

Smart Polypeptides

By

Jin Huang (MSc)

Supervisor: **Dr. Andreas Heise**

A thesis submitted to Dublin City University
in partial fulfilment of the requirements
for the degree of
Doctor of Philosophy



January 2013

Declaration

I hereby certify that this material, which I now submit for assessment on the programme of study leading to the award of a degree of Doctor of Philosophy is entirely my own work, that I have exercised reasonable care to ensure that the work is original, and does not to the best of my knowledge breach any law of copyright, and has not been taken from the work of others save and to the extent that such work has been cited and acknowledged within the text of my work.

Signed: _____ (**Jin Huang**)

ID No. **58125621**

Date:

Acknowledgement

Time flies... More than three years and a half have already gone. It has been so hard for me to start this part, since the whole PhD journey has been so special to me and I have learned so much both on a personal and scientific level. However, I would like to express my sincerest appreciation to all the people I meet before I say goodbye to my PhD.

First of all, my sincerest gratitude goes to the greatest supervisor Dr. Andreas Heise. Andreas, thanks a million for being my best-ever mentor as well as a good friend. Thank you for your unreserved trust and understanding, motivating me to be confident, raising me up whenever I was down, offering me enormous freedom and constant support all the time. Thank you for everything you have already done for me. I know it was tough to have a very demanding student, so please also accept my apologies for all of the troubles and inconveniences I made.

I would like to thank Prof. Harm-Anton Klok from EPFL/Switzerland, Prof. Dermot Diamond and Dr. Kieran Nolan from DCU/Ireland for being my examiners. Also, I want to acknowledge Prof. Han Vos from DCU and Dr. Xiao Yan (Jenny) for their initial recommendations; otherwise I would have missed the best supervisor.

During my PhD, I got massive support from DCU Chemistry Community. I am really grateful for your great help. Thank all of you in DCU Chemistry Technical Office. Veronica, thanks a lot for your support all the time, in particular lots of urgent requests such as purchasing orders. Catherine, thank you for ordering lots of chemicals and lab consumables, listening to my complaints and cheering me up. Brendan, you are my hero, thank you for helping me out with SEM/UV/ATR. Ambrose, you are a legend, thanks for your patience and help whenever I came to you. John, I appreciate your great help on many NMR measurements. Damien, thanks a lot for lab safety and bringing me to the clinic after the accident of “broken acryloylchloride bottle in the fridge”. I also want to acknowledge the great help

from Vinny, Mary, Niamh, Stephen, Christina. Julie, I appreciate the countless supports on administration from you very much. Thanks a lot for being helpful as always. Dr. Brian Kelleher, Shane and Brian, you guys are very nice to help me out with freezing dryer. Dr. Dermot Brougham and Eoin, thank you for DLS measurement. Eoin, many thanks for many helps on DLS and I always enjoyed a little chats with you, good luck to your PhD. And I also would like to thank Dr. Lynn Dennany for fluorescence measurements.

It is a great honor for me to work with many different groups and individuals during my PhD. First of all, I would like to give the special gratitude to Dr. Gijs Habraken from Eindhoven University of Technology/The Netherlands. Gijs, you are my big hero, and thank you very much for bringing me into NCA world as well as tremendous help in the initial stage of my PhD. And also thanks for taking care of me during my stay in Eindhoven. It was a great experience to be involved in “IUPAC Glycopeptides Project” and work with the top polymer chemistry groups. Thanks all of you for having meetings and sharing knowledge together. In particular, I would like to thank Prof. Sebastien Lecommandoux and Dr. Colin Bonduelle from University of Bordeaux/France. I was lucky to have the chance to work with you, and I am always impressed by your vast knowledge of self-assembly. Our collaboration has been so amazing, as proven by our very productive results. I would like to extend my sincere gratitude to Dr. Dave Adams and Jaclyn Raeburn from University of Liverpool/UK for the rheological measurement and Cryo-TEM in the hydrogel projects. Thanks for looking after me when I was in Liverpool, and correcting the manuscript of hydrogel story. I also want to thank Conn Hastings, Dr. Garry Duffy, Dr. Helena Kelly from Royal College of Surgeons in Ireland for helping me sort out the application of the hydrogel. Conn, you are very helpful and I enjoyed working with you a lot, good luck to your PhD. I am grateful for the collaboration with Prof. David Haddleton and Dr. Remzi Becer from the University of Warwick/UK on the binding kinetics of glycopeptides. I must thank Anne Shanahan from Dublin Institute of Technology for CD measurements. Thanks for reserving the CD machine for me whenever I wanted to use it. I also appreciate the great help from Dr. Anja Palmans from Eindhoven University of Technology/The

Netherlands for temperature-dependent CD measurement, and valuable suggestions and corrections on the manuscript of hydrogel story.

Four-month stay in Eindhoven University of Technology was a pleasant and special experience for me. I would like to thank Prof. Cor Koning for offering me the precious opportunity to be a part of SPC for four months. Pleunie is appreciated for solving a lot of administrative issues such as work permit and accommodation. Many thanks to my labmates there: Gijs, Karel, Hermant, Eirk, Bahar, Inge... for a lot of help, discussion and fun in the lab. Martin, thanks a lot for your generosity to let me work in your fumehood and helping me analyze lots of SEC/HFIP during my whole PhD. Bahar, Thank you for your help on SEC/HFIP as well. It was great to know Donglin and Jing there, thanks for coming to Dublin and visiting me. Jing, thanks for taking care of me when I was back to TU/e, as well as a lot of encouragement and help during my job-hunting. I wish you all the best in your new life chapter.

Being a part of PRG is more than brilliant and unforgettable. Thank all of PRGers, and my PhD would not be the same without you. Thank you for working together in the lab daily, having lunch or going out together, and sharing happiness and sadness of our life here. I am also very sorry for making any trouble or mess in the lab, and please accept my sincere apologies if it bothered you. Paul, thanks for correcting my English and your company to gigs and movies. I wish you all the best in Durham. Fabrice, I am always impressed by your solid knowledge of polymer chemistry, and thank you for being there whenever I need your help, bringing me nice chocolates and being “caustic” to me as well. Hope you will have great success in your academy life. Claudia, thanks for being a great friend here, running the column to purify azido lactose for me, organizing the surprise birthday party, making very delicious tiramisu and wine chicken, and sharing the life in Dublin. Good luck to your PhD, I am sure you will have a bright new life ahead. Tushar, thanks a lot for shopping together on the weekend and waiting for me to finish my labwork later evening sometimes. I wish you all the best with finishing your PhD sooner. Good luck in your academic or political future. Ida, you are always very kind, thank you

for sharing the lab and having lunch together when we started our PhD in X-150. 加油(jia you), you are almost there. Zeliha, you are a great “baker”, thank you for your nice muffins and Turkish delights, and they were really delicious. I also wish you good luck with finishing your PhD sooner. Mark, you are my favorite Irish buddy, and you are a great lab buddy as well. I believe you will be very productive in your PhD and I wish you all the best. Anton, thanks for the nice journey together in California, please take it easy in your life and I wish you will enjoy your PhD in Dublin. Jaco, I always enjoy the conversions with you, good luck to your PhD as well. Marcello, it is a great honor to work with you, and I wish you all the best with your PhD.

Special thanks owe to some friends I meet here. Zhang Yu, thanks a lot for picking me up in the airport when I arrived in Dublin for the first time, sharing me a bedroom and traveling together. Tons of thanks and appreciation go to Fu Na, Qiu Zhengwei and Anna for giving me huge help and support during my PhD in Dublin. Thanks for sharing the house for more than two years, giving me a lift to the supermarket or airport all the time, cooking nice meals for me, cheering me up, and sharing my routine life. I wish you all with the new baby will have a great time here. I also would like to thank Yuan Zhenhui and Zhang Xin for lots of help when we shared the big house. And I would like to thank Barry for being patient to listen to me and teach me lots of English. Zhang Yang, I enjoy being the flatmate with you a lot, and thank you for a lot of chatting, sharing nice food and giving me the lift. I wish you the best with your PhD and the life ahead. Special thanks also go to Josh, thanks for your music and your show on Sunday. With the company of your show, my labwork on Sunday was always more enjoyable and exciting. Josh, I hope you will enjoy the life more.

Many thanks are also given to my previous supervisors and friends in China who have always trusted and encouraged me. Especially, I would like to thank Prof. Wang Shilong and Prof. Li Dongming from Tongji University for writing the recommendation letters and giving me lots of encouragement. I would like to extend

my gratitude to Luo Xianji, He Haidong, Yang Rong and Zhou Lei. I really appreciate you guys for helping me out with many troubles and taking care of me whenever I was back to Shanghai. And many thanks go to Zeng Lei, Wang Wei, Zhang Liping, etc for being there to support me all the time.

I am pretty sure that I would not finish my PhD without the massive support and love from my dearest family. Thus, huge thanks go to Dad, Mum, Brother, Sister-in-law and my cutest niece.

Thanks, all of you I have ever met!!!

List of Publications

- Jin Huang, Andreas Heise; Stimuli responsive synthetic polypeptides derived from N-carboxyanhydride (NCA) polymerisation; *Chem. Soc. Rev.* **2013**, DOI: 10.1039/C3CS60063G.
- Jin Huang, Conn L. Hastings, Garry P. Duffy, Helena M. Kelly, Jaclyn Raeburn, Dave J. Adams, Andreas Heise; Supramolecular hydrogels with reverse thermal gelation properties from (oligo)tyrosine containing block copolymers; *Biomacromolecules* **2013**, *14*, 200.
- Jin Huang, Colin Bonduelle, Julie Thévenot, Sébastien Lecommandoux, Andreas Heise; Biologically active polymersomes from amphiphilic glycopeptides; *J. Am. Chem. Soc.* **2012**, *134*, 119.
- Jin Huang, Gijs Habraken, Fabrice Audouin, Andreas Heise; Hydrolytically stable bioactive synthetic glycopeptide homo- and copolymers by combination of NCA polymerisation and click reaction; *Macromolecules* **2010**, *43*, 6050.
- Jin Huang, Qiang Zhang, Guang-Zhao Li, David M. Haddleton, Russell Wallis, Daniel Mitchell, Andreas Heise, and C. Remzi Becer; Glycopeptides as potential inhibitory agents for dendritic cell and HIV-1. (submitted)
- Jin Huang, Andreas Heise; Salt-triggered supramolecular hydrogel. (to be submitted)
- Colin Bonduelle, Jin Huang, Emmanuel Ibarboure, Andreas Heise, Sébastien Lecommandoux; Synthesis and self-assembly of “tree-like” amphiphilic glycopolypeptides; *Chem. Commun.* **2012**, *48*, 8353.

- Kai-Steffen Krannig, Jin Huang, Andreas Heise, Helmut Schlaad; Photochemical thiol-yne functionalization of polypeptide scaffolds; *Polym. Chem.* **2013**, DOI: 10.1039/C3PY00428G.
- Fabrice Audouin, Mary Fox, Ruth Larragy, Paul Clarke, Jin Huang, Brendan O'Connor, Andreas Heise; Polypeptide-grafted macroporous polyHIPE by surface-Initiated N-carboxyanhydride (NCA) polymerisation as a platform for bioconjugation; *Macromolecules* **2012**, *45*, 6127.
- Fabrice Audouin, Rutger J. I. Knoop, Jin Huang, Andreas Heise; Star polymers by cross-linking of linear poly(benzyl-L-glutamate) macromonomers via free-radical and RAFT polymerisation. A simple route toward peptide-stabilized nanoparticles; *J. Polym. Sci. A; Polym. Chem.* **2010**, *48*, 6402.

Conference presentations

- Jin Huang, Andreas Heise; A highly efficient route to bio-active glycopeptides by combination of NCA polymerisation and click reaction; *Macro UK Young Researcher Meeting*, Nottingham/UK, April 2010.
- Jin Huang, Andreas Heise; A highly efficient route to bio-active glycopeptides by combination of NCA polymerisation and click reaction; *43rd IUPAC World Polymer Congress*, Glasgow/UK, July 2010.
- Jin Huang, Andreas Heise; From organogel to hydrogel: PEGylated tyrosine-based polypeptides by NCA polymerisation; *24th European Conference on Biomaterials*, Dublin/Ireland, September 2011.
- Jin Huang, Andreas Heise; Self-assembly of amphiphilic polypeptides for the formation of polymersomes and hydrogels; *243rd ACS National Meeting*, San Diego/USA, March 2012.

Abstract

In order to design the next generation polypeptide-based biomaterials, novel synthetic strategies and materials with well-defined structures as well as selective responsiveness are needed. The aim of this PhD project was to develop novel synthetic stimuli-responsive polypeptides (so-called “smart” polypeptides), which can selectively bind to biomolecules and/or respond to environmental changes for applications in drug delivery and tissue engineering. The synthetic strategies were versatile amino-acid N-carboxyanhydride (NCA) polymerisation and precise orthogonal conjugation chemistries. Two different platforms have been developed including biologically active glycopolypeptides and responsive tyrosine-based polypeptide hydrogels.

Platform 1: Biologically active glycopolypeptides: Propargylglycine without any potentially hydrolytically unstable ester bond was utilized to prepare glycopeptides by the combination of NCA polymerisation and quantitative Huisgen [3+2] cycloaddition click reaction with azide-functionalized galactose. Highly selective bioactivity of the glycosylated poly(DL-propargylglycine) was demonstrated by galactose specific lectin recognition experiment. The synthetic concept also offered a facile route to bioactive polymersomes fully based on glycopeptides. Poly(γ -benzyl-L-glutamate-*b*-galactosylated propargylglycine) copolymers were proposed as candidates to prepare glycopeptidic vesicles with lectin binding galactose presented at the polymersome surface. In this amphiphilic block copolymer design, carbohydrates were introduced on the side chains of the hydrophilic segment that fulfill a dual function by promoting self-assembly and specific binding. Depending on the block copolymer composition and the self-assembly protocol, the morphology of the self-assembly could be controlled, ranging from (wormlike) micelles to polymersomes.

Platform 2: Responsive tyrosine-based polypeptide hydrogels: Within this project new PEGylated amphiphilic tyrosine-based polypeptides were obtained by NCA polymerisation. In this concept, tyrosine building blocks are able to display multiple interactions triggering self-assembly into the hydrogel matrix. Most

interestingly, PEGylated tyrosine-based polypeptides can undergo unusual sol-gel transition at a low polymer concentration range of 0.25-3.0 wt% when the temperature increases. A preliminary *in vitro* application confirmed the hydrogels are biocompatible and biodegradable, and produced a sustained release of a small-molecule drug. Moreover, tyrosine-based amphiphilic copolypeptides poly(L-glutamate-*b*-L-tyrosine) were explored as salt-triggered hydrogel materials. Upon the addition of the salt (i.e. CaCl₂), amphiphiles at certain concentration (typically 1.0-4.0 wt%) can be triggered to form hydrogels by hydrophobic interaction and electrostatic interaction. Furthermore, the amphiphiles can also spontaneously self-assemble into macroscopic transparent membrane-like aggregates in the salty medium.

Keywords:

α -amino acid N-carboxyanhydride (NCA), ring-opening polymerisation, synthetic polypeptides, stimuli-responsive, glycopolypeptides, propargylglycine, click chemistry, self-assembly, polymersomes, hydrogel, tyrosine

Contents

Acknowledgement	iii
List of publications	viii
Abstract.....	x
Chapter 1.....	1
“Smart” polypeptides	1
1.1 Synthetic polypeptides	2
1.2 Ring-opening polymerisation of α -amino acid N-carboxyanhydride (NCA)	3
1.2.1 Mechanism of NCA polymerisation	4
1.2.2 “Living” NCA polymerisation	6
1.3 Biologically responsive polypeptides	9
1.4 Temperature responsive polypeptides.....	15
1.5 pH responsive polypeptides.....	18
1.6 Photo responsive polypeptides	22
1.7 Redox responsive polypeptides	25
1.8 Miscellaneous responsive polypeptides	28
1.9 Conclusions.....	31
1.10 Aim and outline of the thesis.....	32
1.11 References.....	33
Chapter 2.....	45
Hydrolytically stable bioactive synthetic glycopeptide by combination of NCA polymerisation and click reaction	45
2.1 Introduction	46
2.2 Experimental section.....	48
2.3 Results and Discussion.....	54
2.4 Conclusions.....	70
2.5 References.....	71

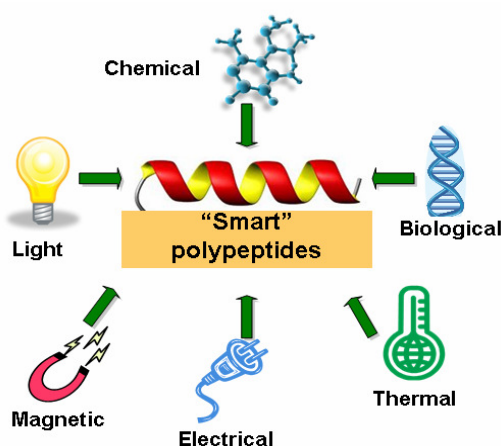
Chapter 3.....	74
Biologically active polymersomes from amphiphilic glycopeptides.....	74
3.1 Introduction	75
3.2 Experimental section.....	76
3.3 Results and Discussion.....	82
3.4 Conclusions.....	95
3.5 References.....	96
 Chapter 4.....	 98
Supramolecular hydrogels with reverse thermal gelation properties from	
(oligo)tyrosine containing block copolymers	98
4.1 Introduction	99
4.2 Experimental section.....	101
4.3 Results and Discussion.....	107
4.4 Conclusions.....	122
4.5 References.....	123
 Chapter 5.....	 127
Salt-triggered self-assembly of amphiphilic poly(L-glutamate-<i>b</i>-L-tyrosine) towards	
the formation of hydrogel	127
5.1 Introduction	128
5.2 Experimental section.....	131
5.3 Results and Discussion.....	135
5.4 Conclusions.....	151
5.5 References.....	152
 Chapter 6.....	 156
Summary and Outlook.....	156

Chapter 1

"Smart" polypeptides

Abstract

By the combination of NCA polymerisation and various synthetic chemistries, well-defined synthetic stimuli-responsive polypeptides ("smart" polypeptides) with incorporated different functionalities have been extensively explored over the past decades. These novel materials have potential applications in biomedicine and biotechnology including tissue engineering, drug delivery and biodiagnostics. "Smart" polypeptides are capable of undergoing conformational changes and phase transition accompanied by variations in the chemical and physical changes of the polypeptides in response to an external stimulus such as biologically relevant species (i.e. enzyme, biomarker), the environment (i.e. temperature, pH), the irradiation with light or exposure to a magnetic field. In this chapter, we review the recent developments including synthetic strategies and applications of synthetic stimuli-responsive homo- and block polypeptides.



This chapter was published in
Huang, J.; Heise, A. *Chem. Soc. Rev.* 2013, DOI: 10.1039/C3CS60063G.

1.1 Synthetic polypeptides

Synthetic polypeptides (i.e. poly(amino acids)) are of great interest because of the potential applications in biomedicine and biotechnology such as tissue engineering, drug delivery, and as therapeutics.¹ Depending on the amino acid side chain they can adopt certain ordered conformations (e.g. helices, sheet and turns) and self-assemble into precisely defined biomimic structures through non-covalent interactions such as hydrogen bonding, van der Waals forces and π - π stacking.² Traditionally solid phase peptide synthesis (SPPS) has been employed to prepare polypeptides with precisely controlled amino acid sequences on laboratory scale.³ While SPPS is widely accepted as a routine and robust technique, the labour-intensive step-by-step amino acid coupling involving deprotection/coupling steps and the limitation of achievable maximum chain length of around 50 amino acid residues can be restricting factors.⁴ In contrast, the ring-opening polymerisation of amino acid N-carboxyanhydrides (NCA), while lacking the ability to synthesize specific sequences, is a highly versatile technique for the fast preparation of higher molecular weight synthetic polypeptides.^{5,6} Thanks to the continuous progress in NCA polymerisation in the last decades, synthetic polypeptides with controllable (high) molecule weight, narrow polydispersity, sophisticate polymeric architectures and unaffected chirality can be prepared in high yield and large quantity.^{7,8,9,10} This progress in NCA polymerisation combined with advanced orthogonal functionalization techniques as well as the integration with other controlled polymerisation techniques significantly widens the scope of polypeptide building blocks in a variety of material designs.^{11, 12} Targeted applications for novel polypeptide hybrid materials are often sought in biomedicine and biotechnology including tissue engineering, drug delivery and biondiagnostics. Particularly, stimuli-responsive polypeptides (so-called "smart" polypeptides) have been extensively explored. "Smart" polypeptides are capable of undergoing conformational changes and/or phase transition accompanied by variations in the chemical and physical changes of the polypeptides in response to an external stimuli such as biologically relevant species (i.e. enzyme, biomarker), the environment (i.e. temperature, pH),

the irradiation with light or exposure to an magnetic field (Figure 1.1).¹³ This paper will review the recent developments in this active field including synthetic strategies and applications of synthetic "smart" homo- and block polypeptides derived from NCA polymerisation.

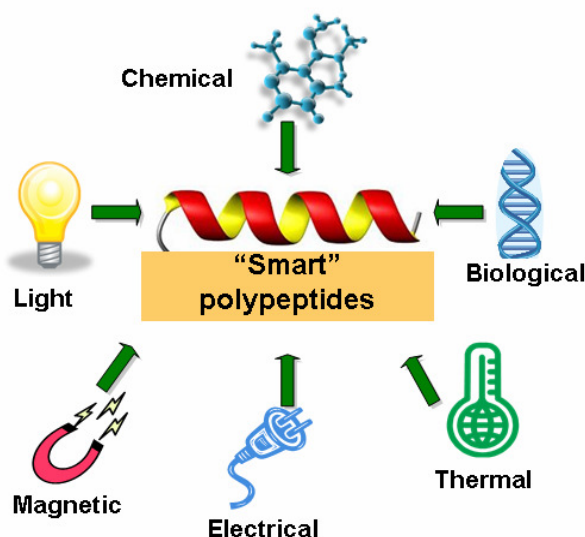
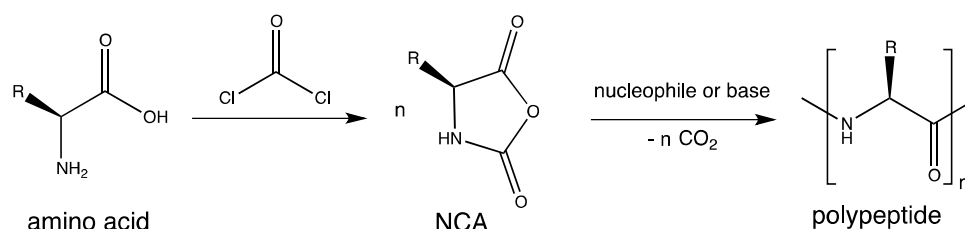


Figure 1.1: The range of stimuli-responsive synthetic polypeptides.

1.2 Ring-opening polymerisation of α -amino acid N-carboxyanhydride (NCA)

The synthesis and polymerisations of NCAs was first reported by Hermann Leuchs in 1906.^{14,15} After 1921, Curtius¹⁶, Wessely¹⁷ and their coworkers used NCAs with water, alcohol or primary amines as initiators in the ring-opening polymerisation for the first time to prepare high molecule weight polypeptides. NCAs can be synthesized either by the reaction of N-alkyloxycarbonyl-amino acids with halogenating agents (Leuchs method¹⁵) or the treatment of α -amino acids with phosgene (Fuchs-Farthing method¹⁸; Scheme 1.1). Triphosgene, diphosgene and di-tert.-butyltricarboxylate have been used as phosgene substitutes, allowing phosgene to form gradually during NCA synthesis.¹⁹ Mostly recrystallization but also flash chromatography can be applied for the purification of NCAs to remove by-products

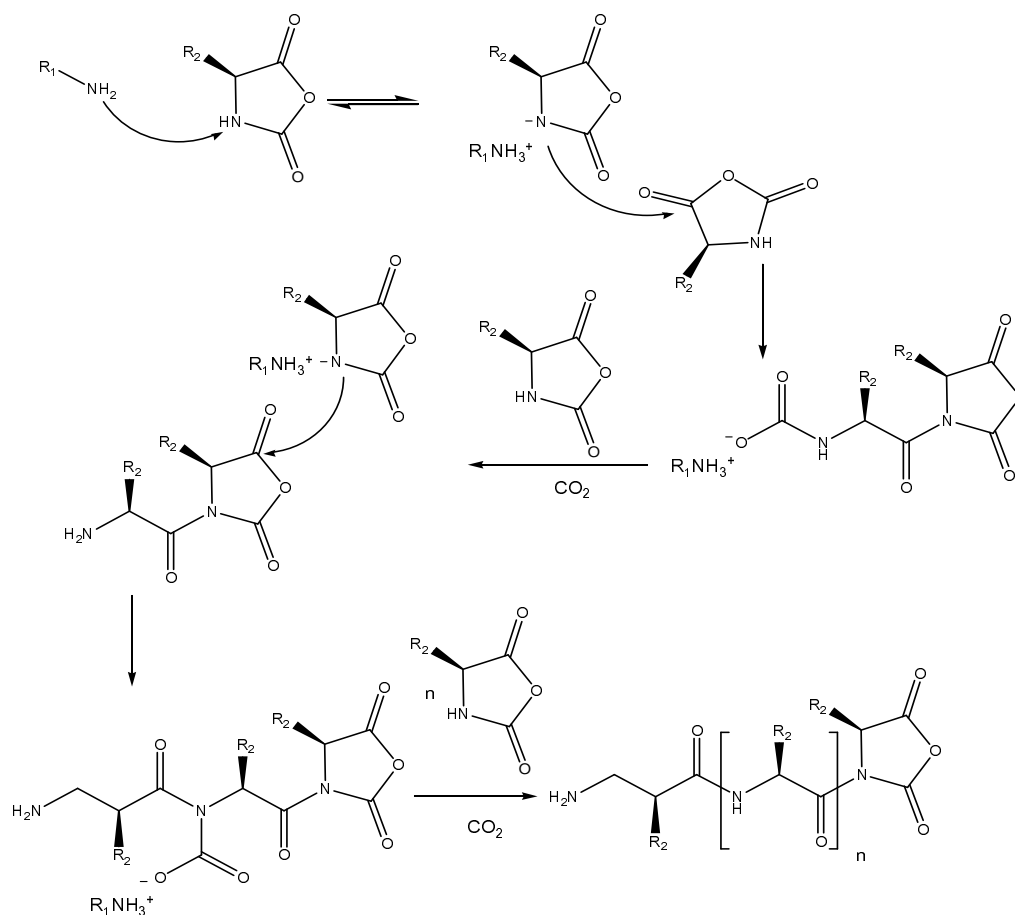
generated during NCA synthesis including HCl, HCl-amino acid salts and 2-isocyanatoacyl chlorides as these electrophilic by-products can inhibit or quench the propagation of the polymer chain and thus affect the synthesis of polypeptides.²⁰



Scheme 1.1: General reaction pathway for synthesis of α -amino acid N-carboxyanhydrides (NCA) and their ring-opening polymerisation.

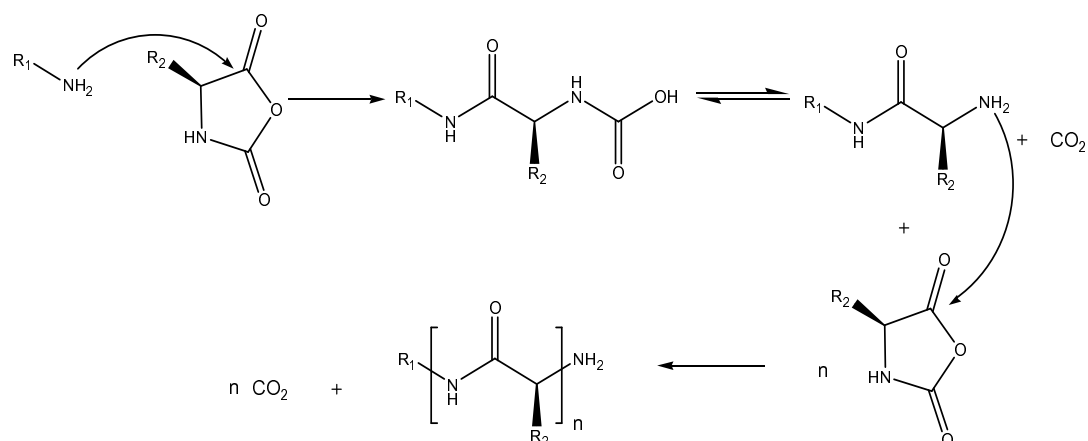
1.2.1 Mechanism of NCA polymerisation

NCA ring-opening polymerisation can be initiated by a range of nucleophiles and bases such as amines and metal alkoxides (Scheme 1.1).²¹ The two widely accepted pathways for the polymerisation of NCAs are the “normal amine” (NAM) and the “activated monomer” (AMM) mechanisms.²² Initiators for the latter typically include bases (i.e. tertiary amines) and alkoxides, which abstract the proton from the NCA nitrogen (3-N) resulting in the formation of an NCA anion. The deprotonated NCA anion can initiate the NCA polymerisation and promote the propagation by attacking the 5-CO of another NCA thereby creating a new anion under the release of CO_2 (Scheme 1.2). Polymerisations following the AMM are generally fully uncontrolled and thus less favoured in the synthesis of well-defined polypeptides.



Scheme 1.2: Activated Monomer Mechanism for NCA polymerisation.

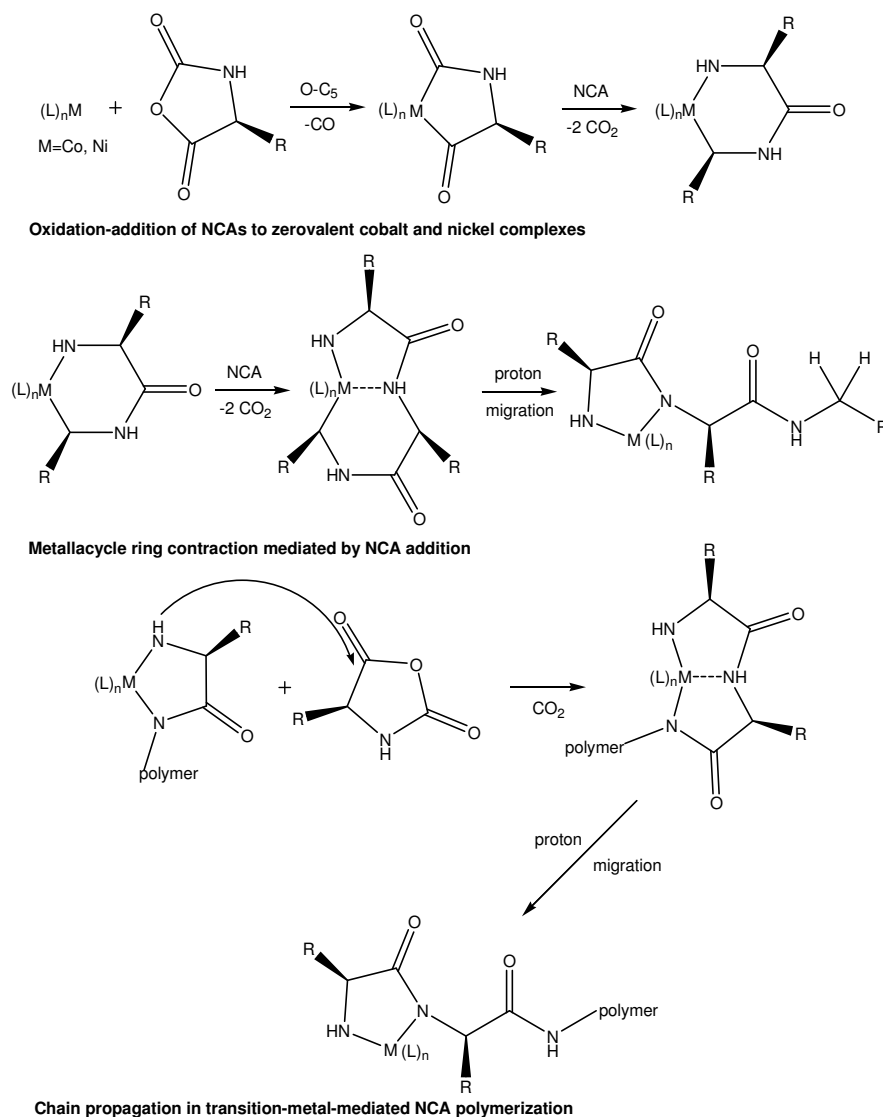
The NAM is generally observed for NCA polymerisations initiated by nonionic initiators bearing at least a mobile hydrogen atom such as primary and secondary amines, alcohol and water. The initiation step is based on the nucleophilic attack on the carbonyl (5-CO) of the NCA ring (Scheme 1.3).²² The ring is opened and the unstable intermediate carbamic acid is formed by proton transfer. The carbamic acid subsequently decarboxylates by the elimination of CO_2 and the newly-formed primary amine promotes the propagation of the polymerisation. The NAM offers control over the molecular weight and end-group fidelity. However, due to a variety of possible side reactions such as the termination of the end group²³ or the formation of cyclic structures²⁴ caused by impurities in the NCAs or the reaction solvent, or the presence of water, the reaction control can be significantly restricted.²⁵



Scheme 1.3: Normal Amine Mechanism for NCA polymerisation.

1.2.2 “Living” NCA polymerisation

Deming was the first to introduce the concept of “living” NCA polymerisation using transition metal catalysts (Scheme 1.4).²⁶ By using zerovalent nickel and cobalt initiators²⁷ (i.e., $(\text{PMe}_3)_4\text{Co}$, and $\text{bpyNi}(\text{COD})$, bpy =2,2'-bipyridine and COD =1,5-cyclooctadiene) to avoid side reactions, homo- and block polypeptides with excellent control over the molecular weight with low polydispersity index (PDI) were obtained. In this approach the formation of the chelating metallacyclic intermediates by the transition metal complex and NCA is necessary for living NCA polymerisation. However, introducing end-group functionality through the initiator is tedious and has only been reported in one literature example using a bifunctional initiator containing an activated bromide group for Atom Transfer Radical Polymerisation (ATRP) and a Ni amido amidate complex for NCA polymerisation.²⁸ Sequential nickel initiated polymerisation of γ -benzyl-L-glutamate (BLG) NCA and ATRP of methyl methacrylate yielded a rod-coil block hybrid copolymer poly(γ -benzyl-L-glutamate-*b*-methyl methacrylate).



Scheme 1.4: Mechanism of transition-metal-mediate NCA polymerisation.

Primary amine initiated NCA polymerisation is thus still the most widely used technique and different experimental techniques have been investigated and optimized to give well-defined polypeptides. Hadjichristidis and co-workers showed that using highly purified chemicals and high vacuum techniques, homo- and block polypeptides with high and controlled molecular weight can be prepared.²⁹ In this approach, the highly purified polymerisation solvent and initiator, the suppression of the carbamic acid- CO_2 equilibrium after the efficient removal of CO_2 as well as the side reaction between DMF and the end-group of propagating polymer chain were accounted for the polymerisation control. The advantages of the high vacuum

technique for the preparation of well-defined polypeptides were also demonstrated by Messman and coworkers.³⁰ Using Matrix-assisted laser desorption/ionization time-of-flight mass spectrometry (MALDI-TOF MS), Nano-assisted laser desorption/ionization time-of-flight mass spectrometry (NALDI-TOF MS), and ¹³C NMR spectroscopy they demonstrated that the high-vacuum polymerisation proceeded exclusively by the NAM with minimal termination. In 2004 another innovative approach to eliminate side reactions in the NAM NCA polymerisation was reported by Vayaboury and coworkers.³¹ The group systematically investigated the hexylamine initiated polymerisation of N ϵ -trifluoroacetyl-L-lysine NCA in DMF at different temperatures. The living amine chain-ends as analyzed by size exclusion chromatography (SEC) and non-aqueous capillary electrophoresis (NACE) increased dramatically from 22% to 99% when the polymerisation temperature was lowered from 20 to 0°C. The elimination of the termination reactions at low temperature was attributed to higher activation energies of the side reactions than that of chain propagation.³² However, an obvious drawback of the polymerisation at 0°C is the long reaction times. Very recently, Heise and Habraken investigated NCA polymerisation of a range of different NCAs to optimize the NAM by combining the high-vacuum and the low-temperature techniques.³³ The combination of two different approaches not only promoted the NCA polymerisation in the controllable manner but also significantly shortened the polymerisation time. A tetrablock copolymer with low PDI and high structural control comprising poly(γ -benzyl-L-glutamate), poly(L-alanine), poly(N ϵ -benzyloxycarbonyl-L-lysine) and poly(β -benzyl-L-aspartate) blocks was synthesized via the combination of the optimal parameters of temperature and pressure. In 2007, a novel organosilicon-mediated NCA polymerisation approach was reported by Cheng and coworkers.³⁴ The synthesis of homo- and hybrid polypeptides with defined composition and narrow molecular weight distribution could be achieved by the use of organo-silicon amines such as hexamethyldisilazane (HMDS) and *N*-trimethylsilyl (TMS) amines as the initiator. A mechanistic study of the polymerisation revealed that the N-terminus of the polymer contains an unexpected trimethylsilyl carbamate (TMS-CBM) end group in both the initiation and the propagation steps. Importantly, nearly quantitative polymerisation with the degree of polymerisation (DP) of 300 could be

completed within 24 hours or less at ambient temperature.³⁵ In 2011, a library of rare earth complexes were first introduced by Ling and coworkers to initiate NCA polymerisation of γ -benzyl-L-glutamate NCA and L-alanine NCA including rare earth isopropoxide ($\text{RE}(\text{OiPr})_3$), rare earth tris(2,6-di-tert-butyl-4-methylphenolate) ($\text{RE}(\text{OAr})_3$), rare earth tris(borohydride) ($\text{RE}(\text{BH}_4)_3(\text{THF})_3$), rare earth tris[bis(trimethylsilyl)amide] ($\text{RE}(\text{NTMS})_3$) and rare earth trifluoromethanesulfonate.³⁶ Homo-, random and block copolymers were prepared in high yield with expected molecular weights and relatively low PDIs (~ 1.1 - 1.6), thereby showing the livingness of the polymerisation. According to the proposed mechanism investigated by MALDI-TOF MS analysis, both NAM and AMM were involved in the NCA polymerisation since nucleophilic attack by the rare earth catalysts on the 5-CO of NCA and deprotonation of 3-NH of NCA simultaneously occurred in the initiation process.³⁷

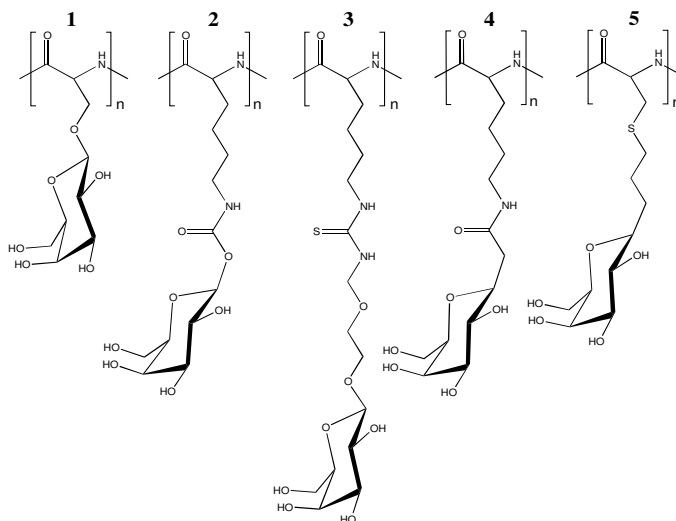
1.3 Biologically responsive polypeptides

Synthetic polypeptides offer an interesting and advantageous platform for the development of biomaterials for controlled drug delivery, biosensor or biodiagnostics and smart matrices for tissue engineering. The polypeptides can be engineered with (bio)functionalities or conjugated with other biomolecules, which are able to respond to a stimulus inherently present in relevant biological systems such as enzymatic degradation and cell-surface receptor recognition.³⁸ Due to their nature, polypeptide chains can be selectively cleaved or hydrolyzed by proteolytic enzymes in some cases with high specificity.³⁹ Recently, much attention has been drawn to the synthesis and application of glycosylated polypeptides due to the fact that natural glycoproteins are involved in many complex biological responsive processes as diverse as signal transmission, fertilization, inflammation, protein folding and many more.⁴⁰ The bioresponsiveness of synthetic glycopeptides is usually assessed with lectins, which is class of sugar binding proteins. Lectins are highly sugar (glycan) specific and typically display multivalent binding, meaning that in the case of polymeric glycomaterials positive binding can be demonstrated by precipitation or turbidity measurements.

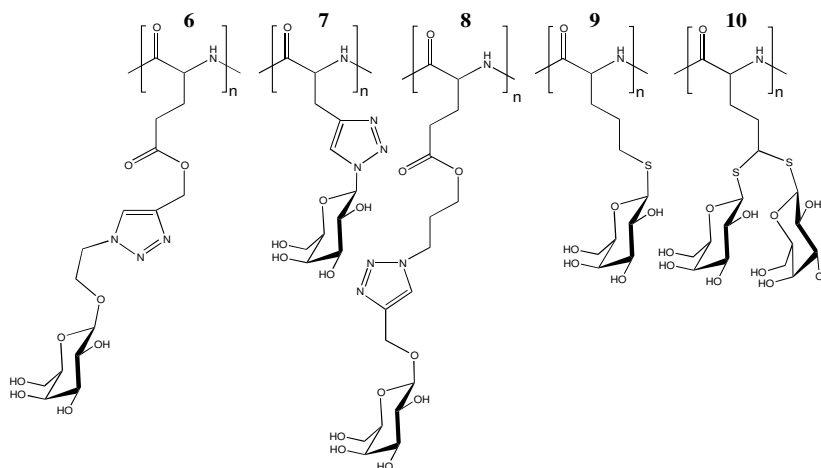
Two different approaches have been employed for the synthesis of glycopolypeptides: (1) the direct ring-opening polymerisation of glycosylated NCA monomer and (2) the post-polymerisation modification of polypeptide side chains (Scheme 1.5). Following the synthesis of O-linked glyco-serine NCAs by Rude et al⁴¹, Okada and coworkers were the first to utilize O-linked glyco-serine NCA (**1**; numbers refer to the polymer structures in Scheme 1.5) to prepare glycopolypeptides in a controlled manner.⁴² However, the monomer synthesis was tedious and only low degrees of polymerisation were obtained attributed to steric effects and hydrogen bonding interaction between the sugar residue and NCA ring. Recently, using a stable glycosyl donor and a commercially available protected lysine, a series of O-linked glyco-lysine NCAs (**2**) including O-benzoylated-D-glyco-L-lysine carbamate NCA and O-acetylated-D-glyco-L-lysine were efficiently prepared by Sen Gupta and coworkers.⁴³ Both glycosylated NCAs bearing protected mannose, galactose and lactose were easily polymerized to yield well-controlled high molecular weight homo- and block glycopolypeptides. The deprotection of acetyl groups from the sugar moieties of glycopolypeptides was more accessible than the deprotection of benzoate to give fully deprotected water-soluble glycopeptides. The biological responsive behavior of the glycopeptides was evaluated by specific carbohydrate-lectin interaction using precipitation and hemagglutination assays as well as isothermal titration calorimetry (ITC). The lectin binding results indicated that the glycopolypeptides poly(α -mannose-O-Lys) can bind specifically to the lectin Concanavalin A (Con A). Interestingly, the binding affinity between glycopolypeptides having a non-helical structure and the corresponding polypeptide adopting an α -helical structure, was proven to be nearly the same. Wenz and coworkers also synthesized well-defined O-glycosylated polylysine upon polymerizing NCAs of O-glycosylated lysine derivatives (**3**) bearing peracetylated sugars (glucose, mannose, galactose) via a thiourea linker.⁴⁴ The significant biological interactions between the galactosylated polypeptides with the human T cells were demonstrated by flow cytometry and fluorescence microscopy and it was found that the galactosylated polymers were specifically incorporated into human T lymphocytes at 37 °C for 6 hours.

The synthesis of glycopolypeptides via polymerisation of C-linked glycosylated-L-lysine NCA monomers (**4**) using transition metal initiator $(\text{PMe}_3)_4\text{Co}$ was first reported by Deming and Kramer.⁴⁵ Well-defined homo-glycopolypeptides as well as block and statistical glycopolypeptides with 100% glycosylation and high molecular weights ($>100\ 000\text{Da}$) were obtained to produce a highly α -helical conformation. Very recently, the same group also employed glycosylated L-cysteine NCA (**5**) for the preparation of conformation-switchable glycopolypeptides.⁴⁶ Those NCA monomers were prepared by thiol-ene click chemistry between alkene-terminated C-linked glycosides of D-galactose or D-glucose and L-cysteine, followed by their conversion to the corresponding glycosylated NCAs. Interestingly, the oxidation of the side-chain thioether linkages in these glycopolypeptides to sulfone groups can make the conformation of the glycopolypeptides undergo helix-to-coil transitions without loss of water solubility.

(a) glycopeptides obtained by polymerisation of glycosylated NCAs



(b) glycopeptides obtained by 'click' chemistry



Scheme 1.5: Glycopolypeptides prepared via polymerisation of glycosylated NCA monomer⁴²⁻⁴⁶ and via post-polymerisation approaches.⁴⁹⁻⁵²

To omit the demanding and labour-intensive synthesis of glycosylated NCA monomers, the synthesis of glycopeptides by versatile post-polymerisation modification approaches has been proposed (Scheme 1.5). The challenge in this approach is to achieve complete glycosylation. Besides the coupling of β -D-galactosylamine to poly(glutamic acid) in the protein by Kiick et al⁴⁷ and D-gluconolactone or lactobionolactone to poly(L-lysine) by Feng et al⁴⁸, in the last few years facile orthogonal conjugation chemistries including copper-catalysed azide-alkyne cycloaddition reaction (6-8), thiol-ene (9) and thiol-yne (10) click reaction

have been reported for the synthesis of biologically responsive glycopolypeptides. These approaches employ a variety of new NCAs bearing "clickable" side-chain functional groups. These new "clickable" NCAs include γ -propargyl-L-glutamate NCA by Chen et al⁴⁹, DL-propargylglycine NCA by Heise et al⁵⁰, γ -3-chloropropyl-L-glutamate NCA by Zhang et al⁵¹ and DL-allylglycine NCA by Schlaad et al⁵². Chen and coworkers found the mannose epitope density of the glycopolypeptides bearing different sugars could significantly influence the rate of multivalent ligand-lectin clustering in the selective lectin recognition experiment.⁴⁹ In contrast to NCAs of γ -propargyl-L-glutamate and γ -3-chloropropyl-L-glutamate with hydrolytically unstable ester linkage in the side chains, DL-propargylglycine without any ester bond was also used for the preparation of stable bioactive glycosylated poly(DL-propargylglycine) via Huisgens cycloaddition click reaction. The latter allows (ester) deprotection chemistry of comonomers like γ -benzyl-L-glutamate for the design of more complex biomimic structures.⁵³ Selective lectin binding experiments revealed that the glycopeptides could be used for biorecognition application. No adverse effect of the triazole ring on the lectin binding was observed.

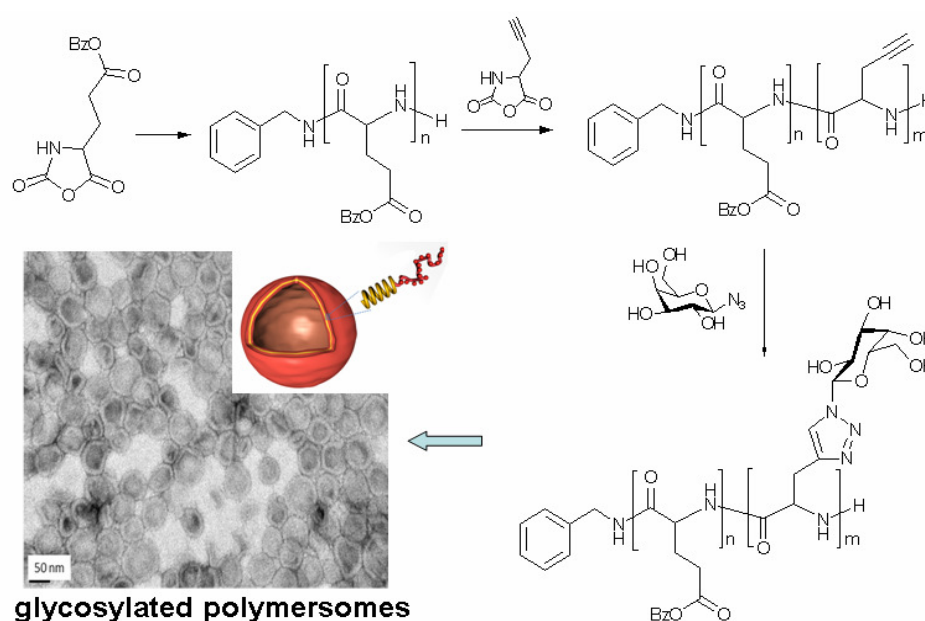


Figure 1.2: Synthesis of poly(γ -benzyl-L-glutamate-*b*-glycosylated propargylglycine) glycopeptides block copolymers and their self-assembly into polymersomes (vesicles).⁵³

Using sequential NCA polymerisation of γ -benzyl-L-glutamate and DL-propargylglycine and further glycosylation by cycloaddition click reaction, a library of well-defined amphiphilic galactose-containing block copolypeptides were prepared to investigate the self-assembly behaviour in aqueous solution.⁵³ Depending on the block copolymer composition and the nanoprecipitation conditions, the morphology of the self-assembly could be controlled, ranging from (wormlike) micelles to polymersomes (Figure 1.2). The biological responsiveness of these structures was proven by selective RCA₁₂₀ lectin recognition. Self-assembled supramolecular structures such as nanorods, micelles, and organogels, reported by Sen Gupta and coworkers, were achieved based on amphiphilic glycopolypeptide-oligo(ethylene glycol)-dendron conjugates.⁵⁴ The self-assembly was affected by the generation of the dendron, the length of the glycopolypeptide segment, the protected or unprotected form of sugar residue, and the extent of helicity of the polypeptide backbone. The bioactivity of these assemblies was also demonstrated by the selective interaction of mannose-functionalized nanorods with Con A. Very recently, Deming et al. reported block copolypeptides containing poly(L-leucine) as α -helical hydrophobic segment and either α -helical poly(α -D-galactopyranosyl-L-lysine) or disordered poly(α -D-galactopyranosyl-L-cysteine sulfone) as hydrophilic segments. Interestingly, different conformations of galactosylated hydrophilic domains significantly affect the assembly morphologies of glycosylated amphiphilic block copolypeptide. The polypeptides with disordered poly(α -D-galactopyranosyl-L-cysteine sulfone) segments favour the formation of vesicles, and proven by lectin binding experiment, the galactose residues present in the vesicle can selectively bind to RCA₁₂₀.⁵⁵

Other specific biologically responsive polypeptides like a glucose-responsive polypeptide was reported by Chen and coworkers, which holds promise for potential applications in glucose sensing and insulin delivery.⁵⁶ The glucose-sensitive group phenylboronic acid was engineered into the pendent carboxyl group of poly(L-glutamic acid) to synthesize poly(ethylene glycol)-*b*-poly(L-glutamic acid-co-*N*-3-L-glutamylamidophenylboronic acid) (mPEG-*b*-P(GA-co-GPBA)). The phenylboronic acid functionalized amphiphilic block copolymers self-assembled

into glucose-responsive micelles, and the release of encapsulated insulin from the micelles was triggered by the addition of glucose at physiological pH.

1.4 Temperature responsive polypeptides

Temperature has been used as a useful external stimulus for the design of stimuli-responsive polypeptides owing to its physiological significance.⁵⁷ In the last few years a variety of novel well-defined polypeptides have been synthesized to respond to temperature variation.⁵⁸ Typically, thermoresponsive polypeptides can undergo a hydration-to-dehydration transition or conformational changes upon temperature changes, resulting in the changes of assemblies and morphologies in an aqueous solution. The thermoresponsivity of the polypeptides can potentially be used in various applications involving thermoresponsive nanoreactors and drug delivery systems.⁵⁹

A range of thermoresponsive polymers, displaying a tunable lower critical solution temperature (LCST), were utilized as building blocks in temperature responsive polypeptides. The thermosensitive polymers were usually employed as the macroinitiator for NCA polymerisation including poly(N-isopropylacrylamide)⁶⁰ (PNIPAM), poly(2-isopropyl-2-oxazoline)⁶¹, Jeffamine⁶² and poly(N-isopropylacrylamide-*co*-N-hydroxy-methyl-acrylamide)⁶³. Post-polymerisation modification (i.e. chemical coupling or "click" chemistry) with thermoresponsive building blocks such as poly(N-isopropylacrylamide)⁶⁴ and poly[2-(dimethylamino)ethyl methacrylate] were also reported by Lecommandoux and coworkers.⁶⁵ These polymers were able to self-assemble into micelles and then underwent subsequent switching of corona and core to form reversed structures upon applying a temperature stimulus.

Recently, great interest in thermogelling polypeptides has emerged because of their potential applications in drug delivery and tissue regeneration. Using amine-functionalized poly(ethylene glycol) (PEG) as the macroinitiator for NCA polymerisation, Jeong and coworkers explored a series of amphiphilic hybrid block copolymers as reverse thermogelling polypeptides including PEG-*b*-poly(alanine), PEG-*b*-poly(phenylalanine) and PEG-*b*-poly(alanine-*co*-phenylalanine).⁶⁶ These

materials underwent sol-to-gel transition at a typical concentration range of 3.0-14.0 wt% in aqueous solution when the temperature was increased. The dehydration of PEG and inter-micellar aggregation either by higher concentration of the polymer in deionized (DI) water or by a conformational change such as strengthening of the secondary structure were suggested to be the driving force of the sol-to-gel transition.⁶⁷ Most importantly, *in vitro* and *in vivo* drug release, and enzymatic degradation experiments revealed the potential of those thermoreponsive polypeptides in the field of tissue engineering, cell therapy, and drug delivery.⁶⁸ Very recently, novel thermoresponsive tyrosine-based polypeptide hydrogels was reported (Figure 1.3). The gel formation was attributed to the precise hydrophobic interaction between PEG and tyrosine building blocks as well as the unique feature of the tyrosine that is hydrophobic but contains a polar phenol group in the side chain. The hydrogelation profile is highly sensitive to the polymer composition. Interestingly, PEGylated tyrosine-based polypeptide can undergo sol-to-gel transition at a low polymer concentration range of 0.25-3.0 wt% when the temperature increases, which is rarely observed as most gels melt with increasing temperature.⁶⁹

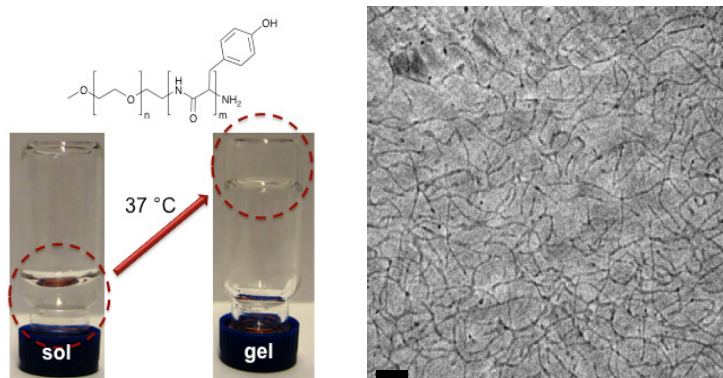


Figure 1.3: Temperature-responsive hydrogel from PEGylated tyrosine-based polypeptide and the morphology of the hydrogel at 0.25 wt% as observed in cryogenic transmission electron microscopy, TEM (the scale bar presents 200 nm).⁶⁹

Chen and coworkers prepared a series of novel temperature responsive polypeptides via click reaction between poly(γ -propargyl-L-glutamate) (PPLG) and 1-(2-

methoxyethoxy)-2-azidoethane ($\text{MEO}_2\text{-N}_3$) or 1-(2-(2-methoxyethoxy)ethoxy)-2-azidoethane ($\text{MEO}_3\text{-N}_3$).⁷⁰ Sharp thermal phase transitions were demonstrated by PPLG-*g*- MEO_x with LCSTs depending on the chain length of the polypeptide backbone and MEO_x in the side chain, polymer concentration and salt concentration. Moreover, the drug release from the temperature-sensitive amphiphilic nanoparticles could be greatly accelerated by increasing the temperatures above their LCSTs, which suggested thermoresponsive polypeptides hold promise as potential candidates for drug delivery. Very recently, a new thermosensitive polypeptide poly(L-glutamate-*g*-2-(2-methoxyethoxy)ethyl methacrylate) (PLG-*g*-P MEO_2MA) was synthesized by ATRP of 2-(2-methoxyethoxy)-ethyl methacrylate using the poly(γ -2-chloroethyl-L-glutamate) as the macroinitiator.⁷¹ Different from the post-modification approach, a series of novel PEGylated L-glutamic acid (EG_xGlu) NCA monomers were developed by Li et al. to prepare well-controlled thermoresponsive homopolypeptide using Deming's catalyst $\text{Ni}(\text{COD})\text{depe}$ as an initiator (Figure 1.4).⁷² Depending on the length of oligo(ethylene glycol) (OEG) units, these polypeptides adopted different secondary structures and demonstrated different thermoresponsive behaviors. The LCSTs of the (co)polypeptides could be modulated by varying OEG length and the ratios of the comonomers. Interestingly, the chirality of the polypeptide can significantly affect the LCST behaviour and it was proven that racemic poly(γ -(2-(2-(2-Methoxyethoxy)ethoxy)ethoxy)esterlyl-L-glutamate) (poly(rac- EG_3Glu)) adopting a random coil conformation did not show any LCST up to 70 °C. Most recently, Dong and coworkers also found that thermosensitive poly(L- EG_2Glu) can self-assemble into nanostructures in aqueous solution, and upon increasing chain length their morphologies altered from spherical micelles to worm-like micelles, then to fiber micelles.⁷³

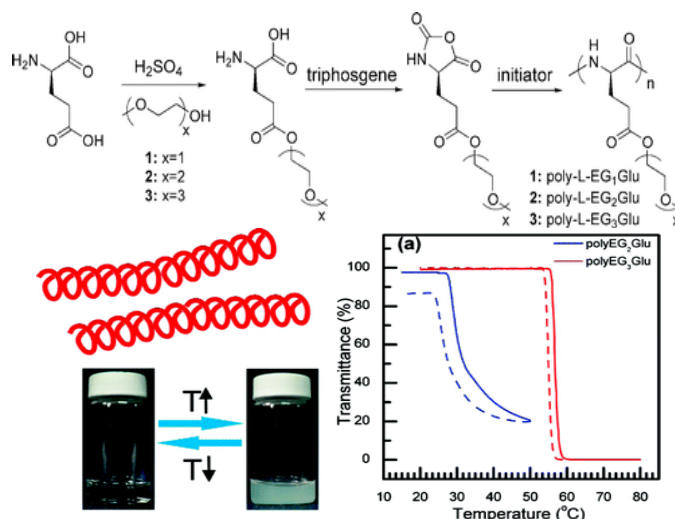


Figure 1.4: Synthetic routes to poly(L-EG_xGlu) homopolypeptides and the plots of transmittance as a function of temperature for aqueous solutions (2 mg.mL⁻¹) of poly(L-EG₂Glu) and poly(L-EG₃Glu) (Solid line: heating; dashed line: cooling).⁷²

1.5 pH responsive polypeptides

Compared to the normal physiological pH of 7.4 in the human body, extracellular pH in tumoral tissues can be as acidic as 5.7 (though on average it is 6.8-7.0).⁷⁴ Even the pH of the extracellular environment (pH 7.4) is different from the one in intracellular compartments such as the endosomes and lysosomes (pH 4.5-6.5).⁷⁵ The synthesis of pH responsive polypeptides for drug delivery systems, which can be exploited to trigger the release of a drug from a carrier system (i.e. micelles, vesicles) in a pH-responsive fashion, has been a focus recent decades.⁷⁶ Upon a variation in pH of the surrounding environment to promote the protonation and deprotonation of the polypeptides containing an amine or carboxylic acid in the side chains, these polypeptides might undergo a reversible transitions in conformation and self-assembly behaviour, and further affect the solubility and aggregation. Polyelectrolytes such as poly(glutamic acid)⁷⁷ and poly(lysine)⁷⁸ have been considerably employed as the building blocks for the preparation of pH-sensitive synthetic polypeptides due to pH-driven solubility in response to pH around their pK_a. Moreover, by introducing hydrophilic thermosensitive building blocks including poly(N-isopropylacrylamide)⁷⁹ and poly(propylene oxide)⁸⁰ as

macroinitiators in NCA polymerisations, thermo and pH dual responsive micelles bearing polyelectrolyte have been developed. Typically, upon varying pH and temperature, the micelles were able to undergo subsequent switching of corona and core to form the reversed structures.⁸¹ The preparation of vesicles from pH responsive amphiphilic block polypeptides has been significantly highlighted.⁸² In 2005, Lecommandoux and coworkers utilized the self-assembly of poly(L-glutamic acid)₁₅-*b*-poly(L-lysine)₁₅ for the formation of pH-sensitive vesicles (Figure 1.5).⁸³ The polypeptide is dispersed as soluble chains when both building blocks are charged at near neutral pH ($5 < \text{pH} < 9$). At $\text{pH} < 4$, the poly(L-lysine) segment is still in a coil confirmation while the poly(L-glutamic acid) block is neutralized and prone to adopt α -helical conformation, which induced vesicle formation with insoluble poly(L-glutamic acid) as the membrane layer and poly(L-lysine) block as the corona. At $\text{pH} > 10$, poly(L-glutamic acid) is in a coil confirmation and poly(L-lysine) becomes α -helical and insoluble, forming vesicles with poly(L-glutamic acid) as corona and poly(L-lysine) as membrane.

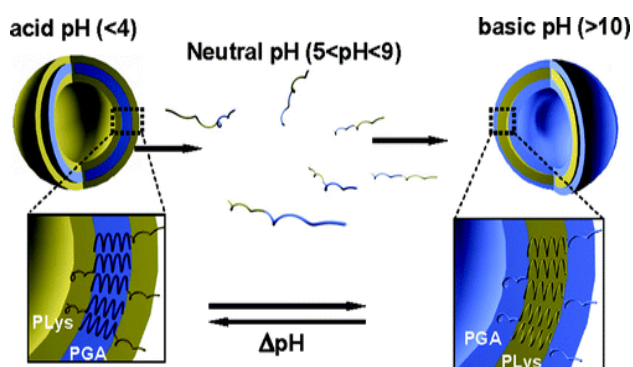
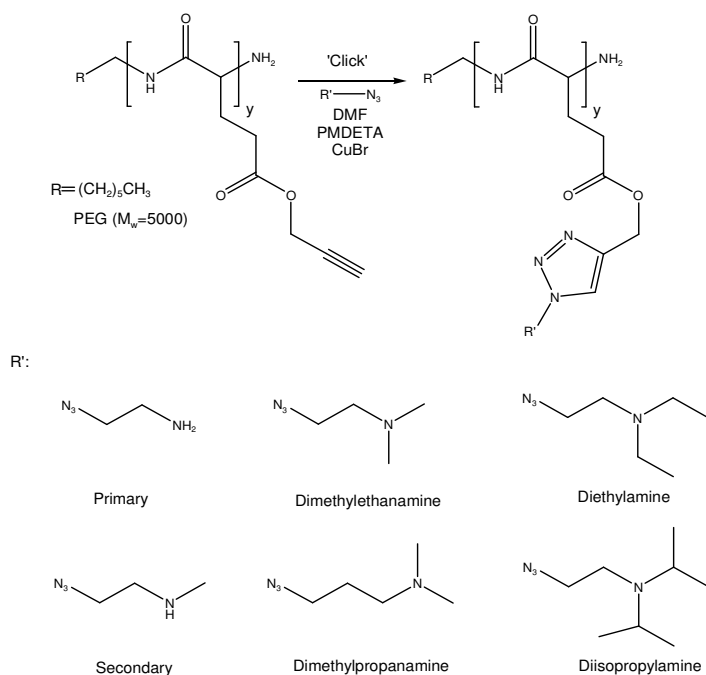


Figure 1.5: Schematic representation of the self-assembly into vesicles of the diblock copolymer poly(L-glutamic acid)₁₅-*b*-poly(L-lysine)₁₅ in different pH solutions.⁸³

Deming's group developed a pH-responsive vesicle by using poly(N ϵ -2-[2-(2-methoxyethoxy) ethoxy] acetyl-L-lysine)₁₆₀-*b*-poly(L-leucine_{0.3}-*co*-L-lysine_{0.7})₄₀ (K^P₁₆₀(L_{0.3}/K_{0.7})₄₀).⁸⁴ The formation of pH responsive vesicles with a hydrophobic P(L_{0.3}/K_{0.7})₄₀ layer and hydrophilic K^P₁₆₀ inner and outer shells was demonstrated in the presence of Fura-2 dye at pH 10.6. As the pH was reduced by the addition of

acid, the vesicle membranes were disrupted rapidly, resulting in the release of the encapsulated Fura-2 dye. pH-responsive vesicles can also be prepared from a variety of block copolypeptides including poly(L-lysine)-*b*-poly(γ -benzyl-L-glutamate)-*b*-poly(L-lysine),⁸⁵ poly(L-lysine)-*b*-poly(L-phenylalanine)⁸⁶, poly(L-lysine)-*b*-poly(L-glycine)⁸⁷ and poly(L-glutamic acid)-*b*-poly(L-phenylalanine)⁸⁸. The concept of pH responsive poly(glutamic acid) has also been employed for pH responsive polypeptide core-shell nanoparticles.⁸⁹ To improve the efficiency in targeting various solid tumors with a lower extracellular pH than normal tissues⁹⁰, poly(histidine) (polyHis) has been explored by Bae and coworkers for the design of smart pH-sensitive tumor-targeted nanocarriers (i.e. micelles, nanogels). The imidazole ring of poly(histidine) with a pKa of ~6.0 has lone pairs of electrons on the unsaturated nitrogen that endow pH dependent amphoteric properties.⁹¹ For example, when the virus-like infectious nanogel consisting of a hydrophobic core [poly(histidine-*co*-phenylalanine)] and two layers of hydrophilic shells [PEG and bovine serum albumin (BSA)] were exposed to early endosomal pH of 6.4, attributed to the protonation of polyHis, the nanogel abruptly swelled to release a significant amount of incorporated DOX to kill the tumor cells in a pH-dependent manner.⁹²

Very recently, a post-modification approach has been used for the synthesis of novel pH responsive polypeptides. As illustrated in Scheme 1.6, Hammond and co-workers⁹³ developed a library of pH-responsive polypeptides via the click reaction between poly(γ -propargyl-L-glutamate) and amino azides including primary amine, secondary amine, dimethylethanamine, dimethylpropanamine, diethylamine, and diisopropylamine. It was found that all of these amine-functionalized polypeptides had strong buffering capacity in the pH range of 5.0-7.35, which is identical to the pH range of typical extracellular tissue to late endosomal pH. The potential use of these materials for systemic drug and gene delivery was demonstrated by reversible micellisation with block copolymers of the polypeptides and nucleic acid encapsulation in different pH mediums.



Scheme 1.6: Functionalization of poly(γ -propargyl-L-glutamate) by the alkyne-azide cycloaddition click reaction and the pH responsive side groups.⁹³

A dual responsiveness of polypeptides with the temperature and pH dependent solubility, was also demonstrated through the utility of poly(γ -propargyl-L-glutamate) grafted with a combination of short oligo(ethylene glycol) side chains that yield a thermoresponsive highly tuneable polypeptide and tertiary amine groups that confer pH sensitivity in a biologically relevant range.⁹⁴

Kataoka et al synthesized poly(aspartic acid)-based pH responsive polypeptide by the aminolysis reaction of poly(β -benzyl-L-aspartate) with ethylenediamine (EDA), diethylenetriamine (DET), triethylenetetramine (TET), or tetraethylenepentamine (TEP).⁹⁵ A distinctive odd-even effect was observed in the buffering capacity of the polypeptides between pH 7.4 and 5.5 as well as subsequent gene transfection profiles. Demonstrated by *in vivo* investigation, poly(γ -benzyl-L-glutamate) with pH-labile hydrazone linkage⁹⁶, and poly(β -benzyl-L-aspartate) incorporated with N', N'-diisopropylaminoethyl group into the side chain were also reported for the preparation of pH-controlled cancer-targeted drug delivery.⁹⁷

1.6 Photo responsive polypeptides

Triggered by an external light stimulus at an appropriate wavelength, photochromic compounds are capable of conformational changes such as reversible isomerization or dimerization or even a phase transition.⁹⁸ The incorporation of photochromic molecules into polypeptides towards novel photoactive materials was achieved using different synthetic approaches including (1) using photoresponsive species as the initiator of NCA polymerisation, (2) synthesizing new NCA monomers bearing light-responsive groups in the side chain, or (3) introducing photochromic moieties into the side chain of polypeptide by post-modification. Common photoresponsive species that have been incorporated into synthetic polypeptide include azobenzenes, spiropyrans, coumarin and 2-nitrobenzyl.^{99, 100} Using bifunctional photochromic amine initiators, di[(mercaptoethylamine)-methylpropanamide]azobenzene (DMMPAB) and diaminoazobenzene (DAAB), Gupta and Williams investigated the effect of the photochromic hinge on the dielectric and photoisomerization behavior of poly(γ -benzyl-L-glutamate).¹⁰¹ Structural characterization revealed that the basicity of the initiator played an important role in determining the hinged structure of poly(γ -benzyl-L-glutamate) while the photoisomerization of the hinged polypeptides by DMMPAB and DAAB showed a negligible influence on the dielectric behavior. Minoura et al¹⁰² synthesized photoresponsive poly(γ -methyl-L-glutamate) using the corresponding NCA and amine-bifunctionalised azobenzene as the initiator. After the subsequent selective deprotection by the monolayer reaction method, the amphiphilic poly[(γ -methyl-L-glutamate)-*co*-(L-glutamic acid)] was able to self-assemble into micelles. Upon UV radiation, the photoinduced isomerization of azobenzene groups in the center resulted in changes in the assembly structures of helical polypeptide rods such as the disaggregation of the micelles or the destabilisation of the transmembrane bundle. Employing poly(γ -benzyl-L-glutamate) as a functional linker and chromophores coumarin 1 and coumarin 343 as a donor and an acceptor at the chain ends, respectively, an effective photo-induced energy transfer system was built. Araki and coworkers demonstrated that this polymer could be switched on and off by a helix-coil secondary transition of the oligopeptide linker.¹⁰³ The photochromic behaviour of different photochromic

polypeptides with incorporated azobenzene and spiropyran groups in the side chains of various polypeptides such as poly(L-phenylalanine)¹⁰⁴, poly(L-aspartate)¹⁰⁵, poly(L-glutamate)¹⁰⁶, poly(L-lysine)¹⁰⁷, poly(L-ornithine)¹⁰⁸, and other poly(L-lysine) analogues¹⁰⁹ have been well described in the literatures. When exposed to light at the given wavelength, those photochromic polypeptides underwent the conformational and structural changes accompanied by variations of the physical and chemical properties such as the transitions between random coil and α -helix, photo-triggered aggregation/disaggregation processes, reversible changes of viscosity and solubility.¹¹⁰ Recently, Mezzenga and coworkers designed amphiphilic polypeptide block copolymers bearing spiropyran (SP) in the side chain of poly(L-glutamic acid). The SP-decorated amphiphilic polypeptides were able to go through a reversible aggregation-dissolution-aggregation process in water in response to UV exposure, which might potentially be applied for photo-triggered drug control-release process or light-controlled biomedical applications (Figure 1.6).¹¹¹

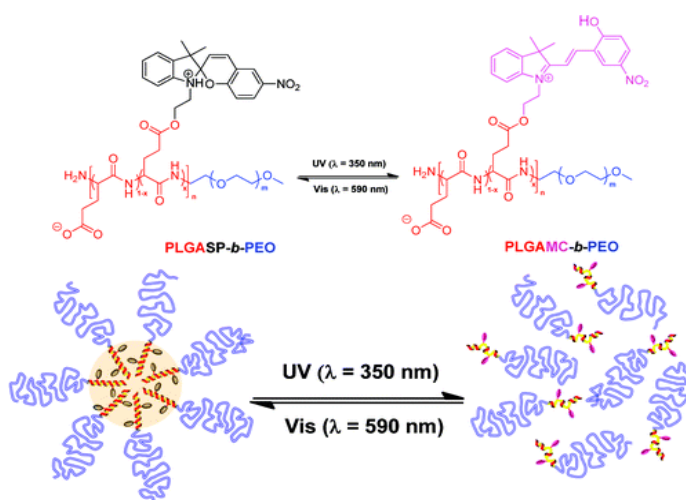


Figure 1.6: Schematic illustration of photoresponsive micellisation/dissolution process for spiropyran-decorated poly(glutamic acid)-*b*-poly(ethylene glycol) (PLGASP-*b*-PEO) block copolymer.¹¹¹

Owing to cycloaddition reactions between coumarin moieties in the side chains upon irradiation, a series of novel photoresponsive cross-linked gels prepared by

coumarin-containing polypeptides were reported by Yamamoto et al.¹¹² Different from Yamamoto's post-modification strategy where the coumaryloxyacetyl group was coupled to the side chains of the polypeptides for photodimerization, γ -cinnamyl-L-glutamate N-carboxyanhydride was recently employed for NCA polymerisation. An amphiphilic block copolymer comprising a hydrophobic poly(γ -cinnamyl-L-glutamate) core was self-assembled into micelles in aqueous solution.¹¹³ The cross-linked micelles formed by UV-irradiation at 254 nm via photodimerisation of the cinnamyl pendant groups showed a slow drug release in comparison with the non-cross-linked micelles in Paclitaxel-loading and release experiment.¹¹⁴ Most recently, photocleavable moieties such as 6-bromo-7-hydroxycoumarin-4-ylmethyl¹¹⁵ and 2-nitrobenzyl¹¹⁶ groups (Figure 1.7) were also introduced for the preparation of light sensitive polypeptides to trigger drug-release from the self-assembly of amphiphilic polypeptides (i.e. micelles) upon light irradiation as the removal of the photocleavable groups can destabilize the self-assembly of amphiphilic polypeptides in aqueous solution.

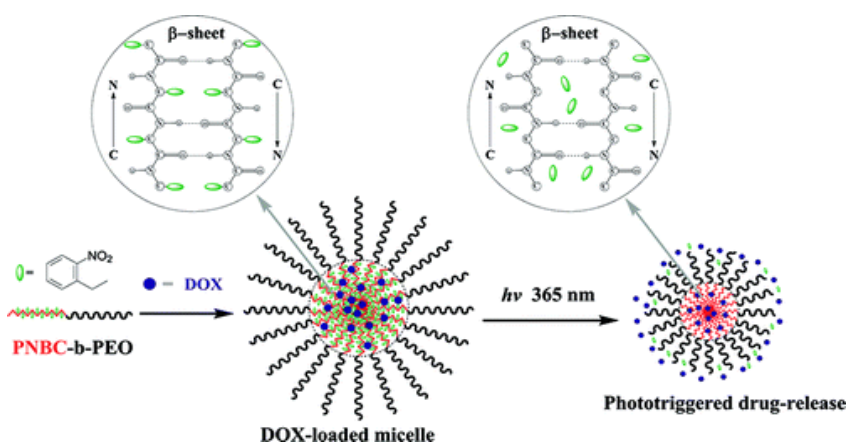


Figure 1.7: Photoresponsive self-assembly and phototriggered drug-release of amphiphilic poly(S-(o-nitrobenzyl)-L-cysteine)-*b*-poly(ethylene glycol) (PNBC-*b*-PEO) block copolymers in aqueous solution.¹¹⁶

1.7 Redox responsive polypeptides

In recent years much interest has been focused on the design and synthesis of redox (reduction-oxidation) responsive polypeptides, which usually possess disulfide linkages in the main chain, at the side chain, or in the cross-linker.¹¹⁷ The disulfide bonds can be readily and rapidly cleaved under a reductive environment such as the presence of the most abundant intracellular reducing molecule Glutathione (GSH, γ -glutamyl-cysteinyl-glycine).¹¹⁸ The high stability in extracellular physiological conditions and their selective disulfide cleavage makes these types of redox responsive polypeptides promising candidates for the development of sophisticated delivery systems including DNA, siRNA, antisense oligonucleotide (asODN), proteins, anti-cancer drugs.¹¹⁹ Using PEG bearing disulfide linkage as a macroinitiator of NCA polymerisation, the novel redox-sensitive peptides PEG-SS-poly[[N-(2-aminoethyl)-2-aminoethyl]- α,β -aspartamide] and PEG-SS-poly(α,β -aspartic acid) were first prepared as PEG-detachable system by Kataoka and coworkers.¹²⁰ These materials not only showed substantially higher transfection efficiency against cultured cells but it was also demonstrated that the reduction of disulfide bonds could be used to induce morphological transitions of the self-assembly of the block copolymers in solution.¹²¹ As revealed in Figure 1.8, polymeric micelles with polyions as the core and PEG linked by disulfide bonds (SS) as the corona can assemble in a vesicular structure after the PEG segments were detached from the micelles in the presence of dithiothreitol (DTT). The innovative "self-templating" approach to the formation of vesicles has many potential applications in drug delivery and gene therapy.



Figure 1.8: Schematic illustration of the preparation of hollow nanocapsules by self-templating strategy. Upon addition of reducing agent DTT into hetero-PEG-detachable PICmicelle A solution, a morphology transition occurred.¹²¹

Recently, PEG-SS-poly(ϵ -benzyloxycarbonyl-L-lysine)¹²², PEG-SS-poly(γ -benzyl-L-glutamate)¹²³, PEG-SS-poly(phenylalanine)¹²⁴ and PEG-SS-poly(rac-leucine)¹²⁵ were synthesized as redox-sensitive nanocarriers (micelles) for drug delivery, and upon reduction by GSH or DTT, the cleavage of the disulfide-linked PEG triggered micellar rearrangement associated with the rapid release of the encapsulated doxorubicin (DOX). Rather than utilizing 3,3'-dithiobis (sulfosuccinimidylpropionate) (DTSSP) as disulfide-containing cross-linkers for the preparation of redox triggered polypeptide-based micelles consisting of poly(ethylene glycol)-*b*-poly(L-lysine)-*b*-poly(L-phenylalanine),¹²⁶ Kataoka et al also employed thiolated PEG-poly(L-lysine) to design a series of polyion complex (PIC) micelles with a reversible disulfide cross-linked core as vehicles for the targeted-delivery of DNA and siRNA.¹²⁷ Remarkably, different thiolation reagents resulted in different cationic charge densities of PEG-poly(L-lysine) and the different linkages, which significantly affected the sensitivity of polyion complex to a reductive environment, micelle formation behaviour and stability, *in vitro* and *in vivo* performance.¹²⁸ Owing to self-crosslinking by the oxidation of thiol groups in the air, recently NCAs of cysteine derivatives have been used for the synthesis of

redox-responsive block polypeptides.¹²⁹ Typically, those polypeptide-based block copolymers can self-assemble into reversible shell-crosslinked micelles in aqueous solutions by control over the addition of reducing agent, which can greatly prevent the loss of the loaded drug and further trigger the drug release under a reductive environment.¹³⁰ Very recently, a novel difunctional NCA monomer of L-cystine NCA bearing two NCA rings and a disulfide bond was reported by Qiao and coworkers to prepare core cross-linked star (CCS) polypeptides composed exclusively of poly(L-lysine) or poly(L-glutamic acid) as the arm and poly(L-cystine) as the core in one pot (Figure 1.9).¹³¹ The star polypeptides, with a variety of functionalities spanning from the core, the arms and the periphery, were easily achieved via the combination of this facile "arm-first approach" and different chemistries such as click chemistry. Importantly, the disulfide bonds in the core of the CCS polypeptides can be readily cleaved in the presence of excessive DTT. Reduction-responsive PEGylated polypeptide nanogel with cross-linked disulfide core were also prepared via one-step ring opening polymerisation of L-cystine NCA with other hydrophobic amino acid NCAs, which showed great potential to control the release of the drug from the delivery system in response to the reducing environment.¹³²

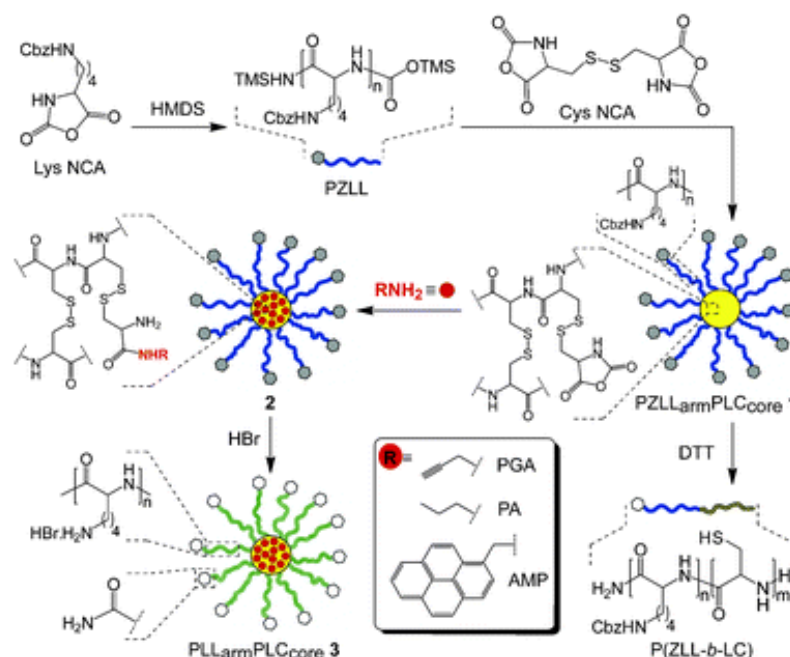


Figure 1.9: Synthesis of amino acid-based core crosslinked star (CCS) polymers having hierarchical functionalities via a one-pot arm-first strategy.¹³¹

1.8 Miscellaneous responsive polypeptides

Metal ions have great potential as a chemical trigger in drug delivery systems as metal ions can be used to induce a conformational transition from an unfolded to a folded state via the binding interaction with metal-sensitive moieties in the polypeptide, for example, the imidazole ring of histidine.¹³³ In 1993, metal responsive poly(γ -benzyl-L-glutamate) having a benzo-15-crown-5 at the end of the polypeptide main chain was first prepared via NCA polymerisation using aminobenzo-15-crown-5 as the initiator, and the polypeptide with a terminal crown ether was able to respond to the alkali metal ions (ie K^+) to form sandwich type complex (helix head-to-head association) in 1,2-dichloroethane.¹³⁴

Due to potential applications in separation and purification of biochemical products, magnetic resonance imaging contrast agents, targeted drug delivery labeling, enzyme immobilization and hyperthermia treatment cancers, magnetic responsive

polypeptide-based hybrid materials have been developed recently.¹³⁵ Peptide brush-magnetic microspheres were obtained through surface initiated polymerisation of alanine NCA from the amine functionalized Fe_3O_4 .¹³⁶ Revealed by the saturation magnetization experiment and the drug loading/release test, the microspheres have a strong magnetic core with a hydrophobic poly-L-alanine chain exterior, and exhibit strong hydrophobic interactions with hydrophobic molecules. Soon after, well-defined magnetic Fe_3O_4 -silica-poly(γ -benzyl-L-glutamate) hybrid microspheres with a diameter of 340 nm were also prepared via NCA polymerisation.¹³⁷ The magnetic polypeptide microspheres could be separated quickly by using an external magnetic field (Figure 1.10), showing a high saturation magnetization of 34.1 emu.g^{-1} and the expected rapid magnetic responsivity.

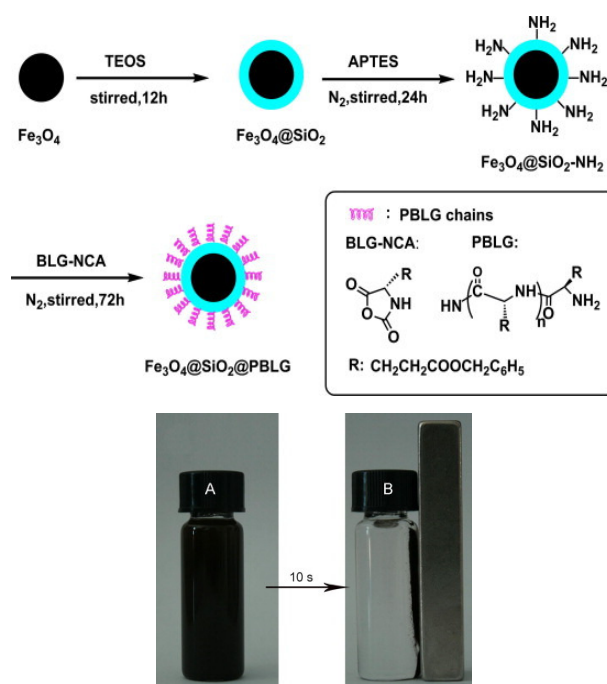


Figure 1.10: Schematic illustration of the synthesis of $\text{Fe}_3\text{O}_4@SiO_2@PBLG$ composite microspheres, and separability of $\text{Fe}_3\text{O}_4@SiO_2@PBLG$ by placing an external magnetic field.¹³⁷

Hybrid polypeptide grafted magnetic nanoparticles can be also obtained via ring-opening polymerisation of γ -benzyl-L-glutamate NCA initiated from a natural adhesive (dopamine) strongly attached to the magnetite surface.¹³⁸ Very recently,

using NCA ring-opening polymerisation to graft an alkyne-functionalized peptide from the particle surface followed by glycosylation through click chemistry, novel glycopeptide-grafted superparamagnetic Fe_3O_4 nanoparticles have been synthesized (Figure 1.11).¹³⁹ The 10 nm size particles have a high sugar density, optimal dispersion and T_1 -weighted MRI properties. Moreover, Bio-responsiveness was demonstrated by lectin binding which classifies these materials as possessing dual responsiveness.

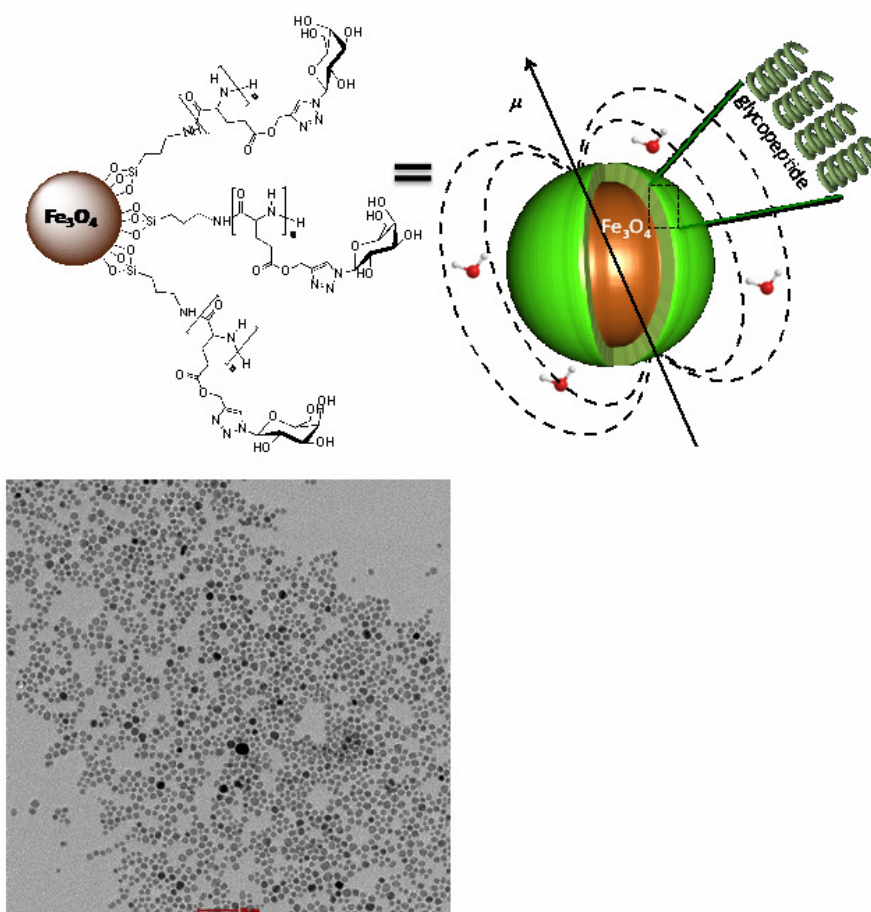


Figure 1.11: Structure of glycopeptide-grafted magnetic nanoparticles (ca. 10 nm) and transmission electron micrograph of the nanoparticles.¹³⁹

1.9 Conclusions

Many polymerisation techniques have experienced a boost after controlled or living techniques have been discovered. Probably the most prominent example is the discovery of controlled radical polymerisation that now allows researchers to combine vinyl monomers in unprecedented compositions and polymer architectures. While fundamentally different in the nature of the monomers, NCA polymerisation follows a similar development. It was the increased understanding of the polymerisation fundamentals and eventually the development of controlled NCA ring-opening polymerisation that opened up an exciting platform for the design and synthesis of new functional biomaterials. Polypeptides with controllable molecular weight, well-defined structure, end-group fidelity and narrow molecular weight distribution can now be obtained. Combined with newly developed selective and highly efficient conjugation chemistries the possibility of manipulating the polypeptide structures and consequently their properties has significantly increased. As summarized in this review paper, researchers have taken advantage of these opportunities and developed a range of stimuli-responsive polypeptides capable of responding to external triggers including biomolecules, pH, temperature, and light in a "smart" manner. What can be observed is that these materials get more sophisticated in terms of their polymer structures but also in their response behaviour, which certainly will be necessary to take the step from academic to applicable materials. Future materials will often be required to fulfil several functions, for example to carry a drug and respond to stimuli or to combine a response with a diagnostic function. It is thus inspiring to already see a number of polypeptide materials with dual responsiveness as highlighted in this review article. Overall, stimuli-responsive polypeptides have the potential to significantly facilitate the development of the next generation biomaterials, particularly new biomedical and pharmaceutical materials.

1.10 Aim and outline of the thesis

The aim of this thesis was the development of novel synthetic stimuli-responsive polypeptides, which can selectively bind to biomolecules and/or respond to environmental changes for applications in drug delivery and tissue engineering. The synthetic approach was the combination of amino-acid NCA ring-opening polymerisation and orthogonal conjugation chemistries. While being a “chemistry project”, translational biomedical data were sought thereafter to advance the chain of knowledge from synthesis to application.

In **Chapter 1**, recent developments of NCA polymerisation techniques, as well as synthetic strategies and applications of stimuli-responsive homo- and block polypeptides via NCA polymerisation were reviewed.

The design and preparation of novel biologically responsive glycopolypeptides was described in **Chapter 2** and **Chapter 3**. The synthesis of galactosylated poly(DL-propargylglycine) by the combination of NCA polymerisation and Huisgen [3+2] cycloaddition click reaction was focused in **Chapter 2**, and the selective bioactivity of the glycopeptide was demonstrated by lectin recognition experiment as well. Inspired by the developed chemistry from **Chapter 2**, a versatile route to bioactive polymersomes fully based on glycopeptides was discussed in **Chapter 3**.

Chapter 4 and **Chapter 5** presented two different stimuli-responsive tyrosine-based polypeptide hydrogels. In **Chapter 4**, a new PEGylated tyrosine-based thermoresponsive polypeptide poly(ethylene glycol-*b*-L-tyrosine) obtained by facile NCA polymerisation was developed. The thermo-hydrogelation mechanism, as well as the preliminary biological application of the hydrogel was also explored. **Chapter 5** described a novel salt-triggered hydrogel material from amphiphilic poly(L-glutamate-*b*-L-tyrosine).

Chapter 6 highlighted the key results, conclusions and outlook from the work presented in the thesis.

1.11 References

- ¹ Deming, T. J. *Prog. Polym. Sci.* **2007**, 32, 858.
- ² Jones, R. *Nat. Nanotechnol.* **2008**, 3, 699.
- ³ Merrifield, R. B. *J. Am. Chem. Soc.* **1963**, 14, 2149.
- ⁴ Cavalli, S.; Alabericio, F.; Kros, A. *Chem. Soc. Rev.* **2010**, 39, 241.
- ⁵ Kricheldorf, H. R. Polypeptides. Models of biopolymers by ring opening polymerisation. **1990**, CRC, Boca Raton, 1.
- ⁶ Kricheldorf, H. R. α -Amino acid-N-carboxyanhydrides and related materials. **1987**, Springer, New York.
- ⁷ Deming, T. J. *Adv. Mater.* **1997**, 9, 299.
- ⁸ Deming, T. J. *J. Polym. Sci., Part A: Polym. Chem.*, **2000**, 38, 3011.
- ⁹ Kricheldorf, H. R. *Angew. Chem. Int. Ed.* **2006**, 45, 5752.
- ¹⁰ Deming, T. J. *Adv. Polym. Sci.* **2006**, 202, 1.
- ¹¹ Klok, H.-A. *Macromolecules* **2009**, 42, 7990.
- ¹² Habraken, G. J. M.; Heise, A.; Thornton, P. D. *Macromol. Rapid Commun.* **2012**, 33, 272.
- ¹³ Stuart, M. A.; Huck, W. T.; Genzer, J.; Müller, M.; Ober, C.; Stamm, M.; Sukhorukov, G. B.; Szleifer, I.; Tsukruk, V. V.; Urban, M.; Winnik, F.; Zauscher, S.; Luzinov, I.; Minko, S. *Nat Mater.* **2010**, 9, 101.
- ¹⁴ (a) Leuchs, H. *Ber.* **1906**, 39, 857. (b) Leuchs, H.; Manasse, W. *Ber.* **1907**, 40, 3235. (c) Leuchs, H.; Geiger, W. *Ber.* **1908**, 41, 1721.
- ¹⁵ Kricheldorf, H. *Angew. Chem. Int. Ed.* **2006**, 45, 5752.
- ¹⁶ (a) Curtius, T.; Sieber, W. *Ber. Dtsch. Chem. Ges. B.* **1921**, 54, 1430. (b) Curtius, T.; Sieber, W. *Ber. Dtsch. Chem. Ges. B.* **1922**, 55, 1543. (c) Curtius, T.; Hochschwender, K.; Meier, H.; Lehmann, W.; Benckiger, A.; Schenk, M.; Nirbatz, W.; Gaier, J.; Muhlhauser, W. *J. Prakt. Chem.* **1930**, 125, 211.
- ¹⁷ (a) Wessely, F. *Z. Physiol. Chem.* **1925**, 146, 72. (b) Wessely, F.; Sigmund, F. *Z. Physiol. Chem.* **1926**, 159, 102. (c) Sigmund, F.; Wessely, F. *Z. Physiol. Chem.* **1926**, 157, 91. (d) Wessely, F.; John, M.; *Z. Physiol. Chem.* **1927**, 170, 38. (e) Wessely, F.; Mayer, J. *Monatsh. Chem.* **1928**, 50, 439. (f) Wessely, F.; Riedel, K.;

Tuppy, H.; *Monatsh. Chem.* **1950**, *81*, 861. (g) Wessely, F.; Swoboda, W.; *Monatsh. Chem.* **1951**, *82*, 621. (h) Wessely, F.; Schlogl, K.; Korgers, G. *Monatsh. Chem.* **1952**, *83*, 845.

¹⁸ (a) Farthing, A. C.; Reynolds, R. J. W. *Nature* **1950**, *165*, 647. (b) Coleman, D.; Farthing, A. C. *J. Chem. Soc.* **1951**, 3218.

¹⁹ (a) Daly, W.H.; Poche, D. S. *Tetrahedron Lett.* **1988**, *29*, 5859. (b) Katakai, R.; Iizuka, Y. *J. Org. Chem.* **1985**, *50*, 715. (c) Nagai, A.; Sato, D.; Ishikawa, J.; Ochiai, B.; Kudo, H.; Endo, T. *Macromolecules* **2004**, *37*, 2332.

²⁰ (a) Iwakura, Y.; Uno, K.; Kang, S. *J. Org. Chem.* **1965**, *30*, 1158. (b) Kramer J. R.; Deming T. J. *Biomacromolecules* **2010**, *11*, 3668.

²¹ Szwarc, M. *Adv. Polymer Sci.* **1965**, *4*, 1.

²² Hadjichristidis, N.; Iatrou, H.; Pitsikalis, M.; Sakellariou, G. *Chem. Rev.* **2009**, *109*, 5528.

²³ Habraken, G. J. M.; Peeters, M.; Dietz, C. H. J. T.; Koning, C. E.; Heise, A. *Polym. Chem.* **2010**, *1*, 514.

²⁴ (a) Kricheldorf, H. R.; Lossow, C. von; Schwarz, G. *Macromol. Chem. Phys.* **2005**, *206*, 282. (b) Kricheldorf, H. R.; Lossow, C. von; Schwarz, G. *Macromolecules* **2005**, *38*, 5513.

²⁵ (a) Barz, M.; Luxenhofer, R.; Zentel R.; Vicenta, M. J. *Polym. Chem.* **2011**, *2*, 1900. (b) Dimitrov, I.; Kukula, H.; Cölfen, H.; Schlaad, H. *Macromol. Symp.* **2004**, *215*, 383.

²⁶ (a) Deming, T. J. *Nature* **1997**, *390*, 386. (b) Pattabiraman, V.; Bode, J. W. *Nature* **2011**, *480*, 471.

²⁷ (a) Deming, T. J. *Nature* **1997**, *390*, 386. (b) Deming, T. J. *J. Am. Chem. Soc.* **1998**, *120*, 4240. (c) Deming, T. J. *Macromolecules* **1999**, *32*, 4500. (d) Deming, T. J.; Curtin, S. *J. Am. Chem. Soc.* **2000**, *122*, 5710.

²⁸ Steig, S.; Cornelius, F.; Witte, P.; Staal, B. B. P.; Koning, C. E.; Heise, A.; Menzel, H. *Chem. Commun.* **2005**, 5420.

²⁹ Aliferis, T.; Iatrou, H.; Hadjichristidis, N. *Biomacromolecules* **2004**, *5*, 1653.

³⁰ Pickel, D. L.; Politakos, N.; Avgeropoulos, A.; Messman, J. M. *Macromolecules* **2009**, *42*, 7781.

- ³¹ Vayaboury, W.; Giani, O.; Cottet, H.; Deratani, A.; Schue, F. *Macromol. Rapid Commun.* **2004**, 25, 1221.
- ³² Vayaboury, W.; Giani, O.; Cottet, H.; Bonaric, S.; Schue, F. *Macromol. Chem. Phys.* **2008**, 209, 1628.
- ³³ (a) Habraken, G. J. M.; Wilsens, K. H. R. M.; Koning, C. E.; Heise, A. *Polym. Chem.* **2011**, 2, 1322. (b) Habraken, G. J. M.; Peeters, M.; Dietz, C. H. J. T.; Koning, C. E.; Heise, A. *Polym. Chem.* **2010**, 1, 514.
- ³⁴ Lu, H.; Cheng, J. *J. Am. Chem. Soc.* **2007**, 129, 14114.
- ³⁵ (a) Lu, H.; Cheng, J. *J. Am. Chem. Soc.* **2008**, 130, 12562. (b) Lu, H.; Wang, J.; Lin, Y.; Cheng, J. *J. Am. Chem. Soc.* **2009**, 131, 13582.
- ³⁶ Peng, H.; Ling, J.; Shen, Z. Q. *J. Polym. Sci. Part A: Polym. Chem.* **2012**, 50, 1076.
- ³⁷ Peng, H.; Ling, J.; Zhu, Y. H.; You, L. X.; Shen, Z. Q. *J. Polym. Sci. Part A: Polym. Chem.* **2012**, 50, 3016.
- ³⁸ (a) Ratner, B. D.; Bryant, S. J.; *Annu. Rev. Biomed. Eng.* **2004**, 6, 41. (b) Roy, D.; Cambre, J. N.; Sumerlin, B. S. *Progress in Polymer Science* **2010**, 35, 278. (c) Randolph, L.M.; Chien, M. P.; Gianneschi, N. C. *Chem. Sci.* **2012**, 3, 1363.
- ³⁹ (a) Habraken, G. J. M.; Peeters, M.; Thornton, P. D.; Koning, C. E.; Heise, A. *Biomacromolecules* **2011**, 12, 3761. (b) Thornton, P. D.; Billah, S. M. R.; Cameron, N. R. *Macromol. Rapid Commun.* **2013**, 34, 257. (c) Byrne, M.; Thornton, P. D.; Cryan, S.-A.; Heise, A. *Polym. Chem.* **2012**, 3, 2825.
- ⁴⁰ (a) Gamblin, D. P.; Scanlan, E. M.; Davis, B. G. *Chem. Rev.* **2009**, 1, 131. (b) Ambrosi, M.; Cameron, N. R.; Davis, B. G. *Org. Biomol. Chem.* **2005**, 3, 1593.
- ⁴¹ (a) Rude, E.; Westphal, O.; Hurwitz, E.; Sela, M. *Immunochemistry* **1966**, 3, 137. (b) Rude, E.; Meyer-Delius, M. *Carbohydr. Res.* **1968**, 8, 219.
- ⁴² (a) Aoi, K.; Tsutsumiuchi, K.; Okada, M. *Macromolecules* **1994**, 27, 875. (b) Tsutsumiuchi, K.; Aoi, K.; Okada, M. *Macromol. Rapid Commun.* **1995**, 16, 749. (c) Aoi, K.; Tsutsumiuchi, K.; Aoki, E.; Okada, M. *Macromolecules* **1996**, 29, 4456. (d) Tsutsumiuchi, K.; Aoi, K.; Okada, M. *Macromolecules* **1997**, 30, 4013.
- ⁴³ (a) Pati, D.; Shaikh, A. Y.; Hotha, S.; Sen, Gupta S. *Polym. Chem.* **2011**, 2, 805. (b) Pati, D.; Shaikh, A.Y.; Das, S.; Nareddy, P. K.; Swamy, M. J.; Hotha, S.; Sen Gupta S. *Biomacromolecules* **2012**, 13, 1287.

- ⁴⁴ Stohr, T.; Blaudszun, A.; Steinfeld, U.; Wenz, G. *Polym. Chem.* **2011**, 2, 2239.
- ⁴⁵ Kramer, J. R.; Deming, T. J. *J. Am. Chem. Soc.* **2010**, 132, 15068.
- ⁴⁶ Kramer, J. R.; Deming, T. J. *J. Am. Chem. Soc.* **2012**, 134, 4112.
- ⁴⁷ Wang, Y.; Kiick, K. L. *J. Am. Chem. Soc.* **2005**, 127, 16392.
- ⁴⁸ (a) Tian, Z.; Wang, M.; Zhang, A.; Feng, Z. *Front. Mater. Sci. China* **2007**, 1, 162.
(b) Tian, Z.; Wang, M.; Zhang, A.; Feng, Z. *Polymer* **2008**, 49, 446.
- ⁴⁹ Xiao, C.; Zhao, C.; He, P.; Tang, Z.; Chen, X.; Jing, X. *Macromol. Rapid Commun.* **2010**, 31, 991.
- ⁵⁰ Huang, J.; Habraken, G.; Audouin, F.; Heise, A.; *Macromolecules* **2010**, 43, 6050.
- ⁵¹ (a) Tang, H.; Zhang, D. *Biomacromolecules* **2010**, 11, 1585. (b) Tang, H.; Zhang, D. *Polym. Chem.* **2011**, 2, 1542.
- ⁵² (a) Sun, J.; Schlaad, H. *Macromolecules* **2010**, 43, 4445. (b) Krannig, K.; Schlaad, H. *J. Am. Chem. Soc.* **2012**, 134, 18542.
- ⁵³ Huang, J.; Bonduelle, C.; Thévenot, J.; Lecommandoux, S.; Heise, A. *J. Am. Chem. Soc.* **2012**, 134, 119.
- ⁵⁴ Pati, D.; Kalva, N.; Das, S.; Kumaraswamy, G.; Sen Gupta, S.; Ambade, A.V. *J. Am. Chem. Soc.* **2012**, 134, 7796.
- ⁵⁵ Kramer, J. R.; Rodriguez, A. R.; Choe, U.-J.; Kamei, D. T., Deming, T. J. *Soft Matter* **2013**, 9, 3389.
- ⁵⁶ Zhao, L.; Ding, J. X.; Xiao, C. S.; He, P.; Tang, Z. H.; Pang, X.; Zhuang, X. L.; Chen, X. S. *J. Mater. Chem.* **2012**, 22, 12319.
- ⁵⁷ Ward, M. A.; Georgiou, T. K. *Polymers* **2011**, 3, 1215.
- ⁵⁸ Ratner, B. D.; Bryant, S. J.; *Annu. Rev. Biomed. Eng.* **2004**, 6, 41.
- ⁵⁹ (a) Randolph, L. M.; Chien, M. P.; Gianneschi, N. C. *Chem. Sci.* **2012**, 3, 1363. (b) Löwik, D. W. P. M.; Leunissen, E. H. P.; van den Heuvel, M.; Hansen, M. B.; van Hest, J. C. M. *Chem. Soc. Rev.* **2010**, 39, 3394.
- ⁶⁰ (a) Cho, C. S.; Cheon, J. B.; Jeong, Y. I.; Kim, I. S.; Kim, S. H.; Akaike, T. *Macromol. Rapid Commun.* **1997**, 18, 361. (b) Cheon, J. B.; Jeong, Y. I.; Cho, C. S. *Polymer* **1999**, 40, 2041. (c) He, C. L.; Zhao, C.W.; Chen, X. S.; Guo, Z. J.; Zhuang, X. L.; Jing, X. B. *Macromol Rapid Commun* **2008**, 29, 490. (d) Zhao, C. W.; Zhuang, X. L.; He, C. L.; Chen, X. S.; Jing, X. B. *Macromol Rapid Commun* **2008**, 29, 1810.

- (e) Chung, T. W.; Kim, B. J.; Park, S. Y.; Akaike, T.; Nah, J. W.; Cho, C. S.; *Macromolecules* **2000**, *33*, 8921. (f) Zhang, X.; Li, J., Li, W.; Zhang, A. *Biomacromolecules* **2007**, *8*, 3557. (g) Rao, J., Luo, Z., Ge, Z., Liu, H., Liu, S. *Biomacromolecules* **2007**, *8*, 3871. (h) Li, J.; Wang, T.; Wu, D.; Zhang, X.; Yan, J.; Du, S.; Guo, Y.; Wang, J., Zhang, A. *Biomacromolecules* **2008**, *9*, 2670.
- ⁶¹ Park, J. S.; Akiyama, Y.; Yamasaki, Y.; Kataoka, K. *Langmuir* **2007**, *23*, 138.
- ⁶² Agut, W.; Brûlet, A.; Taton, D.; Lecommandoux, S. *Langmuir* **2007**, *23*, 11526.
- ⁶³ Liu, Y.; Li, C.; Wang, H. Y.; Zhang, X. Z.; Zhuo, R. X. *Chem. Eur. J.* **2012**, *18*, 2297.
- ⁶⁴ (a) Tu, Y. L., Wang, C. C.; Chen, C. Y. *J. Polym. Sci. A Polym. Chem.* **2011**, *49*, 2866. (b) He, C.; Zhao, C.; Guo, X.; Guo, Z.; Chen, X.; Zhuang, X.; Liu, S.; Jing, X. *J. Polym. Sci. A Polym. Chem.* **2008**, *46*, 4140.
- ⁶⁵ (a) Agut, W.; Taton, D.; Lecommandoux, S. *Macromolecules* **2007**, *40*, 5653. (b) Agut, W.; Agnaou, R.; Lecommandoux, S.; Taton, D. *Macromol. Rapid Commun.* **2008**, *29*, 1147. (c) Agut, W.; Taton, D.; Brûlet, A.; Sandre, O.; Lecommandoux, S. *Soft Matter* **2011**, *7*, 9744. (d) Agut, W.; Brûlet, A.; Schatz, C.; Taton, D.; Lecommandoux S. *Langmuir* **2010**, *26*, 10546
- ⁶⁶ (a) Choi, Y. Y.; Jang, J. H.; Park, M. H.; Choi, B. G.; Chi, B.; Jeong, B. *J. Mater. Chem.* **2010**, *20*, 3416. (b) Oh, H. J.; Joo, M. K.; Sohn, Y. S.; Jeong, B. *Macromolecules* **2008**, *41*, 8204. (c) Jeong, Y. ; Joo, M. K.; Bahk, K. H.; Choi, Y. Y.; Kim, H. T.; Kim, W. K.; Lee, H. J.; Sohn, Y. S.; Jeong, B. *Journal of Controlled Release* **2009**, *137*, 25. (d) Joo, M. K.; Park M. H.; Choi, B. G.; Jeong, B. *J. Mater. Chem.* **2009**, *19*, 5891. (d) Shinde, U. P.; Joo, M. K.; Moon, H. J.; Jeong, B. *J. Mater. Chem.* **2012**, *22*, 6072.
- ⁶⁷ Park, M. H.; Joo, M. K.; Choi, B. G.; Jeong, B. *Acc. Chem. Res.* **2012**, *45*, 424.
- ⁶⁸ (a) Jeong, Y.; Joo, M. K.; Bahk, K. H.; Choi, Y. Y.; Kim, H. T.; Kim, W. K.; Lee, H. J.; Sohn, Y. S.; Jeong, B. *Journal of Controlled Release* **2009**, *137*, 25. (b) Yun, E. J.; Yon, B.; Joo, M. K.; Jeong, B. *Biomacromolecules* **2012**, *13*, 1106.
- ⁶⁹ Huang, J.; Hastings, C.; Duffy, G.; Kelly, H.; Raeburn, J.; Adams, D. J.; Heise, A.; *Biomacromolecules* **2013**, *14*, 200.

- ⁷⁰ Cheng, Y.; He, C.; Xiao, C.; Ding, J.; Zhuang, X.; Chen, X. *Polym. Chem.* **2011**, *2*, 2627.
- ⁷¹ Ding, J.; Xiao, C.; Tang, Z.; Zhuang, X.; Chen, X. *Macromol. Biosci.* **2011**, *11*, 192.
- ⁷² Chen, C.; Wang, Z.; Li, Z. *Biomacromolecules* **2011**, *12*, 2859.
- ⁷³ Liao, Y.; Dong, C. M.; *J. Polym. Sci. A Polym. Chem.* **2012**, *50*, 1834.
- ⁷⁴ (a) Lee, E. S.; Gao, Z.; Bae, Y. H.; *Journal of Controlled Release* **2008**, *132*, 164. (b) Ganta, S.; Devalapally, H.; Shahiwala, A.; Amiji, M. *Journal of Controlled Release* **2008**, *126*, 187.
- ⁷⁵ Mellman, I.; Fuchs, R.; Helenius, A. *Annu. Rev. Biochem.* **1986**, *55*, 663.
- ⁷⁶ Felber, A. E.; Dufresne, M. H.; Leroux, J. C.; *Advanced Drug Delivery Reviews* **2012**, *64*, 979.
- ⁷⁷ (a) Tian, H.; Chen, X.; Lin, H.; Deng, C.; Zhang, P.; Wei, Y.; Jing, X. *Chem. Eur. J* **2006**, *12*, 4305. (b) Huang, H. H.; Li, J. Y.; Liao, L. H.; Li, J. H.; Wu, L. X.; Dong, C. K.; Lai, P. B.; Liu, D. J. *European Polymer Journal* **2012**, *48*, 696. (c) Kim, M. S.; Dayanandb, K.; Choi, E. K.; Park, H. J.; Kim, J. S.; Lee, D. S. *Polymer* **2009**, *50*, 2252. (d) Audouin, F.; Knoop, R. J. I.; Huang, J.; Heise, A. *J. Polym. Sci. A; Polym. Chem.* **2010**, *48*, 6402. (e) Byrne, M.; Thornton, P.D.; Cryan, S.-A.; Heise, A. *Polym. Chem.* **2012**, *3*, 2825. (f) Knoop, R. J. I.; de Geus, M.; Habraken, G. J. M.; Koning, C. E.; Menzel, H.; Heise, A. *Macromolecules* **2010**, *43*, 4126. (g) Borase, T.; Iacono, M.; Ali, S. I.; Thornton, P. D.; Heise, A. *Polym. Chem.* **2012**, *3*, 1267.
- ⁷⁸ (a) Li, Y.Y.; Hua, S. H.; Xiao, W.; Wang, H. Y.; Luo, X. H.; Li, C.; Cheng, S. X.; Zhang, X. Z.; Zhuo, R. X. *J. Mater. Chem.* **2011**, *21*, 3100. (b) Yan, Y. S.; Li, J. Y.; Zheng, J. H.; Pan, Y.; Wang, J. Z.; He, X. Y.; Zhang, L. M.; Liu, D. J. *Colloids and Surfaces B: Biointerfaces* **2012**, *95*, 137. (c) Yuan, R.X.; Shuai, X. T. *J. Polym. Sci. B Polym. Phys.* **2008**, *46*, 782. (d) Wang, C.; Kang, Y. T.; Liu, K.; Li, Z. B.; Wang, Z. Q.; Zhang, X. *Polym. Chem.* **2012**, *3*, 3056.
- ⁷⁹ (a) He, C. L.; Zhao, C. W.; Chen, X. S.; Guo, Z. J.; Zhuang, X. L.; Jing, X. B.; *Macromol Rapid Commun* **2008**, *29*, 490. (b) Zhang, X.; Li, J.; Li, W.; Zhang, A. *Biomacromolecules* **2007**, *8*, 3557. (c) Rao, J.; Luo, Z.; Ge, Z.; Liu, H.; Liu, S.

- Biomacromolecules* **2007**, *8*, 3871. (d) Li, J.; Wang, T.; Wu, D.; Zhang, X.; Yan, J.; Du, S.; Guo, Y.; Wang, J.; Zhang, A. *Biomacromolecules* **2008**, *9*, 2670.
- ⁸⁰ (a) Cai, C. H.; Zhang, L. S.; Lin, J. P.; Wang, L. Q. *J. Phys. Chem. B* **2008**, *112*, 12666. (b) Ray, J. G.; Naik, S. S.; Hoff, E. A.; Johnson, A. J.; Ly, J. T.; Easterling, C. P.; Patton, D. L.; Savin, D. A. *Macromol. Rapid Commun.* **2012**, *33*, 819.
- ⁸¹ (a) Rao, J.; Luo, Z.; Ge, Z.; Liu, H.; Liu, S. *Biomacromolecules* **2007**, *8*, 3871. (b) Rao, J. Y.; Zhang, Y. F.; Zhang, J. Y.; Liu, S. Y. *Biomacromolecules* **2008**, *9*, 2586.
- ⁸² Carlsten, A.; Lecommandoux, S. *Curr. Opin. Colloid Interface Sci.* **2009**, *14*, 329.
- ⁸³ Rodríguez-Hernández, J.; Lecommandoux, S., *J. Am. Chem. Soc.* **2005**, *127*, 2026.
- ⁸⁴ Bellomo, E. G.; Wyrsta, M. D.; Pakstis, L.; Pochan, D. J.; Deming, T. J. *Nat. Mater.* **2004**, *3*, 244.
- ⁸⁵ Iatrou, H.; Frielinghaus, H.; Hanski, S.; Ferderigos, N.; Ruokolainen, J.; Ikkala, O.; Richter, D.; Mays, J.; Hadjichristidis, N. *Biomacromolecules* **2007**, *8*, 2173.
- ⁸⁶ (a) Sun, J.; Chen, X. S.; Deng, C.; Yu, H. J.; Xie, Z. G.; Jing, X. B. *Langmuir* **2007**, *23*, 8308. (b) Sun, J.; Huang, Y. B.; Shi, Q.; Chen, X. S.; Jing, X. B. *Langmuir* **2009**, *25*, 13726.
- ⁸⁷ Gaspard, J.; Silas, J. A.; Shantz, D. F.; Jan, J. *Supramol. Chem.* **2010**, *22*, 178.
- ⁸⁸ Kim, M. S.; Dayananda, K.; Choi, E. K.; Park, H. J.; Kim, J. S.; Lee, D. S. *Polymer* **2009**, *50*, 2252.
- ⁸⁹ (a) Knoop, R. J. I.; de Geus, M.; Habraken, G. J. M.; Koning, C. E.; Menzel, H.; Heise, A. *Macromolecules* **2010**, *43*, 4126. (b) Audouin, F.; Knoop, R. J. I.; Huang, J.; Heise, A. *J. Polym. Sci. A; Polym. Chem.* **2010**, *48*, 6402. (c) Borase, T.; Iacono, M.; Ali, S. I.; Thornton, P. D.; Heise, A. *Polym. Chem.* **2012**, *3*, 1267.
- ⁹⁰ Lee, E. S.; Gao, Z. G.; Bae, Y. H. *J. Controlled Release* **2008**, *132*, 164.
- ⁹¹ (a) Kim, G. M.; Bae, Y. H.; Jo, W. H. *Macromol. Biosci.* **2005**, *5*, 1118. (b) Gao, Z. G.; Tian, L.; Hu, J.; Park, I.; Bae, Y. H. *J. Controlled Release* **2011**, *152*, 84. (c) Lee, E. S.; Na, K.; Bae, Y. H. *J. Controlled Release* **2003**, *91*, 103. (d) Lee, E. S.; Shin, H. J.; Na, K.; Bae, Y. H. *J. Controlled Release* **2003**, *90*, 363. (e) Lee, E. S.; Na, K.; Bae, Y. H. *Nano Lett.* **2005**, *5*, 325. (f) Kim, D.; Lee, E. S.; Oh, K. T.; Gao, Z. G.; Bae, Y. H. *Small* **2008**, *4*, 2043. (g) Yin, H. Q.; Kang, H. C.; Huh, K. M.; Bae, Y. H. *J. Mater. Chem.* **2012**, *22*, 19168.

- ⁹² Lee, E. S.; Kim, D.; Youn, Y. S.; Oh, K. T.; Bae, Y. H. *Angew. Chem. Int. Ed.* **2008**, *47*, 2418.
- ⁹³ Engler, A. C.; Bonner, D. K.; Buss, H. G.; Cheung, E. Y.; Hammond, P. T. *Soft Matter* **2011**, *7*, 5627.
- ⁹⁴ Chopko, C. M.; Lowden, E. L.; Engler, A. C.; Griffith, L. G.; Hammond, P. T. *ACS Macro Lett.* **2012**, *1*, 727.
- ⁹⁵ Uchida, H.; Miyata, K.; Oba, M.; Ishii, T.; Suma, T.; Itaka, K.; Nishiyama, N.; Kataoka, K. *J. Am. Chem. Soc.* **2011**, *133*, 15524.
- ⁹⁶ Xiao, Y. L.; Hong, H.; Javadi, A.; Engle, J. W.; Xu, W. J.; Yang, Y. N.; Zhang, Y., Barnhart, T. E.; Cai, W. B.; Gong, S. Q. *Biomaterials* **2012**, *33*, 3071.
- ⁹⁷ Wang, W. W.; Cheng, D.; Gong, F. M.; Miao, X. M.; Shuai, X. T. *Adv. Mater.* **2012**, *24*, 115.
- ⁹⁸ (a) Lowe, A. B.; McCormick, C. L. *Stimuli Responsive Water-Soluble and Amphiphilic (Co)polymers* **2001**, *1*, 1. (b) Pieroni, O.; Fissi, A.; Angelini, N.; Lenci, F. *Acc. Chem. Res.* **2001**, *34*, 9. (c) Pieroni, O.; Fissi, A.; Ciardelli, F.; *Reactive & Functional Polymers* **1995**, *26*, 185.
- ⁹⁹ (a) Zhao, Y. *Macromolecules* **2012**, *45*, 3647. (b) Pieroni, O.; Fissi, A.; Angelini, N.; Lenci, F. *Acc. Chem. Res.* **2001**, *34*, 9.
- ¹⁰⁰ Hernández, J. R.; Klok, H.-A. *J. Polym. Sci. Part A: Polym. Chem.* **2003**, *41*, 1167.
- ¹⁰¹ Williams, A. J.; Gupta, V. K. *J. Polym. Sci. Part B: Polym. Phys.* **2001**, *39*, 2759.
- ¹⁰² Minoura, N.; Higuchi, M.; Kinoshita, T. *Mater. Sci. Eng.* **1997**, *4*, 249.
- ¹⁰³ Kishimoto, A.; Mutai, T.; Araki, K. *Chem. Commun.* **2003**, 742.
- ¹⁰⁴ Goodman, M.; Falxa, M. L. *J. Am. Chem. Soc.* **1967**, *89*, 3863.
- ¹⁰⁵ (a) Ueno, A.; Takahashi, K.; Anzai, J.; Osa, T. *Macromolecules* **1980**, *13*, 459. (b) Ueno, A.; Takahashi, K.; Anzai, J.; Osa, T. *J. Am. Chem. Soc.* **1981**, *103*, 6410. (c) Ueno, A.; Adachi, K.; Nakamura, J.; Osa, T. *J. Polym. Sci., Part A: Polym. Chem.* **1990**, *28*, 1161.
- ¹⁰⁶ (a) Pieroni, O.; Fissi, A.; Houben, J. L.; Ciardelli, F. *J. Am. Chem. Soc.* **1985**, *107*, 2990. (b) Pieroni, O.; Fabbri, D.; Fissi, A.; Ciardelli, F. *Makromol. Chem. Rapid Commun.* **1988**, *9*, 637. (c) Fissi, A.; Pieroni, O. *Macromolecules* **1989**, *22*,

1115. (d) Higuchi, M.; Takizawa, A.; Kinoshita, T.; Tsujita, Y. *Macromolecules* **1987**, *20*, 2888. (e) Sato, M.; Kinoshita, T.; Takizawa, A.; Tsujita, Y. *Macromolecules* **1988**, *21*, 1612. (f) Aoyama, M.; Youda, A.; Watanabe, J.; Inoue, S. *Macromolecules* **1990**, *23*, 1458. (g) Sisido, M.; Ishikawa, Y.; Itoh, K.; Tazuke, S. *Macromolecules* **1991**, *24*, 3993. (h) Narisawa, H.; Kishi, R.; Sisido, M. *Macromol. Chem. Phys.* **1995**, *196*, 1419. (i) Menzel, H.; Hallensleben, M. L.; Schmidt, A.; Knoll, W.; Fischer, T.; Stumpe, J. *Macromolecules* **1993**, *26*, 3644. (j) Menzel, H. *Macromol. Chem. Phys.* **1994**, *195*, 3747. (k) Menzel, H.; Weichart, B.; Schmidt, A.; Paul, S.; Knoll, W.; Stumpe, J.; Fischer, T. *Langmuir* **1994**, *10*, 1926. (l) Ciardelli, F.; Fabbri, D.; Pieroni, O.; Fissi, A. *J. Am. Chem. Soc.* **1989**, *111*, 3470. (m) Fissi, A.; Pieroni, O.; Ciardelli, F.; Fabbri, D.; Ruggeri, G.; Umezawa, K. *Biopolymers* **1993**, *33*, 1505. (n) Fissi, A.; Pieroni, O.; Angelini, N.; Lenci, F., *Macromolecules* **1999**, *32*, 7116.

¹⁰⁷ (a) Fissi, A.; Pieroni, O.; Ciardelli, F. *Biopolymers* **1987**, *26*, 1993. (b) Yamamoto, H.; Nishida, A. *Macromolecules* **1986**, *19*, 943. (c) Pieroni, O.; Fissi, A.; Vieg, A.; Fabbri, D.; Ciardelli, F. *J. Am. Chem. Soc.* **1992**, *114*, 2734. (d) Fissi, A.; Pieroni, O.; Ruggeri, G.; Ciardelli, F. *Macromolecules* **1995**, *28*, 302.

¹⁰⁸ (a) Yamamoto, H.; Nishida, A.; Takimoto, T.; Nagai, A. *J. Polym. Sci., Polym. Chem.* **1990**, *28*, 67. (b) Yamamoto, H.; Ikeda, K.; Nishida, A. *Polym. Int.* **1992**, *27*, 67.

¹⁰⁹ (a) Yamamoto, H.; Nishida, A.; Kawaura, T. *Int. J. Biol. Macromol.* **1990**, *12*, 257. (b) Yamamoto, H.; Nishida, A. *Polym. Int.* **1991**, *24*, 145. (c) Cooper, T. M.; Stone, M. O.; Natarajan, L. V.; Crane, R. L. *Photochem. Photobiol.* **1995**, *62*, 258.

¹¹⁰ (a) Pieroni, O., Fissi, A., Angelini, N., Lenci, F. *Acc. Chem. Res.* **2001**, *34*, 9. (b) Pieroni, O., Fissi, A., Ciardelli F. *Reactive & Functional Polymers* **1995**, *26*, 185.

¹¹¹ Kotharangannagari, V. K.; Sanchez-Ferrer, A.; Ruokolainen, J.; Mezzenga, R. *Macromolecules* **2011**, *44*, 4569.

¹¹² (a) Yamamoto, H.; Kitsuki, T.; Nishida, A.; Asada, K.; Ohkawa, K. *Macromolecules* **1999**, *32*, 1055. (b) Ohkawa, K.; Shoumura, K.; Yamada, M.; Nishida, A.; Shirai, H.; Yamamoto, H.; *Macromol. Biosci.* **2001**, *1*, 149. (c) Ohkawa, K.; Shoumura, K.; Shirakabe, Y.; Yamamoto, H. *J. Mater. Sci.* **2003**, *38*, 3191.

- ¹¹³ Ding, J. X.; Zhuang, X. L.; Xiao, C. S.; Cheng, Y. L.; Zhao, L.; He, C. L.; Tang, Z. H.; Chen, X. S. *J. Mater. Chem.* **2011**, *21*, 11383.
- ¹¹⁴ Yan, L.; Yang, L.; He, H.; Hu, X.; Xie, Z.; Huang, Y.; Jing, X. *Polym. Chem.* **2012**, *3*, 1300.
- ¹¹⁵ Kumar, S.; Allard, J. F.; Morris, D.; Dory, Y.; Lepage, M.; Zhao, Y. *J. Mater. Chem.* **2012**, *22*, 7252.
- ¹¹⁶ Liu, G.; Dong, C. M. *Biomacromolecules* **2012**, *13*, 1573.
- ¹¹⁷ (a) Raina, S.; Missiakas, D. *Annu Rev Microbiol* **1997**, *51*, 179. (b) Meng, F.; Hennink, W.E.; Zhong, Z. *Biomaterials* **2009**, 2180.
- ¹¹⁸ (a) Elias, S. J.; Arner, A. H. *Eur. J. Biochem.* **2000**, 267, 6102. (b) Townsend, D. M.; Tew, K. D.; Tapiero, H. *Biomed Pharmacother* **2003**, *57*, 145. (c) Go, Y. M.; Jones, D. P.; *Biochim Biophys Acta* **2008**, 1780, 1273.
- ¹¹⁹ (a) Kim, T. I.; Kim, S. W. *Reactive & Functional Polymers* **2011**, *71*, 344. (b) Saito, G.; Swanson, J. A.; Lee, K. D.; *Adv. Drug Deliv. Rev.* **2003**, *55*, 199.
- ¹²⁰ Takae, S.; Miyata, K.; Oba, M.; Ishii, T.; Nishiyama, N.; Itaka, K.; Yamasaki, Y.; Koyama, H.; Kataoka, K. *J. Am. Chem. Soc.* **2008**, *130*, 6001.
- ¹²¹ Dong, W. F.; Kishimura, A.; Anraku, Y.; Chuanoi, S.; Kataoka, K. *J. Am. Chem. Soc.* **2009**, *131*, 3804.
- ¹²² (a) Wen, H. Y.; Dong, H. Q.; Xia, W. J.; Li, Y. Y.; Wang, K.; Pauletti, G. M.; Shi D. L. *Chem. Commun.* **2011**, *47*, 3550. (b) Cai, X. J.; Dong, H. Q.; Xia, W. J.; Wen, H. Y.; Li, W. Q.; Yu, J. H.; Li, Y. Y.; Shi, D. L. *J. Mater. Chem.* **2011**, *21*, 14639. (c) Cai, X. J.; Dong, C. Y.; Dong, H. Q.; Wang, G. M.; Pauletti, G. M.; Pan, X. J.; Wen, H. Y.; Mehl, I.; Li, Y. Y.; Shi, D. L. *Biomacromolecules* **2012**, *13*, 1024. (d) Ding, J. X.; Chen, J. J.; Li, D.; Xiao, C. S.; Zhang, J. C.; He, C. L.; Zhuang, X. L.; Chen X. S. *J. Mater. Chem. B* **2013**, *1*, 69.
- ¹²³ Thambi, T.; Yoon, H. Y.; Kim, K.; Kwon, I. C.; Yoo, C. K.; Park, J. H.; *Bioconjug. Chem.* **2011**, *22*, 1924.
- ¹²⁴ Waku, T.; Matsumoto, M.; Matsusaki, M.; Akashi, M.; *Chem. Commun.* **2010**, 46, 7025.
- ¹²⁵ Ren, T. B.; Xia, W. J.; Dong, H. Q.; Li, Y. Y. *Polymer* **2011**, *52*, 3580.

- ¹²⁶ Koo, A. N.; Lee, H. J.; Kim, S. E.; Chang, J. H.; Park, C.; Kim, C.; Park, J. H.; Lee, S. C. *Chem. Commun.* **2008**, 6570.
- ¹²⁷ (a) Kakizawa, Y.; Harada, A.; Kataoka, K. *Biomacromolecules* **2001**, 2, 491. (b) Miyata, K.; Kakizawa, Y.; Nishiyama, N.; Harada, A.; Yamasaki, Y.; Koyama, H.; Kataoka, K. *J. Am. Chem. Soc.* **2004**, 126, 2355. (c) Matsumoto, S.; Christie, R. J.; Nishiyama, N.; Miyata, K.; Ishii, A.; Oba, M.; Koyama, H.; Yamasaki, Y.; Kataoka, K. *Biomacromolecules* **2009**, 10, 119. (d) Christie, R.J.; Miyata, K.; Matsumoto, Y.; Nomoto, T.; Menasco, D.; Lai, T.C.; Pennisi, M.; Osada, K.; Fukushima, S.; Nishiyama, N.; Yamasaki, Y.; Kataoka, K. *Biomacromolecules* **2011**, 12, 3174.
- ¹²⁸ Miyata, K.; Nishiyama, N.; Kataoka, K. *Chem. Soc. Rev.* **2012**, 41, 2562.
- ¹²⁹ Habraken, G. J. M.; Koning, C. E.; Heuts, J. P.; Heise, A. *Chem. Commun.* **2009**, 3612.
- ¹³⁰ (a) Sun, J., Chen, X. S.; Lu, T.; Liu, S.; Tian, H.; Guo, Z.; Jing, X.; *Langmuir* **2008**, 24, 10099. (b) Wang, K.; Luo, G. F.; Liu, Y.; Li, C.; Chen, X. S.; Zhuo, R. X.; Zhang, X. Z. *Polym. Chem.* **2012**, 3, 1084.
- ¹³¹ (a) Sulistio, A.; Blencowe, A.; Widjaya, A.; Zhang, X.; Qiao, G. G. *Polym. Chem.* **2012**, 3, 224. (b) Sulistio, A.; Lowenthal, J.; Blencowe, A.; Bongiovanni, M. N.; Ong, L.; Gras, S. L.; Zhang, X.; Qiao, G. G. *Biomacromolecules* **2011**, 12, 3469. (c) Sulistio, A.; Widjaya, A.; Blencowe, A.; Zhang, X.; Qiao, G. G. *Chem. Commun.* **2011**, 47, 1151.
- ¹³² (a) Xing, T.; Lai, B.; Ye, X.; Yan, L. *Macromol. Biosci.* **2011**, 11, 962. (b) Ding, J.; Shi, F.; Xiao, C.; Lin, L.; Chen, L.; He, C.; Zhuang, X.; Chen, X. S. *Polym. Chem.* **2011**, 2, 2857. (c) Shi, F. H.; Ding, J. X.; Xiao, C. S.; Zhuang, X. L.; He, C. L.; Chen, L.; Chen, X. S. *J. Mater. Chem.* **2012**, 22, 14168.
- ¹³³ Löwik, D.W. P. M.; Leunissen, E. H. P.; van den Heuvel, M.; Hansen, M. B.; van Hest J. C. M. *Chem. Soc. Rev.* **2010**, 39, 3394.
- ¹³⁴ (a) Minoura, N. *J. Chem. Soc., Chem. Commun.* **1993**, 196. (b) Minoura, N.; Higuchi, M.; Kinoshita, T. *Mater. Sci. Eng.* **1997**, 4, 249.
- ¹³⁵ (a) Mornet, S.; Vasseur, S.; Grasset, F.; Duguet, E. *J. Mater. Chem.* **2004**, 14, 2161. (b) Bae, S.; Lee, S. W.; Takemura, Y. *Appl. Phys. Lett.* **2006**, 89, 252503. (c)

Jun, Y. W.; Huh, Y. M.; Choi, J. S.; Lee, J. H.; Song, H. T.; Kim, S.; Yoon, S.; Kim, K. S.; Shin, J. S.; Suh, J. S.; Cheon, J. *J. Am. Chem. Soc.* **2005**, *127*, 5732.

¹³⁶ Xu, Z. G.; Feng, Y. Y.; Liu, X. Y.; Guan, M.; Zhao, C. D.; Zhang, H. X. *Colloids and Surfaces B: Biointerfaces* **2010**, *81*, 503.

¹³⁷ Liu, D.; Li, Y.; Deng, J. P.; Yang, W. T. *Reactive & Functional Polymers* **2011**, *71*, 1040.

¹³⁸ (a) Marcelo, G.; Muñoz-Bonilla, A.; Rodríguez-Hernández, J.; Fernández-García, M. *Polym. Chem.* **2013**, *4*, 558. (b) Marcelo, G.; Muñoz-Bonilla, A.; Fernández-García, M. *J. Phys. Chem. C* **2012**, *116*, 24717.

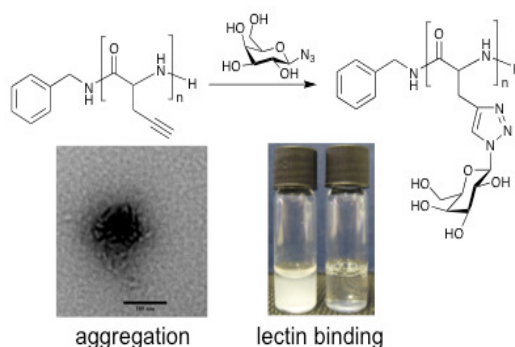
¹³⁹ Borase, T.; Ninjabdar, T.; Kapetanakis, A.; Roche, S.; O'Connor, R.; Kerskens, C.; Heise, A.; Brougham, D. F. *Angew. Chem. Int. Ed.* **2013**, *52*, 3164.

Chapter 2

Hydrolytically stable bioactive synthetic glycopeptide by combination of NCA polymerisation and click reaction

Abstract

The synthesis of poly(DL-propargylglycine) and poly(γ -benzyl-L-glutamate-*co*-DL-propargylglycine) was performed by NCA polymerisation at 0 °C to yield well-defined polypeptides with polydispersity indices below 1.3. FTIR results confirm β -sheet and α -helical conformation of the homopolymer and copolymer, respectively. The subsequent glycosylation was achieved by Huisgen [3+2] cycloaddition click reaction with azide-functionalized galactose. FTIR, NMR, SEC and MALDI-TOF analyses verify the successful glycosylation and suggest a high efficiency of the click reaction. The homo-glycopeptide was found to be water-soluble and to form aggregates in water above a critical concentration of 0.079 mg/mL. Selective lectin binding experiments confirm that the glycopeptides can be used in biorecognition applications. Moreover, the selective hydrolysis of the benzyl ester groups in the copolymer was achieved without loss of the galactose.



This chapter was published in
Huang, J.; Habraken, G.; Audouin, F.; Heise, A. *Macromolecules* 2010,
43, 6050.

2.1 Introduction

Carbohydrates are important in many complex biological processes as diverse as signal transmission, fertilization, inflammation, protein folding and many more. In particular, glycoproteins are seen to play a key role in these processes and in the last decade many efforts were directed towards their synthesis.¹ Well-defined artificial glycoconjugates are an interesting alternative to glycoproteins (biomimetic analogues). Glycopolymers, i.e. sugar-conjugated synthetic macromolecules, are nowadays synthetically well accessible, and often show biological activity useful in biomedical applications. Not least the advances in controlled radical polymerisation techniques and highly efficient coupling reactions have accelerated the development of synthetic glycopolymers.²⁻⁸ While the majority of the reported glycopolymers are acrylate-based, it is desirable to develop systems with a higher resemblance to natural glycopeptides by employing synthetic polypeptides. Useful in that respect are recently developed techniques for the ring-opening polymerisation of amino acid N-carboxy-anhydrides (NCA) allowing a high level of control over the polypeptide structures.⁹⁻¹⁵ Availability of a versatile synthetic protocol to glycopeptides derived from NCAs would give access to a promising class of biomimetic analogues and open new application areas owing to their structural similarity to natural peptides. However, up to now only a very limited number of examples of synthetic polypeptide-sugar conjugates were reported. This is primarily due to the inability to readily synthesize glycopolypeptides in a controlled manner. For example, the polymerisation of sugar-functional NCA has been described, but the monomer synthesis is challenging and requires the use of protected sugars.^{16, 17} The polymer analogous glycosylation of polypeptides offers a possible alternative. It is widely applied for the glycosylation of individual amino acids in natural proteins by reaction of functional and in some cases activated sugars with an asparagine (N-linkage) or with a serine or threonine (O-linkage) of the polypeptide.¹ While both strategies make use of the functionalities of the natural amino acids in the polypeptide and could also be applied for the glycosylation of synthetic polypeptides, they have two major drawbacks. Firstly, they would require protection

of the amino acids before NCA synthesis, and secondly, the nature of the glycosidic linkage between the saccharide and the peptides makes it prone to chemical and enzymatic hydrolysis.

“Click”-type reactions address both drawbacks and are ideally suited for peptide glycosylation due to their high efficiency.^{18,19} Reactions such as the Huisgen [3 + 2] cycloaddition between organic azides and acetylenes have already proven to be highly versatile for the glycosylation of synthetic polyacrylates.⁸ However, reports on the application of this reaction in peptide modification and more specifically in the synthesis of glycopeptides are still rare. Directed mutagenesis was, for example, used to replace a natural amino acid in a defined position of the amino acid sequence of peptides with a non-natural azide or alkyne functional amino acid. Selective glycosylation of these individual amino acids was then achieved by click reaction with the corresponding alkyne or azide sugar.²⁰⁻²² For synthetic NCA-derived polypeptides Lecommandoux described the synthesis of amphiphilic block copolymers including the coupling of oligosaccharides by Huisgen cycloaddition to polypeptide end-groups.²³⁻²⁶ A few recent publications report on the side-chain modification of NCA-derived polypeptides. Thiol-ene coupling was used by us for the modification of a cystein containing copolypeptide²⁷ and Schlaad applied the same technique to couple thiol functional sugars to poly(DL-allylglycine).²⁸ Hammond first described azide-alkyne click reactions for the modification of NCA-derived polypeptides.²⁹ Poly(ethylene glycol) (PEG) azide was coupled to an alkyne functional homopolypeptide synthesized from γ -propargyl-L-glutamate NCA. Very recently, Xuesi Chen reported the application of click reactions to synthesize a mannose functional polypeptide using the same NCA³⁰ and Donghui Zhang applied the same technique to click alkyne functional sugar to an azide functional polypeptide³¹. The latter was obtained by a multi-step synthesis and a final azide-halogen exchange on poly(γ -3-chloropropanyl-L-glutamate). All azide-alkyne systems reported so far rely on glutamic acid esters thereby introducing a potentially hydrolytically unstable ester bond between the carbohydrate and the polypeptide. This could have disadvantages in a biological environment as enzymatic ester cleavage could result in reduced activity. It has been suggested that the use of non-

natural amino acid with the amino acid side chain connected to the sugar unit via an isosteric linkage may lead to a chemically and metabolically more stable analogue while retaining biological activity.³² Moreover, ester linkages potentially limit the possibilities to combine this approach with common deprotection techniques applied in synthetic polypeptide chemistry and thus the possibility to design more complex polypeptides. We therefore investigated the applicability of the commercial non-natural alkyne functional amino acid DL-propargylglycine for the synthesis of glycopeptides. In this paper we report on the synthesis and characterization of homo- and copolymers with benzyl glutamate and their glycosylation by Huisgen click reactions. We show that a high degree of conjugation can be achieved by this method and investigate the influence of the glycosylation on the peptide conformation. Furthermore, we provide first evidence for the bioactivity of the glycopeptides and their stability under selective ester deprotection conditions.

2.2 Experimental section

Materials

All chemicals were purchased from Sigma-Aldrich and used as received unless otherwise noted. γ -Benzyl-L-glutamate and DL-propargylglycine were supplied by Bachem. Diethylether was purchased from VWR. Anhydrous DMF, DMSO, ethyl acetate, THF, methanol were used directly from the bottle under an inert and dry atmosphere. *Ricinus communis* (castor bean) Agglutinin RCA₁₂₀ (10 mg/mL in buffered aqueous solution) and Concanavalin A (Con A, Type IV, lyophilized powder) from *Canavalia ensiformis* (Jack bean) were purchased from Aldrich and used as received. 0.01 M Phosphate- buffered saline (PBS) at pH 7.4 was prepared by dissolving one tablet of PBS (Sigma-Aldrich) into 200 mL of distilled water. γ -Benzyl-L-glutamate NCA was synthesized following a literature procedure.³³ 1- β -Azido-2,3,4,6-tetraacetyl-D-galactose was synthesized following a literature procedure.³⁴ The spectroscopic data were in agreement with literature data.

Methods

^1H and ^{13}C NMR spectra were recorded at room temperature with a Bruker Avance 400 (400 MHz) and a Bruker Avance Ultrashield 600 (600 MHz). DMSO-d^6 , CDCl_3 , Acetone- d^6 and D_2O were used as solvents and signals were referred to the signal of residual protonated solvent signals. TMS was used as an internal standard for DMSO-d^6 and CDCl_3 . ATR-FTIR spectra were collected on a Perkin Elmer Spectrum 100 in the spectral region of $650\text{--}4000\text{ cm}^{-1}$ and were obtained from 4 scans with a resolution of 2 cm^{-1} . A background measurement was taken before the sample was loaded onto the ATR unit for measurements. SEC analysis using Hexafluoroisopropanol (HFIP, Biosolve, AR-S from supplier or redistilled) as eluent was carried out using a Shimadzu LC-10AD pump (flow rate 0.8 mL/min) and a WATERS 2414 differential refractive index detector (at $35\text{ }^\circ\text{C}$) calibrated with poly(methyl methacrylate) standard (range 1000 to 2000000 g/mol). Two PSS PFG-lin-XL ($7\text{ }\mu\text{m}$, $8\times 300\text{ mm}$) columns at $40\text{ }^\circ\text{C}$ were used. Injections were done by a Spark Holland MIDAS injector using a $50\text{ }\mu\text{L}$ injection volume. Before SEC analysis was performed, the samples were filtered through a $0.2\text{ }\mu\text{m}$ PTFE filter (13 mm , PP housing, Alltech). Matrix assisted laser desorption / ionization - time of flight - mass spectroscopy (MALDI-ToF) analysis was carried out on a Voyager DE-STR from Applied Biosystems (laser frequency 20 Hz , 337 nm and a voltage of 25 kV). The matrix material used was trans-2-[3-(4-tert-Butylphenyl)-2-methyl-2-propenylidene] malononitrile (DCTB; 40 mg/mL). Potassium trifluoroacetic acid (KTFA) was added as cationic ionization agent (5 mg/mL). The polymer sample was dissolved in HFIP (1 mg/mL), to which the matrix material and the ionization agent were added ($5:1:5$), and the mixture was placed on the target plate. Samples were precipitated from the reaction medium in diethylether, filtered and placed in a freezer before measuring. Melting points were measured by Differential scanning calorimetry (DSC) on a TA DSC Q200 calorimetry in nitrogen at a heating rate of $10\text{ }^\circ\text{C/min}$ and a cooling rate of $5\text{ }^\circ\text{C/min}$ in the range from $-20\text{ }^\circ\text{C}$ to $200\text{ }^\circ\text{C}$. TEM images were obtained using a JEOL 2100 TEM scan instrument (at an accelerating voltage of 200 kV) for samples deposited on carbon-coated (400 mesh) copper grids. The preparation of samples for TEM analysis involved depositing a drop ($15\text{ }\mu\text{L}$) of the glycopeptide solution, which was dissolved in DI water onto the grids and

allowing water to evaporate prior to imaging. The turbidity assay of the lectin with different concentrations of glycopeptides was monitored at 450 nm in Varian Cary 50 by UV quartz cuvette. The dynamic light scattering (DLS) experiments of glycopeptides in DI water solution were performed at 25 °C on a Zetasizer Nano ZS particle analyzer (Malvern Instruments, Worcestershire UK) using a detection angle of 173° and a 4 mW He-Ne laser operating at a wavelength of 633 nm. Emission spectra for the critical aggregation concentration were recorded on a Varian Cary Eclipse fluorescence spectrophotometer at an excitation wavelength of 340 nm using a 1 cm optical path length quartz cuvette. The spectra were averaged from triplicate recorded spectra. CD spectroscopy was performed on a Jasco J-815 spectrometer with 0.0045 mM solution of the peptide in demineralized water.

Synthesis of *DL*-propargylglycine NCA (2). *DL*-propargylglycine **1** (2.5 g, 22.1 mmol) and α -pinene (14.88 g, 109 mmol) were dissolved in 60 mL anhydrous THF in a three-neck round-bottom flask. The reaction mixture was heated to 50 °C under nitrogen and then triphosgene (4.92 g, 16.6 mmol) in 20 mL THF was added dropwise over a period of 1 hour. The reaction was continued for 4 hours until the mixture became clear gradually. The mixture was concentrated under reduced pressure and the NCA precipitated by addition of 100 mL *n*-heptane. The mixture was then placed in a freezer overnight. After filtration, the crude product was dissolved in dry THF, and re-crystallized twice by addition of *n*-heptane. The obtained solid was washed with *n*-heptane, yielding off-white crystals in 75% yield. $^1\text{H-NMR}$ (400 MHz, Acetone- d_6 , δ , ppm): 2.62 (t, $J=2.5$ Hz, 1H, $\equiv\text{CH}_2$), 2.84 (dd, $J=4.5, 2.5$ Hz, 2H, $-\text{CH}_2-\text{C}\equiv$), 4.75 (t, $J=4.5$ Hz, 1H, CH), 8.04 (s, 1H, NH), $^{13}\text{C-NMR}$ (400 MHz, Acetone- d_6 , δ , ppm): 22.26 ($-\text{CH}_2-\text{C}\equiv$), 57.30 (CH), 73.64 ($\equiv\text{CH}$), 78.23 ($-\text{C}\equiv\text{CH}$), 152.71 ($-\text{O}(\text{CO})\text{NH}-$), 170.62 ($-\text{O}(\text{CO})\text{CH}$). FTIR (neat, cm^{-1}): 3363, 3247, 1854, 1771, 1286, 1195, 1111, 1089, 934, 893, 777, 756, 723, 698, 668. Mp: 114 °C.

Synthesis of poly(*DL*-propargylglycine) (3). *DL*-propargylglycine NCA (800 mg, 5.76 mmol) and anhydrous LiBr (261 mg, 3 mmol) were dissolved in 28 mL dry DMF in a Schlenk tube. A solution of benzylamine (31.08 mg, 0.288 mmol) in 2 mL dry DMF was added after the NCA and LiBr were totally dissolved. The reaction was maintained for 5 days at 0 °C under an inert atmosphere. The reaction

mixture was precipitated into an excess diethylether, filtered and dried under vacuum to yield a pale yellow solid. Yield: 84%. M_n : 2250 g/mol, PDI: 1.16.

Synthesis of 1-Azido-1-deoxy- β -D-galactopyranoside (1-azido- β -galactose) (5).

The synthesis was carried out following a slightly modified literature procedure.³⁵ 1- β -Azido-2,3,4,6-tetraacetyl-D-galactose (373 mg, 1 mmol) was dissolved in 5 mL anhydrous methanol in a Schlenk tube. To this solution a catalytic amount of anhydrous potassium carbonate (6 mg, 0.04 mmol) was added and the reaction mixture was vigorously stirred at room temperature under a nitrogen atmosphere for 3 hours. Amberlite IR-120 ion-exchange resin was washed with methanol and then added to and stirred with the reaction mixture for 1 hour. The resin was then filtered off under gravity and the resulting solution was concentrated to dryness in vacuum to yield a white powder (184 mg, Yield 90%). Mp 150 °C. ¹H-NMR (400 MHz, D₂O, δ , ppm): 3.49 (dd, J_{2-1} =8.7 Hz, J_{2-3} =9.8 Hz, 1H, H-2), 3.66 (dd, J_{3-2} =9.8 Hz, J_{3-4} =3.3 Hz, 1H, H-3), 3.72-3.78 (m, 3H, H-5, H-6a', H-6b'), 3.94 (d, J_{4-3} =3.3 Hz, 1H, H-4), 4.64 (d, J_{1-2} =8.7 Hz, 1H, H-1). ¹³C-NMR (400 MHz, D₂O, δ , ppm): 63.44 (C-6), 71.00 (C-4), 72.81 (C-3), 75.13 (C-5), 79.70 (C-2), 93.05 (C-1).

Glycosylation of poly(DL-propargylglycine) using protected galactose (6).

Poly(DL-propargylglycine) (100 mg, ca. 0.938 mmol of alkyne units), 1- β -azido-2,3,4,6-tetraacetyl-D-galactose (526 mg, 1.407 mmol, 1.5 equiv.) and triethylamine (68 μ L, 0.492 mmol, 0.5 equiv) were dissolved in 5 mL of anhydrous DMSO in a Schlenk tube. The mixture was stirred and degassed by bubbling with nitrogen for 30 min. (PPh₃)₃CuBr (88 mg, 0.094 mmol, 0.1 equiv) was then added and nitrogen was bubbled through the resulting solution for another 30 min. Then the Schlenk tube was placed in an oil bath at 30 °C for 72 hours under nitrogen atmosphere. The reaction solution was precipitated into a large excess of diethyl ether. The filtrated solid was dissolved in THF and passed through a short neutral aluminium oxide column eluting with THF. The polymer was recovered by precipitation in diethyl ether and dried under high vacuum. Yield: 40%. M_n : 6450 g/mol, PDI: 1.25.

The deacetylation of glycopeptides clicked with protected galactose was carried out following a slightly modified literature procedure.⁴ 75 mg acetylated glycopeptide was dissolved in 6 mL of CHCl₃/CH₃OH mixture (v/v=2:1) in a Schlenk tube. The solution was degassed with nitrogen for 15 min, and 11 mg sodium methoxide was

added. After few seconds, the reaction solution became very turbid and the mixture was stirred under N₂ atmosphere at room temperature overnight to allow maximum deacetylation of the glycopeptide. The mixture was dried under reduced pressure. Yield: 99%.

Glycosylation of poly(DL-propargylglycine) using unprotected galactose (7):

Poly(propargylglycine) **3** (100 mg, 0.938 mmol of clickable alkyne units), 1-Azido-1-deoxy- β -D-galactopyranoside **4** (289 mg, 1.407 mmol, 1.5 equiv.) and triethylamine (68 μ L, 0.492 mmol, 0.5 equiv) were dissolved in 5 mL of anhydrous DMSO in a Schlenk tube. The mixture was stirred and degassed by bubbling nitrogen for 30 min. (PPh₃)₃CuBr (88 mg, 0.0938 mmol, 0.1 equiv) was then added and nitrogen was bubbled through the resulting solution for another 30 min. Then the Schlenk tube was placed in an oil bath at 30 °C for 72 hours under nitrogen atmosphere. The solution was precipitated into THF twice to remove the catalyst, and then the obtained solid was redissolved in DMSO and precipitated twice in methanol. The polymer was filtered and dried in vacuum oven. Yield: 55%. M_n : 4150 g/mol, PDI: 1.13.

Synthesis of poly(γ -benzyl-L-glutamate-co-DL-propargylglycine) (8).

γ -Benzyl-L-glutamate NCA **1** (1.01 g, 3.82 mmol), propargylglycine NCA **2** (267 mg, 1.91 mmol) and anhydrous LiBr (261 mg, 3 mmol) were dissolved in 28 mL anhydrous DMF. A solution of benzylamine (20.44 mg, 0.191 mmol) in 2 mL dry DMF was added after both of NCAs were dissolved. The reaction was maintained for 5 days at 0 °C under an inert atmosphere. The reaction mixture was precipitated into an excess diethylether, filtered and dried under vacuum as a pale yellow solid. Yield: 80%. M_n : 5800 g/mol, PDI: 1.15.

Glycosylation of poly(γ -benzyl-L-glutamate-co-DL-propargylglycine) (9).

Poly(γ -benzyl-L-glutamate-co-DL-propargylglycine) (400 mg, ca. 0.735 mmol of alkyne units), 1-Azido-1-deoxy- β -D-galactopyranoside (226 mg, 1.102 mmol, 1.5 equiv. to alkyne) and triethylamine (51 μ L, 0.367 mmol, 0.5 equiv) were dissolved in 8 mL of anhydrous DMSO in the Schlenk tube. The mixture was stirred and degassed by bubbling nitrogen for 30 min. (PPh₃)₃CuBr (68 mg, 0.0735 mmol, 0.1 equiv.) was then added and nitrogen was bubbled through the resulting solution for another 30 min. Then the Schlenk tube was placed in an oil bath at 30 °C for 72 h under

nitrogen atmosphere. The amphiphilic nature of the copolymer after glycosylation makes the identification of a proper precipitation solvent difficult. After the reaction, the polymer solution was added drop-wise to an excess diethyl ether, the obtained polymer re-dissolved in DMSO and precipitated twice in a 1:2 THF/methanol mixture. The polymer was centrifuged and dried in vacuum oven. Yield: 30%. M_n : 7050 g/mol, PDI: 1.21.

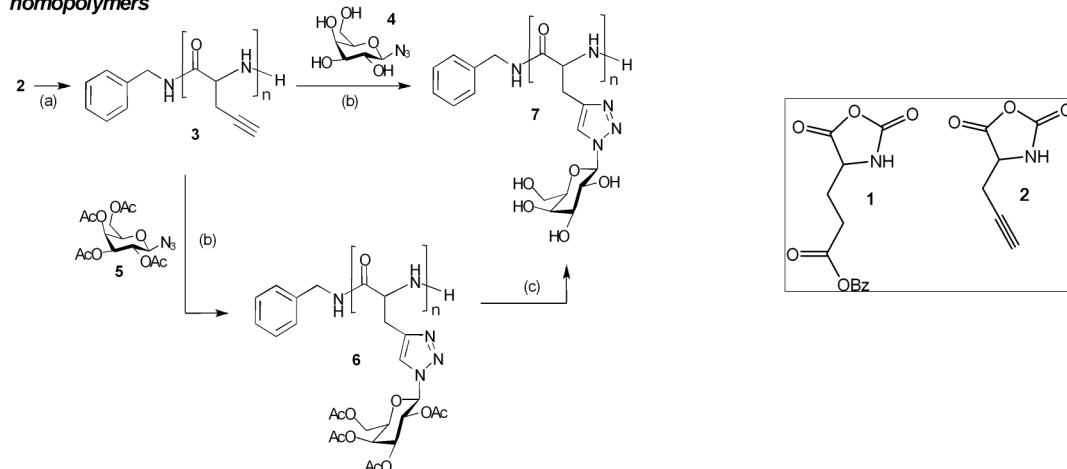
Benzyl ester hydrolysis of glycosylated poly(γ -benzyl-L-glutamate-co-DL-propargylglycine) (10). The hydrolysis was done following a modified literature procedure.³⁶ The glycosylated copolymer (100 mg) was dissolved in 2.0 ml trifluoroacetic acid (TFA). A six-fold excess with respect to benzyl-L-glutamate of a 33% of HBr in acetic acid (0.3 mL) was added. After 16 hours, the mixture was added drop-wise into diethyl ether. The precipitates were redissolved in DMF, precipitated twice in diethyl ether and dialyzed in water for three days. The polymer was filtered and dried under reduced pressure. Yield: 60%.

Critical aggregation concentration. The critical aggregation concentration of the glycopeptide was determined following a literature procedure.³⁷ A stock solution of the glycopeptide with a concentration of 1.0 mg/mL was prepared by dissolving the glycopeptides in DI water. This stock solution was further diluted to yield a series of solutions with concentrations varying from 1.0 mg/mL to 0.001 mg/mL. A defined amount of the fluorescence probe N-phenyl-1-naphthalamine (PNA) in acetone was added to each of the solutions in a 20 mL volumetric flask and then acetone was evaporated overnight. The concentration of PNA in the final solution was 2.0×10^{-6} mol/L. In total the samples were kept for 48 h to equilibrate the PNA and aggregates before the fluorescence spectra were measured.

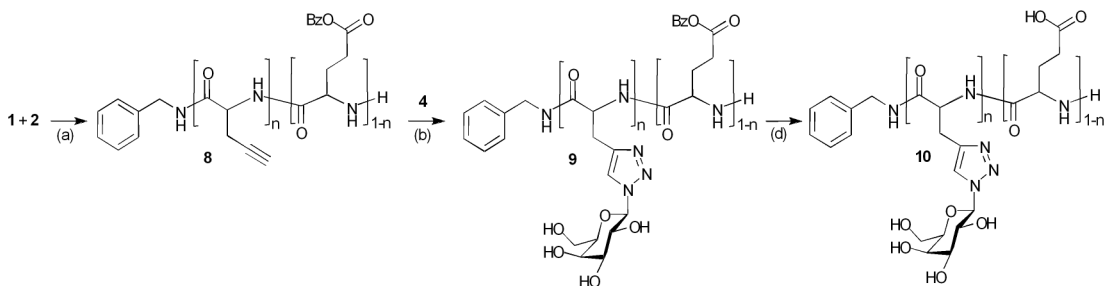
Carbohydrate-lectin binding recognition. The lectin recognition activity of the glycopeptide solution was analyzed by the change of the turbidity at 450 nm at room temperature. 2 mg/mL of RCA₁₂₀ lectin was first prepared in 0.01 M phosphate buffered saline (PBS) at pH 7.4. 600 μ L lectin solutions were transferred into a cuvette and a baseline measured. A solution of 60 μ L glycopeptide with different concentrations in PBS buffer solution was added into the cuvette containing the lectin solution. The solution in the cuvette was gently mixed using a pipette and immediately the absorbance at 450 nm was recorded every 5 min. As a control

lectin Con A was used under the same experimental conditions as well as PBS buffer solution without any glycopeptide.

homopolymers



copolymers



Scheme 2.1: Synthesis of glycopeptides. (a) LiBr, DMF, benzylamine, 0 °C; (b) Cu(PPh₃)₃Br, Et₃N, DMSO, 30 °C; (c) MeONa, DCM/MeOH, r.t.; (d) TFA, HBr/acetic acid, r.t.

2.3 Results and Discussion

γ -Benzyl-L-glutamate and DL-propargylglycine were converted into the corresponding NCAs **1** and **2** by reaction with triphosgene. The homopolymerisation of **2** was carried out with benzylamine as an initiator in DMF at 0 °C to prevent side-reactions and maintain structural control (Scheme 2.1).³⁸ The only previous report on the synthesis and polymerisation of NCA **2** was by Schlögel and Pelousek in 1960, who observed a low solubility of the poly(DL-propargylglycine) in most solvents.³⁹ Indeed, under the applied polymerisation conditions a fast gelling of the reaction medium was observed and only very low molecular weight

oligopeptides were obtained. This is most likely caused by intermolecular hydrogen bonding (β -sheets), which limits the polymer growth. Addition of LiBr to the polymerisation medium improved the polymerisation results and poly(DL-propargylglycine) **3** with a number average molecular weight (M_n) of 2250 g/mol and a low polydispersity index (PDI) of 1.16 was obtained (Table 2.1, Figure 2.1). In agreement with the report of Schlögel and Pelousek, the solubility of this polypeptide is very poor in most common solvents. MALDI-ToF spectra analysis confirms the low polydispersity and the structural homogeneity of the material, evident from the presence of peaks exclusively corresponding to propargylglycine repeating units and benzyl amide and amine end-groups, respectively (Figure 2.2). Inspection of the ^1H - and ^{13}C -NMR spectra further confirms the structure of the poly(DL-propargylglycine) (Figure 2.3 and Figure 2.4). Most characteristic for this polymer are the carbon peaks at 22 ppm (*f*) 73 ppm (*h*) and 80 ppm (*g*) and the proton peak at 2.6 ppm (*d*) and 2.8 ppm (*e*) from the alkyne moiety. From the integrated peak area ratio of the benzyl amine *a* at 7.27 ppm and the combined peaks *b* and *c* (4.2 - 4.6 ppm) in the ^1H -NMR spectrum a molecular weight of 1912 g/mol can be calculated, which is slightly lower than the SEC molecular weight (PMMA standards).

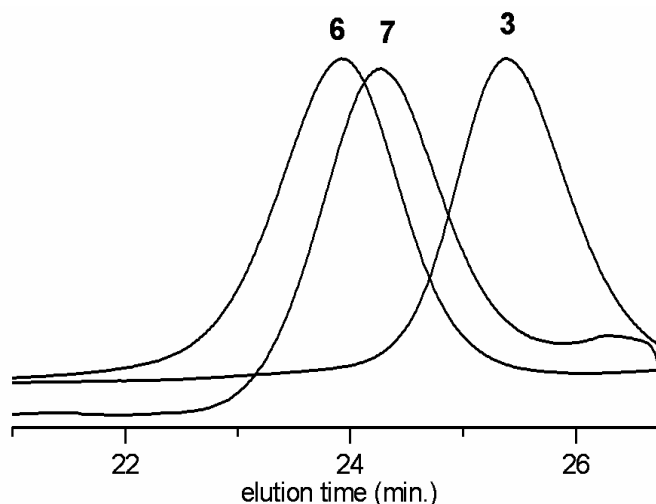


Figure 2.1: SEC traces (HFIP, PMMA standards) of poly(DL-propargylglycine) (**3**, M_n : 2250 g/mol, PDI: 1.16) and the glycosylated poly(DL-propargylglycine) by click reaction with protected (**6**, M_n : 6450 g/mol, PDI: 1.25) and unprotected galactose (**7**, M_n : 4150 g/mol, PDI: 1.13).

Table 2.1: Molecular weights and polydispersity indices (PDI) of polypeptides before and after click reaction.

polymer	M_n (GPC) (g/mol)	PDI
3	2250	1.16
6	6450	1.25
7	4150	1.13
8	5800	1.15
9	7050	1.21

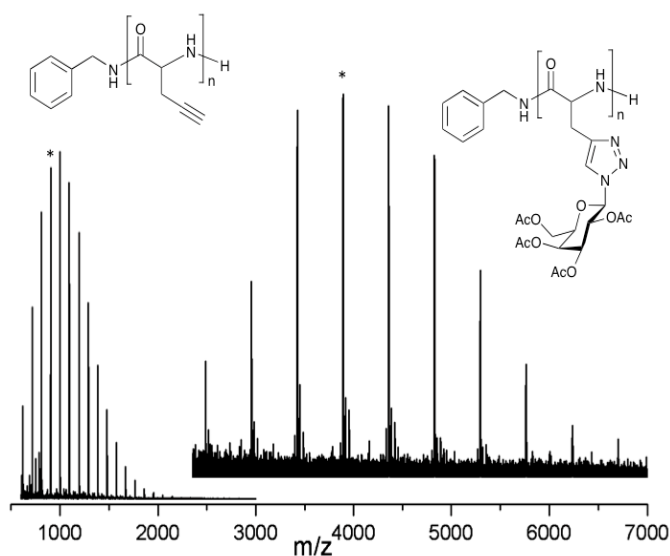


Figure 2.2: MALDI-ToF-MS spectra of poly(DL-propargylglycine) (**3**) and the glycosylated poly(DL-propargylglycine) by click reaction with protected galactose (**6**) (small peaks represent copper adducts). * denotes the polymers with $n = 8 + K^+$: m/z 905.91 (**3**) and m/z 3892.26 (**6**).

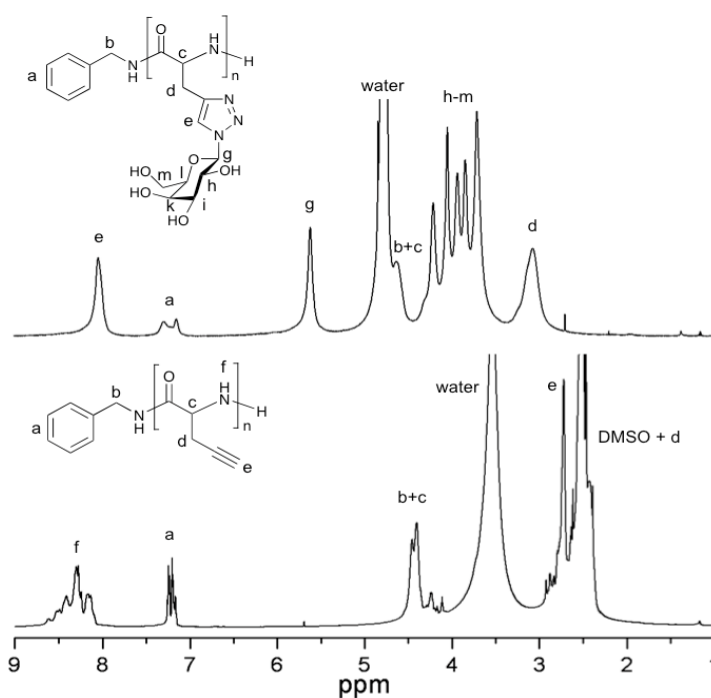


Figure 2.3: ^1H -NMR spectra of poly(DL-propargylglycine) **3** in DMSO-d_6 and glycosylated polypeptide **7** after click reaction with unprotected galactose **4** in D_2O .

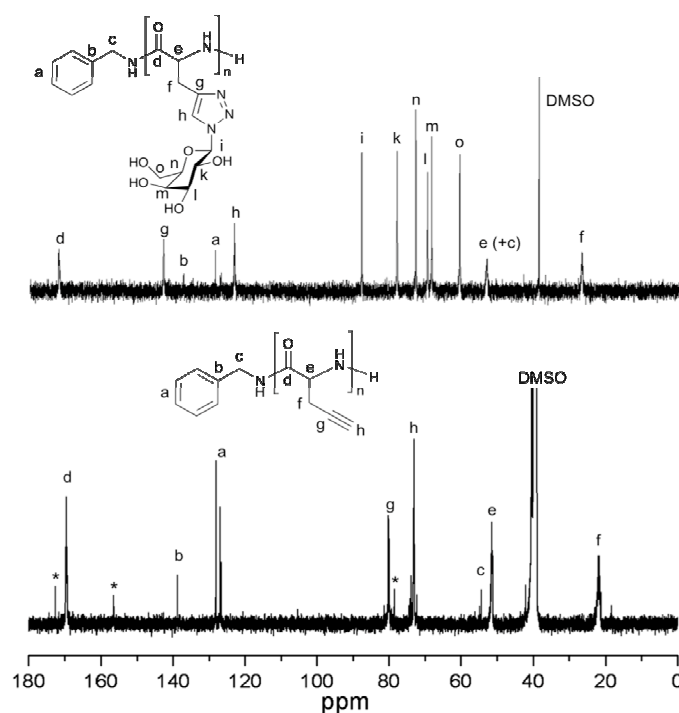


Figure 2.4: ^{13}C -NMR spectra of poly(DL-propargylglycine) **3** in DMSO-d_6 and glycosylated polypeptide **7** after click reaction with unprotected galactose **4** in D_2O (* denotes residual NCA signals).

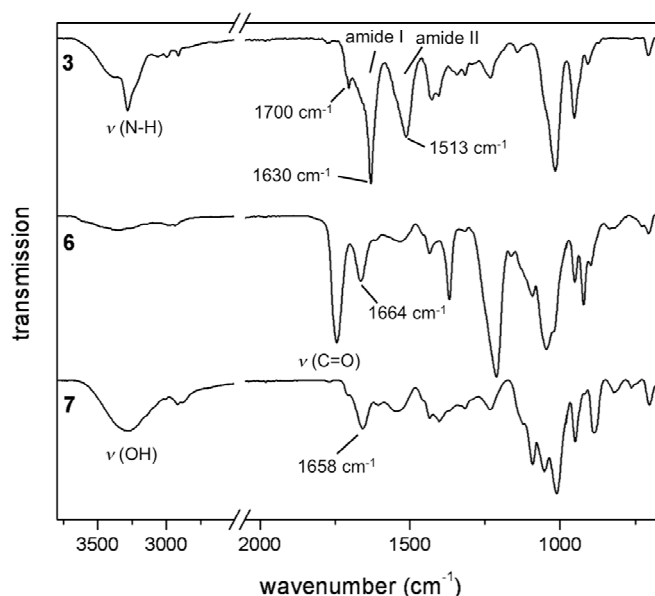


Figure 2.5: FTIR spectra of poly(DL-propargylglycine) (**3**) and the glycosylated poly(DL-propargylglycine) by click reaction with protected (**6**) and unprotected galactose (**7**).

Besides the amide II band at 1513 cm^{-1} , IR spectroscopy reveals the presence of two amide I bands at 1630 (strong) and 1700 (weak) cm^{-1} characteristic of a β -sheet conformation (Figure 2.5).^{40,41} This is in agreement with an investigation by Akaike who found that poly(valine) containing various ratios of D- and L-amino acids all had IR-spectra and X-ray diffraction patterns that were consistent with a β -sheet configuration.⁴² The only noticeable effect of the D-enantiomer was an increased spacing between the sheets. Due to the low solubility of **3** in suitable solvents it was not possible to confirm the secondary structure by Circular dichroism (CD) spectroscopy.

The copolymerisation of **2** with γ -benzyl-L-glutamate NCA **1** at a monomer feed ratio of 1:2 was carried out under similar conditions as the homopolymerisation. Owing to the slightly higher solubility of the copolymer a higher molecular weight of 5800 g/mol (PDI: 1.15) was obtained. $^1\text{H-NMR}$ spectroscopy confirms the presence of both monomers in the copolymer in a ratio corresponding to the monomer feed ratio (Figure 2.6). Moreover, the MALDI-ToF spectrum shows the complex signal pattern of a copolymer (Figure 2.7).

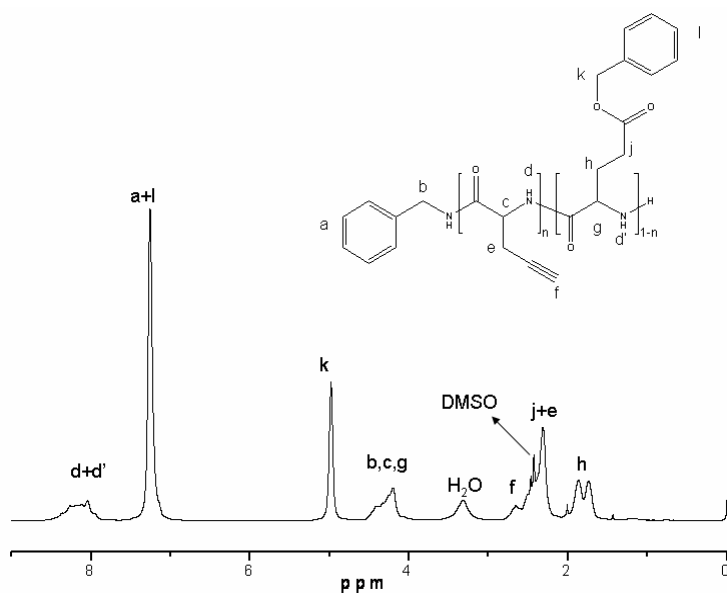


Figure 2.6: ^1H -NMR spectrum of poly(γ -benzyl-L-glutamate-*co*-DL-propargylglycine) **8** in $\text{DMSO}-d_6$.

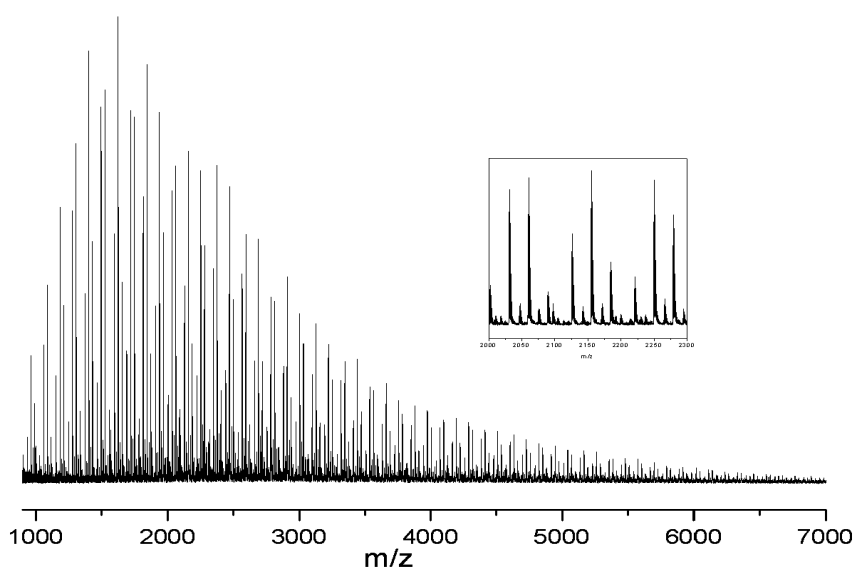


Figure 2.7: MALDI-ToF-MS spectrum of poly(γ -benzyl-L-glutamate-*co*-DL-propargylglycine) **8**. The spectrum shows a complex signal pattern typical for copolymers. By software supported deconvolution the copolymer contour plot in Figure 2.8 of the main document was calculated.

Using a software based MALDI-TOF deconvolution method developed in our group, the spectrum was converted into composition contour plots.⁴³⁻⁴⁵ The shape of the contour plot allows conclusions to be drawn concerning the molecular distribution of the comonomers in the chain. The contour plot of copolymer **8** exhibits a directional coefficient and a single distribution with a maximum at five γ -benzyl-L-glutamate and three propargylglycine units (Figure 2.8). This is characteristic for a random copolymer and in good agreement with the monomer feed ratio. Interestingly, the copolymer adopts an α -helical conformation as evident from the positions of the IR amide bands at 1655 and 1543 cm^{-1} (Figure 2.9) and the CD spectrum (Figure 2.10). It can be speculated that the strong helix-forming ability of the γ -benzyl-L-glutamate units is the driving force for the helical conformation but without further data the role of both amino acids in the secondary structure cannot be determined.

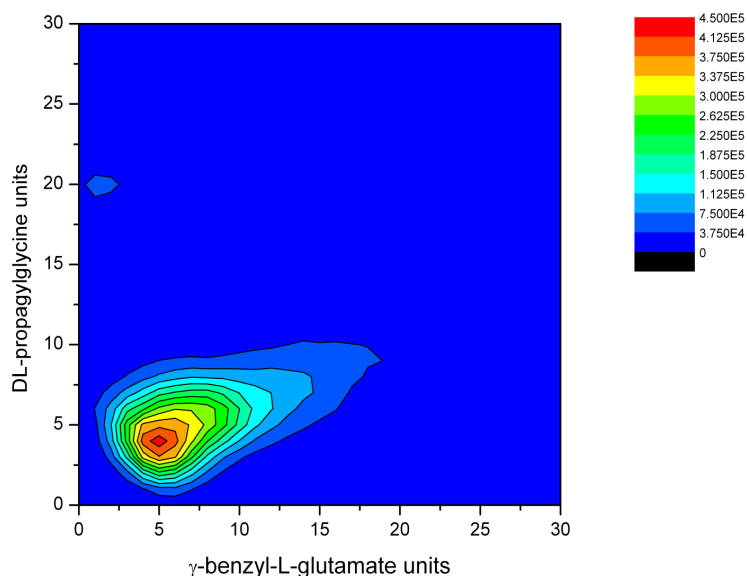


Figure 2.8: MALDI-ToF-MS contour plot of copolymer **8**.

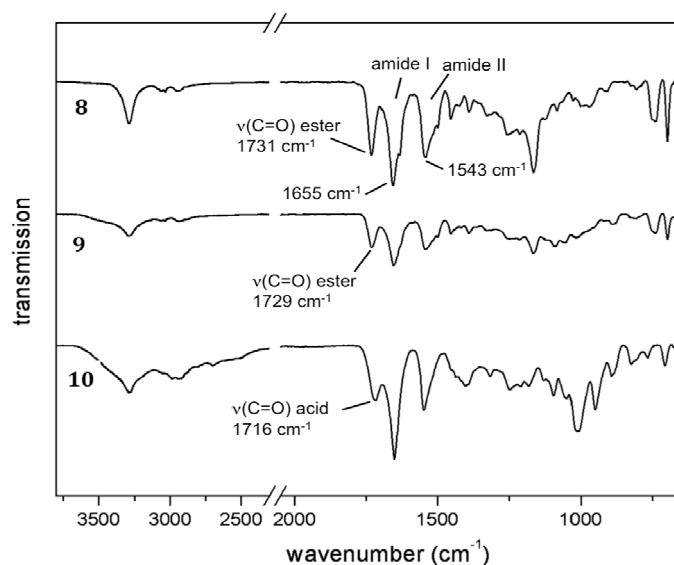


Figure 2.9: FTIR spectra of poly(γ -benzyl-L-glutamate-*co*-DL-propargylglycine) (**8**), the glycosylated poly(γ -benzyl-L-glutamate-*co*-DL-propargylglycine) obtained by click reaction with unprotected galactose (**9**) and the glycosylated poly(L-glutamic acid-*co*-DL-propargylglycine) (**10**).

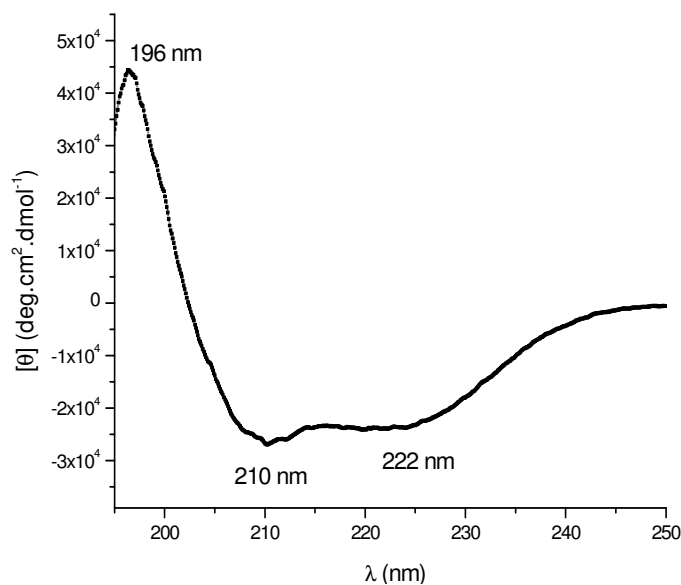


Figure 2.10: CD spectrum of poly(γ -benzyl-L-glutamate-*co*-DL-propargylglycine) **8** in acetonitrile. The spectrum is in agreement with an α -helical structure, which is consistent with FTIR results (Figure 2.9).

The glycosylation of both polymers was done with galactose, which can be readily converted to the corresponding azide. In order to investigate the influence of the free sugar hydroxy groups on the results of the click reaction both the acetyl-protected galactose **5** and the unprotected galactose **4** were employed for the glycosylation of **3**. Immediately noticeable was the improved solubility of the polypeptide in common organic solvents after conjugation with the acetylated galactose. A clear shift of the SEC trace to higher molecular weights was observed after attachment of both the protected and unprotected galactose (Figure 2.1). While in the latter case an M_n of 4150 g/mol was calculated from SEC, functionalization with the protected galactose produced a polymer with an M_n of 6450 g/mol in accordance with the higher molecular weight of the sugar units (Table 2.1). Spectroscopic evidence for the successful glycosylation was obtained from NMR spectra, which are in agreement with the proposed structure (data not shown). An approximation of the click reaction yield was obtained from the MALDI-ToF spectrum of **6** (Figure 2.2). The spectrum reveals one dominating polymer species with repeating units corresponding to the propargylglycine with the protected galactose attached via a triazole unit and benzyl amide and amino end-groups (other small signals were identified as copper aggregates of **6**). Although any quantification of MALDI-ToF spectra has to be viewed with caution, this result suggests a very high glycosylation yield. Equally successful was the direct glycosylation of **3** with the unprotected galactose **4**. Direct evidence for the attachment of the sugar to the polymer backbone via the click reaction was obtained from NMR spectroscopy. Figure 2.4 shows the ^{13}C -NMR spectrum of **7** in which peaks characteristic of the galactose (*i-o*) as well as the polypeptide carbons (*a-e*) can be identified. Most importantly, peaks *g* at 143 ppm and *h* at 123 ppm can be assigned to triazole carbons, which experience a significant downfield shift upon click reaction. Similarly, the ^1H -NMR spectrum of **7** reveals proton peaks characteristic of the polymer backbone, the triazole and the sugar (Figure 2.3). Most significant are the downfield shifts of protons *d* and *e* to 3.0 and 7.97 ppm, respectively, upon formation of the triazole ring. Polymer **7** is soluble in water and polar organic solvents like DMF and DMSO, which suggests similarly high functionalization efficiency as for **6**. This is supported by the fact that all spectroscopic and solubility results are identical irrespective of

whether **7** was synthesized directly from the unprotected galactose or from the protected galactose with subsequent deprotection.

Besides further evidence for the presence of galactose in the polymer, the FTIR spectra (Figure 2.5) provide valuable information about the secondary structure of the polypeptide after glycosylation. In the case of the protected galactose, the FTIR-spectrum of **6** clearly shows the presence of a carbonyl band at 1744 cm^{-1} owing to the acetyl protecting groups. Interestingly, both amide bands are shifted to higher wave numbers when compared to the spectrum of **3**. The amide I band can now be found at 1664 cm^{-1} (1630 cm^{-1} in **3**). A similar shift of amide bands was observed for polymer **7**, which contains the unprotected galactose. Moreover, the characteristic OH bands between 1100 and 1050 cm^{-1} as well as a broad band centred at 3290 cm^{-1} confirm the presence of the unprotected galactose. The positions of the amide bands suggest a random coil conformation of the glycopeptide.⁴⁰ Apparently, the presence of the bulky galactose moieties prevents the formation of intermolecular hydrogen bonds and thus the arrangement of the polypeptides into β -sheets. However, in aqueous solution the CD spectrum of **7** clearly confirms β -sheet conformation by a characteristic minimum at 214 nm (Figure 2.11). This apparent contradiction can be rationalized by the sample history; FTIR spectra were recorded from solid polymers obtained by evaporation of a DMSO solution. The interruption of hydrogen bonding between the amino acid units of the polypeptides by DMSO is apparently sufficient to prevent the formation of β -sheets and thus force the polymers into a random coil conformation in the solid state. In water, on the other hand, the glycopeptides can form weak hydrogen bonds sufficient enough to assemble as β -sheets.

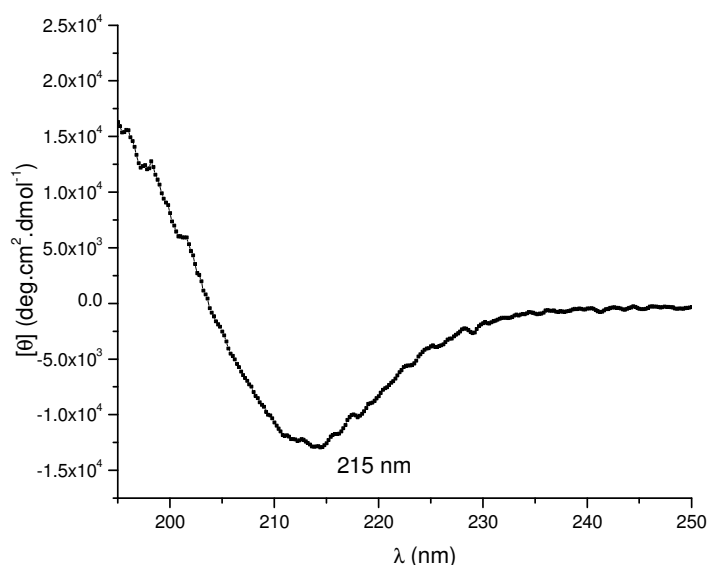


Figure 2.11: CD spectrum of glycopeptides **7** in water.

While polymer **7** is readily soluble in water, we hypothesized that this behaviour must cause the formation of aggregates at higher concentration. Indeed, Dynamic Light Scattering (DLS) revealed the formation of aggregates in the range of 540 nm (0.5 mg/mL). In order to determine the critical aggregation concentration of **7** more accurately, we carried out fluorescent probe experiments in the presence of N-phenyl-1-naphthalamine (PNA). PNA strongly emits in a hydrophobic environment while it is quenched in polar media.⁴⁶ When the fluorescence of solutions of **7** in the presence of PNA was monitored at different concentrations, only low fluorescence was detected at concentrations below 0.1 mg/mL. At higher concentrations the fluorescence drastically increased caused by the incorporation of PNA in the hydrophobic regions of the aggregates (Figure 2.12). The critical aggregation concentration of 0.079 mg/mL was determined by intersecting the two straight lines. A similar self-association was described by Li for glycosylated polyacrylates.⁴⁷ It appears that, although these highly glycosylated polymers are usually considered hydrophilic, hydrophobic interaction of the polypeptide backbone, and possibly hydrogen bonding via β -sheets as confirmed by CD spectroscopy, results in aggregation. TEM micrographs confirmed that these aggregates are non-uniform with large size variation in water. From the enlarged micrograph shown in the inset

of Figure 2.12 it seems that the aggregates consist of smaller tape-like assemblies. A detailed study into these phenomena is currently under way.

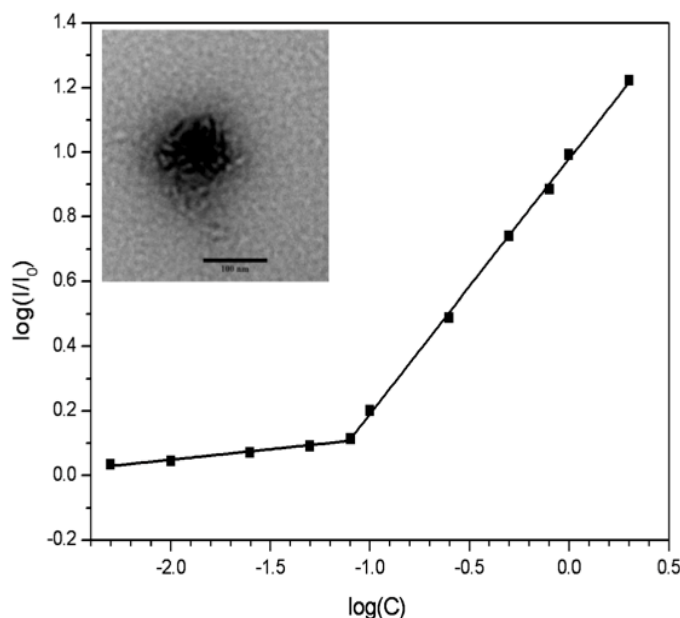


Figure 2.12: Relative fluorescence intensity of PNA as a function of the concentration of glycopeptides **7** in aqueous solution (C: concentration in mg/mL). The intersection of both lines marks the critical aggregation concentration. The inset shows a TEM micrograph of **7** in water (0.5 mg/mL); the scale bar represents 100 nm.

The glycosylation of copolymer **8** was carried out with the objective to investigate whether a selective deprotection of the benzyl ester groups of γ -benzyl-L-glutamate can be achieved. The success of the click reaction and the presence of galactose in the copolymer were confirmed from both $^1\text{H-NMR}$ (Figure 2.13) as well as FTIR spectra (Figure 2.9). This coincides with an increase of the molecular weight of the copolymer from 5800 to 7050 g/mol (Figure 2.14).

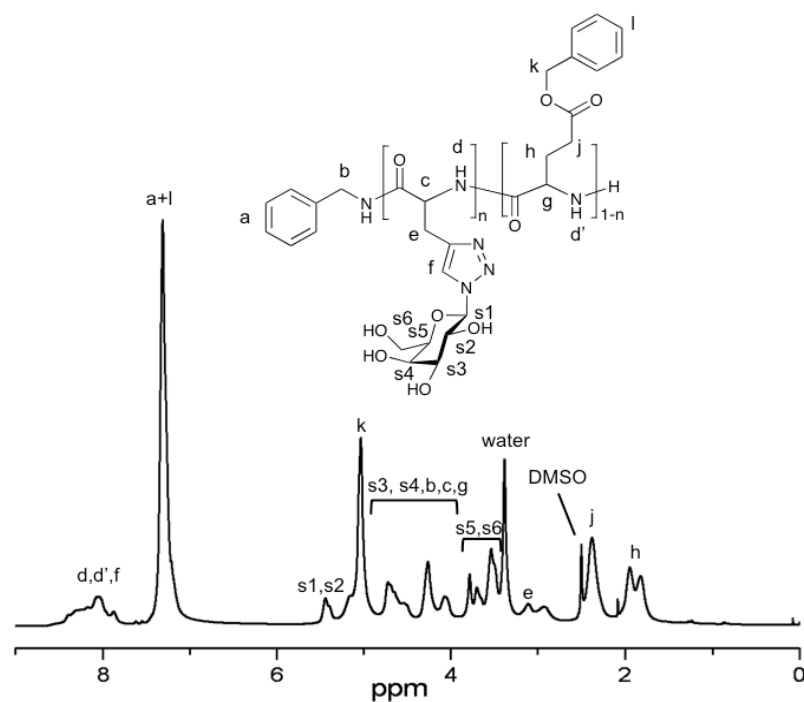


Figure 2.13: ^1H -NMR spectrum of glycosylated poly(γ -benzyl-L-glutamate-*co*-DL-propargylglycine) after click reaction (**9**) in DMSO-d^6 .

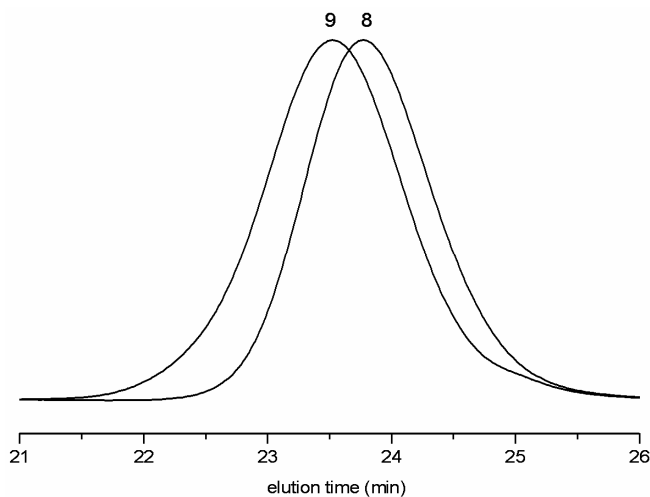


Figure 2.14: SEC traces (HFIP, PMMA standards) of poly(γ -benzyl-L-glutamate-*co*-DL-propargylglycine) (**8**, M_n : 5800 g/mol, PDI: 1.15) and the glycosylated poly(γ -benzyl-L-glutamate-*co*-DL-propargylglycine) obtained by click reaction with unprotected galactose (**9**, M_n : 7050 g/mol, PDI: 1.21).

In contrast to the homopolymer, glycosylation does not result in a change of the polypeptide helical conformation as neither the amide I nor the amide II band experience a shift in the spectrum. The benzyl ester hydrolysis of the glycosylated copolymer **9** was carried under acid conditions with HBr. Of analytical relevance is the shift of the carbonyl band from 1731 (ester) to 1716 cm^{-1} (acid). Moreover, the ^1H -NMR spectrum shows the complete disappearance of the signal at 7.5 ppm previously assigned to the aromatic benzyl ester protons (Figure 2.15). Most importantly, signals of the galactose units are still present. These experiments emphasize a major advantage over recently reported systems in which the alkyne functionality was introduced via ester bonds (e.g., using glutamic acid) and are potentially prone to hydrolysis under these conditions.²⁹⁻³¹

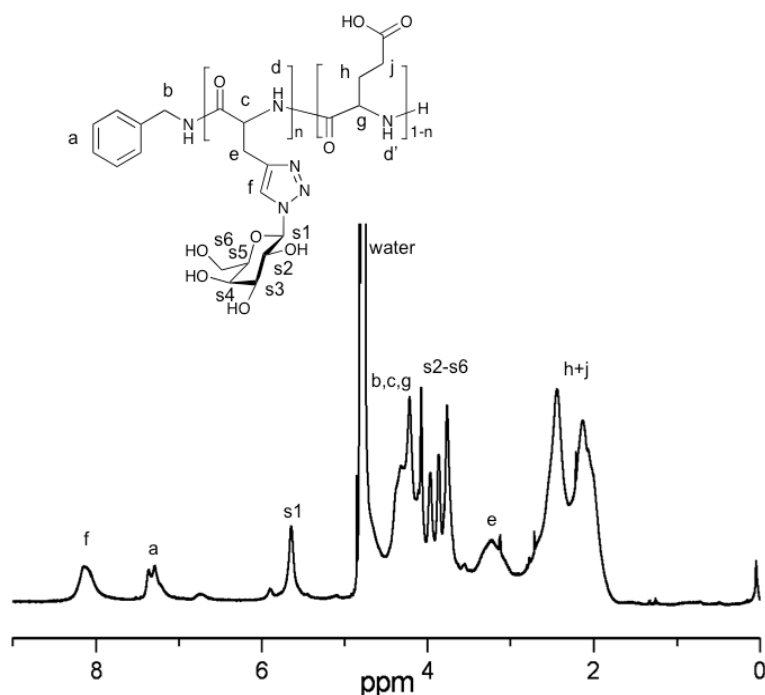


Figure 2.15: ^1H -NMR spectrum of crude polymer obtained after benzyl ester hydrolysis of glycosylated poly(γ -benzyl-L-glutamate-*co*-DL-propargylglycine) (**10**) in D_2O .

Finally, the ability of the synthesized glycopeptides **7** to interact with biological systems was assessed. Carbohydrates play a major role in biological recognition events mediated by specific carbohydrate-lectin interaction. While the exact mechanism of this interaction is still unknown, many studies show that it is highly specific and non-covalent. The *in vitro* evaluation of this specific binding event is thus a first test for the ability of a synthetic glycopolymer to interact with biological systems, for example for the development of drug delivery, tissue engineering or other biomedical materials.⁴⁸ Typically, these tests are conducted by mixing the glycopolymer with a lectin that is selective for the sugar conjugated to the polymer.^{4,8,49} A positive result is obtained by the appearance of a precipitation due to the aggregation of lectins measured as a reduced transparency of the solution. Since single sugar units only bind weakly to the lectin receptors, only multivalent binding will lead to lectin clustering and precipitation. *Ricinus Communis* Agglutinin (RCA₁₂₀) is a known specific lectin for the selective binding of galactosyl residues. We therefore systematically investigated the change in absorbance of solutions of glycopeptides **7** with RCA₁₂₀ at 450 nm. Upon addition of the glycopeptide in buffer solution to the lectin an immediate precipitation was visible (inset Figure 2.16). Further inspection of Figure 2.16 shows that the absorbance (i.e. turbidity) is higher for higher concentrations of glycopeptides. Moreover, at a glycopeptides concentration of 2 mg/mL the precipitation is so rapid that no change of absorbance was measured over time. At a concentration of 0.1 mg/mL the absorbance increases within the first 5 min. of the experiment and reaches a plateau. As a control experiment, PBS buffer solution without glycopeptide was added to RCA₁₂₀. Only a slight increase in absorbance was detected, however, significantly lower than for the samples containing glycopeptides. When the same reaction was carried out with Concanavalin A lectin (Con A), which is selective for glucosyl and mannosyl but unable to bind galactosyl residues, no significant precipitation was monitored. The slight increase in absorbance monitored for Con A is in the range of the change detected for the control. These experiments confirm that the glycopeptides synthesized by the click reaction of azido galactose to poly(DL-propargylglycine) are active in biorecognition. The lectin binding is selective and, depending on the concentration,

instantaneous. In particular, no adverse effect of the triazole ring on the lectin binding was observed.

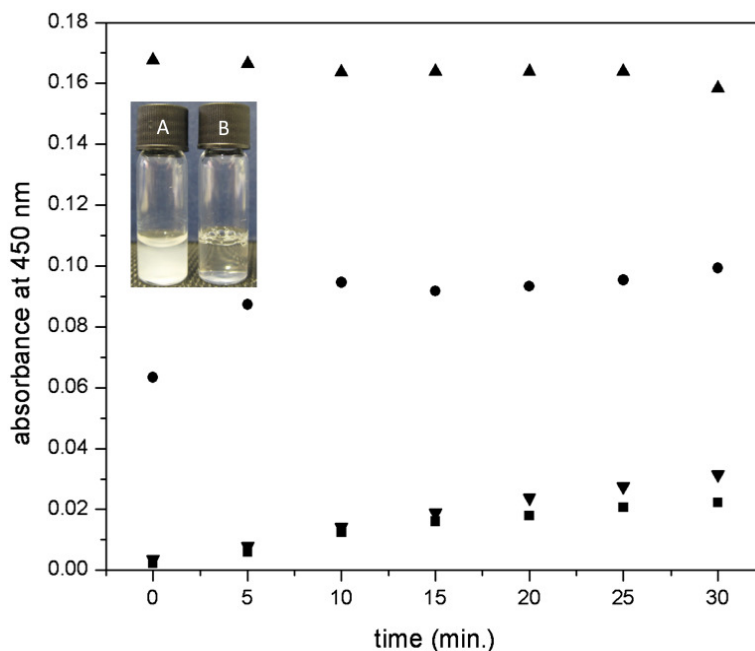


Figure 2.16: Absorbance (450 nm) of glycopeptides **7** solution upon reaction with two different lectins in PBS buffer: (▲) lectin RCA₁₂₀, glycopeptide concentration 2 mg/mL; (●) lectin RCA₁₂₀, glycopeptide concentration 0.1 mg/mL; (■) lectin RCA₁₂₀, PBS buffer without glycopeptide; (▼) lectin Con A, glycopeptide concentration 2 mg/mL. The inset shows the glycopeptide solution at 2 mg/mL with (A) RCA₁₂₀ and (B) Con A present.

2.4 Conclusions

We have shown that synthetic glycopeptides can be readily obtained by Huisgen [3+2] cycloaddition of azide functional galactose to alkyne-functional homo and copolypeptides. The fast and selective biorecognition was demonstrated by lectin clustering experiments. The fact that no labile bond was used to link the alkyne to the amino acid allows applying common amino acid deprotection chemistry on the glycopeptides as was shown for γ -benzyl-L-glutamate copolymer. The isosteric linkage thus improves the chemical and potentially metabolic stability while retaining biological activity. This presents a major advantage for the application of this approach for the synthesis of more complex polypeptides for a variety of structurally diverse biomimetic analogues.

2.5 References

- ¹ Gamblin, D. P.; Scanlan, E. M.; Davis, B. G. *Chem. Rev.* **2009**, *1*, 131.
- ² Spain, S. G.; Gibson, M. I.; Cameron, N. R. *J. Polym. Sci. A; Polym. Chem.* **2007**, *11*, 2059.
- ³ Ladmiral, V.; Melia, E.; Haddleton, D. M. *Eur. Polym. J.* **2004**, *3*, 431.
- ⁴ Ting, S.R.S.; Min, E. H.; Escalé, P.; Save, M.; Billon, L.; Stenzel, M. H. *Macromolecules* **2009**, *42*, 9422.
- ⁵ Albertin, L.; Cameron, N. R. *Macromolecules* **2007**, *40*, 6082.
- ⁶ Chen, G. J.; Tao L.; Mantovani, G.; Geng, J.; Nystrom, D.; Haddleton, D. M. *Macromolecules* **2007**, *40*, 7513.
- ⁷ Deng, Z. C.; Ahmed, M.; Narain, R. *J. Polym. Sci A: Polym. Chem.* **2009**, *47*, 614.
- ⁸ Ladmiral, V.; Mantovani, G.; Clarkson, G. J.; Cauet, S.; Irwin, J. L.; Haddleton, D. M. *J. Am. Chem. Soc.* **2006**, *14*, 4823.
- ⁹ Klok, H.-A. *Macromolecules* **2009**, *42*, 7990.
- ¹⁰ Kricheldorf, H. R. *Angew. Chem. Int. Ed.* **2006**, *45*, 572.
- ¹¹ Hadjichristidis, N.; Iatrou, H.; Pitskalis, M.; Sakellariou, G. *Chem. Rev.* **2009**, *109*, 5528.
- ¹² Deming, T. J. *Adv. Polym. Sci.* **2006**, *202*, 1.
- ¹³ Schlaad, H. *Adv. Polym. Sci.* **2006**, *202*, 53.
- ¹⁴ Lu, H.; Cheng, J. *J. Am. Chem. Soc.* **2007**, *129*, 14114.
- ¹⁵ Klok, H.-A.; Lecommandoux, S. *Adv. Polym. Sci.* **2006**, *202*, 75.
- ¹⁶ Aoi, K.; Tsutsumiuchi, K.; Okada, M. *Macromolecules* **1994**, *3*, 875.
- ¹⁷ Gibson, M. I.; Hunt, G. J.; Cameron, N. R. *Org. Biomol. Chem.* **2007**, *17*, 2756.
- ¹⁸ Wu, P.; Feldman, A. K.; Nugent, A. K.; Hawker, C. J.; Scheel, A.; Voit, B.; Pyun, J.; Frechet, J. M.; Sharpless, K. B.; Fokin, V. V. *Angew. Chem., Int. Ed.* **2004**, *43*, 3928.
- ¹⁹ Malkoch, M.; Schleicher, K.; Drockenmuller, E.; Hawker, C. J.; Russell, T. P.; Peng Wu; Fokin, V. V. *Macromolecules*, **2005**, *38*, 3663.
- ²⁰ van Kasteren, S. I.; Kramer, H. B.; Jensen, H. H.; Campbell, S. J.; Kirkpatrick, J.; Oldham, N. J.; Anthony, D. C.; and Davis, B. G. *Nature* **2007**, *446*, 1105.

- ²¹ Lin, H.; Walsh, C. T. *J. Am. Chem. Soc.* **2004**, 126, 13998.
- ²² Wan, Q.; Chen, J.; Chen, G., and Danishefsky, S. J. *J. Org. Chem.* **2006**, 71, 8244.
- ²³ Agut, W.; Taton, D.; Lecommandoux S. *Macromolecules* **2007**, 40, 5653.
- ²⁴ Schatz, C. ; Louguet, S.; Le Meins, J. F. ; Lecommandoux, S. *Angew. Chem. Int. Ed.* **2009**, 48, 2572.
- ²⁵ Upadhyay, K. K.; Meins, J. F.; Misra, A.; Voisin, P.; Bouchaud, V.; Ibarboure, E.; Schatz, C.; Lecommandoux, S. *Biomacromolecules* **2009**, 10, 2802.
- ²⁶ Upadhyay, K. K.; Bhatt, A. N.; Mishra, A. K.; Dwarakanath, B. S; Jain, S.; Schatz, C.; Le Meins, J. F.; Farooque, A.; Chandraiah, G.; Jain, A. K.; Misra, A.; Lecommandoux, S. *Biomaterials*, **2010**, 31, 2882.
- ²⁷ Habraken, G. J. M.; Koning, C. E.; Heuts, J. P. A.; Heise, A. *Chem. Commun.* **2009**, 24, 3612-3614.
- ²⁸ Sun, J.; Schlaad, H. *Macromolecules* **2010**, 43, 4445.
- ²⁹ Engler, A. C., Hyung-il Lee, Hammond, P. T. *Angew. Chem. Int. Ed.* **2009**, 48, 9334.
- ³⁰ Chunsheng Xiao, Changwen Zhao, Pan He, Zhaohui Tang, Xuesi Chen, Xiabin Jing *Macromol. Rapid Commun.* **2010**, 31, 991.
- ³¹ Tang, H. Y.; Zhang, D. H. *Biomacromolecules* **2010**,
- ³² Kuijpers, B. H. M.; Groothuys, S.; Keereweer, A. R.; Quaedflieg, P. J. L. M.; Blaauw, R. H.; van Delft, F. L.; and Rutjes, F. P. J. T. *Org. Lett.* **2004**, 6, 3123.
- ³³ Habraken, G. J. M.; Koning, C. E.; Heise, A. *J. Polym. Sci. A; Polym. Chem.* **2009**, 47, 6883.
- ³⁴ Maier, M. A.; Yannopoulos, C. G.; Mohamed, N.; Roland, A.; Fritz, H.; Mohan, V, Just, G.; Manoharan, M. *Bioconjugate Chem.* **2003**, 14, 18.
- ³⁵ Hayes, W.; Osborn, H. M. I.; Osborne, S. D.; Rastall, R. A.; Romagnoli, B. *Tetrahedron* **2003**, 59, 7983.
- ³⁶ Tian, Z.; Wang, M.; Zhang A. Y.; Feng, Z. G. *Polymer* **2008**, 49, 446.
- ³⁷ Liang, Y. Z.; Li, Z. C.; Li, F. C. *J. Colloid Interface Sci.* **2000**, 224, 84.
- ³⁸ Habraken, G. J. M.; Peeters, M.; Dietz, C. H. J. T.; Koning, C. E.; Heise, A. *Polym. Chem.* **2010**, 1, 514.
- ³⁹ Schlögl, K.; Pelousek, H. *Monatsh. Chem.* **1960**, 91, 227.

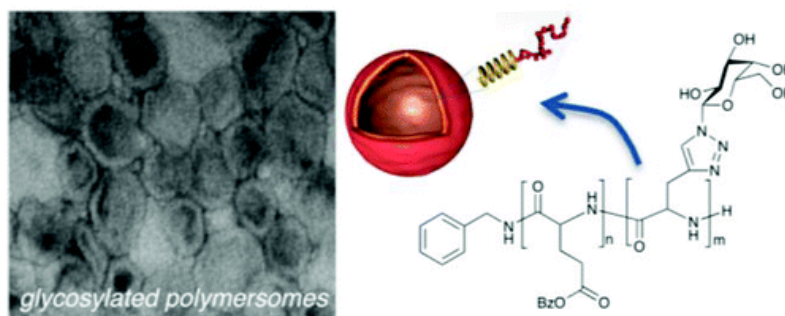
- ⁴⁰ Guinn, R. M.; Margot, A. O.; Taylor, J. R.; Schumacher, M.; Clark, D. S.; Blanch, H. W. *Biopolymers* **1995**, *35*, 503.
- ⁴¹ Henkel, B.; Bayer, E. *J. Peptide Sci.* **1998**, *4*, 461.
- ⁴² Akaike, T.; Inoue, S.; Itoh, K. *Biopolymers* **1976**, *15*, 1863.
- ⁴³ Willemse, R. X. E.; Staal, B. B. P.; Donkers, E. H. D.; Herk, A. M. *Macromolecules* **2004**, *15*, 5717.
- ⁴⁴ Huijser, S. In *Synthesis and characterization of biodegradable polyesters: polymerisation mechanisms and polymer microstructures revealed by MALDI-ToF-MS*. 2009. thesis Eindhoven: Technische Universiteit.
- ⁴⁵ Willemse, R.X.E., Herk A.M. *J. Am. Chem. Soc.* **2006**, *128*, 4471.
- ⁴⁶ McClure, W. O.; Edelman, G. M. *Biochem.* **1966**, *5*, 1908.
- ⁴⁷ Liang, Y. Z.; Li, Z. C.; Li, F. M. *J. Colloid Interface Sci.* **2000**, *1*, 84.
- ⁴⁸ Ambrosi, M.; Cameron, N. R.; Davis, B.G. *Org. Biomol. Chem.* **2005**, *3*, 1593.
- ⁴⁹ Park, J.; Rader, L. H.; Thomas, G. B.; Danoff, E. J.; English, D. S.; D., P. *Soft Matter* **2008**, *4*, 1916.

Chapter 3

Biologically active polymersomes from amphiphilic glycopeptides

Abstract

Polypeptide block copolymers with different block length ratios were obtained by sequential ring opening polymerisation of benzyl-L-glutamate (BLG) and propargyl-glycine (PG) N-carboxyanhydrides (NCA). Glycosylation of the poly(propargylglycine) block was obtained by Huisgens cycloaddition click reaction using azide functional galactose. All copolymers were self-assembled using the nanoprecipitation method to obtain spherical and worm-like micelles as well as polymersomes, depending on the block length ratio and the nanoprecipitation conditions. These structures display bioactive galactose units in the polymersome shell as proven by selective lectin binding experiments.



This chapter was published in
Huang, J.; Bonduelle, C.; Thévenot, J.; Lecommandoux, S.; Heise, A. J.
***Am. Chem. Soc.* 2012, 134, 119.**

The "Self-assembly" work of this chapter was done in collaboration with Prof. Sébastien Lecommandoux in Université de Bordeaux.

3.1 Introduction

The targeted delivery of highly specific next generation drugs such as biopharma therapeutics (peptides, proteins and nucleic acids) requires the development of new smart drug delivery systems.¹ In this respect, carriers resulting from the self-assembly of amphiphilic block copolymers offer a wide scope of possibilities.² Important factors that determine the morphology obtained from these molecules are the block length ratio of the hydrophilic and hydrophobic block as well as the processing conditions.³ Accordingly, morphologies can range from spherical to worm-like micelles and vesicles.⁴ While micelles are the most intensively studied and worm-like micelles have recently shown very promising long-term blood circulation, their use being mainly limited to the loading of hydrophobic drugs.^{5,6} Polymersomes, on the other hand, are ideally suited containers as they combine the ability to carry a high payload of both hydrophobic and hydrophilic drugs.⁷ For targeted drug delivery, polymersomes should display biological recognition units on the surface for specific interactions with cells. For the latter, glycans, i.e. carbohydrates, are ideal candidates as they play an important role in cell interaction and recognition.^{8,9} Three different approaches have been explored so far for the synthesis of glycopolymeric vesicles: (1) conjugation of glycans to preformed polymersomes¹⁰, (2) formation of polymersomes from end-functionalized synthetic block copolymers¹¹ and (3) formation of polymersomes from polymers comprising biomolecules-containing hydrophilic blocks.¹² The last approach favors the formation of polymersomes with a highly functionalized inner and outer surface. This allows biomolecules to be located in deeper layers, resulting in enhanced interaction with the biological target compared to end-functionalized block copolymers approaches.

Alternative to purely synthetic polymers, polypeptide-based copolymers show considerable promise as building blocks for polymersomes. Besides their biodegradability, the supramolecular organization of peptides offers an opportunity to produce hierarchical structures and can also be used to promote specific “bioactivity”.¹³ For example, it has been highlighted that the helical conformation of

a hydrophobic peptide segment such as poly(γ -benzyl-L-glutamate) (PBLG) is an efficient way to form and stabilize vesicles.¹⁴ Block copolymers combining a polypeptide and an oligosaccharide block have previously been used to prepare glycoprotein biomimetic polymersomes.¹⁵ This promising approach allowed the preparation, by chemical coupling, of dextran-*b*-PBLG and hyaluronan-*b*-PBLG. In aqueous solution, these simple glycoprotein analogues self-assemble in glycopeptidic polymersomes (glycopeptosomes) with structure and properties similar to viral capsids. However, this approach is not cost-effective and requires well-defined oligosaccharides.

We therefore disclose the efficient synthesis of novel amphiphilic glycopeptide block copolymers and their formulation into lectin binding polymersomes. In this design, carbohydrates are introduced on the side chains of the hydrophilic segment that fulfill a dual function by promoting self-assembly and specific binding. The synthetic protocol, using controlled polypeptide synthesis and post-glycosylation, as well as the self-assembly protocol permit extensive control over the morphology of the structures formed. Composed entirely of amino acids and natural carbohydrates our approach omits the use of synthetic polymers, and offers a fully biocompatible system.

3.2 Experimental section

Materials

All chemicals were purchased from Sigma-Aldrich and used as received unless otherwise noted. γ -Benzyl-L-glutamate and DL-propargylglycine were supplied by Bachem. Anhydrous DMF, DMSO, ethyl acetate, THF, methanol were used directly from the bottle under an inert and dry atmosphere. *Ricinus communis* (castor bean) Agglutinin RCA₁₂₀ (10 mg/mL in buffered aqueous solution) and Concanavalin A (Con A, Type IV, lyophilized powder) from *Canavalia ensiformis* (Jack bean) were purchased from Aldrich and used as received.

Methods

^1H and ^{13}C NMR spectra were recorded at room temperature with a Bruker Avance 400 (400 MHz) and a Bruker Avance Ultrashield 600 (600 MHz). DMSO- d_6 , CDCl_3 , Acetone- d_6 and D_2O were used as solvents and signals were referred to the signal of residual protonated solvent signals. TMS was used as an internal standard for DMSO- d_6 and CDCl_3 . ATR-FTIR spectra were collected on a Perkin Elmer Spectrum 100 in the spectral region of $650\text{--}4000\text{ cm}^{-1}$ and were obtained from 4 scans with a resolution of 2 cm^{-1} . A background measurement was taken before the sample was loaded onto the ATR unit for measurements. SEC analysis using HFIP (Biosolve, AR from supplier or redistilled) as eluent was carried out using a Shimadzu LC-10AD pump (flow rate 0.8 mL/min) and a WATERS 2414 differential refractive index detector (at $35\text{ }^\circ\text{C}$) calibrated with poly(methyl methacrylate) (range 1000 to 2000000 g/mol). Two PSS PFG-lin-XL ($7\text{ }\mu\text{m}$, $8\times 300\text{ mm}$) columns at 40°C were used. Injections were done by a Spark Holland MIDAS injector using a $50\text{ }\mu\text{L}$ injection volume. Before SEC analysis was performed, the samples were filtered through a $0.2\text{ }\mu\text{m}$ PTFE filter (13 mm , PP housing, Alltech). The turbidity assay of the lectin with different concentrations of glycopeptides was monitored at 450 nm in Varian Cary 50 by UV quartz cuvette. CD data were collected on a Jasco J-810 CD spectrometer (Japan Spectroscopic Corporation) with a path length of 0.1 cm and a band width of 1 nm . Three scans were conducted and averaged between 185 nm and 250 nm at a scanning rate of 20 nm min^{-1} with a resolution of 0.2 nm . The data were processed by subtracting the DI water as background and smoothing with Means-Movement method with a convolution of 5. Transmission Electron Microscopy (TEM) images were recorded on a Hitachi H7650 microscope working at 80 kV equipped with a GATAN Orius 11 Megapixel camera. Samples were prepared by spraying a 1 g/L solution of the block copolymer onto a copper grid (200 mesh coated with carbon) using a homemade spray tool and negatively stained with 1% uranyl acetate. Dynamic Light Scattering (DLS) and Static Light Scattering (SLS) was used to obtain the average size of the particles right after dialysis by using a Malvern ZetaSizer NanoZS instrument with 90° backscattering measurements at $25\text{ }^\circ\text{C}$. To determine radius of gyration (R_G) and hydrodynamic radius (R_H), multiangle light-scattering analysis was achieved with

an ALV laser goniometer, with a 22 mW linearly polarized laser (632.8 nm HeNe) and an ALV-5000/EPP multiple tau digital correlator (125 ns initial sampling time). All the measurements were performed at a constant temperature of 25 °C. The accessible scattering angles range from 40 to 140°. The solutions were placed in 10 mm diameter glass cells. Data were acquired with ALV correlator control software, and the counting time was fixed for each sample at 60 s. The hydrodynamic radius was calculated from the diffusion coefficient using the Stokes-Einstein relation and the gyration radius was calculated from a guinier plot. Atomic Force Microscopy (AFM) images were recorded in air with a Nanoscope III microscope operating in dry Tapping mode. The probes were commercially available silicon tips with a spring constant of 42 N/m, a resonance frequency of 285 kHz and a typical radius of curvature in the 10-12 nm range. Freshly cleaved mica was used as sample substrate materials.

Synthesis of γ -benzyl-L-glutamate NCA. α -Pinene (31.29 g, 229.68 mmol) and γ -benzyl-L-glutamate (15.0 g, 63.3 mmol) were dissolved in 120 mL anhydrous ethyl acetate in a three-neck round-bottomed flask. The mixture was stirred and heated to reflux. Then a solution of triphosgene (10.34 g, 34.8 mmol) in anhydrous ethyl acetate (60 mL) was added drop-wise. Two-third of the solution was added within 1 h, and the reaction was left at reflux for another hour. Then, the rest of the triphosgene solution was added until the γ -benzyl-L-glutamate completely disappeared. Subsequently, around 90 mL of the solvent was removed under pressure and 180 mL n-heptane was added slowly to precipitate NCA. The mixture was allowed to cool down to room temperature and then placed in a freezer overnight. After filtration, the solid was recrystallized by ethyl acetate and n-heptane twice, and then washed with n-heptane. The NCA was recovered as white crystal after being dried under vacuum. Mp 94 °C, Yield: 12.6 g (83%). $^1\text{H-NMR}$ (400MHz, CDCl_3 , δ , ppm): 2.13 (m, 2H, CH_2), 2.59 (t, 2H, CH_2 , $J=7.09$ Hz), 4.37 (t, 1H, CH , $J=6.56$ Hz), 5.13 (s, 2H, CH_2O), 6.75 (s, 1H, NH), 7.35 (m, 5H, ArH). $^{13}\text{C-NMR}$ (400MHz, CDCl_3 , δ , ppm): 26.98 (CH_2CH), 29.87 (CH_2CO), 57.01 (CH), 67.22 (CH_2O), 128.48 (ArH), 128.71 (ArH), 128.83 (ArH), 135.30 (ArH), 152.10 (NHC(O)O), 169.53 ($\text{CH}_2\text{C(O)O}$), 172.51 (CHC(O)O).

Synthesis of DL-propargylglycine NCA. DL-propargylglycine (2.5 g, 22.1 mmol) and α -pinene (14.88 g, 109 mmol) were dissolved in 60 mL anhydrous THF in a three-neck round-bottom flask. The reaction mixture was heated to 50 °C under nitrogen and then triphosgene (4.92 g, 16.6 mmol) in 20 mL THF was added dropwise over a period of 1 hour. The reaction was continued for 4 hours until the mixture became gradually clear. The mixture was concentrated under reduced pressure and the NCA precipitated by addition of 100 mL n-heptane. The mixture was then placed in a freezer overnight. After filtration, the crude product was dissolved in dry THF, and re-crystallized twice by addition of n-heptane. The obtained solid was washed with n-heptane, yielding white crystals in 75% yield. ^1H -NMR (400 MHz, Acetone- d_6 , δ , ppm): 2.62 (t, $J = 2.5$ Hz, 1H, $\equiv\text{CH}$), 2.86 (dd, $J = 4.5$ and 2.5 Hz, 2H, $-\text{CH}_2-\text{C}\equiv$), 4.75 (t, $J = 4.5$ Hz, 1H, CH), 8.05 (s, 1H, NH), ^{13}C -NMR (400 MHz, Acetone- d_6 , δ , ppm): 22.26 ($-\underline{\text{C}}\text{H}_2-\text{C}\equiv$), 57.30 ($\underline{\text{C}}\text{H}$), 73.64 ($\equiv\text{CH}$), 78.23 ($-\underline{\text{C}}\equiv\text{CH}$), 152.71 ($-\text{O}(\underline{\text{C}}\text{O})\text{NH}-$), 170.62 ($-\text{O}(\underline{\text{C}}\text{O})\text{CH}$). FTIR (neat, cm^{-1}): 3363, 3247, 1854, 1771, 1286, 1195, 1111, 1089, 934, 893, 777, 756, 723, 698, 668. Mp: 114 °C.

Typical synthesis procedure of poly(γ -benzyl-L-glutamate-*b*-DL-propargylglycine). The NCA monomer of γ -benzyl-L-glutamate (1.01 g, 3.82 mmol) was dissolved in 9 mL DMF in a Schlenk tube. A solution of benzylamine (20.44 mg, 0.191 mmol) in 2 mL dry DMF was added after NCA was dissolved. The reaction was left to stir in a cold water bath of 0 °C for 4 days under an inert atmosphere. After BLG-NCA had been completely consumed as monitored by FTIR and NMR, and the PBLG macroinitiator was added to a solution of DL-propargylglycine NCA (267 mg, 1.9 mmol) in DMSO at room temperature. The reaction mixture was left to stir for another five days. The reaction mixture was precipitated into an excess diethylether, filtered and dried under vacuum as off-white solid (Yield 80%).

Synthesis of 1-Azido-1-deoxy- β -D-galactopyranoside (1-azido- β -galactose). To a solution of 1- α -Bromo-2,3,4,6-tetraacetyl-D-galactose (5.69 g, 13.8 mmol) in 57 mL CH_2Cl_2 at room temperature was added NaN_3 (4.5 g, 69.1 mmol), tetrabutylammonium hydrogen sulfate (4.7 g, 13.8 mmol) and 57 mL of a saturated solution of NaHCO_3 . The reaction mixture was stirred vigorously at room

temperature for 4 hours and then diluted with 500 mL ethyl acetate. The organic layer was washed with 200 mL of a saturated solution of NaHCO_3 and evaporated under reduced pressure. 1- β -Azido-2,3,4,6-tetraacetyl-D-galactose was obtained as a pale yellow solid. Recrystallization from methanol yielded as white crystals (4.10 g, Yield 80%). Mp 94-96 °C, ^1H -NMR (400 MHz, CDCl_3 , δ , ppm): 1.99, 2.07, 2.10, 2.18 (4s, 12H, 4 \times CH_3CO), 4.00-4.03 (m, 1H, H-6a'), 4.13-4.21 (m, 2H, H-5 and H-6b'), 4.61 (d, 1H, H-1), 5.06 (dd, 1H, H-3), 5.17 (dd, 1H, H-2), 5.42 (dd, 1H, H-4). ^{13}C -NMR (400 MHz, CDCl_3 , δ , ppm): 20.44, 20.53, 20.57, 20.58 (CH_3CO), 61.20 (C-6), 66.84 (C-4), 68.00 (C-3), 70.63 (C-5), 72.75 (C-2), 88.15 (C-1), 169.31, 169.90, 170.06, 170.29 (CH_3CO).

1- β -Azido-2,3,4,6-tetraacetyl-D-galactose (373 mg, 1 mmol) was dissolved in 5 mL anhydrous methanol in a Schlenk tube. To this solution a catalytic amount of anhydrous potassium carbonate (6 mg, 0.04 mmol) was added and the reaction mixture was vigorously stirred at room temperature under a nitrogen atmosphere for 3 hours. Amberlite IR-120 ion-exchange resin was washed with methanol and then added to and stirred with the reaction mixture for 1 hour. The resin was then filtered off under gravity and the resulting solution was concentrated to dryness in vacuum to yield a white powder (184 mg, Yield 90%). Mp 150 °C. ^1H -NMR (400 MHz, D_2O , δ , ppm): 3.49 (dd, $J_{2-1}=8.7\text{Hz}$, $J_{2-3}=9.8\text{Hz}$, 1H, H-2), 3.66 (dd, $J_{3-2}=9.8\text{Hz}$, $J_{3-4}=3.3\text{Hz}$, 1H, H-3), 3.72-3.78 (m, 3H, H-5, H-6a', H-6b'), 3.94 (d, $J_{4-3}=3.3\text{Hz}$, 1H, H-4), 4.64 (d, $J_{1-2}=8.7\text{Hz}$, 1H, H-1). ^{13}C -NMR (400 MHz, D_2O , δ , ppm): 63.44 (C-6), 71.00 (C-4), 72.81 (C-3), 75.13 (C-5), 79.70 (C-2), 93.05 (C-1).

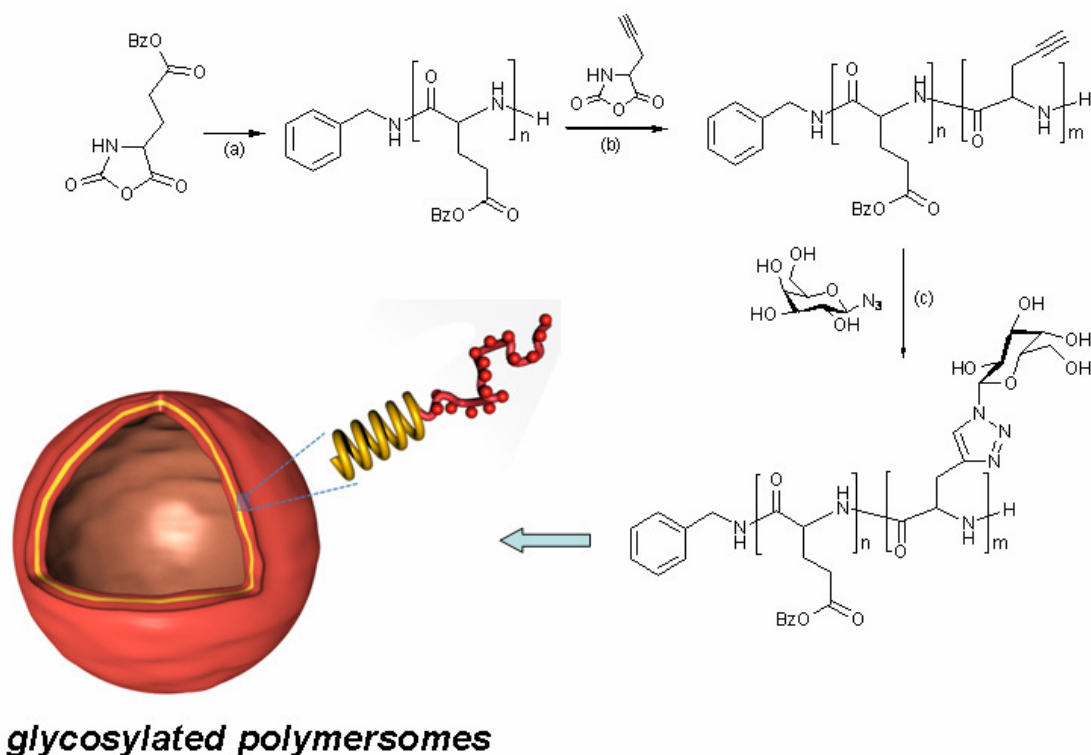
Typical glycosylation procedure of poly (γ -benzyl-L-glutamate-*b*-DL-propargylglycine). Poly(γ -benzyl-L-glutamate-*b*-DL-propargylglycine) (400 mg, ca. 0.735 mmol of alkyne units), 1-Azido-1-deoxy- β -D-galactopyranoside (226 mg, 1.102 mmol, 1.5 equiv. to alkyne groups) and triethylamine (51 μL , 0.367 mmol, 0.5 equiv) were dissolved in 8 mL of anhydrous DMSO in the Schlenk tube. The mixture was stirred and degassed by bubbling nitrogen for 30 min. $(\text{PPh}_3)_3\text{CuBr}$ (68 mg, 0.0735 mmol, 0.1 equiv.) was then added and nitrogen was bubbled through the resulting solution for another 30 min. The Schlenk tube was placed in an oil bath at 30 °C for 72 h under nitrogen atmosphere. Ion exchange resin (150 mg) was added, and the suspension gently stirred at ambient temperature overnight. After filtration

and centrifugation, the polymer solution precipitated in a 2:1 THF/diethyl ether mixture and was washed by THF twice. The polymer was separated by centrifugation and dialyzed against distilled water for 3 days, then lyophilized as off-white polymer (Yield 60%). ^1H -NMR and ^{13}C -NMR spectra are shown in Figure 3.2 and 3.3.

Carbohydrate-lectin binding experiments. The lectin recognition activity of the glycopeptide solution was analyzed by the change of the turbidity at 450 nm at room temperature. 2 mg/mL of RCA₁₂₀ lectin was prepared in DI water. 600 μL lectin solution were transferred into a cuvette and a baseline measured. A solution of 60 μL glycopeptide with different concentrations in DI water was added into the cuvette containing the lectin solution. The solution in the cuvette was gently mixed using a pipette and immediately the absorbance at 450 nm was recorded every 10 min. As a control lectin Con A was used under the same experimental conditions.

Nanoprecipitation. Method 1: 0.5 mL of block copolymer solution in DMSO (10 mg/mL, filtered with 0.22 μm polypropylene membrane) was placed into a glass vial and 4.5 mL of ultrapure water was added instantaneously (1 s) under magnetic stirring (500 rpm). The mixture was dialyzed 24 h against water (Spectra/Por[®] MWCO 50 kDa membrane) to remove DMSO.

Method 2: 0.5 mL of block copolymer solution in DMSO (10 mg/mL, filtered with 0.22 μm polypropylene membrane) was added instantaneously (1 s) into a glass vial containing 4.5 mL of ultrapure water under magnetic stirring (500 rpm). The mixture was dialyzed 24 h against water (Spectra/Por[®] MWCO 50 kDa membrane) to remove DMSO.



Scheme 3.1: Synthesis of (PBLG-*b*-PGG) glycopeptides block copolymers. (a) DMF, benzylamine, 0 °C; (b) DMSO, r.t.; (c) Cu(PPh₃)₃Br, Et₃N, DMSO, 30 °C.

3.3 Results and Discussion

We propose PBLG-*b*-poly(galactosylated propargylglycine) (PBLG-*b*-PGG) copolymers as candidates to prepare glycopeptidic vesicles with lectine binding galactose presented at the polymersome surface (Scheme 3.1). The preparation of the block copolymer is based on our previously reported synthesis of glycopeptides by Huisgens click reaction of azide-functionalized galactose to poly(propargylglycine).¹⁶ The latter can easily be obtained by ring-opening polymerisation of the N-carboxyanhydride (NCA) of propargylglycine (PG). Building on this synthetic strategy, amphiphilic block copolymers were obtained by sequential polymerisation of γ -benzyl-L-glutamate (BLG) NCA and propargylglycine (PG) NCA, and subsequent glycosylation by click reaction (Scheme 3.1). Due to the better solubility of the PBLG block, BLG-NCA

polymerisation was carried out first in DMF at 0 °C in order to prevent end-group termination.¹⁷ After 4 days, BLG-NCA had been completely consumed as monitored by FTIR and NMR, and the PBLG macroinitiator was added to PG-NCA in DMSO at room temperature for chain extension. While the ratio of initiator to BLG-NCA was kept constant at 1:20, the ratio of PG-NCA to BLG-NCA was successively increased from 5:20 to 40:20 to obtain a library of block copolymers with increasing ratios of hydrophilic (glycosylated) to hydrophobic blocks.

Analysis of the block copolymers by size exclusion chromatography (SEC) and ¹H-NMR spectroscopy confirmed a low polydispersity index (PDI) of ~ 1.1 and good agreement of the polymer composition with the monomer feed ratio. As shown in Figure 3.1, FTIR spectra of block copolymers displayed amide bands typical of both α -helical (1651 and 1544 cm⁻¹) and β -sheet conformations (1630 and 1513 cm⁻¹). As the latter band became more pronounced with increasing chain length of PG, these were assigned to the β -sheet conformation of this block.

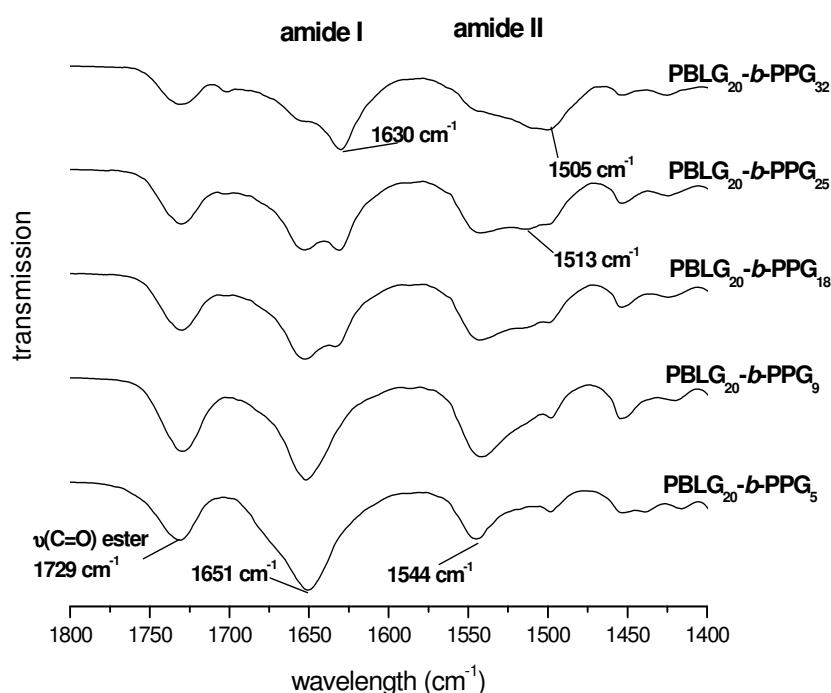


Figure 3.1: FTIR spectra of different block copolymers before glycosylation.

Table 3.1: Glycosylated peptide block copolymers (BLG: γ -benzyl-L-glutamate, PG: propargylglycine, PGG: glycosylated poly(propargylglycine)).

Block Copolymer^a	M_n^b before glycosylation (g/mol)	M_n^b after glycosylation (g/mol)	PDI^b after glycosylation	Hydrophilic weight ratio
PBLG ₂₀ - <i>b</i> -PGG ₅	5800	9200	1.10	25%
PBLG ₂₀ - <i>b</i> -PGG ₉	7400	9700	1.07	38%
PBLG ₂₀ - <i>b</i> -PGG ₁₈	7800	11200	1.08	55%
PBLG ₂₀ - <i>b</i> -PGG ₂₅	8200	11500	1.17	63%
PBLG ₂₀ - <i>b</i> -PGG ₃₂	9300	16200	1.17	68%

^a Calculated from ¹H NMR using the integrated peak ratios of PBLG at 5.0 ppm (-O-CH₂-C₆H₅) and the combined PPG/PBLG backbone (C_α) signals at 3.8-4.6 ppm (-CH-CO-) while using the PBLG aromatic signal at 7.3 ppm as an internal standard.

^b Determined by SEC in HFIP with PMMA standards.

Glycosylation of the block copolymers was subsequently carried out with azide-functionalized galactose via Huisgens cycloaddition click reaction (Scheme 3.1). The success of the click reaction and presence of galactose in the block copolymers were monitored by SEC, ¹H and ¹³C NMR (Figure 3.2 and Figure 3.3), as well as FTIR spectroscopy (Figure 3.4). The addition of galactose to the PG block coincides with a significant increase of the molecular weight of all block copolymers (Table 3.1). Moreover, the complete disappearance of alkyne peaks at 73 ppm and 80 ppm in the ¹³C NMR spectra of the block copolymers suggests a nearly quantitative glycosylation of the materials.

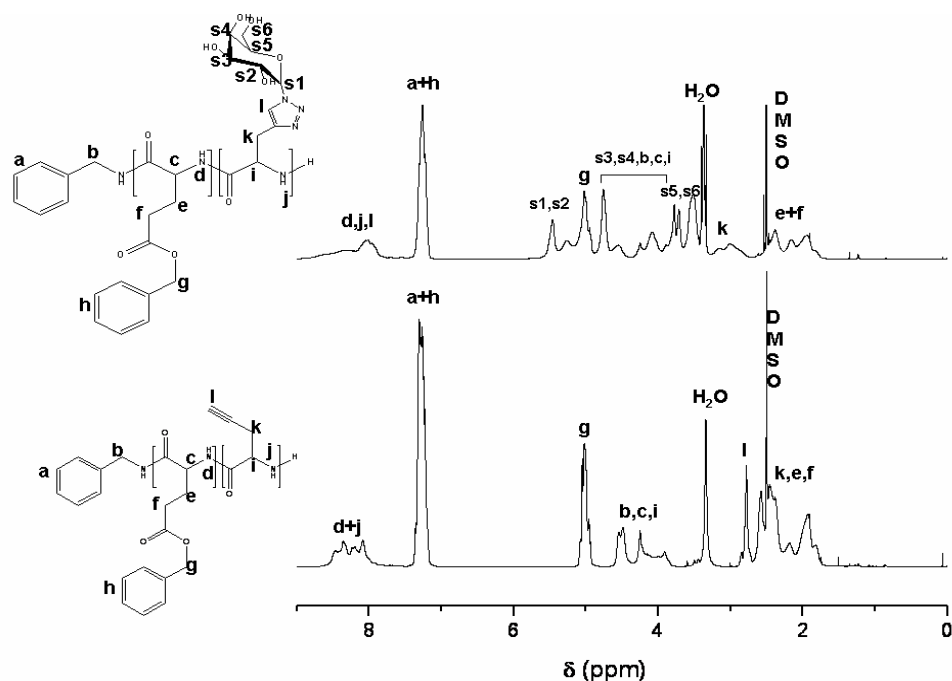


Figure 3.2: ^1H -NMR spectra of poly(γ -benzyl-L-glutamate-*b*-DL-propargylglycine) (PBLG₂₀-*b*-PG₂₅) before (bottom) and after glycosylation (top) in DMSO- d^6 .

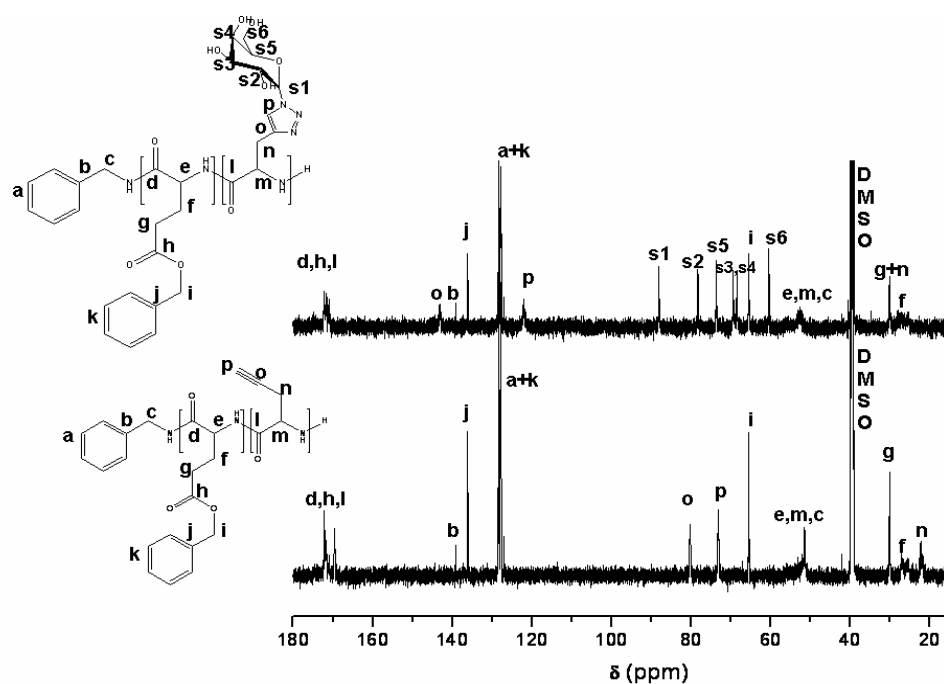


Figure 3.3: ^{13}C -NMR spectra of poly(γ -benzyl-L-glutamate-*b*-DL-propargylglycine) (PBLG₂₀-*b*-PG₂₅) before (bottom) and after glycosylation (top) in DMSO- d^6 .

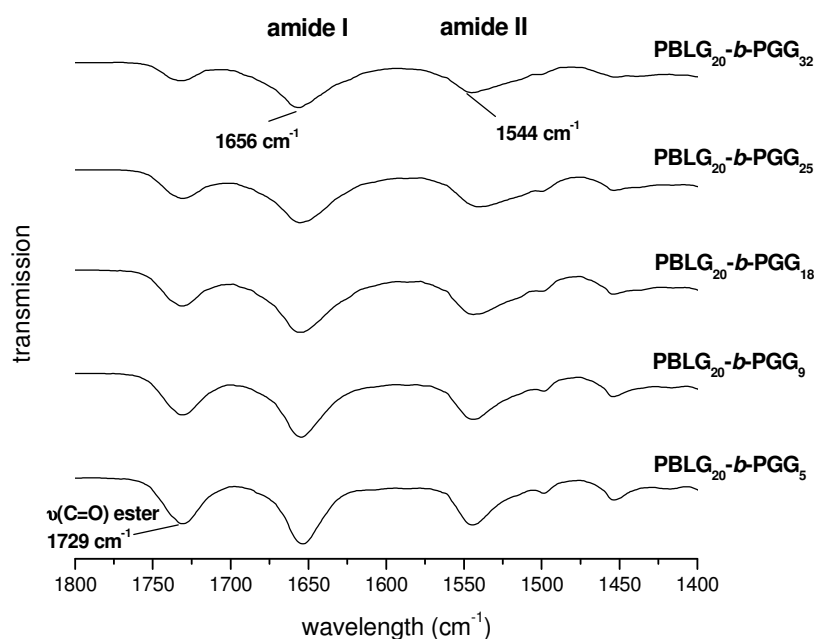


Figure 3.4: FTIR spectra of different block copolymers after glycosylation.

Interestingly, the (solid state) conformation of block copolymers after glycosylation is different from that of the polymers before glycosylation (Figure 3.4). Amide I and II bands can be found at 1656 cm^{-1} and 1544 cm^{-1} , respectively, in the FTIR spectra. These positions are indicative of an α -helical conformation imposed by the PBLG block. The presence of the bulky galactose moieties conjugated to the side chains of the PGG block appears to prevent the formation of β -sheets.

All block copolymers were self-assembled using the nanoprecipitation method, which consists of adding a non-solvent [here deionized (DI) water] for the hydrophobic segment to a copolymer solution (10 mg/mL) in a common solvent for both blocks (here DMSO). During this process, DMSO quickly diffuses into the water phase, leading to the aggregation of the hydrophobic chains and driving the self-assembly process of the amphiphilic block copolymers. The obtained morphology was generally predetermined by the molecular composition, but the system could be kinetically trapped when the kinetics of solvent diffusion is faster than the kinetic of the self-assembly, leading to metastable morphologies. The

material morphology can also be controlled by the order of addition (DMSO in water or water in DMSO) and the addition speed.¹⁸

Dynamic light scattering (DLS) analysis was performed after removal of DMSO by dialysis, except for samples with hydrophilic weight ratios of 25 and 38%, which underwent macroscopic aggregation. The three other samples (Table 3.1), appeared perfectly limpid (no macroscopic aggregation) after dialysis. Transmission electron microscopy (TEM) imaging was used to probe the morphology directly after self-assembly. As shown in Figure 3.5 (a-c), mixtures of spherical and worm-like structures were observed irrespective of the hydrophilic weight ratio. Changing the addition speed from a few seconds to 2 hours and/or the copolymer concentration from 0.1 to 10 g/L did not significantly modify the nano-assemblies. In marked contrast, changing the order of addition (DMSO in water instead of water in DMSO) promoted the formation of spherical structures without worm-like assemblies. Small polymersomes with an average diameter of < 100 nm were clearly evidenced by TEM imaging for hydrophilic weight ratios of 55 and 63% (Figure 3.5 d and e). For PBLG₂₀-*b*-PGG₃₂ (Figure 3.5 f), a mixture of spherical micelles and vesicles was observed, indicating the upper hydrophilic weight ratio limit for polymersomes formation with these diblock copolymers. It is worth taking into consideration that in both cases (water in DMSO or DMSO in water), the observed morphologies certainly resulted from the kinetic trapping induced by the rigidity of the PBLG segment.

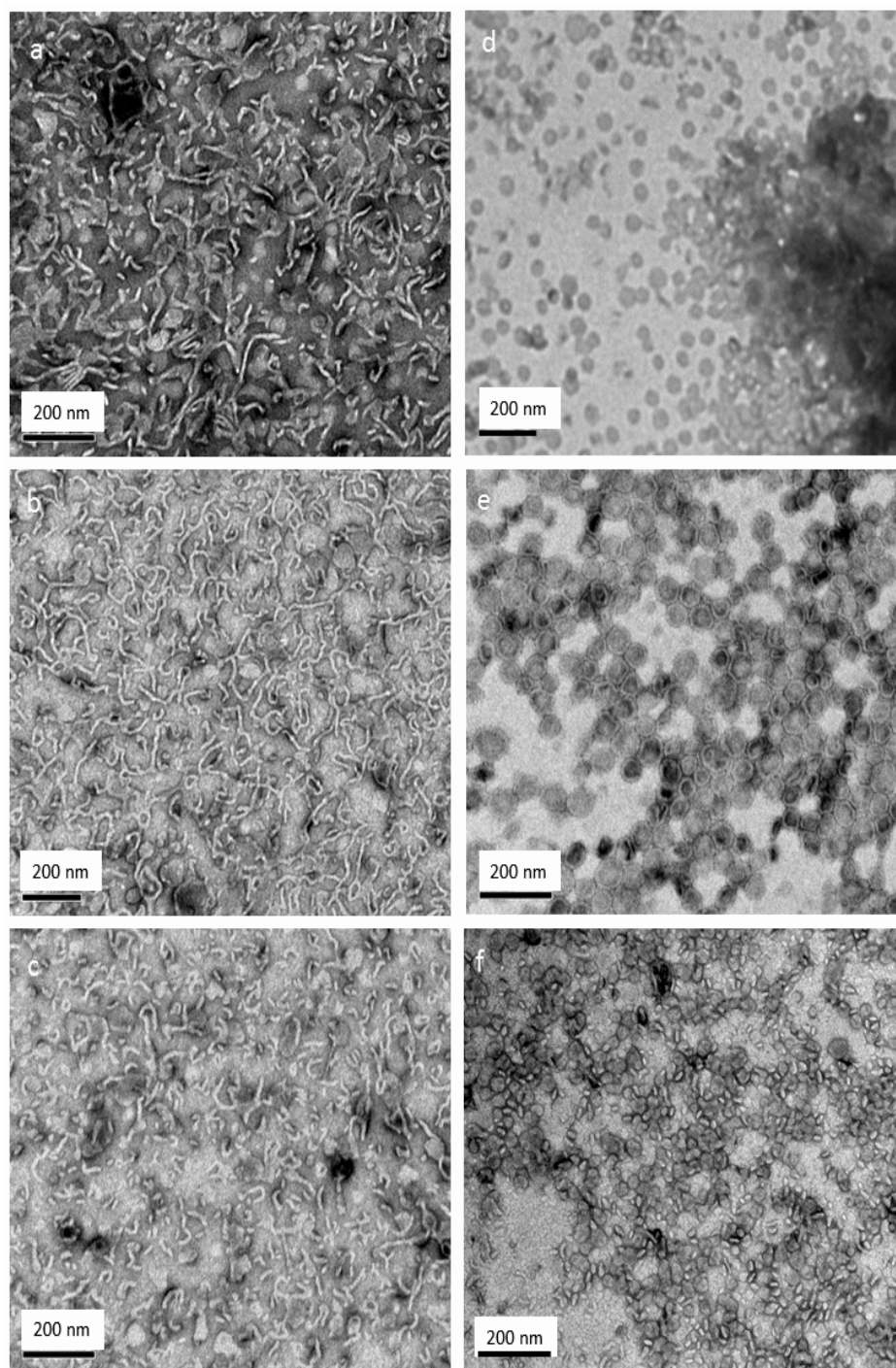


Figure 3.5: TEM images of samples obtained by instantaneously adding water in DMSO (a) PBLG₂₀-*b*-PGG₁₈, (b) PBLG₂₀-*b*-PGG₂₅, (c) PBLG₂₀-*b*-PGG₃₂; by instantaneously adding DMSO in water (d) PBLG₂₀-*b*-PGG₁₈, (e) PBLG₂₀-*b*-PGG₂₅, (f) PBLG₂₀-*b*-PGG₃₂.

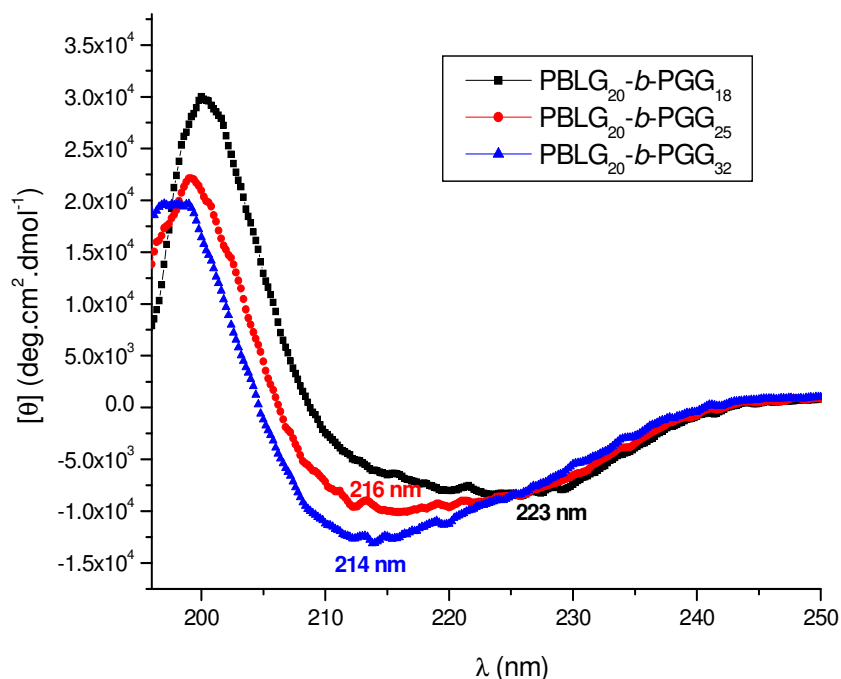


Figure 3.6: Circular dichroism (CD) spectra of glycosylated block copolymers after self-assembly in water (0.25 mg/mL).

Moreover, the PBLG segment adopting a rigid α -helical conformation as membrane layers of the polymersomes was also confirmed by CD spectra of block copolymers after the self-assembly in water (Figure 3.6). Different from the conformation of glycosylated block copolymers in solid state which is characteristic of an α -helical conformation, the self-assemblies of the glycosylated block copolymer in aqueous solution only gave a weak β -sheet conformation with increasing chain length of glycopeptide blocks. And the weak β -sheet conformation might be attributed to inter or intra-molecular hydrogen bondings from glycosylated poly(propargylglycine) domains.

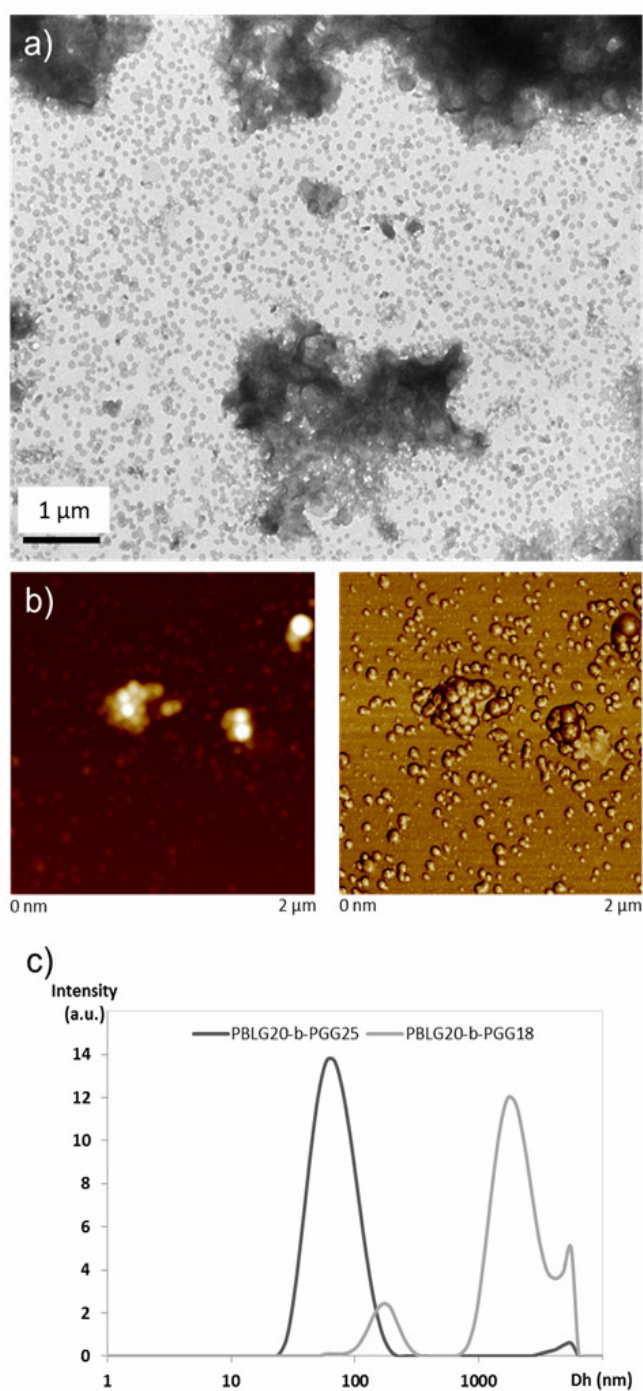


Figure 3.7: Evidence of the aggregation of vesicles made from PBLG₂₀-*b*-PGG₁₈. TEM (a) and AFM (b) images showing the coexistence of isolated vesicles and micrometre size aggregates. (c) Comparison of the DLS intensity distributions obtained from the cumulant analysis for PBLG₂₀-*b*-PGG₁₈ and PBLG₂₀-*b*-PGG₂₅.

Vesicles made of block copolymer PBLG₂₀-*b*-PGG₁₈ were significantly aggregated in solution, as evidenced from TEM, AFM, and DLS (Figure 3.7). On the other hand, vesicles made of copolymer PBLG₂₀-*b*-PGG₂₅ were much more stable, allowing the determination of the radius of gyration (R_G) and the hydrodynamic radius (R_H) by multiangle LS analysis (Figure 3.8).

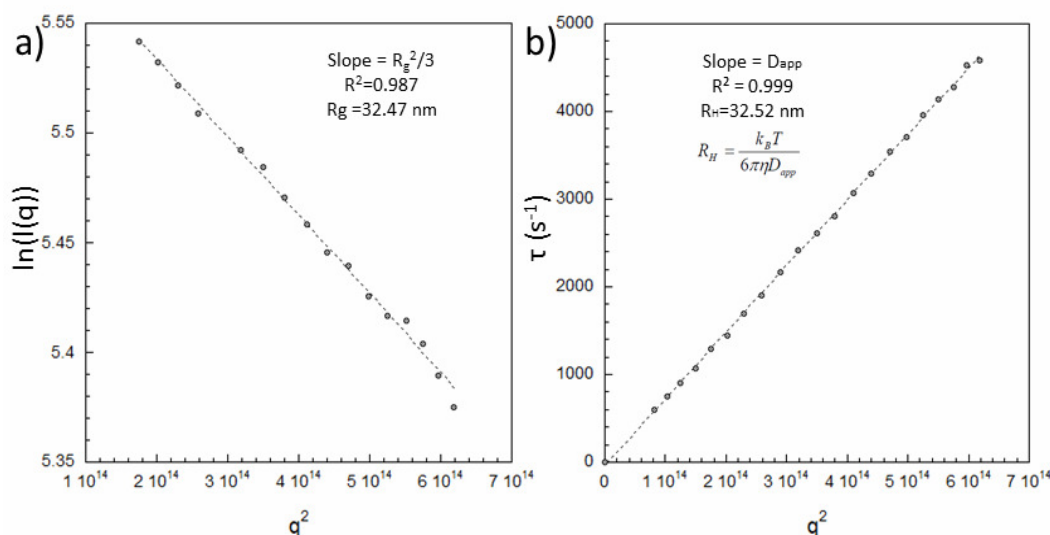


Figure 3.8: Multiangle light scattering analysis of PBLG₂₀-*b*-PGG₂₅. (a) Guinier plot and R_G determination; (b) Variation of decay rate vs squared scattering vector and R_H determination.

As expected, R_G/R_H ratio was found to be close to 1, attesting the formation of polymersomes. High magnification TEM imaging of the vesicles allowed good membrane visualization, the thickness being estimated to 5-10 nm. AFM analysis evidenced a diameter/height ratio in agreement with the hollow structure (Figure 3.9). As a result, by means of a solvent-injection method (the nanoprecipitation method), galactosylated vesicles of small sizes and good dispersity were obtained by using (1) the appropriate block copolypeptides after galactose coupling (2) the appropriate nanoprecipitation process, and in particular, the correct order of solvent addition.

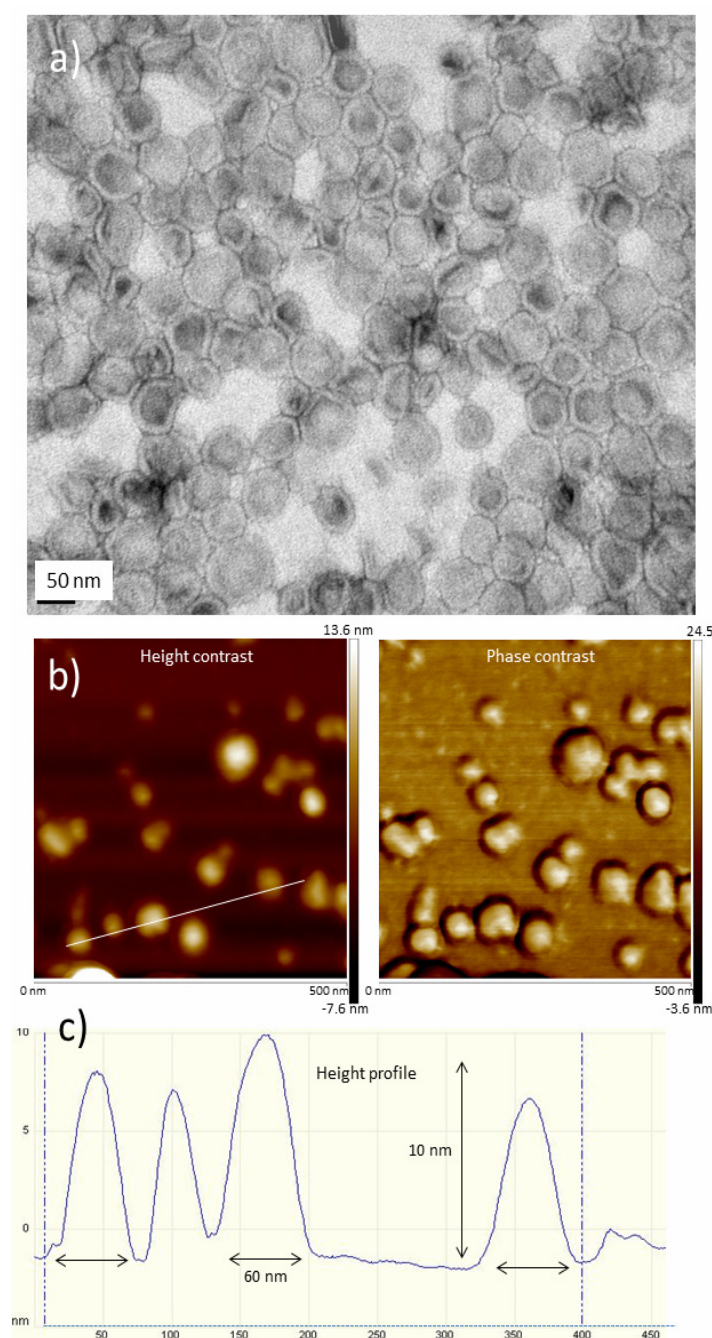


Figure 3.9: Microscopy of galactosylated polymersomes made of PBLG₂₀-*b*-PGG₂₅. (a) high magnification TEM imaging; (b) AFM imaging; (c) section profile of the AFM image along the white line in (b).

The bioactivity of the glycopeptide polymersomes formed from copolymer PBLG₂₀-*b*-PGG₂₅ was assessed by carbohydrate-lectin binding experiments. This involved

the mixing of the glycosylated polymersome solution with a lectin that specifically binds the sugar conjugated to the copolymer. In this case, *Ricinus communis* Agglutinin (RCA₁₂₀) was chosen since it is highly specific and selective for binding galactosyl residues.¹⁹ Upon the addition of different concentrations of the glycopeptide polymersomes to the RCA₁₂₀ solution, instantaneous precipitation was observed. This signifies that the carbohydrate groups present at the surface of the polymersomes are available to mediate the interaction with biological target molecules. In an attempt to quantify the interaction with the RCA₁₂₀, the absorbance spectra of the polymersome/lectin solutions were recorded.

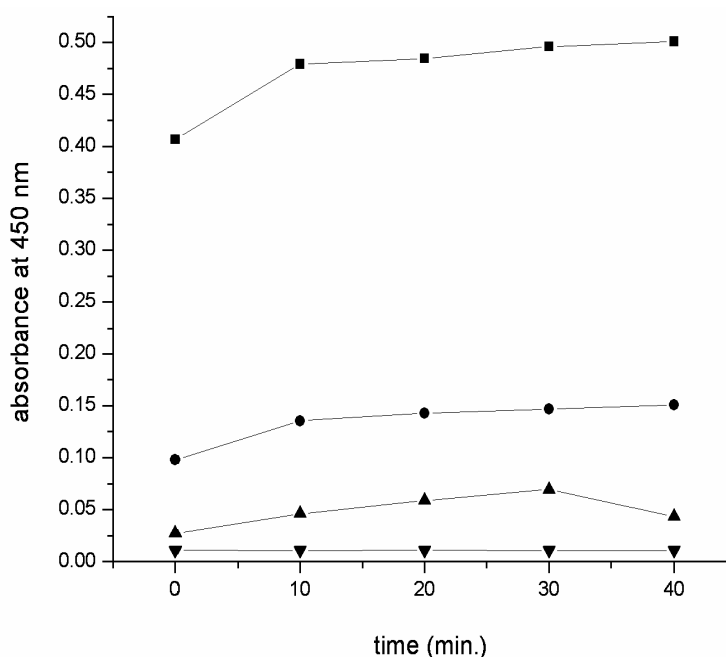


Figure 3.10: Absorbance (450 nm) of PBLG₂₀-*b*-PGG₂₅ polymersomes in the presence of two different lectins in DI water: (■) lectin RCA₁₂₀, glycopeptide concentration 1.0 mg/mL; (●) lectin RCA₁₂₀, glycopeptide concentration 0.25 mg/mL; (▲) lectin Con A, glycopeptide concentration 1.0 mg/mL; (▼) glycopeptide concentration 1.0 mg/mL, without the addition of any lectin.

As shown in Figure 3.10, the absorbance is highest for the greatest concentration of glycopeptide polymersomes. Furthermore, the lectin binding is so rapid that no

change of absorbance was measured over time regardless of the concentration of glycosylated block copolymers. The control experiment with Concanavalin A (Con A), which is selective for mannosyl and glucosyl but unable to bind galactosyl residues,¹⁹ showed no significant precipitation and change of turbidity. In addition, the lectin recognition experiments were also performed using the self-assembled structures obtained from other glycopeptide block copolymers (Table 3.1). It was observed in Figure 3.11 that all structures from different glycosylated block copolymers show biological activity in these tests. For the block copolymers with longer glycopeptides blocks, the absorbance slightly increased, although it is uncertain whether this small difference is caused by the chain length of glycopeptide blocks or the structure of the self-assembly.

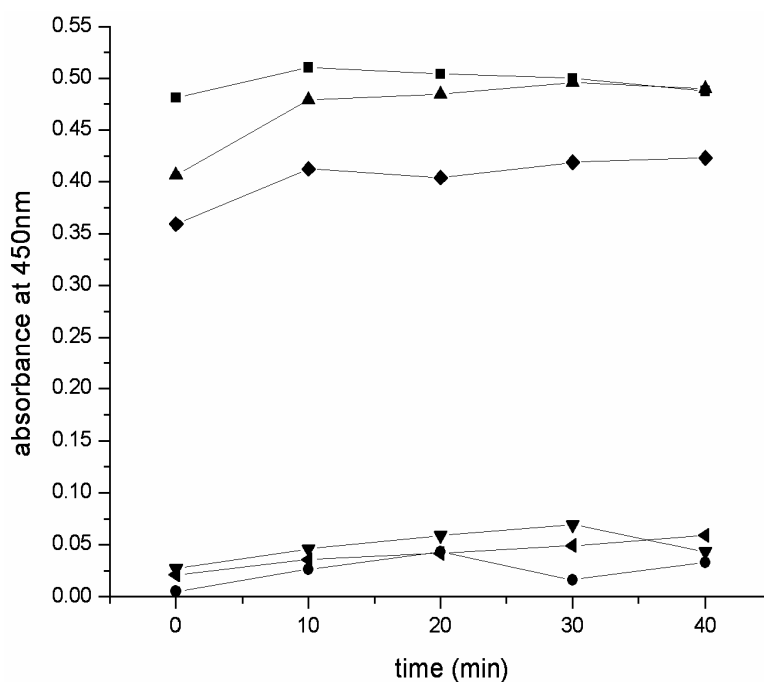


Figure 3.11: Absorbance (450 nm) of glycopeptide block copolymers after self-assembly with two different lectins in DI water: (■) lectin RCA₁₂₀, PBLG₂₀-b-PGG₃₂ 1.0 mg/mL; (▲) lectin RCA₁₂₀, PBLG₂₀-b-PGG₂₅ 1.0 mg/mL; (◆) lectin RCA₁₂₀, PBLG₂₀-b-PGG₁₈ 1.0 mg/mL; (▼) lectin Con A; PBLG₂₀-b-PGG₃₂ 1.0 mg/mL; (◄) lectin Con A; PBLG₂₀-b-PGG₂₅ 1.0 mg/mL; (●) lectin Con A; PBLG₂₀-b-PGG₁₈ 1.0 mg/mL.

3.4 Conclusions

In summary, we have presented a versatile and facile route to bioactive polymersomes fully based on amino acid and carbohydrate building blocks. Using controlled NCA polymerisation and efficient “click” glycosylation afforded well-defined amphiphilic galactose containing block copolymers. Depending on the block copolymer composition and the self-assembly protocol, the morphology of the structures formed could be controlled, ranging from (worm-like) micelles to polymersomes. These materials hold promise as nanosized drug carriers for targeted delivery.

3.5 References

- ¹ (a) Couvreur, P.; Gref, R.; Andrieux, K.; Malvy, C., *Prog. Solid State Chem.* **2006**, *34*, 231. (b) Reischl, D.; Zimmer, A.; *Nanomed.-Nanotechnol.* **2009**, *5*, 8. (c) Itaka, K.; Kataoka, K.; *Eur. J. Pharm. Biopharm.* **2009**, *71*, 475. (d) Du, J.; O'Reilly, R. K.; *Soft Matter* **2009**, *5*, 3544.
- ² Johnston, A. P. R.; Such, G. K.; Ng, S. L.; Caruso, F. *Curr. Opin. Colloid Interface Sci.* **2011**, *16*, 171.
- ³ Discher, D. E. ; Eisenberg, A. *Science* **2002**, *297*, 967.
- ⁴ (a) Jain, S.; Bates, J. S. *Science* **2003**, *300*, 460. (b) Gillies, E. R.; Fréchet, J. M. J. *Chem. Commun.* **2003**, *14*, 1640.
- ⁵ van Dongen, S. F. M.; de Hoog, H.-P. M.; Peters, R. J. R. W.; Nallani, M.; Nolte, R. J. M.; van Hest, J. C. M.; *Chem. Rev.* **2009**, *109*, 6212.
- ⁶ Geng, Y.; Dalhaimer, P.; Cai, S. S.; Tsai, R.; Tewari, M.; Minko, T.; Discher, D. E. *Nat Nanotechnol.* **2007**, *2*, 249.
- ⁷ (a) Brinkhuis, R. P.; Rutjes, F. P. J. T.; van Hest, J. C. M. *Polym. Chem.* **2011**, *2*, 1449. (b) Massignani, M.; Lomas, H.; Battaglia, G. *Adv. Polym. Sci.* **2010**, *229*, 115. (c) Bertin, A.; Hermes F.; Schlaad, H. *Adv. Polym. Sci.* **2010**, *224*, 167. (d) Christian, D. A.; Cai, S.; Bowen, D. M.; Kim, Y.; Pajeroski, D.; Discher, D. E. *Eur. J. Pharm. Bio.* **2009**, *71*, 463. (e) Meng, F.; Zhong, Z.; Feijen, J. *Biomacromolecules* **2009**, *10*, 197. (f) Egli, S.; Nussbaumer, M. G.; Balasubramanian, V.; Chami, M.; Bruns, N.; Palivan, C.; Meier W. J. *Am. Chem. Soc.* **2011**, *133*, 4476.
- ⁸ Gamblin, D. P.; Scanlan, E. M.; Davis, B. G. *Chem. Rev.* **2009**, *109*, 131.
- ⁹ Egli, S.; Schlaad, H.; Bruns, N.; Meier, W. *Polymers* **2011**, *3*, 252.
- ¹⁰ Martin, A. L.; Li, B.; Gillies, E. R. *J. Am. Chem. Soc.* **2009**, *131*, 734.
- ¹¹ (a) Kim, B. S.; Yang, W. Y.; Ryu, J. H.; Yoo, Y. S.; Lee, M. *Chem. Commun.* **2005**, *41*, 2035. (b) Kim, B. S.; Hong, D. J.; Bae, J.; Lee, M. *J. Am. Chem. Soc.* **2005**, *127*, 16333. (c) Toyotama, A.; Kugimiya, S. I.; Yamanaka, J.; Yonese, M.; *Chem. Pharm. Bull.* **2001**, *49*, 169.
- ¹² (a) Hordyjewicz-Baran, Z.; You, L.; Smarsly, B.; Sigel, R.; Schlaad, H. *Macromolecules* **2007**, *40*, 3901. (b) You, L.; Schlaad, H. *J. Am. Chem. Soc.* **2006**,

128, 13336. (c) Schlaad, H.; You, L.; Sigel, R.; Smarsly, B.; Heydenreich, M.; Manton, A.; Mašić, A. *Chem. Commun.* **2009**, 45, 1478. (d) Gress, A.; Smarsly, B.; Schlaad, H. *Macromol. Rapid Commun.* **2008**, 29, 304. (e) Li, Z. C.; Liang, Y. Z.; Li, F. M. *Chem. Commun.* **1999**, 35, 1557. (f) Liang, Y. Z.; Li, Z. C.; Li, F. M. *New J. Chem.* **2000**, 24, 323. (g) Zhou, W.; Dai, X. H.; Dong, C. M. *Macromol. Biosci.* **2008**, 8, 268. (h) Dai, X. H.; Dong, C. M. *J. Polym. Sci. A Polym. Chem.* **2008**, 46, 817. (i) Pasparakis, G.; Alexander, C. *Angew. Chem. Int. Ed.* **2008**, 47, 4847. (j) Ercelen, S.; Zhang, X.; Duportail, G.; Grandfils, C.; Desbrières, J.; Karaeva, S.; Tikhonov, V.; Mély, Y.; Babak, V. *Colloids Surf. B* **2006**, 51, 140. (k) Li, M.; Su, S.; Xin, M.; Liao, Y. *J. Colloid Interf. Sci.* **2007**, 311, 285.

¹³ Carlsten, A.; Lecommandoux, S. *Curr. Opin. Colloid Interface Sci.* **2009**, 14, 329.

¹⁴ (a) Holowka, E. P.; Pochan, D. J.; Deming, T. J. *J. Am. Chem. Soc.* **2005**, 127, 12423. (b) Rodriguez-Hernandez, J.; Lecommandoux, S. *J. Am. Chem. Soc.* **2005**, 127, 2026.

¹⁵ (a) Schatz, C.; Louguet, S.; Le Meins, J.-F.; Lecommandoux, S. *Angew. Chem., Int. Ed.* **2009**, 48, 2572. (b) Upadhyay, K. K.; Le Meins, J.-F.; Misra, A.; Voisin, P.; Bouchaud, V.; Ibarboure, E.; Schatz, C.; Lecommandoux, S. *Biomacromolecules* **2009**, 10, 2802. (c) Upadhyay, K. K.; Bhatt, A. N.; Mishra, A. K.; Dwarakanath, B. S.; Jain, S.; Schatz, C.; Meins, J.-F. L.; Farooque, A.; Chandraiah, G.; Jain, A. K.; Misra, A.; Lecommandoux, S. *Biomaterials* **2010**, 31, 2882.

¹⁶ Huang, J.; Habraken, G.; Audouin, F.; Heise, A. *Macromolecules* **2010**, 43, 6050.

¹⁷ (a) Habraken, G. J. M.; Peeters, M.; Dietz, C. H. J. T.; Koning, C. E.; Heise, A. *Polym. Chem.* **2010**, 1, 514. (b) Habraken, G. J. M.; Wilsens, K. H. R. M.; Koning, C. E.; Heise, A. *Polym. Chem.* **2011**, 2, 1322.

¹⁸ Sanson, C.; LeMeins, J.; Schatz, C.; Brûlet, A.; Soum, A.; Lecommandoux, S. *Langmuir* **2010**, 26, 2751.

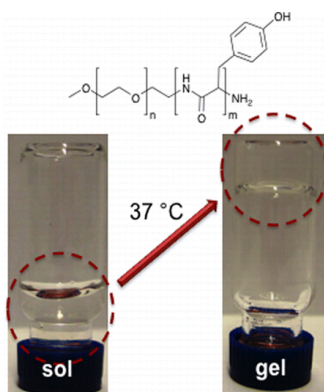
¹⁹ Ambrosi M.; Cameron N. R.; Davis B. G. *Org. Biomol. Chem.* **2005**, 3, 1593.

Chapter 4

Supramolecular hydrogels with reverse thermal gelation properties from (oligo)tyrosine containing block copolymers

Abstract

Novel block copolymers comprising poly(ethylene glycol) (PEG) and an oligo(tyrosine) block were synthesized in different compositions by N-carboxyanhydride (NCA) polymerisation. It was shown that PEG2000-Tyr₆ undergoes thermoresponsive hydrogelation at a low concentration range of 0.25-3.0 wt% within a temperature range of 25 to 50 °C. Cryogenic Transmission Electron Microscopy (Cryo-TEM) revealed a continuous network of fibers throughout the hydrogel sample even at concentrations as low as 0.25 wt%. Circular Dichroism (CD) results suggested that better packing of the β -sheet tyrosine block at increasing temperature induces the reverse thermogelation. A preliminary assessment of the potential of the hydrogel for in vitro application confirmed the hydrogel is not cytotoxic, is biodegradable and produced a sustained release of a small-molecule drug.



Part of this chapter was published in Huang, J.; Hastings, C.; Duffy, G.; Kelly H.; Raeburn, J.; Adams, J.; Heise, A. *Biomacromolecules* 2013, 14, 200.

The application of hydrogel in this chapter was done in collaboration with Dr. Garry Duffy and Dr. Helena Kelly in Royal College of Surgeons/Ireland.

4.1 Introduction

Hydrogels are critical materials in biomedical science. Their high water content and permeability, allied to structural integrity similar to the extracellular matrix means that hydrogels are ideal building blocks in regenerative medicine and as therapeutic delivery systems.¹ Despite the immense progress made in the development of hydrogels, their first clinical applications and the large and diverse number of materials disclosed in the academic and patent literature, there is still a high demand for the development of new hydrogels with material properties that better match application demands. Of particular interest are reverse thermo-responsive gels, that is, solutions, which transform into a gel upon temperature increase.² In particular, thermoresponsive hydrogels are highly amenable to the localised delivery of small-molecule drugs and other therapeutic molecules, due to their tendency to maintain a liquid state at room temperature, thereby enabling a minimally invasive administration via syringing and subsequent ability to rapidly form a robust gel bolus upon heating to physiological temperature, thereby enforcing drug cohesion and facilitating sustained release at the intended site of action. Such systems can potentially achieve local efficacy for extended periods, requiring the administration of smaller doses, thereby reducing the manifestation of off-target effects associated with systemic administration of drugs.³

A promising class of materials is that of synthetic hydrogels obtained by self-assembly of amphiphilic polypeptides.⁴ Amphiphilic peptides can self-assemble into the supramolecular hydrogel matrix through non-covalent interactions such as hydrogen bonding, electrostatic interactions, π -stacking and hydrophobic interactions.⁵ A prominent example is the peptide amphiphiles introduced by Stupp consisting of a hydrophobic chain segment attached to a hydrophilic amino acid sequence.⁶ This design promotes supramolecular self-assembly into three-dimensional networks of fibrils in aqueous solution, stabilized through peptide interactions at a low concentration. While this design concept is very efficient, the self-assembly process is highly sensitive to the length and sequence of the amino acid block and relies on tedious multistep peptide and organic synthesis.⁷

Utilizing a polymerisation approach would potentially simplify the synthetic efforts, however, at the expense of monodispersity and the oligopeptide sequence. Synthetic polypeptides can readily be prepared by the ring-opening polymerisation of amino acid N-carboxyanhydrides (NCA).⁸ Recent advances demonstrate the feasibility of NCA polymerisation for the synthesis of complex polymer structures capable of self-assembly⁹, some of which are reported to form hydrogels. For example, Deming employed NCA polymerisations for the synthesis of hydrogel forming diblock copolypeptide amphiphiles.¹⁰ These materials contain water soluble polyelectrolyte blocks such as poly(L-lysine) or poly(L-glutamate) and a α -helical poly(L-leucine) hydrophobic block. The gelation is driven by the stiff α -helical conformation of the hydrophobic domain and the electrostatic repulsion from the polyelectrolyte segments. However, hydrogelation was only achieved when both the hydrophobic and hydrophilic segments had a sufficiently high molecular weight. Jeong reported a series of amphiphilic hybrid block copolymers obtained by ring-opening polymerisation of alanine or phenylalanine NCAs.¹¹ These materials self-assemble into nanostructures such as micelles in aqueous solutions, and further transition into hydrogels at high polymer concentration in the range of 3.0-14 wt% through intermicellar aggregation when the temperature increases. Very recently, Chen also reported micelle-assembled thermosensitive hydrogels based on poly(L-glutamate)s bearing different hydrophobic side groups via NCA polymerisation. Depending on the nature of the side chains, the polymers underwent sol-gel transitions with increasing temperature up to 62 °C at a high polymer concentration (typically 9.0 wt%).¹²

We were interested in investigating if the advantages of NCA polymerisation for the synthesis of amphiphilic polypeptides could be married with efficient hydrogelation at low concentration and thermoresponsive behavior. In this concept, a single amino acid must be able to display multiple modes of interaction, triggering self-assembly into the hydrogel matrix through non-covalent interactions. We hypothesized that tyrosine is a promising amino acid candidate. Despite its polar phenol group in the side chain, tyrosine residues are relatively hydrophobic when the pH of the solution is lower than the pKa of the phenol.¹³ In addition to the ability to form stable β -sheet assemblies through main chain amide bond driven by hydrogen bonding, it has been

shown that hydrogen bonding from the tyrosine -OH group contributed favorably to protein stability.¹⁴ Because one of the two lone electron pairs is partially delocalized within the aromatic ring, it can act either as hydrogen bonding donor or acceptor.¹⁵ Baker and Hubbard revealed that Tyr-OH groups form more hydrogen bonds to water molecules than intramolecular hydrogen bonds; although, in proteins, the tyrosine phenolic hydroxyl group generally forms a single intramolecular hydrogen bond with a main-chain carbonyl oxygen or a side chain carboxyl group.¹⁶ If desired, tyrosine can also be enzymatically cross-linked¹⁷ for hydrogel stabilization.¹⁸ To explore if the unique features of tyrosine can be utilized to trigger supramolecular hydrogel formation at a low concentration, we designed a range of PEG conjugated tyrosine-based amphiphiles by simple NCA polymerisation. The hydrogelation profile is highly sensitive to the polymer composition and the materials display rare reverse thermogelation. We determine the applicability of this polymer to form an injectable drug delivery vehicle and undertake a preliminary appraisal of the biodegradability and toxicity of the formulation in cultured cells. The release of a model compound, desferrioxamine (DFO), a small-molecule pro-angiogenic, from the thermoresponsive gel was investigated.

4.2 Experimental section

Materials

All chemicals were purchased from Sigma-Aldrich and used as received unless otherwise noted. O-benzyl-L-tyrosine and phenylalanine were supplied by Bachem. Anhydrous DMF, ethyl acetate, THF were used directly from the bottle under an inert and dry atmosphere.

Methods

¹H and ¹³C NMR spectra were recorded at room temperature with a Bruker Avance 400 (400 MHz). CF₃COOD and CDCl₃ were used as solvents, and signals were referred to the signal of residual protonated solvent signals. ATR-FTIR spectra were collected on a Perkin Elmer Spectrum 100 in the spectral region of 650-4000 cm⁻¹, and were obtained from 16 scans with a resolution of 2 cm⁻¹. A background

measurement was taken before the sample was loaded onto the ATR unit for measurements. CD data were collected on a Jasco J-810 CD spectrometer (Japan Spectroscopic Corporation) with a pathlength of 0.1 cm and a bandwidth of 1 nm. Three scans were conducted and averaged between 185 nm and 350 nm at a scanning rate of 20 nm min⁻¹ with a resolution of 0.2 nm. The data were processed by subtracting solvent as background. CD temperature-dependent measurements were performed in a Jasco J-815 spectropolarimeter (Japan Spectroscopic Corporation) with a PFD-425S/15 Peltier-type temperature controller with a temperature range from 10 °C to 60 °C and a temperature slope of 1 °C/min. The solution was allowed to equilibrate for 10 minutes at each temperature prior to data collection. The measurements were done between 185 nm and 350 nm in a 0.1 mm quartz cell. Dynamic rheological experiments were measured using an Anton Paar Physica MCR101 rheometer. For the oscillatory shear measurements, a sandblasted parallel top plate with a 25 mm diameter and 1.0 mm gap distance were used. Evaporation of water from the hydrogel was minimized by covering the sides of the plate with low viscosity mineral oil. The measurements of storage modulus (G') and loss modulus (G'') with gelation were made as a function of time at a frequency of 1.59 Hz (10 rad/s) and at a constant strain of 2% as the temperature increased from 25 °C to 60 °C by a heating rate of 1.0 °C/min. a frequency sweep (1-100 Hz) was performed on the recovered gel at a constant strain of 2%. The morphology images of hydrogel were obtained by using Hitachi S3400n SEM instrument. The preparation of samples for SEM analysis involved placing a drop of hydrogel on the thin carbon-coated film. The hydrogel was subjected to shock-freezing by liquid nitrogen, followed by lyophilization for 2 hours. It was then submitted for SEM scanning after gold-coating for 2 minutes. Cryogenic-transmission electron microscopy (Cryo-TEM): Sample preparation was carried out using a CryoPlunge 3 unit (Gatan Instruments) employing a double blot technique. 3 μ L of sample was pipetted onto a plasma etched (15 s) 400 mesh holey carbon grid (Agar Scientific) held in the plunge chamber at approximately 90% humidity. The samples were blotted, from both sides for 0.5, 0.8 or 1.0 s dependent on sample viscosity. The samples were then plunged into liquid ethane at a temperature of -170 °C. The grids

were blotted to remove excess ethane then transferred under liquid nitrogen to the cryo TEM specimen holder (Gatan 626 cryo holder) at -170 °C. Samples were examined using a Jeol 2100 TEM operated at 200 kV and imaged using a GatanUltrascan 4000 camera; images captured using Digital Micrograph software (Gatan). High-performance liquid chromatography (HPLC) for DFO release studies was performed on an Agilent 1120 Compact LC with a Phenomenex Gemini 5u C18 column, mobile phase acetonitrile: phosphate buffer (10%:90% v/v), containing 2.0 M ethylenediaminetetraacetic acid (EDTA), pH adjusted to 6.5 and UV detection at 440 nm.

Synthesis of *O*-benzyl-*L*-tyrosine (BLT-NCA) and phenylalanine (Phe-NCA). α -Pinene (15 g, 110.3 mmol) and *O*-benzyl-*L*-tyrosine (10.0 g, 36.9 mmol) were dissolved in 80 mL anhydrous ethyl acetate in a three-neck round-bottomed flask. The mixture was stirred and heated to reflux with a slow flow of nitrogen. Then, a solution of triphosgene (5.5 g, 18.4 mmol) in anhydrous ethyl acetate (40 mL) was added drop-wise. Two-thirds of the solution was added within 1 hour, and the reaction was left at reflux for another hour. The rest of the triphosgene solution was added until the reaction mixture became clear. Subsequently, around 60 mL of the solvent was removed under pressure and 120 mL *n*-heptane was added slowly to precipitate NCA. After filtration, the solid was recrystallized from ethyl acetate and *n*-heptane (1:2) four times until the NCA was recovered as an off-white crystal. (8.2 g, Yield 75%) $^1\text{H-NMR}$ (400 MHz, CDCl_3 , δ , ppm): 2.95 (dd, $J=14.13, 8.36$ Hz, 1H, -CH-CH $_2$ -), 3.21 (dd, $J=14.13, 4.10$ Hz, 1H, -CH-CH $_2$ -), 4.49 (dd, $J=4.10, 8.36$ Hz, 1H, -NH-CH-), 5.04 (s, 2H, -CH $_2$ -O-), 5.96 (s, 1H, -NH-CH-), 6.95 (d, $J=8.61$ Hz, 2H, ArH), 7.10 (d, $J=8.61$ Hz, 2H, ArH), 7.39 (m, 5H, ArH). $^{13}\text{C-NMR}$ (400 MHz, CDCl_3 , δ , ppm): 37.1 (-CH-CH $_2$ -), 58.9 (-CH-CH $_2$ -), 70.0 (-O-CH $_2$ -), 115.6 (Ar), 125.9 (Ar), 127.5 (Ar), 128.1 (Ar), 128.7 (Ar), 130.2 (Ar), 136.6 (Ar), 151.5 (Ar), 158.5 (-O-C(O)-CH-), 168.6 (-C(O)-NH-).

The same procedure was applied to the synthesis of phenylalanine NCA. (5.3 g, Yield 45%) $^1\text{H-NMR}$ (400 MHz, CDCl_3 , δ , ppm): 2.99 (dd, $J=14.16, 8.59$ Hz, 1H, -CH-CH $_2$ -), 3.30 (dd, $J=14.16, 4.06$ Hz, 1H, -CH-CH $_2$ -), 4.54 (dd, $J=4.06, 8.59$ Hz, 1H, -NH-CH-), 6.03 (s, 1H, -NH-CH-), 7.20 (m, 2H, ArH), 7.35 (m, 5H, ArH). $^{13}\text{C-NMR}$

NMR (400MHz, CDCl₃, δ , ppm): 38.0 (-CH-CH₂-), 58.9 (-CH-CH₂-), 128.2 (Ar), 129.3 (Ar), 129.4 (Ar), 134.0 (Ar), 151.8 (-O-C(O)-CH-), 168.7 (-C(O)-NH).

General Procedure for the synthesis of PEG-*b*-poly(O-benzyl-L-tyrosine). O-benzyl-L-tyrosine NCA (715 mg, 2.4 mmol) was dissolved in 30 mL of dry DMF in a Schlenk tube. A solution of α -methoxy- ω -amino poly(ethylene glycol) (M_w =2000 g/mol, PDI 1.03, 960 mg, 0.48 mmol) in 10 mL of dry DMF was added after the NCA had dissolved. The reaction was left to stir at room temperature for 4 days in a dry nitrogen atmosphere until NCA was completely consumed (as monitored by FTIR). The reaction mixture was precipitated into an excess diethylether, filtered and dried under vacuum as a pale yellow solid (Yield 80%). ¹H-NMR of PEG2000-*b*-poly(O-benzyl-L-tyrosine)₆ (400 MHz, TFA-d⁶ with CDCl₃, δ , ppm): 2.66-3.03 (br m, 12H), 3.25-4.07 (br m, 176H) 4.5-5.17 (br m, 18H), 6.70-7.44 (br m, 54H).

The synthesis of PEG-*b*-poly(L-tyrosine). PEG-*b*-Poly(O-benzyl-L-tyrosine) (1 g) was dissolved in 10.0 mL hexafluoroisopropanol (HFIP) with 2 mL trifluoroacetic acid (TFA). A six-fold excess with respect to O-benzyl-L-tyrosine of a 33% of HBr in acetic acid (1.6 mL) was added. After 16 hours, the mixture was added dropwise into diethyl ether. The polymer was filtered and redissolved in deionized water and dialyzed against water for 7 days. The solution was lyophilized as a white fluffy powder (Yield 55%). ¹H-NMR of PEG2000-*b*-poly(L-tyrosine)₆ (400 MHz, TFA-d⁶, δ , ppm): 2.62-3.26 (br s, 12H), 3.30-4.23 (br m, 176H), 4.58-4.97 (br s, 6H), 6.70-7.27 (br m, 31H).

Hydrogel preparation and Sol-Gel transition. Hydrogel solutions were prepared by dissolving freeze-dried polypeptide samples in deionized water at the desired concentrations. The homogenous solutions were obtained by sonication at 20 °C until the solutions became clear. The formation of the gel was determined *via* vial inverted method.¹⁹ Each sample at a given concentration was dissolved into distilled water in a 2 mL vial. After equilibration at room temperature overnight, the vials containing samples were immersed in a water bath equilibrated at each given temperature for 15 min. The sol-gel transition was determined after inverting the vial. If no flow was observed within one minute, the sample was regarded as a gel. For the temperature dependent measurements, the temperature was raised in 1 °C steps (the precision of the sol-gel transition temperature was ± 1 °C). Each

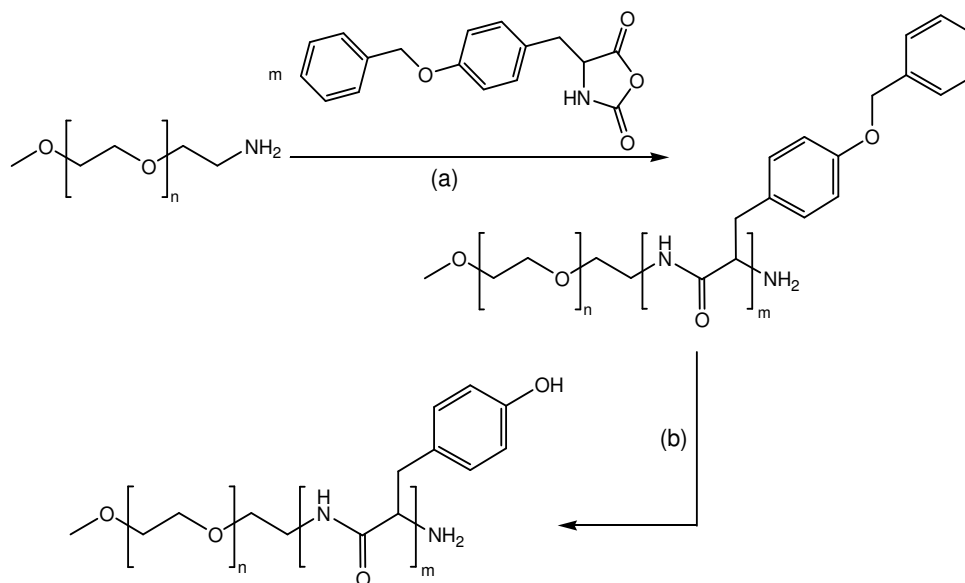
temperature data point represents an average of three measurements. The gelation time as a function of block copolymer concentration at the physiologically relevant temperature of 37 °C was measured in a 37 °C water-bath. The gelpoint was determined *via* vial inversion method every 15 min in the initial 3 h. Thereafter, the gelation was checked every 30 min. The duration from the time point the polymer solution was put into the water bath to the time point the gelation was observed was defined as the gelation time. Each gelation time data point was determined from an average of three measurements.

Hydrogel degradation profiles. Degradation of the hydrogels was assessed by measuring the weight loss every 24 h for nine days in triplicate. A 1 mL aliquot of deionized water containing 1.0 wt% and 2.0 wt% block copolymer, respectively, was placed in a vial and left in a water bath at 37 °C for 30 min to allow gelation to occur. A 2 mL aliquot of prewarmed Krebs buffer solution was gently added into each vial, taking care not to disturb the hydrogels. The vials were then left in the water-bath for the duration of the degradation study. Every 24 h, the Krebs buffer solution was removed along with any gel debris that had accumulated. Vials were then weighed to assess the change in weight of the hydrogels over the duration of the study. In the enzymatic degradation experiment, the enzymes were doped into the hydrogel by dissolving the enzymes in the 5 mg/mL (~0.5 wt%) polymer solution. The activity of both enzymes in the final polymer solution is 28.5 unit/mL. The hydrogelation was triggered by heating the solutions to 37 °C in a water bath (around 4 h). The formation of the hydrogel was determined by the inverted vial method.

Desferrioxamine (DFO) release experiment. Analysis of DFO release from a 2.0 wt% (20 mg/mL) PEG2000-Tyr₆ hydrogel was undertaken as previously described.²⁰ Hydrogels containing DFO of 100 µM concentrations were prepared. A total of 2 g of 20 mg/mL polymer with 100 µM DFO was placed in each of three glass vials and allowed to gel in a water bath for 2 h at 37 °C. A 1mL aliquot of phosphate buffer (pH 7.2) was added to each vial and the samples were allowed to incubate at 37 °C while shaking at 75 rpm for the duration of the release study (2 mL of buffer was used at 4 h and 24 h to ensure appropriate sink conditions in release media at early time points). The phosphate buffer was completely removed and replaced at 4 h, 24

h, day 3, day 5 and day 7, and frozen until analysis. All studies were performed in triplicate. Samples were analyzed for DFO content via HPLC.

Hydrogel biocompatibility. The biocompatibility of the hydrogel was preliminarily assessed through the culture of cell monolayers on a preformed PEG2000-Tyr₆ hydrogel substrate. Mesenchymal stem cells were derived from bone marrow aspirates of Wistar rats (rMSCs) under ethical approval. Cells were cultured in Dulbecco's Modified Eagles medium (DMEM) supplemented with 10% foetal bovine serum (FBS), 1% *L*-glutamine, 2% penicillin/streptomycin, 1% non-essential amino acids and 0.5% Glutamax. 50,000 rMSCs were seeded on a pre-formed gel layer consisting of 100 µL of 2.0 wt% gel allowed to set at 37 °C for 1 h in wells of a 24-well plate. Cell viability and morphology was assessed qualitatively at 48 h, as previously described,²¹ through use of a Live/Dead stain (Molecular Probes), which labels cells with calcein or ethidium homodimer to stain live cells green and dead cells red, respectively. The proportion of live to dead cells, and the ability of cells to spread and attach to the gel substrate were assessed qualitatively through visual inspection of stained cells at 48 h.



Scheme 4.1: Synthesis of PEG-Tyr block copolymers. (a) DMF, 0 °C; (b) HBr/acetic acid, hexafluoroisopropanol/TFA, r.t.

4.3 Results and Discussion

Poly(ethylene glycol-*b*-O-benzyl-L-tyrosine) (PEG-PBLT) block copolymers were synthesized by ring-opening polymerisation of O-benzyl-L-tyrosine NCA using α -methoxy- ω -amino poly(ethylene glycol) ($M_w = 2000$ and 5000 g/mol) as the macroinitiator (Scheme 4.1). The ratio of PEG macroinitiator to NCA was systematically varied to obtain block copolymers at different block lengths ratios (Table 4.1). ^1H NMR analysis confirmed the very good agreement between the PEG to NCA monomer feed ratio with the composition of the obtained block copolymers, although for PEG5000 a slight deviation was observed at higher ratios. The subsequent quantitative deprotection of the tyrosine benzyl ether was monitored by ^1H NMR spectroscopy by the disappearance of the benzyl ether peaks (7.2-7.4 ppm) and afforded the poly(ethylene glycol-*b*-L-tyrosine) (PEG-Tyr).

Table 4.1: Characteristics of poly(ethylene glycol-*b*-L-tyrosine) (PEG-Tyr) block copolymers obtained by macroinitiation of O-benzyl-L-tyrosine NCA from amine-functionalized PEG (PEG-NH₂).

PEG-NH ₂	Feed ratio PEG/NCA ^a	Composition block copolymer ^b
PEG2000	1:5	PEG2000-Tyr ₆
PEG2000	1:10	PEG2000-Tyr ₁₀
PEG2000	1:15	PEG2000-Tyr ₁₄
PEG5000	1:10	PEG5000-Tyr ₉
PEG5000	1:15	PEG5000-Tyr ₁₃
PEG5000	1:20	PEG5000-Tyr ₁₆
PEG5000	1:30	PEG5000-Tyr ₂₃

^a Molar ratio of PEG macroinitiator to O-benzyl-L-tyrosine NCA. ^b Calculated from ¹H NMR (CF₃COOD) using the integrated peak area ratios of the PEG ethylene signals at 3.25-4.07 ppm and the C_α signal of poly(L-tyrosine) at 4.58-4.97 ppm while using the aromatic groups at 6.70-7.40 ppm and C_β signal at 2.62-3.26 ppm of poly(L-tyrosine) as the internal standards.

Organogel formation was observed from all series of PEG-PBLT block copolymers in a range of common organic solvents including dichloromethane (DCM), tetrahydrofuran (THF), N,N-dimethylformamide (DMF), dimethyl sulfoxide (DMSO) and chloroform. On the contrary to the most protein organogel systems that undergo gel-sol transition as the temperature increases,²² these block copolymers form transparent, thermostable gels in the organic solvents. Moreover, those gels do not melt until the temperature reaches the boiling point of solvents. Taking the gelation in chloroform as the example, the critical gelation concentration of these polymers in chloroform is around 1.3 wt% (20 mg/mL) regardless of the slight increase of the chain lengths from poly(O-benzyl-L-tyrosine) building blocks. Very little amount of chloroform was squeezed out when 1.3 wt% organogel in

chloroform was put in 50 °C water bath for eight hours. Furthermore, the gelation can reversibly occur when the temperature cools down.

It is proposed that these organogels are driven by the formation of hydrogen bonding and aromatic interactions. PEG2000-*b*-poly(O-benzyl-L-tyrosine)₆ was selected to investigate the mechanism of the organogel formation. The amide I carbonyl stretching vibration of the peptide in Figure 4.1 can be used to determine the presence of secondary structure, supporting the driving force of organogelation. The amide I band of PEG2000-*b*-poly(O-benzyl-L-tyrosine)₆ in solid state at 1633 cm⁻¹ suggests that the polymer adopts a β -sheet conformation, which coincides with an investigation by Bonora et al that oligopeptides of O-benzyl-L-tyrosine existed predominantly in the parallel β -sheet structure for the degree of polymerisation (DP) > 4.²³ In addition, after the polymer self-assembled into the organogel in chloroform, the amide I band at 1633 cm⁻¹ still remained, revealing that the secondary structure of PEG2000-*b*-poly(O-benzyl-L-tyrosine)₆ in the organogel is of β -sheet conformation. Circular dichroism (CD) spectroscopy of PEG2000-*b*-poly(O-benzyl-L-tyrosine)₆ (Figure 4.1) also confirms β -sheet conformation by a characteristic minimum peak at 219 nm. However, there is a pronounced positive maximum peak at 238 nm in CD spectrum. This could be assigned to $n-\pi$ and $\pi-\pi$ transitions resulting from aromatic interactions of the aromatic residues.²⁴ Furthermore, addition of few drops of trifluoroacetic acid (TFA) into the gel resulted in the complete loss of gelation, indicating that hydrogen bonding is involved in the gelation process.²⁵

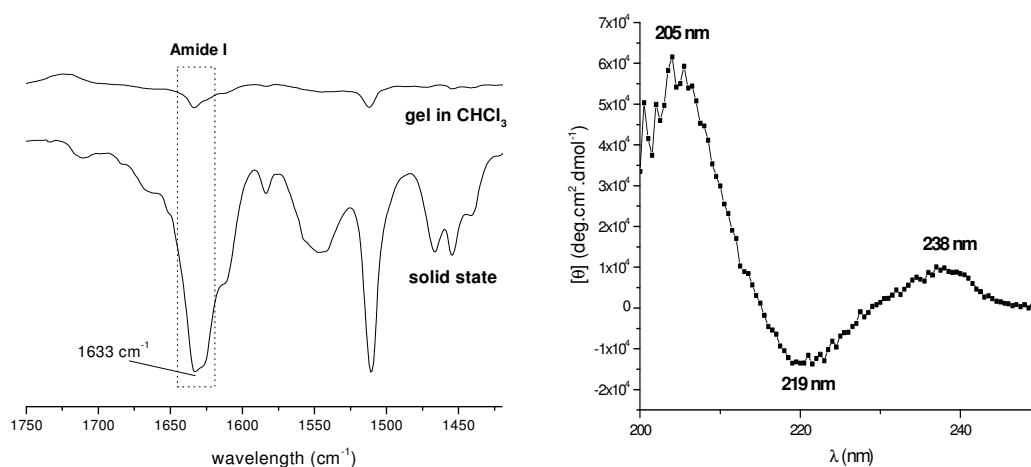


Figure 4.1: FTIR spectra of PEG2000-*b*-poly(O-benzyl-L-tyrosine)₆ in solid state and organogel of PEG2000-*b*-poly(O-benzyl-L-tyrosine)₆ in chloroform (Left); Circular dichroism spectrum of PEG2000-*b*-poly(O-benzyl-L-tyrosine)₆ (0.25 mg/mL) in acetonitrile (Right).

After deprotection, of the PEG5000 series PEG5000-Tyr₂₃ was water insoluble, while all other block copolymers were readily soluble but did not form hydrogels at room temperature, even at polymer concentrations >120 mg/mL (12 wt%, higher concentrations were not investigated). Of the PEG2000 series, both PEG2000-Tyr₁₀ and PEG2000-Tyr₁₄ were water insoluble. PEG2000-Tyr₆, on the other hand, formed transparent hydrogels in deionized (DI) water at a range of concentrations and temperatures. Cryogenic transmission electron microscopy (cryo-TEM) revealed a continuous network of fibers throughout the hydrogel sample, even at concentrations as low as 0.25 wt% (Figure 4.2). The fibers appear interconnected by cross-link points. Scanning electron microscopy (SEM) images of samples treated with liquid nitrogen followed by lyophilization to preserve the hydrogel structure also confirm the three-dimensional interconnected network structure (Figure 4.2).

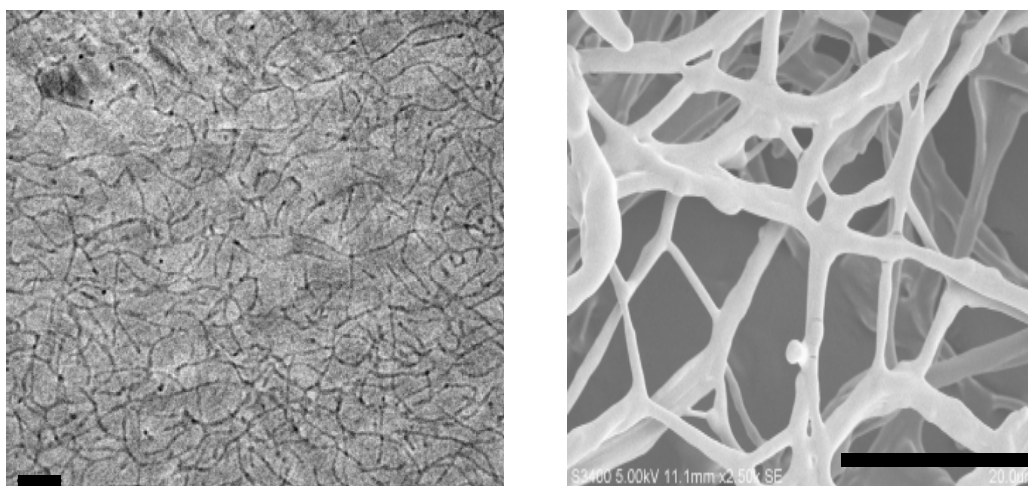


Figure 4.2: Left image: Cryogenic transmission electron microscopy (Cryo-TEM) images of PEG2000-Tyr₆ hydrogels (0.25 wt%), the scale bar represents 200 nm. Right image: Scanning electron microscopy (SEM) images of PEG2000-Tyr₆ hydrogels (0.5 wt%) after lyophilization, the scale bar represents 20 μ m.

Interestingly, the sol-gel phase diagram revealed a temperature-dependent profile at low solid content. Figure 4.3 shows that PEG2000-Tyr₆ undergoes thermoresponsive gelation at a concentration range of 0.25-3.0 wt% within a temperature range of 25 to 50 °C. The sol-to-gel transition temperature depends on the polymer concentration, and increases with decreasing polymer concentration, for example 28 °C at 2.0 wt% and 39 °C at 1.0 wt%. It is remarkable that even at a polymer concentration of 0.25 wt% stable hydrogels can be observed upon heating to 50 °C. The second phase diagram in Figure 4.3 depicts the gelation time as a function of block copolymer concentration at the physiologically relevant temperature of 37 °C. The data signify that the hydrogelation time can be completely controlled by the polymer concentration in water. Moreover, at concentrations >2.0 wt%, hydrogelation occurs immediately at this temperature. The thermogelation profile observed for PEG2000-Tyr₆ is contrary to most polypeptide aqueous systems that form a stable hydrogel via hydrogen bonding or ionic interactions at a low temperature and then undergo gel-to-sol transition (gel melting) when the temperature increases.^{26,27} Most relevant in that respect is the example of telechelic Fmoc protected dityrosine end-capped PEG recently published by Hamley.

Self-assembled β -sheet fibril-based hydrogels from these materials exhibited a gel-to-sol transition with increasing temperature.²⁸

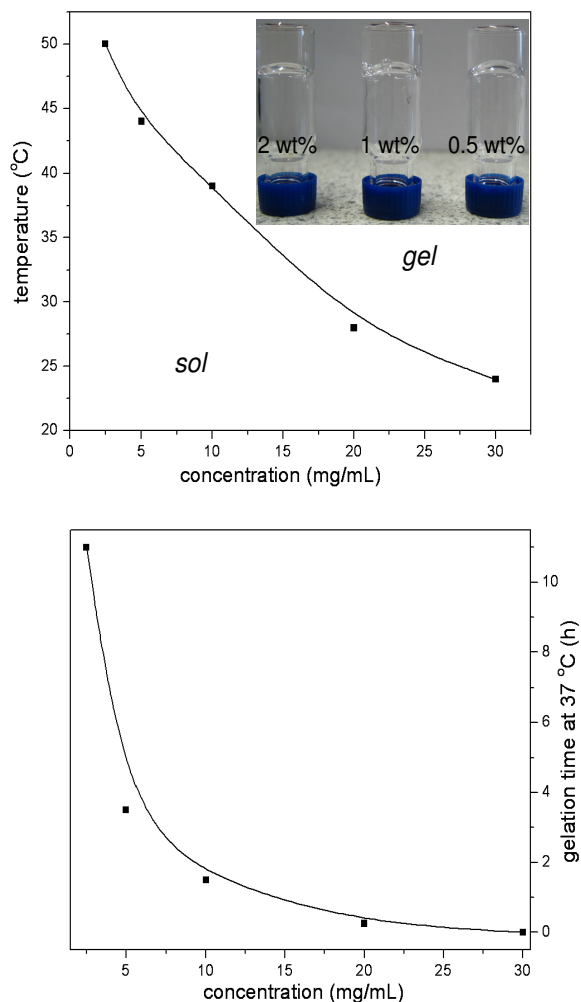


Figure 4.3: Hydrogelation temperature as a function of PEG2000-Tyr₆ concentration (top). Hydrogelation time at 37 °C as a function of PEG2000-Tyr₆ concentration (bottom).

All these results suggest that there is a very delicate block length ratio that needs to be met in this system for efficient hydrogel formation to occur since the hydrogelation was not observed for PEG2000-Tyr₁₀ and PEG2000-Tyr₁₄. An obvious explanation is the hydrophilic-hydrophobic balance between the PEG and the tyrosine block that is determining for the hydrogel formation.^{14,29} Moreover, the self-assembly of the PEG2000-Tyr₆ in water can to a large extent be ascribed to the

β -sheet interaction in agreement with previously reported peptide hydrogels.³⁰ FTIR and CD spectra confirm that the tyrosine block adopts a typical β -sheet conformation when the hydrogel is formed as evident from the amide I band at 1623 cm^{-1} and the minimum at 220 nm in the CD spectrum. The hydrogels are stable up to pH 13.0, which coincides with the complete deprotonation of the tyrosine hydroxy groups (Figure 4.4). Further evidence for the importance of the tyrosine phenolic groups in the current hydrogels was obtained from block copolymers in which the tyrosine was replaced by phenylalanine (Phe). Although the FTIR spectra of both PEG2000-Phe₅ and PEG2000-Phe₁₀ confirmed a β -sheet conformation, with a higher hydropathy index of 2.8 than Tyr (-1.3),³¹ neither of the polymers were water-soluble and could form hydrogels. Apparently, the phenolic hydroxy groups render the tyrosine block more polar and better soluble than the phenylalanine block. This slight difference in structure favorably tips the amphiphilic balance, and affects the self-assembly in aqueous solution. Furthermore, the partly polar phenolic group could promote intermolecular hydrogen bonds with water molecules or main-chain carbonyls and, thus, contributes to the molecular interaction in the hydrogels.¹⁶

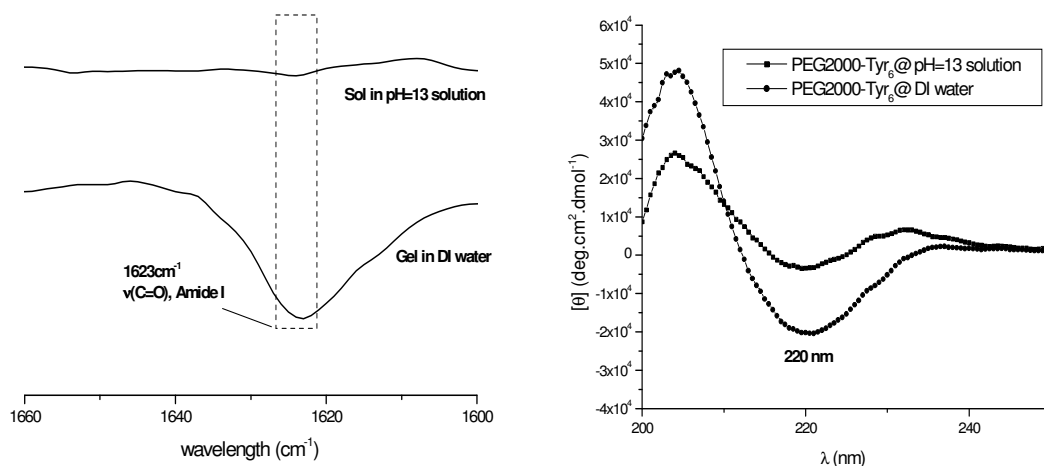


Figure 4.4: FTIR spectra of PEG2000-Tyr₆ (40 mg/mL) hydrogel in DI water and in a solution of pH=13.0 (Left); Circular dichroism spectra of PEG2000-Tyr₆ (0.25 mg/mL) in DI water and in pH=13.0 solution (Right).

While these results explain the hydrogel formation, they do not rationalize the reverse thermoresponsive sol-to-gel transition of PEG2000-Tyr₆. To investigate the conformational changes of the block copolymer in aqueous solution, temperature dependent CD spectra were recorded. As revealed in Figure 4.5, the negative band at 220 nm, corresponding to β -sheet conformation, gradually increased as the temperature increased from 10 to 60 °C, in particular, above 30 °C. This implies that the increment of β -sheet conformation at increased temperature increases, thereby promoting better intermolecular interaction and hydrogelation. We hypothesize that two phenomena contribute to this behavior. The first is the known dehydration of PEG at higher temperatures, causing the PEG blocks to become more hydrophobic.³² This offsets the hydrophobic/hydrophilic balance in the block copolymer and decreases the molecular motion of the PEG block. On the other hand, an increase in temperature increases the molecular motion of the Tyr domain, promoting better phase packing and also enhancing its molecular self-organization *via* hydrogen bonding, as demonstrated by the stronger β -sheet conformation at elevated temperatures. This process facilitates block copolymer self-assembly and hydrogel network formation. The sensitivity of the hydrogelation to the block lengths composition highlights the delicate balance of these interactions.

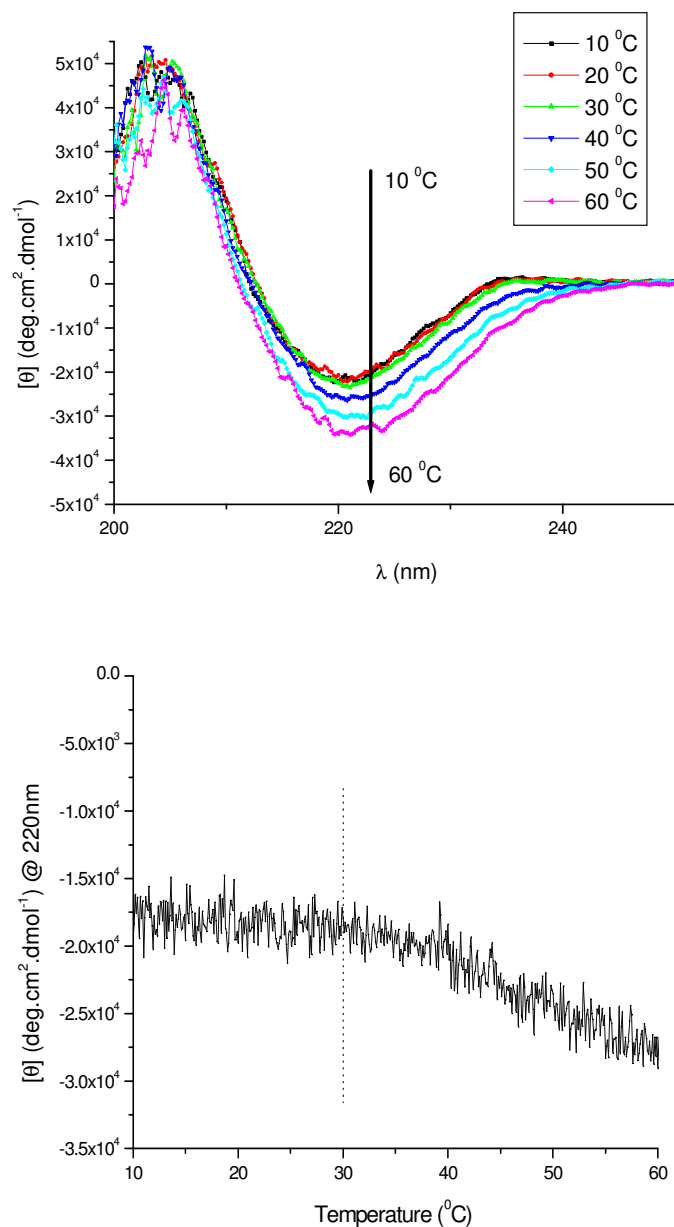


Figure 4.5: Circular dichroism spectra of PEG2000-Tyr₆ aqueous solution (0.25 mg/mL) as a function of temperature (Top). Ellipticity change of PEG2000-Tyr₆ (0.25 mg/mL) at 220 nm as a function of temperature (Bottom).

The viscoelastic properties of the gels were explored using oscillatory rheology, in which the temporal evolution of storage modulus (G') and loss modulus (G'') is typically measured to observe the gelation behavior.³³ Figure 4.6 shows the dynamic mechanical changes in the modulus of PEG2000-Tyr₆ at different concentrations of 2.0 wt% and 1.0 wt% as a function of temperature. The G' of the polymer in both cases is an order of magnitude higher than G'' as the temperature gradually increases from 25 °C to 60 °C. This is indicative of the formation of an elastic solid-like material as the temperature increases. At higher polymer concentrations, higher values of G' and G'' were obtained, indicating a more rigid gel. G' was found to be insensitive to the frequency in a range of 1~100 rad/s, and only increase slightly with increasing frequency in all different concentrations.³⁴ The dependence of the gel modulus on concentration is weak when compared to that seen for many gelling systems (Figure 4.7), with a power law of approximately 1.2 for concentrations with $r^2=0.99$. Such a low power law is surprising. Studies of self-assembling peptides have in the past shown power laws in the range of 2.5, although we recently showed that for gels formed from Fmoc-dipeptides a low power law of 1.4 was observed.³⁵ A power law of 1.4 was reported for hydrogels prepared from a peptide amphiphile when cross-linked by calcium; a higher power law was obtained when acid was used to induce gelation, implying that the difference in power law is due to cross-link density. One possible explanation for the low power law observed in the current system is that the conditions of gelation are not identical at different concentrations.

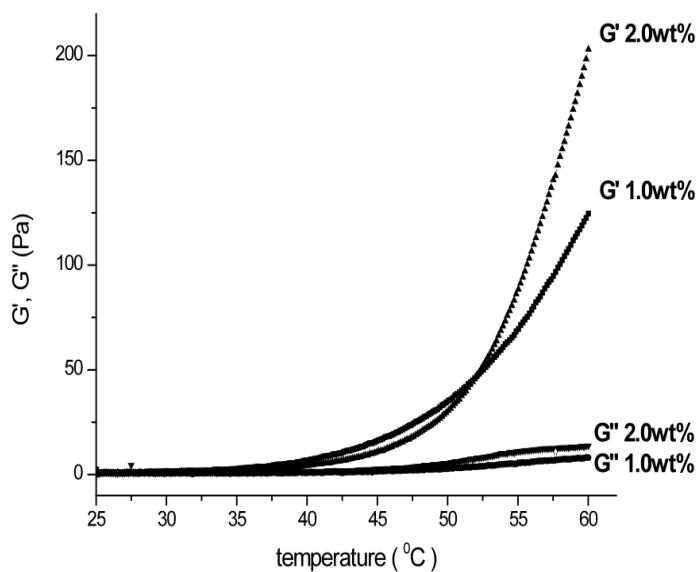


Figure 4.6: Dynamic mechanical changes in the modulus of PEG2000-Tyr₆ at 2.0 wt% and 1.0 wt% as a function of temperature.

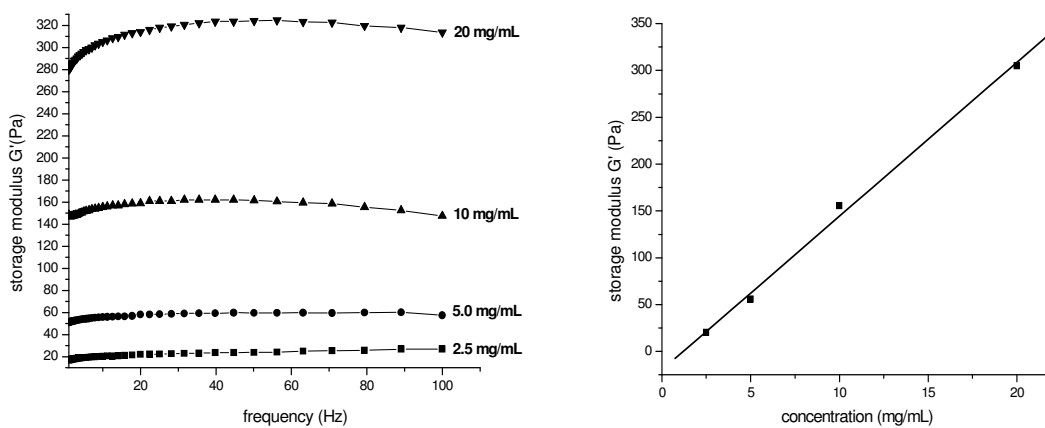


Figure 4.7: (Left) Frequency sweep data for the gel with different concentrations; (Right) Storage modulus (G') as a function of concentration, where the line represents a linear fit of the data.

The information obtained from the spectroscopic and rheological analysis suggests that the hydrogel formation of PEG2000-Tyr₆ is collectively driven by several factors including amphiphilic balance between PEG and Tyr blocks, hydrogen bonding by β -sheet conformation and phenolic group, possibly also aromatic interaction from the side chains of poly(L-tyrosine). Better packing of the β -sheet tyrosine block at increasing temperature induces a reverse thermogelation. Therefore, as indicated in Figure 4.2, with the increase of the temperature, amphiphilic PEG2000-Tyr₆ block copolymers in aqueous solution can entangle with each other through hydrogen bonding or other non-covalent interactions to form a fibrous three-dimensional network as the matrices of the hydrogels. This is a desirable property for biomedical hydrogels because at room temperature, a liquid gel-precursor solution could be administered by injection, possibly together with drugs or growth factors, followed by *in-situ* gelling at body temperature thus avoiding surgical implantation. The applicability of PEG2000-Tyr₆ as biomedical hydrogels was therefore assessed in preliminary experiments.

Biostability and resorbability under simulated physiological conditions are essential criteria in the assessment of biomedical hydrogels. The stability of the hydrogel at block copolymer concentrations of 2.0 and 1.0 wt% was measured in Krebs buffer solution. Krebs buffer is a physiological buffer that, to some degree, mimics the ionic composition, pH, and osmotic behavior of tissue fluid and, so, is a useful medium to examine the behavior of biomaterials *in vitro*. Figure 4.8 reveals a weight loss of around 20 % and 5 % after nine days for the gel of 1.0 and 2.0 wt%, respectively. While both hydrogels remained quite stable over the monitored time, the 2.0 wt% hydrogel displayed higher stability and lower weight loss due to its higher mechanical stability as shown in Figure 4.8. This lack of mechanical strength of the 1.0 wt% hydrogel could allow for more uptake of water, resulting in more swelling, with concomitant structural breakdown. Second, a weaker gel will be more prone to mechanical disruption due to physical manipulation associated with buffer changes. Both of these factors together could account for the observed change in weight. In a second set of experiments, enzymes were encapsulated into the hydrogel (0.5 wt% PEG2000-Tyr₆). Chymotrypsin was chosen as a positive control because it preferentially cleaves peptide amide bonds adjacent to an aromatic amino

acid such as tyrosine, tryptophan and phenylalanine.³⁶ Trypsin was selected as negative control as it cleaves peptide chains mainly at the carboxyl side of the amino acids like lysine or arginine.³⁷ The enzymes of 28.5 unit/mL were doped into the hydrogels by dissolving them in a 0.5 wt% polymer solution and subsequently triggering hydrogelation by heating to 37 °C. The hydrogel containing chymotrypsin showed a gradual disintegration within 24 hours and completely broke into pieces after 7 days (inset Figure 4.8). In contrast, no visible change was observed for the hydrogels containing trypsin or no enzyme in the same time period highlighting the selective enzymatic degradation by chymotrypsin. This experiment further shows that certain biomolecules can be incorporated without compromising the hydrogel formation.

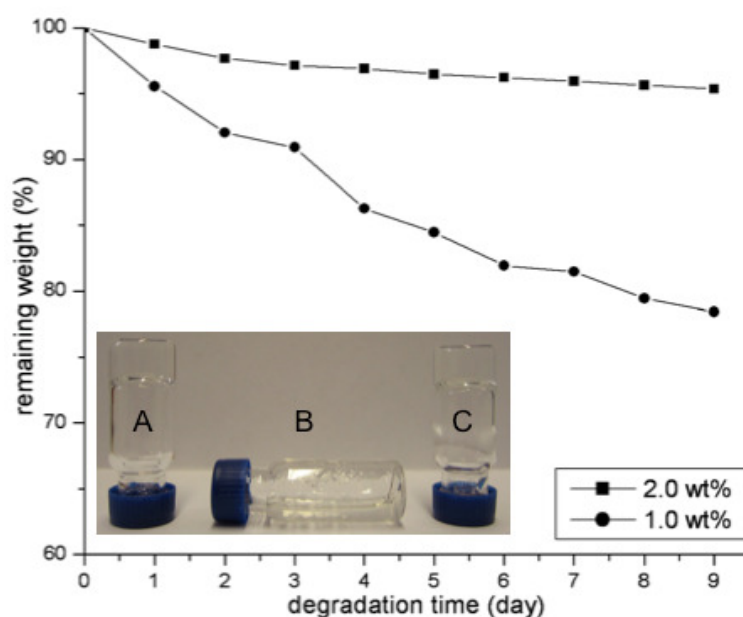


Figure 4.8: Weight loss of PEG2000-Tyr₆ hydrogel at 2.0 and 1.0 wt% in Krebs buffer solution. Inset: Degradation of hydrogels in the presence of (A): no enzyme, (B): chymotrypsin, (C): trypsin. Enzymes (28.5 unit/mL) were incorporated in the hydrogel at 0.5 wt% in 37 °C water bath; pictures taken after 7 days.

We also explored the use of the hydrogel for the entrapment and release of small drug molecules. A 2.0 wt% PEG2000-Tyr₆ hydrogel was utilized to release the

pharmacological pro-angiogenic desferrioxamine (DFO) over a period of 7 days. DFO was dissolved within the gel as it is a water-soluble drug. Release of DFO from the hydrogel into phosphate buffer by diffusion at 37 °C was measured via HPLC. As shown in Figure 4.9, the gel produced a burst release within the first 24 h and then a sustained, albeit decreasing, release over the period of seven days. Interestingly, the gel released ~20% of the total encapsulated drug within seven days. However, the amount of drug released is sufficient to exert a biological effect.²⁰ The remainder of the drug may have become degraded, within both the gel and release buffer. The sustained release of the small-molecule drug confirmed that the PEG2000-Tyr₆ hydrogel could potentially function as an injectable drug depot, which could exert sustained drug release and local efficacy for an extended period.

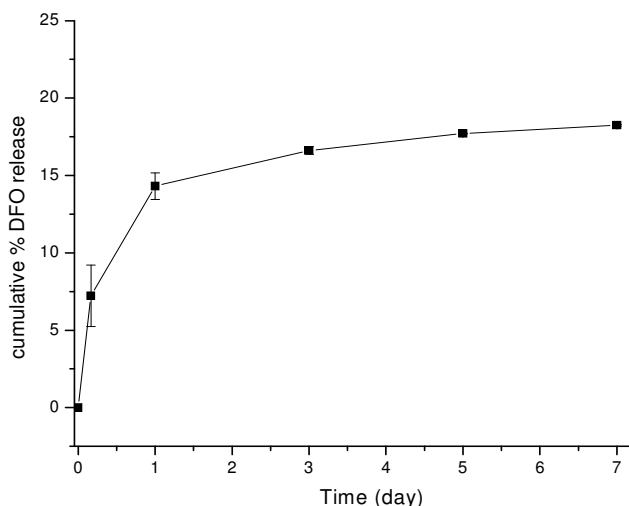


Figure 4.9: Cumulative release profile of DFO from 2.0 wt% hydrogel containing 100 μ M DFO at 37 °C over seven days ($n=3$, mean + standard deviation plotted).

Finally, the cytotoxicity of the hydrogel was assessed by seeding rMSCs onto a preformed 2.0 wt% PEG2000-Tyr₆ gel layer and staining with a Live/Dead stain. No dead cells were apparent and cells were adherent to the gel layer, suggesting that the gel did not exert significant cytotoxicity after 48 hours. As revealed in Figure 4.10, at 48 hours the majority of cells appeared rounded, suggesting that the cells were not presented with sufficient attachment sites to enable spreading.

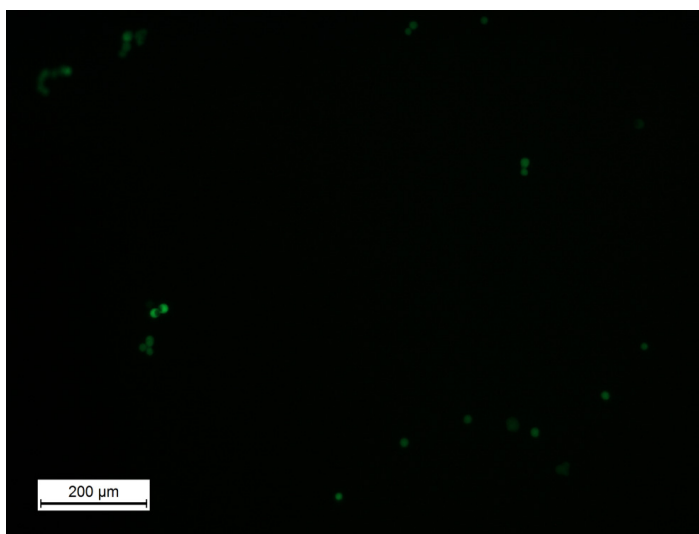


Figure 4.10: Live/Dead image of rMSCs seeded on a preformed PEG2000-Tyr₆ gel layer after 48 hours. Live cells are stained green. No dead cells were present. Cells were adherent but the majority appeared rounded.

4.4 Conclusions

Novel block copolymers comprising a PEG and an oligo(tyrosine) block were synthesized in different compositions by NCA polymerisation. The ability to form hydrogels is delicately dependent on the block length ratio with an optimum composition of PEG2000-Tyr₆. This material undergoes thermoresponsive gelation at a low concentration range of 0.25-3.0 wt% within a temperature range of 25 to 50 °C. The hydrogel formation of PEG2000-Tyr₆ is collectively driven by several factors including amphiphilic balance between PEG and Tyr blocks, hydrogen bonding by β -sheet conformation and phenolic group. CD analysis confirms that better packing of the β -sheet tyrosine blocks at increasing temperature induces the reverse thermogelation. A preliminary assessment of biocompatibility *in vitro* indicated that the hydrogel is not cytotoxic, is biodegradable, and produced a sustained release of a small-molecule drug. Therefore, this formulation may have potential as an injectable drug delivery vehicle.

4.5 References

- ¹ (a) Vermonden T.; Censi R.; Hennink W. E. *Chem. Rev.* **2012**, *112*, 2853. (b) Peppas, N. A.; Hilt, J. Z.; Khademhosseini, A.; Langer, R. *Adv. Mater.* **2006**, *18*, 1345. (c) Altunbas, A.; Pochan, D. J.; *Top Curr. Chem.* **2012**, *310*, 135. (d) Seliktar, D., *Science* **2012**, *336*, 1124. (e) Li Y.; Rodrigues J.; Tomás H. *Chem. Soc. Rev.* **2012**, *41*, 2193.
- ² (a) Li, Z. Q.; Guan, J. J. *Expert Opin. Drug Deliv.* **2011**, *8*, 991. (b) Klouda, L.; Mikos, A. G. *Eur. J. Pharm. Biopharm.* **2008**, *68*, 34. (c) Jeong, B.; Kim, S.W.; Bae, Y. H. *Adv. Drug Deliv. Rev.* **2002**, *54*, 37.
- ³ (a) Park M. H.; Joo M. K.; Choi B.G., Jeong B., *Acc. Chem. Res.* **2012**, *45*, 42. (b) Moon, H. J.; Ko, D. Y.; Park, M. H.; Joo, M. K.; Jeong, B. *Chem. Soc. Rev.* **2012**, *41*, 4860. (c) Li, Z. Q.; Guan, J. J., *Expert Opin. Drug Deliv.* **2011**, *8*, 991.
- ⁴ (a) Matson, J. B.; Stupp, S. I. *Chem. Commun.* **2012**, *48*, 26. (b) Branco, M. C.; Schneider, J. P. *Acta Biomaterialia* **2009**, *5*, 817.
- ⁵ (a) Estroff, L.A.; Hamilton, A. D. *Chem. Rev.* **2004**, *104*, 1201. (b) Adams, D. J.; Topham, P. D. *Soft Matter* **2010**, *6*, 3707. (c) Dastidar P. *Chem. Soc. Rev.* **2008**, *37*, 269. (d) Jonker A. M.; Löwik, D W. P. M.; van Hest J. C. M. *Chem. Mater.* **2012**, *24*, 759.
- ⁶ Hartgerink, J. D.; Beniash, E.; Stupp, S.I. *Science* **2001**, *294*, 1684.
- ⁷ (a) Cui, H.; Webber, M. J.; Stupp, S. I. *Biopolymers* **2010**, *94*, 1. (b) Niece, K. L.; Czeisler, C.; Sahni, V.; Tysseling-Mattiace, V.; Pashuck, E. T.; Kessler, J. A.; Stupp, S. I. *Biomaterials* **2008**, *29*, 4501.
- ⁸ (a) Hadjichristidis, N.; Iatrou, H.; Pitsikalis, M.; Sakellariou, G. *Chem. Rev.* **2009**, *109*, 5528. (b) Deming, T. J. *Nature* **1997**, *390*, 386. (b) Dimitrov, I.; Schlaad, H. *Chem. Commun.* **2003**, 2944. (c) Habraken, G. J. M.; Peeters, M.; Dietz, C. H. J. T.; Koning, C. E.; Heise, A. *Polym. Chem.* **2010**, *1*, 514.
- ⁹ (a) Bertin, A.; Hermes, F.; Schlaad, H. *Adv. Polym. Sci.* **2010**, *224*, 167. (b) Cheng, J.; Deming, T. J. *Top. Curr. Chem.* **2012**, *310*, 1. (c) Habraken, G. J. M.; Heise, A.; Thornton, P. D. *Macromol. Rapid Commun.* **2012**, *33*, 272. (d) Colin, B.; Huang, J.; Ibarboure, E.; Heise, A.; Lecommandoux, S. *Chem. Commun.* **2012**, *48*, 8353. (e)

Huang, J.; Bonduelle, C.; Thévenot, J.; Lecommandoux, S.; Heise, A. *J. Am. Chem. Soc.* **2012**, *134*, 119. (f) Schatz, C.; Louguet, S.; Le Meins, J.-F.; Lecommandoux, S. *Angew. Chem., Int. Ed.* **2009**, *48*, 2572.

¹⁰ (a) Nowak, A. P.; Breedveld, V.; Pakstis, L.; Ozbas, B.; Pine, D. J.; Pochan, D.; Deming, T. J. *Nature* **2002**, *417*, 424. (b) Breedveld, V.; Nowak, A. P.; Sato, J.; Deming, T. J.; Pine, D. J. *Macromolecules* **2004**, *37*, 3943. (c) Nowak, A. P.; Breedveld, V.; Pine, D. J.; Deming, T. J. *J. Am. Chem. Soc.* **2003**, *125*, 15666. (d) Nowak, A. P.; Sato, J.; Breedveld, V.; Deming, T. J. *Supramol. Chem.* **2006**, *18*, 423. (e) Deming, T. J. *Soft Matter* **2005**, *1*, 28. (f) Li, Z. B.; Deming, T. J. *Soft Matter* **2010**, *6*, 2546.

¹¹ (a) Choi, Y. Y.; Jang, J. H.; Park, M. H.; Choi, B. G.; Chi, B.; Jeong, B. *J. Mater. Chem.* **2010**, *20*, 3416. (b) Oh, H. J.; Joo, M. K.; Sohn, Y. S.; Jeong, B. *Macromolecules* **2008**, *41*, 8204. (c) Jeong, Y.; Joo, M. K.; Bahk, K. H.; Choi, Y. Y.; Kim, H.-T.; Kim, W.-K.; Lee, H. J.; Sohn, Y. S.; Jeong, B. *J. Control. Release* **2009**, *137*, 25. (d) Kang, E. Y.; Yeon, B.; Moon, H. J.; Jeong, B. *Macromolecules* **2012**, *45*, 2007. (e) Shinde, U. P.; Joo, M. K.; Moon, H. J.; Jeong, B. *J. Mater. Chem.* **2012**, *22*, 6072. (f) Park, M. H.; Joo, M. K.; Choi, B. G.; Jeong, B. *Acc. Chem. Res.* **2012**, *45*, 42.

¹² Cheng, Y.; He, C.; Xiao, C.; Ding, J.; Zhuang, X.; Huang, Y.; Chen, X. *Biomacromolecules* **2012**, *13*, 2053.

¹³ (a) Lesser, G. J.; Rose, G. D. *Proteins: Struct. Funct. Genet.* **1990**, *8*, 6. (b) Glazer, A. N.; Smith, E. L. *J. Biol. Chem.* **1961**, *236*, 2948. (c) Tanford, C.; Hauenstein, J. D.; Rands, D. G. *J. Am. Chem. Soc.* **1955**, *77*, 6409. (d) Tachibana, A.; Murachi, T. *Biochemistry* **1966**, *5*, 2756.

¹⁴ Pace, C. N.; Horn, G.; Hebert, E. J.; Bechert, J.; Shaw, K.; Urbanikova, L.; Scholtz, J. M.; Sevcik, J. *J. Mol. Biol.* **2001**, *312*, 393.

¹⁵ (a) McDonald, I. K.; Thornton, J. M. *J. Mol. Biol.* **1994**, *238*, 777. (b) Boobbyer, D. N.; Goodford, P. J.; McWhinnie, P. M.; Wade, R. C. *J. Med. Chem.* **1989**, *32*, 1083. (c) Fersht, A. R.; Shi, J. P.; Knill-Jones, J.; Lowe, D. M.; Wilkinson, A. J.; Blow, D. M.; Brick, P.; Carter, P.; Waye, M. M.; Winter, G. *Nature* **1985**, *314*, 235.

¹⁶ Baker, E. N.; Hubbard, R. E. *Prog. Biophys. Mol. Biol.* **1984**, *44*, 97.

- ¹⁷ (a) Malencik D. A.; Anderson, S. R. *Biochemistry* **1996**, *35*, 4375. (b) Malencik, D. A.; Anderson, S. R. *Amino Acids* **2003**, *25*, 233. (c) Elvin, C. M.; Carr, A. G.; Huson, M. G.; Maxwell, J. M.; Pearson, R. D.; Vuocolo, T.; Liyou, N. E.; Wong, D. C. C.; Merritt, D. J.; Dixon, N. E. *Nature* **2005**, *437*, 999.
- ¹⁸ Liao, S. W.; Yu, T.B.; Guan, Z. *J. Am. Chem. Soc.* **2009**, *131*, 17638.
- ¹⁹ Yu, L.; Zhang, H.; Ding, J. D. *Angew. Chem. Int. Ed.* **2006**, *45*, 2232.
- ²⁰ Hastings, C. L.; Kelly, H. M.; Murphy, M. J.; Barry, F. P.; O'Brien, F. J.; Duffy, G. *P. J. Control. Release* **2012**, *10*, 73.
- ²¹ Liu, T. C. K.; Ismail, S.; Brennan, O.; Hastings, C.; Duffy, G. P. *J. Tissue Eng. Regen. Med.* **2011**, *5*, 501.
- ²² (a) Kim, K.T.; Park, C.; Vandermeulen, G.W.M.; Rider, D.A.; Kim, C.; Winnik, M. A.; Manners, I. *Angew Chem. Int. Ed.* **2005**, *44*, 7964. (b) Naik, S. S.; Savin, D. A. *Macromolecules* **2009**, *42*, 7114. (c) Gibson, M. I.; Cameron, N. R. *Angew. Chem. Int. Ed.* **2008**, *47*, 5160.
- ²³ (a) Bonora, G. M.; Moretto, V.; Toniolo, C.; Anzinger, H.; Mutter, M. *Int. J. Pept. Protein Res.* **1983**, *21*, 336. (b) Lee, N. H.; Frank, C. W. ; *Langmuir* **2003**, *19*, 1295.
- ²⁴ (a) Mahalakshmi, R.; Raghothama, S.; Balaram, P. *J. Am. Chem. Soc.* **2006**, *128*, 1125. (b) Castelletto, V.; Hamley, I.W. *Biophysical Chemistry.* **2009**, *141*, 169.
- ²⁵ Gibson, M. I.; Cameron, N. R. *Angew. Chem. Int. Ed.* **2008**, *47*, 5160.
- ²⁶ Petka, W. A.; Harden, J. L.; McGrath, K. P.; Wirtz, D.; Tirrell, D. A. *Science* **1998**, *281*, 389.
- ²⁷ Joo, M. K.; Park, M. H.; Choi, B. G.; Jeong, B. *J. Mater. Chem.* **2009**, *19*, 5891.
- ²⁸ Hamley, I. W.; Cheng, G.; Castelletto, V. *Macromol.Biosci.* **2011**, *11*, 1068.
- ²⁹ Barth, A. *Prog. Biophys. Mol. Biol.* **2000**, *74*, 141.
- ³⁰ Rughani, R.V.; Salick, D. A.; Lamm, M. S.; Yucel, T.; Pochan, D. J.; Schneider J.P. *Biomacromolecules* **2009**, *10*, 1295.
- ³¹ Kyte, J.; Doolittle, R. F. *J. Mol. Biol.* **1982**, *157*, 105.
- ³² Yu, L.; Zhang, H.; Ding, J. D. *Angew.Chem. Int. Ed.* **2006**, *45*, 2232.
- ³³ Yan, C. Q.; Pochan, D. J. *Chem. Soc. Rev.* **2010**, *39*, 3528.
- ³⁴ Tzokova, N.; Fernyhough, C. M.; Butler, M. F.; Armes, S. P.; Ryan, A. J.; Topham, P. D.; Adams, D. J. *Langmuir* **2009**, *25*, 11082.

³⁵ Chen, L.; Pont, G.; Morris, K.; Lotze, G.; Squires, A.; Serpell, L. C.; Adams, D. J., *Chem. Commun.* **2011**, 47, 12071.

³⁶ (a) Wilcox P.E. *Methods in Enzymology* **1970**, 19, 64. (b) Plunkett, K. N.; Berkowski, K. L.; Moore, J. S. *Biomacromolecules* **2005**, 6, 632.

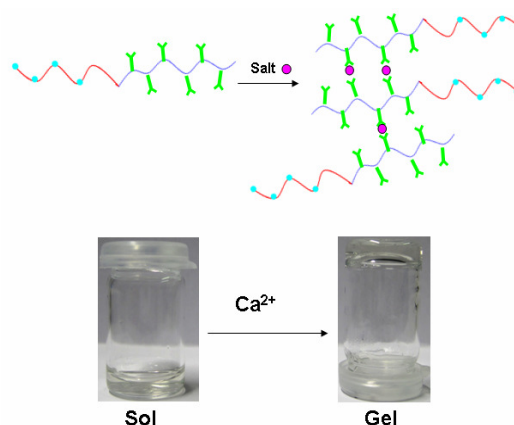
³⁷ Thornton, P. D.; McConnell, G.; Ulijn, R. V. *Chem. Commun.* **2005**, 5913.

Chapter 5

Salt-triggered self-assembly of amphiphilic poly(L-glutamate-*b*-L-tyrosine) towards the formation of hydrogel

Abstract

Novel amphiphilic poly(L-glutamate-*b*-L-tyrosine) block copolymer can spontaneously self-assemble into macroscopic transparent membrane-like aggregates in the presence of salt solutions. Upon the addition of Ca^{2+} to screen the carboxylates of poly(L-glutamate), the delicate balance between the forces favoring assembly by hydrophobic interaction and the forces disfavoring assembly by electrostatic repulsion can be manipulated, further resulting in conformation changes and self-assembly. Most importantly, amphiphilic poly(L-glutamate-*b*-L-tyrosine) at certain concentrations (typically 1.0-4.0 wt%) can be triggered by the sufficient electrostatic screening and salt bridge from Ca^{2+} to form self-supporting hydrogels. These materials might be useful for biological applications such as slow-diffusion drug-delivery systems and regenerative medicine.



5.1 Introduction

The design and fabrication of novel peptide-based amphiphiles through peptide self-assembly has been intensively explored over the last decades. Their excellent biocompatibility and unique biomimetic structures make them ideal candidates for a range of biomedical applications such as controlled drug delivery, tissue engineering, biomineralisation, and membrane protein stabilization.¹ Through non-covalent interactions such as hydrogen bonding, van der Waals interaction, electrostatic interaction, π - π stacking and hydrophobic interaction, amphiphilic peptides can self-assemble into well-defined supramolecular organizations including nanofibers, nanotubes, vesicles and micelles.² Advances in peptide synthesis enabled the design of more sophisticated amphiphilic peptides, of which the self-assembly can be controlled in a “smart” manner. In particular, the self-assembly of peptide-based amphiphiles can be triggered in response to a range of external stimulus, including pH,³ salt concentration,⁴ light,⁵ temperature⁶ or the presence of enzymes.⁷ Ionic strength is a powerful and facile approach used to trigger the self-assembly of polypeptide amphiphiles into different nanostructures as the salt can significantly contribute to hydrophobic and electrostatic interactions through charge screening.⁸ By incorporating charged amino acids like glutamic acid or lysine into the peptide sequences, Stupp and coworkers have pioneered the use of the salt (i.e. calcium ions) to promote the self-assembly of amphiphilic molecules into supramolecular nanofibril network and further the formation of self-supporting hydrogel.⁹ Zhang employed charged amino acids including glutamic acid and lysine to design a series of ionic self-complementary oligopeptides.¹⁰ Upon the addition of the salt, due to electrostatic interactions, these self-assembling peptides (i.e. EAK16, so-called “zuotin”) can spontaneously self-organize into ordered nanofibers and further into artificial three-dimensional scaffolds such as macroscopic membranes or hydrogels for regenerative medicine.¹¹ Recently, Adams et al. demonstrated that the addition of divalent cations to a solution of a dipeptide-based hydrogelators that formed worm-like micelles at high pH led to the formation of a stiff self-supporting hydrogel.¹² Ulijn et al. revealed that salts could have a pronounced effect on

molecular assembly and material properties of a series of anionic Fmoc-peptide-based gelators as ions were found to have a significant influence on the hydrophobic interactions, leading to more organized supramolecular structures.¹³ Xu also used calcium ions to cross-link the supramolecular nanofibers of small peptides consisting of multiple carboxylic acid and aromatic groups for the formation of hydrogel.¹⁴

The self-assembly process of these peptide amphiphiles triggered by salt highly relies on the length and sequence of the amino acid blocks. To omit tedious peptide amphiphile synthesis by coupling chemistry and to simplify the preparation of amphiphilic peptide in a scalable manner, facile N-carboxyanhydride (NCA) ring-opening polymerisation can be applied for the synthesis of amphiphilic block copolymers. NCA polymerisation has been demonstrated for the synthesis of complex polymer structures capable of self-assembly.¹⁵ The formation of hydrogels from diblock polypeptide amphiphiles via NCA polymerisation was first reported by Deming.¹⁶ These materials contain water soluble polyelectrolyte blocks such as poly(L-lysine) or poly(L-glutamate) and a α -helical poly(L-leucine) hydrophobic block. The gelation is driven by the stiff α -helical conformation of the hydrophobic domain and the electrostatic repulsion from the polyelectrolyte segments. In addition, the gel is highly stable both in the presence and absence of ionic species. However, hydrogelation is only achieved when both of the hydrophobic and hydrophilic segments have a sufficiently high molecular weight. A series of micelle-assembled thermosensitive hydrogels from amphiphilic hybrid block copolymers obtained by ring-opening polymerisation of alanine or phenylalanine NCAs were also demonstrated.¹⁷ These materials self-assemble into nanostructures such as micelles in aqueous solutions and further transit into hydrogels at high polymer concentration in the range of 3.0-14.0 wt% through intermicellar aggregation when the temperature increases. Very recently, we developed a new PEGylated tyrosine-based polypeptide obtained by NCA polymerisation. In this concept, tyrosine building blocks in the amphiphiles are able to display multiple interactions triggering self-assembly into the hydrogel matrix. The gel formation is attributed to the precise hydrophobicity interaction between PEG and tyrosine building blocks, as well as the unique feature of the tyrosine that has a polar but hydrophobic phenol

group in the side chain. Surprisingly, the PEGylated tyrosine-based polypeptide underwent thermoresponsive hydrogelation at a low concentration range of 0.25-3.0 wt% within a temperature range of 25 to 50 °C.¹⁸

In this paper, we continued to explore tyrosine for the design of new amphiphilic copolypeptides, as the previous work demonstrated that due to its unique features tyrosine is a promising amino acid candidate for the self-assembly of amphiphiles, in particular for the formation of hydrogel. To investigate the self-assembly of the polypeptide amphiphiles in response to the salt, poly(L-glutamic acid) was chosen as the corresponding polyelectrolyte segment. Owing to the different pK_a of the side chains, amphiphiles can be simply prepared by the deprotonation of poly(L-glutamic acid) under mild basic condition. Interestingly, in this molecular design, the amphiphilic block copolypeptides comprise two completely different motifs, in which the hydrophilic building block poly(L-glutamate) prefers a random coil conformation when the side chains are charged while the hydrophobic but polar poly(L-tyrosine) building block favors a β -sheet secondary structure.¹⁸ The intriguing question is whether the salt would induce conformational changes and trigger the self-assembly of the polypeptide into three-dimensional network and hydrogel. Thereby, poly(L-glutamate-*b*-L-tyrosine) amphiphiles with different chain lengths were prepared, and then the self-assembly of the amphiphiles triggered by the salt was investigated.

5.2 Experimental section

Materials

All chemicals were purchased from Sigma-Aldrich and used as received unless otherwise noted. γ -Benzyl-L-glutamate, O-benzyl-L-tyrosine and phenylalanine were supplied by Bachem. Anhydrous DMF, ethyl acetate, THF were used directly from the bottle under an inert and dry atmosphere.

Methods

^1H and ^{13}C NMR spectra were recorded at room temperature with a Bruker Avance 400 (400 MHz). CF_3COOD and CDCl_3 were used as solvents, and signals were referred to the signal of residual protonated solvent signals. ATR-FTIR spectra were collected on a Perkin Elmer Spectrum 100 in the spectral region of $650\text{--}4000\text{ cm}^{-1}$, and were obtained from 16 scans with a resolution of 2 cm^{-1} . A background measurement was taken before the sample was loaded onto the ATR unit for measurements. CD data were collected on a Jasco J-810 CD spectrometer (Japan Spectroscopic Corporation) with a pathlength of 0.1 cm and a bandwidth of 1 nm. Three scans were conducted and averaged between 185 nm and 250 nm at a scanning rate of 20 nm min^{-1} with a resolution of 0.2 nm. The data were processed by subtracting the solvent as background. The percentages of α -helical and β -sheet contents were determined by DichroWeb using the SELCON3 analysis program, based on a reference set of 56 proteins in the 185-240 nm wavelength range. The morphology of membrane-like aggregates was obtained by using Hitachi S3400n SEM instrument. The preparation of samples for SEM analysis involved placing a drop of amphiphilic peptide onto the salt solution on the thin carbon-coated film. After the polymer self-assembled into the membrane-like aggregate, the sample was left to air dry. It was then submitted for SEM scan after gold coating for 2 minutes. SEC analysis using HFIP (Biosolve, AR from supplier or redistilled) as eluent was carried out using a Shimadzu LC-10AD pump (flow rate 0.8 mL/min) and a WATERS 2414 differential refractive index detector (at $35\text{ }^\circ\text{C}$) calibrated with poly(methyl methacrylate) standards (range 1000 to 2000000 g/mol). Two PSS

PFG-lin-XL (7 μ m, 8*300 mm) columns at 40 °C were used. Injections were done by a Spark Holland MIDAS injector using a 50 μ L injection volume. Before SEC analysis was performed, the samples were filtered through a 0.2 μ m PTFE filter (13 mm, PP housing, Alltech).

Synthesis of *O*-benzyl-L-tyrosine NCA (BLT-NCA), γ -benzyl-L-glutamate NCA (BLG-NCA), phenylalanine NCA (Phe-NCA). α -Pinene (15 g, 110.3 mmol) and *O*-benzyl-L-tyrosine (10.0 g, 36.9 mmol) were dissolved in 80 mL anhydrous ethyl acetate in a three-neck round-bottomed flask. The mixture was stirred and heated to reflux with a slow flow of nitrogen. Then, a solution of triphosgene (5.5 g, 18.4 mmol) in anhydrous ethyl acetate (40 mL) was added dropwise. Two-thirds of the solution was added within 1 hour after which the reaction was left at reflux for another hour. The rest of the triphosgene solution was added until the reaction mixture became clear. Subsequently, around 60 mL of the solvent was removed under pressure and 120 mL *n*-heptane was added slowly to precipitate NCA. After filtration, the solid was recrystallized from ethyl acetate and *n*-heptane (1:2) four times until the NCA was recovered as an off-white crystal. (8.2 g, Yield 75%). ^1H -NMR (400 MHz, CDCl_3 , δ , ppm): 2.95 (dd, $J=14.13$, 8.36 Hz, 1H, $-\text{CH}-\underline{\text{CH}}_2-$), 3.21 (dd, $J=14.13$, 4.10 Hz, 1H, $-\text{CH}-\underline{\text{CH}}_2-$), 4.49 (dd, $J=4.10$, 8.36 Hz, 1H, $-\text{NH}-\underline{\text{CH}}-$), 5.04 (s, 2H, $-\underline{\text{CH}}_2-\text{O}-$), 5.96 (s, 1H, $-\text{NH}-\underline{\text{CH}}-$), 6.95 (d, $J=8.61$ Hz, 2H, ArH), 7.10 (d, $J=8.61$ Hz, 2H, ArH), 7.39 (m, 5H, ArH). ^{13}C -NMR (400 MHz, CDCl_3 , δ , ppm): 37.1 ($-\text{CH}-\underline{\text{CH}}_2-$), 58.9 ($-\underline{\text{CH}}-\text{CH}_2-$), 70.0 ($-\text{O}-\underline{\text{CH}}_2-$), 115.6 (Ar), 125.9 (Ar), 127.5 (Ar), 128.1 (Ar), 128.7 (Ar), 130.2 (Ar), 136.6 (Ar), 151.5 (Ar), 158.5 ($-\text{O}-\underline{\text{C}}(\text{O})-\text{CH}-$), 168.6 ($-\underline{\text{C}}(\text{O})-\text{NH}-$).

The same procedure was applied to the synthesis of γ -benzyl-L-glutamate NCA. (Yield 83%). ^1H -NMR (400 MHz, CDCl_3 , δ , ppm): 2.13 (m, 2H, $\underline{\text{CH}}_2$), 2.59 (t, 2H, $\underline{\text{CH}}_2$, $J=7.09$ Hz), 4.37 (t, 1H, $\underline{\text{CH}}$, $J=6.56$ Hz), 5.13 (s, 2H, $\underline{\text{CH}}_2\text{O}$), 6.75 (s, 1H, $\underline{\text{NH}}$), 7.35 (m, 5H, ArH). ^{13}C -NMR (400 MHz, CDCl_3 , δ , ppm): 26.98 ($\underline{\text{CH}}_2\text{CH}$), 29.87 ($\underline{\text{CH}}_2\text{CO}$), 57.01 ($\underline{\text{CH}}$), 67.22 ($\underline{\text{CH}}_2\text{O}$), 128.48 (ArH), 128.71 (ArH), 128.83 (ArH), 135.30 (ArH), 152.10 ($\text{NHC}(\text{O})\text{O}$), 169.53 ($\text{CH}_2\underline{\text{C}}(\text{O})\text{O}$), 172.51 ($\text{CHC}(\text{O})\text{O}$).

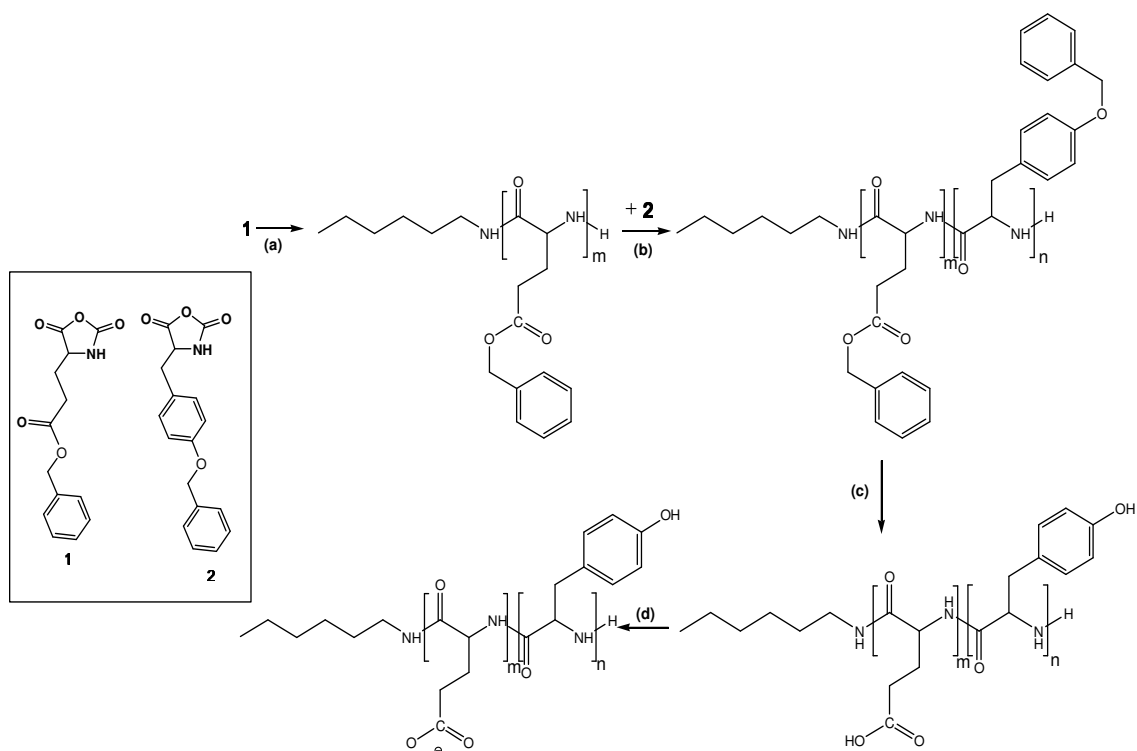
The same procedure was applied to the synthesis of phenylalanine NCA. (Yield 45%). ^1H -NMR (400 MHz, CDCl_3 , δ , ppm): 2.99 (dd, $J=14.16$, 8.59 Hz, 1H, $-\text{CH}-$

CH₂-), 3.30 (dd, *J*=14.16, 4.06 Hz, 1H, -CH-CH₂-), 4.54 (dd, *J*=4.06, 8.59 Hz, 1H, -NH-CH-), 6.03 (s, 1H, -NH-CH-), 7.20 (m, 2H, ArH), 7.35 (m, 5H, ArH). ¹³C-NMR (400 MHz, CDCl₃, δ, ppm): 38.0 (-CH-CH₂-), 58.9 (-CH-CH₂-), 128.2 (Ar), 129.3 (Ar), 129.4 (Ar), 134.0 (Ar), 151.8 (-O-C(O)-CH-), 168.7 (-C(O)-NH).

The synthesis of poly(γ-benzyl-L-glutamate-*b*-O-benzyl-L-tyrosine). The NCA monomer of γ-benzyl-L-glutamate (1.01 g, 3.82 mmol) was dissolved in 9 mL DMF in a Schlenk tube. A solution of hexylamine (19.2 mg, 0.191 mmol) in 2 mL dry DMF was added after NCA was dissolved. The reaction was left to stir in a cold water bath of 0 °C for 4 days under an inert atmosphere. After BLG-NCA had been completely consumed as monitored by FTIR and NMR, and the solution of O-benzyl-L-tyrosine NCA (565 mg, 1.9 mmol) in 20 mL DMF was added. The reaction mixture was left to stir for another 7 days at 0 °C until O-benzyl-L-tyrosine NCA was completely consumed. The reaction mixture was precipitated into an excess diethyl ether, filtered and dried under vacuum as an off-white solid (Yield 80%). ¹H-NMR of poly(γ-benzyl-L-glutamate-*b*-O-benzyl-L-tyrosine) (400 MHz, TFA-d⁶ with CDCl₃, δ, ppm): 0.73-0.82 (s, 3H), 1.11-1.25 (s, 6H), 1.35-1.46 (s, 2H), 1.72-2.20 (br m, 42H), 2.27-2.56 (br m, 42H), 2.60-2.91 (br m, 20H), 4.48-4.72 (br m, 31H), 4.75-5.13 (br m, 64H), 6.65-7.02 (br m, 40H), 7.12-7.35 (br m, 155H).

The synthesis of poly(L-glutamate-*b*-L-tyrosine). Poly(γ-benzyl-L-glutamate-*b*-O-benzyl-L-tyrosine) (1 g) was dissolved in 15.0 mL trifluoroacetic acid (TFA) with 1 mL chloroform. A six-fold excess with respect to benzyl ester (and benzyl ether) of a 33% of HBr in acetic acid (5.0 mL) was added. After 16 hours, the mixture was added dropwise into diethyl ether. The polymer was filtered and suspended in deionized water by ultrasonication, and dialyzed against water for 3 days. The solution was lyophilized as a white solid (Yield 55%). The polymer was suspended in pH=11.0 NaOH solution, and ultrasonicated until it was completely dissolved. The polymer solution was transferred to a dialysis bag (MWCO = 1000 Da) and dialyzed against DI water for 3 days. After dialysis, the polymer was lyophilized to give the product as a white fluffy powder. ¹H-NMR of poly(L-glutamic acid-*b*-L-tyrosine) (400 MHz, TFA-d⁶, δ, ppm): 0.75-0.90 (s, 3H), 1.16-1.40 (s, 6H), 1.46-1.60 (s, 2H), 1.86-2.40 (br m, 42H), 2.42-2.74 (br m, 42H), 2.74-3.12 (br m, 20H), 3.43-3.25 (s, 2H), 4.36-5.06 (br m, 31H), 6.46-7.22 (br m, 52H).

Hydrogel preparation. Hydrogels were prepared by mixing poly(L-glutamate-*b*-L-tyrosine) stock solution with various concentrations of calcium chloride solution directly at room temperature. The homogeneous gels were left to stand at room temperature overnight, and the gelation was confirmed by the inverted vial method.



Scheme 5.1: Synthesis of poly(L-glutamate-*b*-L-tyrosine) block copolymers. (a) hexylamine, DMF, 0 °C; (b) DMF, 0 °C; (c) HBr/acetic acid, TFA/CHCl₃, r. t.; (d) NaOH, pH=11.0, r. t.

5.3 Results and Discussion

Block copolymers poly(γ -benzyl-L-glutamate-*b*-O-benzyl-L-tyrosine) or poly(γ -benzyl-L-glutamate-*b*-phenylalanine) were obtained by sequential ring-opening polymerisation of γ -benzyl-L-glutamate (BLG) NCA and O-benzyl-L-tyrosine (BLT) NCA or phenylalanine (Phe) NCA at different monomer ratios (Scheme 5.1).

Table 5.1: The synthesis of block copolymers poly(γ -benzyl-L-glutamate-*b*-O-benzyl-L-tyrosine) [poly(BLG-*b*-BLT)] and poly(γ -benzyl-L-glutamate-*b*-phenylalanine) [poly(BLG-*b*-Phe)].

Entry	Monomer Feed ratio ^a	Monomer ^b	M _w (g/mol) ^c	M _w (g/mol) ^d	PDI ^d
1	[BLG]:[BLT]=20:10	21:10	7230	- ^e	-
2	[BLG]:[BLT]=20:20	20:19	9288	-	-
3	[BLG]:[Phe]=20:10	20:10	6391	6830	1.2

^a Ratio based on molar amounts of used monomers. ^b Determined by ¹H NMR (TFA-d⁶ with CDCl₃) analysis, which was calculated by the integral peak ratios of the methyl group (-CH₃) from hexylamine at 0.73-0.82 ppm and the C_β signal of poly(O-benzyl-L-tyrosine) at 2.60-2.91 ppm and C_β signal of poly(γ -benzyl-L-glutamate) at 1.72-2.56 ppm while using C_α of poly(O-benzyl-L-tyrosine) and poly(γ -benzyl-L-glutamate) at 4.48-4.72 ppm as the internal standards. ^c Determined by NMR calculations. ^d Determined by SEC in HFIP with PMMA standards. ^e Not determined due to unreliable GPC results.

All polymerisations were performed at 0 °C to prevent the termination of the amino end-groups.¹⁹ Because of the better solubility of poly(γ -benzyl-L-glutamate) building block, BLG-NCA polymerisation initiated by hexylamine was carried out first. After 4 days BLG-NCA was completely consumed as monitored by FTIR, and then BLT-NCA or Phe-NCA was sequentially added into the solution of PBLG macroinitiator for chain extension. As summarized in Table 5.1, the structures of

poly(BLG-*b*-BLT) or poly(BLG-*b*-Phe) diblock copolypeptides were confirmed by ^1H NMR. Poly(L-glutamic acid-*b*-L-tyrosine) and Poly(L-glutamic acid-*b*-L-phenylalanine) were obtained by the quantitative deprotection of the benzyl ether and benzyl ester protecting groups.

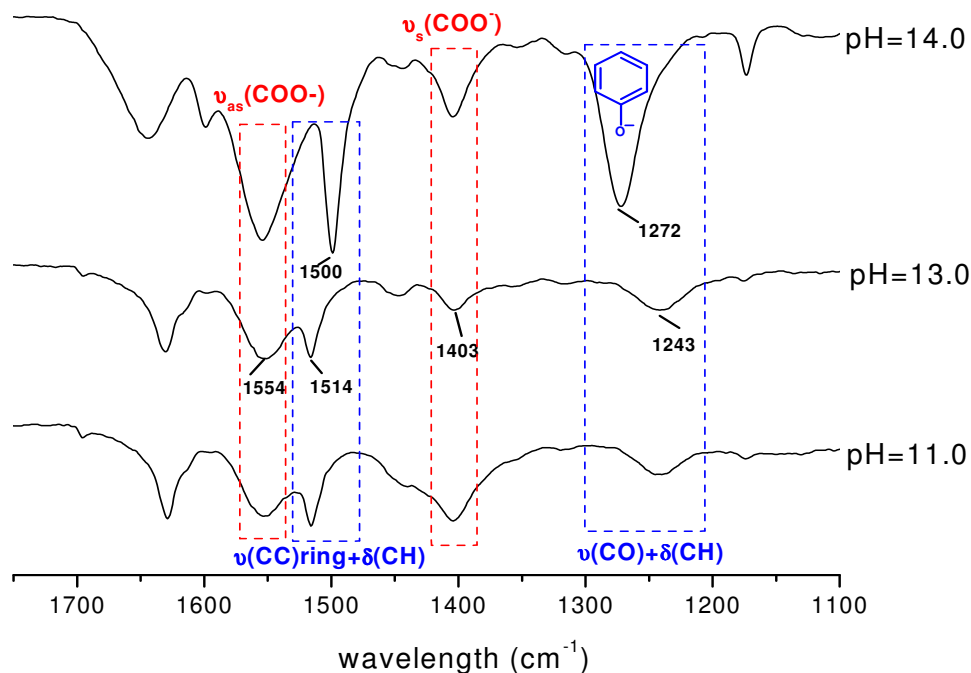


Figure 5.1: FTIR spectra of poly(L-glutamate₂₀-*b*-L-tyrosine₂₀) treated by different pH solutions.

Owing to the different pKa of the side chains, poly(L-glutamic acid-*b*-L-tyrosine) can be selectively deprotonated under basic conditions to yield amphiphilic block copolymer. As the pKa of tyrosine (pKa~10.1) is much higher than the one of glutamic acid (pKa~4.33), the poly(L-glutamic acid) domain is deprotonated under mild basic conditions to give the hydrophilic building block, while the poly(L-tyrosine) block remains hydrophobic.²⁰ Both of block copolypeptides cannot be deprotonated (water soluble) in the solution of pH < 11.0. Thus, different pH solutions were used to determine the optimum conditions for the preparation of amphiphiles. As revealed in FTIR spectra of poly(L-glutamate₂₀-*b*-L-tyrosine₂₀) treated by sodium hydroxide solutions of different pH including pH=11.0, pH=13.0

and pH=14.0 (Figure 5.1), two strong bands at 1403 cm^{-1} and 1554 cm^{-1} characteristic of the symmetric and anti-symmetric stretching vibration confirmed the deprotonation of the carboxylate groups. However, the phenolic hydroxyl groups in the poly(L-tyrosine) block can only be completely deprotonated at pH=14.0. Evidence can be obtained from the downshift of the Tyr $\nu(\text{CC})$ ring and $\delta(\text{CH})$ vibration from 1514 cm^{-1} to 1500 cm^{-1} in the deprotonated state.²¹ Furthermore, the band of $\nu(\text{C-O})$ in the phenolic hydroxyl group was upshifted from 1243 cm^{-1} to 1272 cm^{-1} after the hydroxyl group was ionized. To avoid the deprotonation of the phenyl hydroxy groups,²² pH=11.0 was chosen for the preparation of the amphiphilic polypeptides.

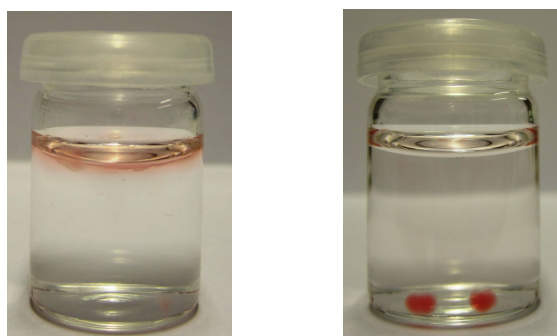


Figure 5.2: Images of poly(L-glutamate₂₀-*b*-L-tyrosine₁₀) membrane-like aggregates (the polymers were dyed by water soluble red dye). Left image: 1.0 wt% in 1.0 M CaCl₂; Right image: 4.0 wt% in 1.0 M CaCl₂.

To investigate the self-assembly of amphiphilic polypeptides in the salt solution, the amphiphilic polypeptides were added via a pipette to different concentrations of calcium chloride. Calcium ions were selected because their strong interaction with carboxylates can promote self-assembly of biomolecules through ion bridges as seen in centrin, cadherin, calmodulin, and laminin.²³ Moreover, the addition of CaCl₂ may screen the negative charges of the carboxylates and thus trigger self-assembly of the amphiphilic polypeptides via hydrophobic interactions.²⁴ The spontaneous self-assembly of both poly(L-glutamate-*b*-L-tyrosine) amphiphiles in a range of polymer concentrations (4.0-1.0 wt%) was observed in different concentrations of

CaCl₂ solutions (1.0 M - 50 mM). The immediate formation of a macroscopic transparent membrane-like aggregate localized at the interface between the amphiphilic polypeptide and the salt solution was found when the poly(L-glutamate-*b*-L-tyrosine) solution was dropped via a pipette into the salt solution. As depicted in Figure 5.2, due to higher density more stable and thicker membrane-like aggregate formed in the polymer solution of 4.0 wt% than the one of 1.0 wt%. Interestingly, those membrane-like aggregates are mechanically stable, but can be broken manually by cutting, tearing, or shearing. Moreover, it was observed that higher polymer content and higher salt concentration lead to more stable macro-aggregation. Scanning electron microscopy (SEM) images of poly(L-glutamate₂₀-*b*-L-tyrosine₁₀) in Figure 5.3 indicate the formation of the membrane-like aggregates from 4.0 wt% amphiphile solution in 1.0 M CaCl₂ is thicker and more homogeneous than 1.0 wt% one.

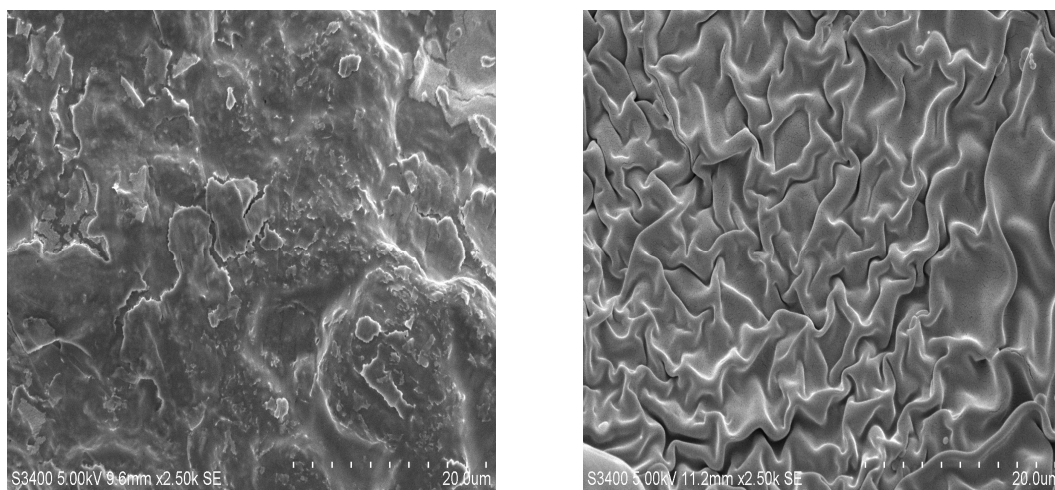


Figure 5.3: Scanning electron microscopy (SEM) images of poly(L-glutamate₂₀-*b*-L-tyrosine₁₀) membrane-like aggregates. Left image: 1.0 wt% in 1.0 M CaCl₂; Right image: 4.0 wt% in 1.0 M CaCl₂, the scale bar represents 20 μm.

As expected, calcium chloride plays a key role in the spontaneous assembly process. Besides mediating the hydrogen bonding interaction between water molecules and the amphiphilic polypeptide, calcium chlorides can significantly screen the charges of poly(L-glutamate), and enhance hydrophobic interaction through electrostatic

interaction to promote the instantaneous self-assembly of the block polypeptide.²⁵ In that context, it is interesting to understand the exact effect of calcium chloride on the conformational changes and the self-assembly.⁸ Hence, the conformational changes of poly(L-glutamate-*b*-L-tyrosine) upon adding different amounts of CaCl₂ were systematically investigated using Circular dichroism (CD) spectroscopy. DichroWeb²⁶, a web-based server, was employed to calculate the secondary structure contents from CD spectra using the SELCON3 analysis program.²⁷

Prior to the addition of calcium ions, poly(L-glutamate₂₀-*b*-L-tyrosine₁₀) displays a random coil conformation with the characteristic negative cotton effect at 198 nm. Due to inter- and intramolecular electrostatic repulsion, the polypeptide can not fold into any ordered structure. The SELCON3 analysis results confirm that the α -helix, β -sheet, β -turn, and disordered structure contents of the amphiphilic polypeptide are 10.8%, 34.2%, 20.8% and 34.2%, respectively. Upon the addition of calcium chloride at $[\text{Ca}^{2+}]/[\text{COO}^-]$ of 0.86, CD spectra (Figure 5.4) reveal that a conformational transition from random coil to extended β -sheet-like was rapidly triggered, and the β -sheet structure content significantly increased to 44% while the α -helix conformation decreased to 6.8%. Apparently, when the negative carboxylate is screened by Ca²⁺, the intramolecular folding is significantly favored, leading to a more β -sheet-like structure. With the increase of $[\text{Ca}^{2+}]/[\text{COO}^-]$, the helicity of poly(L-glutamate₂₀-*b*-L-tyrosine₁₀) significantly increased, resulting in α -helix and β -sheet structure content of 29.7% and 10.9%, respectively. Surprisingly, the conformation of the amphiphilic polypeptide was not altered by the further increase of the salt after the ratio of Ca²⁺ and COO⁻ reached 1.7. It was speculated that the poly(L-glutamate) domain was stabilized and self-assembled into a more rigid structure when Ca²⁺ completely screened the charges of poly(L-glutamate).²⁸ Therefore, the further addition of the salt cannot break the delicate balance between the two domains to trigger the conformational changes. However, by adding excessive CaCl₂, the “salting-out” of the polypeptide was observed, suggesting the increasing salt concentration largely enhanced hydrophobic interactions and further broke the delicate inter and intra-molecular interaction balance. Thereby, the amphiphilic polypeptide can form macroscopic transparent membrane-like aggregates in the presence of high concentrated salt solutions.

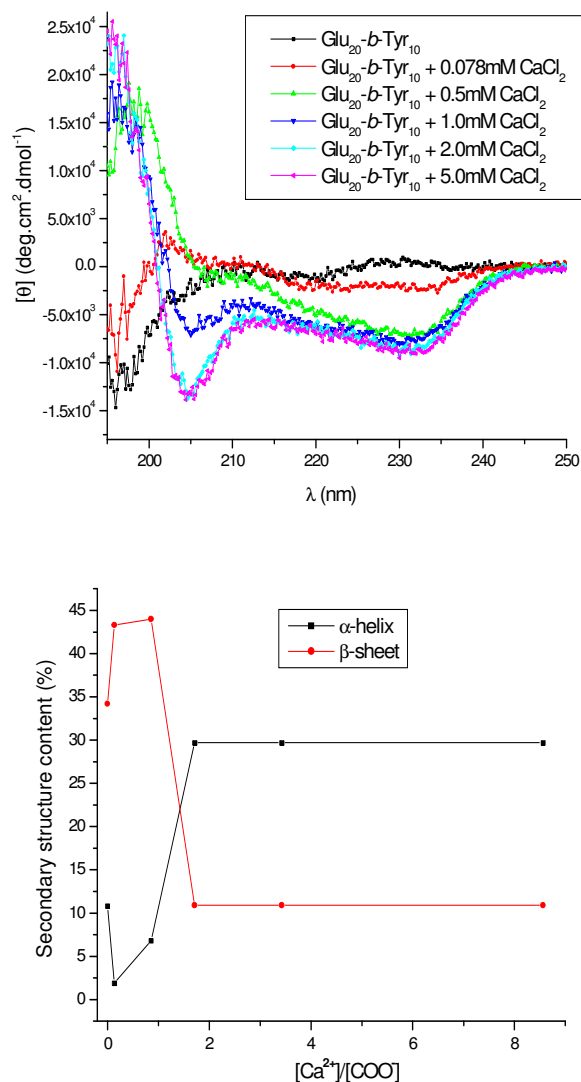


Figure 5.4: (Top) CD spectra of poly(L-glutamate₂₀-*b*-L-tyrosine₁₀) (0.125 mg/mL) upon the addition of different amounts of CaCl₂; (Bottom) Secondary structure content as a function of $[\text{Ca}^{2+}]/[\text{COO}^-]$.

The spontaneous self-assembly was also observed when poly(L-glutamate₂₀-*b*-L-tyrosine₂₀) was dropped into CaCl₂ solutions. However, due to the longer chain length of poly(L-tyrosine) building blocks, as indicated in Figure 5.5, the polymer showed different conformation changes in salt solutions. Without the addition of CaCl₂, poly(L-glutamate₂₀-*b*-L-tyrosine₂₀) adopted an extended β -sheet-like

structure with negative cotton effect at 232 nm. As confirmed by SELCON3 analysis, the α -helix, β -sheet, β -turn, and disordered structure contents of the amphiphilic polypeptide are 9.2%, 36%, 10.9% and 33.9%. More importantly, upon the addition of CaCl_2 the conformation of poly(L-glutamate₂₀-*b*-L-tyrosine₂₀) was not affected until $[\text{Ca}^{2+}]/[\text{COO}^-]$ reached 2.36. The more rigid conformation might be attributed to the different hydrophobicity balance caused by the longer poly(L-tyrosine) domain. However, with the increase of Ca^{2+} ion ($[\text{Ca}^{2+}]/[\text{COO}^-] > 2.36$), the helicity of poly(L-glutamate₂₀-*b*-L-tyrosine₂₀) greatly increased up to 66.5%, indicating that the conformation of the polypeptide amphiphiles was dominated by the poly(L-glutamate) building blocks after the addition of CaCl_2 . Furthermore, the polypeptide also precipitated out in higher concentrated salt solutions. Interestingly, due to the longer poly(L-tyrosine) chain, the critical $[\text{Ca}^{2+}]/[\text{COO}^-]$ ratio (> 4.72) for the salting-out of poly(L-glutamate₂₀-*b*-L-tyrosine₂₀) is much smaller than the one (> 8.56) of poly(L-glutamate₂₀-*b*-L-tyrosine₁₀). This also confirms that the chain length of the building blocks can significantly influence peptide-peptide interactions and hydrophobic interactions in the salt-triggered self-assembly process. Using two polypeptide amphiphiles bearing different chain lengths of tyrosine blocks and adopting two distinct secondary-structure motifs, we demonstrate that the conformation and the self-assembly of polypeptides can be manipulated by the addition of Ca^{2+} . The balance between the forces favoring assembly by hydrophobic interaction and the forces disfavoring assembly (charge repulsion) can be mediated by increasing solution ionic strength.²⁹ The results revealed the potential of using these materials to study peptide-peptide interactions or to design the new biomaterials such as membrane drug-delivery systems.

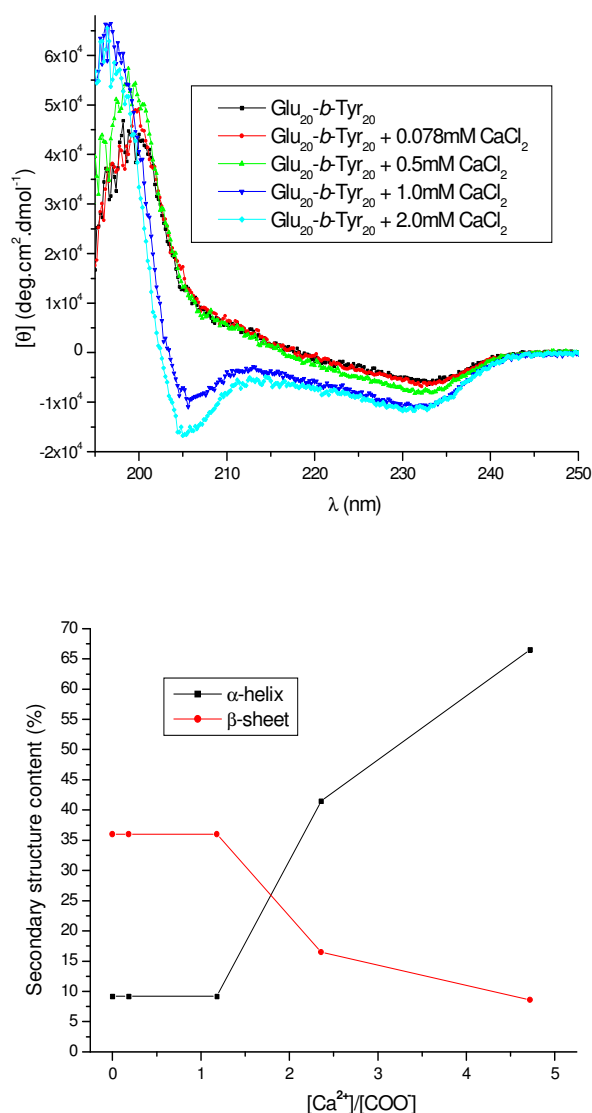


Figure 5.5: (Top) CD spectra of poly(L-glutamate₂₀-*b*-L-tyrosine₂₀) (0.125 mg/mL) upon the addition of different amounts of CaCl₂; (Bottom) Secondary structure content as a function of $[\text{Ca}^{2+}]/[\text{COO}^-]$.

Poly(L-glutamate₂₀-*b*-L-phenylalanine₁₀) was prepared to examine how the different building blocks can alter the salt-induced self-assembly of the amphiphiles. Phenylalanine is also a β -sheet forming amino acid but with a higher hydropathy index of 2.8 than tyrosine (-1.3).³⁰ As shown in Figure 5.6, poly(L-glutamate₂₀-*b*-L-phenylalanine₁₀) is of an extended α -helix structure. Calculated from SELCON3 analysis, the α -helix, β -sheet, β -turn, and disordered structure contents of the

amphiphilic polypeptide are 31.9%, 17.8%, 21.0% and 29.3%, respectively. Interestingly, the conformation of (L-glutamate₂₀-*b*-L-phenylalanine₁₀) did not change upon the addition of CaCl₂. It was speculated that owing to the more rigid and hydrophobic poly(L-phenylalanine) segment, the stronger hydrophobic interaction might result in the self-assembly of the amphiphile with a stable extended α -helix conformation before the addition of the salt. Dynamic Light Scattering (DLS) was employed to investigate the self-assembly of poly(L-glutamate₂₀-*b*-L-phenylalanine₁₀). As revealed by DLS, the polypeptide amphiphile was able to self-assemble into micelles with the size of 45 nm (PDI 0.20), and the critical micelle concentration was about 0.1 mg/mL. Poly(L-glutamate₂₀-*b*-L-phenylalanine₁₀) also coagulated at $[\text{Ca}^{2+}]/[\text{COO}^-] > 1.83$ as excessive Ca²⁺ can easily break the hydrophobicity balance and cross-link the carboxylates in the corona of the micelles to form large macro-aggregates.³¹ It is noteworthy that poly(L-glutamate₂₀-*b*-L-phenylalanine₁₀) can form larger opaque aggregates or precipitation when the polymer was added through a pipette into high concentrated CaCl₂. Apparently, bearing non-polar and hydrophobic side chains poly(L-phenylalanine) is not as “soft” as poly(L-tyrosine) in the amphiphile, leading to the different salt-triggered self-assembly. These findings also suggest that the design of amphiphilic block copolypeptides with advanced properties requires careful amino acid selection and control of their block length to delicately balance the interactions between the different segments.

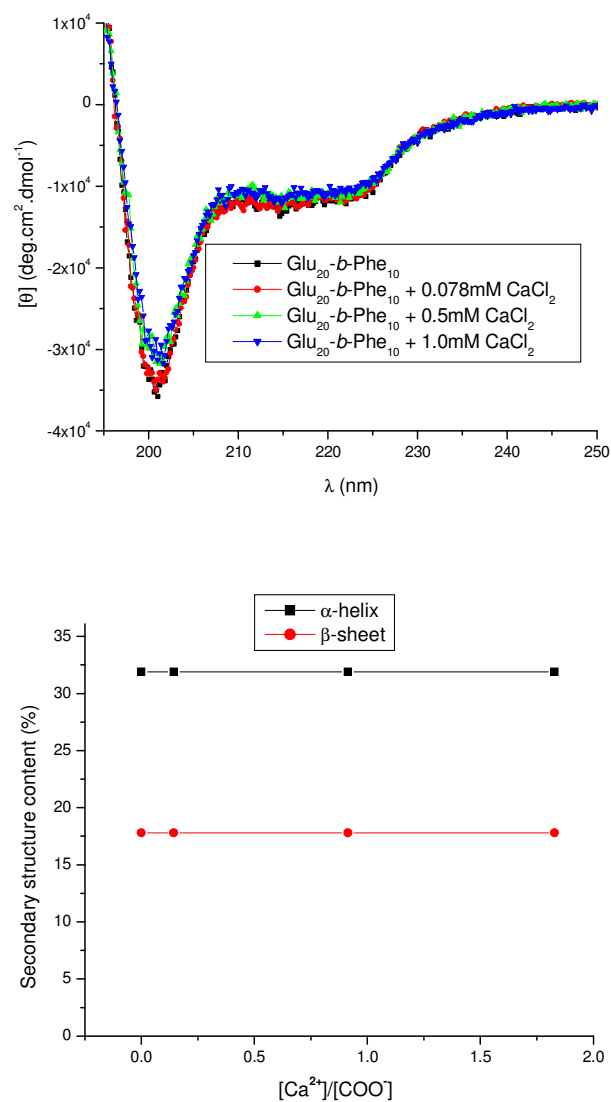
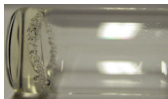
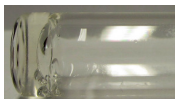
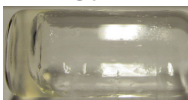
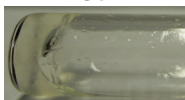
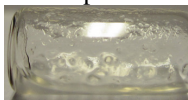

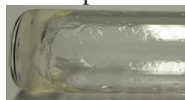
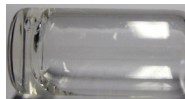
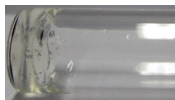


Figure 5.6: (Top) CD spectra of poly(L-glutamate₂₀-*b*-L-phenylalanine₁₀) (0.125 mg/mL) upon the addition of different amounts of CaCl₂; (Bottom) Secondary structure content as a function of $[\text{Ca}^{2+}]/[\text{COO}^-]$.

Learning that the salt can trigger the spontaneous self-assembly of poly(L-glutamate-*b*-L-tyrosine) amphiphiles through breaking the delicate balance between hydrophobic interactions and electrostatic repulsions, we aimed to utilize this unique behavior to develop novel salt-triggered polypeptide hydrogels. Since the gelation of the amphiphile is a macroscopic signature of self-assembly at the molecular level, at certain concentrations and in the presence of sufficient electrostatic screening, these tyrosine-based amphiphiles might form a three-dimensional network that is observed macroscopically as a self-supporting gel. We hypothesized that the driving force of salt-triggered hydrogelation can be attributed to the cooperativity between hydrophobic interactions and electrostatic interactions. Furthermore, divalent ions such as Ca^{2+} can also cross-link the deprotonated carboxylates of the self-assemblies as salt bridges to promote the hydrogelation. Bulky aromatic groups from poly(L-tyrosine) domains would also help stabilize the structures via potential aromatic interactions.¹⁴

We systematically investigated the hydrogelation of the amphiphiles by mixing a polymer solution with a salt solution at a given concentration. Without the addition of salt, poly(L-glutamate₂₀-*b*-L-tyrosine₁₀) at the concentration > 8.0 wt% can self-assemble into stiff and transparent hydrogel directly through non-covalent interactions. Importantly, below that concentration, the hydrogelation can be achieved by controlling the concentration ratio of the amphiphile and the salt (Table 5.2). 4.0 wt% Poly(L-glutamate₂₀-*b*-L-tyrosine₁₀) solution failed to afford a hydrogel when the concentration ratio of CaCl_2 and carboxylates ($[\text{Ca}^{2+}]/[\text{COO}^-]$) was 0.067, indicating that the non-covalent interactions triggered by Ca^{2+} are insufficient to promote hydrogelation under this condition.

Table 5.2: Typical hydrogelation of poly(L-glutamate₂₀-*b*-L-tyrosine₁₀) at different [CaCl₂]/[COO⁻] and their optical images.

	Polymer concentration ^a (wt %)			
	1.0	2.0	4.0	8.0
[CaCl ₂]/[COO ⁻] =0	Sol ^b	Sol	Sol	Gel 
[CaCl ₂]/[COO ⁻] =0.067	Sol	Sol	Viscous Sol	N/A ^b
[CaCl ₂]/[COO ⁻] =0.134	Sol	Viscous Sol	Gel 	N/A
[CaCl ₂]/[COO ⁻] =0.268	Viscous Sol	Gel ^b 	Gel 	N/A
[CaCl ₂]/[COO ⁻] =0.529	Precipitation 	Precipitation ^b 	Precipitation 	N/A
[NaCl]/[COO ⁻] =0.529	Sol	Sol	Sol	N/A
[NaCl]/[COO ⁻] =1.06	Sol	Sol	Gel 	N/A
[NaCl]/[COO ⁻] =2.12	Sol	Sol	Gel 	N/A

^a The concentration is the final concentration of the polymer after being mixed with a salt solution at a given concentration.

^b “Sol”: solution; “Gel”: gelation, the gelation is determined by the inverted vial method. The gels were left to stand overnight before the optical images were taken. No flow was observed after the vial was inverted for 1 minute, suggesting the formation of the hydrogelation; “Precipitation”: the solution turned to the mix of macro-aggregates or failed to afford a homogenous hydrogel; “N/A”: not applicable.

However, after increasing $[\text{Ca}^{2+}]/[\text{COO}^-]$ to 0.134, a sol-gel transition was observed that the solution gradually became a clear hydrogel after being aged for several minutes. This confirms that the interactions between Ca^{2+} and carboxylates are very critical to promote the hydrogelation. While higher calcium concentrations helped fasten the electrostatic-screening rate and cross-linking rate, and further facilitate stronger hydrophobic interactions, an immediate but opaque hydrogel formed at $[\text{Ca}^{2+}]/[\text{COO}^-]$ of 0.268. Upon the continuous increase of CaCl_2 concentration, the polymer formed pieces of solid-like aggregates and failed to assemble into hydrogels, suggesting the excessive Ca^{2+} could break the delicate hydrophobicity balance through the stronger electrostatic interaction, further leading to “salting-out”. Moreover, these results coincide with the findings in the spontaneous self-assembly of the amphiphiles at the different $[\text{Ca}^{2+}]/[\text{COO}^-]$, and support the conclusion that hydrophobic interactions highly depend on the interactions between Ca^{2+} and carboxylates. When the concentration of the polymer was < 2.0 wt%, the hydrogelation was only found at $[\text{Ca}^{2+}]/[\text{COO}^-]$ of 0.268. At lower $[\text{Ca}^{2+}]/[\text{COO}^-]$ inadequate amount of Ca^{2+} cannot trigger the hydrogelation while too strong electrostatic interactions at higher $[\text{Ca}^{2+}]/[\text{COO}^-]$ resulted in the instantaneous precipitation. No salt-triggered gelation occurred at the concentration of 1.0 wt%. This also confirms the fact that polymer concentration is another very important factor for the hydrogelation and a critical entanglement concentration has to be reached to form a three-dimensional network.

To validate that the interactions between Ca^{2+} and carboxylates are responsible for the efficient hydrogelation, the control experiment was carried out by using NaCl to trigger the hydrogelation of poly(L-glutamate₂₀-*b*-L-tyrosine₁₀). The hydrogelation was observed at 4.0 wt% when $[\text{NaCl}]/[\text{COO}^-]$ was > 1.07 . At lower polymer concentration such as 2.0 wt% the solutions were not able to afford hydrogelation until $[\text{NaCl}]/[\text{COO}^-]$ was > 4.28 . Furthermore, the solution of 1.0 wt% could not afford hydrogelation even in the presence of much higher concentrations of sodium chloride. It is noteworthy to mention that hydrogelation of 4.0 wt% polymer triggered by sodium chloride at $[\text{NaCl}]/[\text{COO}^-]$ of 1.06 showed a very slow sol-gel transition, and the hydrogel was observed over a period of approximate 60 minutes. The control experiments demonstrate that electrostatic interactions by Na^+ are not as

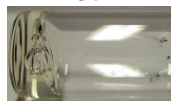
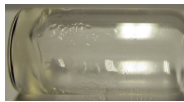
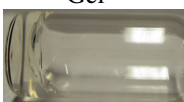

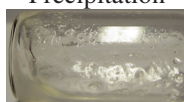
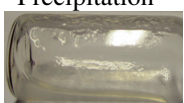
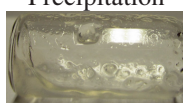
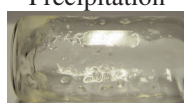
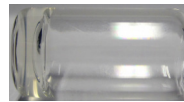
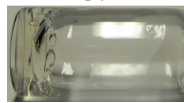
sufficient as Ca^{2+} to induce the hydrogelation of the amphiphiles until the concentration of NaCl is higher than the critical coagulation concentration.³¹ Apparently, Ca^{2+} ions are more effective in screening charges, and promoting self-assembly and hydrogel formation. Meanwhile, Ca^{2+} could also potentially be involved in bridging the carboxylates of poly(L-glutamate) through the coordination interactions (“salt bridge” effect).³² However, it remains uncertain whether aromatic interactions from the bulky aromatic groups of the poly(L-tyrosine) segments contributed to the hydrogelation.

The hydrogelation behavior of poly(L-glutamate₂₀-*b*-L-tyrosine₂₀) was also studied by mixing different concentrations of the amphiphile with CaCl_2 and NaCl, respectively. As shown in Table 5.3, similar results as for poly(L-glutamate₂₀-*b*-L-tyrosine₁₀) were found. The amphiphile can also form a transparent hydrogel without any addition of the salt at a concentration of 8.0 wt%. Owing to the longer tyrosine chain length resulting in the different hydrophobicity balance, poly(L-glutamate₂₀-*b*-L-tyrosine₂₀) demonstrated a fast sol-gel transition than poly(L-glutamate₂₀-*b*-L-tyrosine₁₀) at the same polymer and salt concentration. 4.0 wt% poly(L-glutamate₂₀-*b*-L-tyrosine₂₀) can form a clear self-supporting hydrogel in few seconds at $[\text{Ca}^{2+}]/[\text{COO}^-] = 0.184$. In addition, different from poly(L-glutamate₂₀-*b*-L-tyrosine₁₀) (4.0 wt%) which can afford hydrogel in a rather broad range of salt solutions, poly(L-glutamate₂₀-*b*-L-tyrosine₂₀) (4.0 wt%) can not self-assemble into a hydrogel, but precipitated out at $[\text{Ca}^{2+}]/[\text{COO}^-] > 0.369$. Most interestingly, a stable hydrogel instantaneously occurred when 1.0 wt% poly(L-glutamate₂₀-*b*-L-tyrosine₂₀) was mixed with 12.5 mM CaCl_2 ($[\text{Ca}^{2+}]/[\text{COO}^-] = 0.369$). These further indicate that different compositions (i.e. chain length) can significantly affect the self-assembly of the amphiphiles, further leading to different hydrogelation behaviors.

To understand the interactions between the salt and the amphiphiles during the hydrogelation, rheological properties of the hydrogels formed by different amphiphiles with different amount of CaCl_2 are evaluated at present. Moreover, transmission electron microscopy (TEM) will be also used to confirm the microstructure of CaCl_2 -triggered hydrogel. These findings open versatile platforms for the biological applications such as injectable gel (liquid before being injected, slow gelling upon the addition of the salt) as the hydrogelation can be easily

controlled by the design of polymers with different compositions or by the addition of salts.

Table 5.3: Typical hydrogelation of poly(L-glutamate₂₀-*b*-L-tyrosine₂₀) at different $[\text{CaCl}_2]/[\text{COO}^-]$ and their optical images.

	Polymer concentration ^a (wt %)			
	1.0	2.0	4.0	8.0
$[\text{CaCl}_2]/[\text{COO}^-]$ =0	Sol ^b	Sol	Sol	Gel 
$[\text{CaCl}_2]/[\text{COO}^-]$ =0.092	Sol	Sol	Viscous Sol	N/A ^b
$[\text{CaCl}_2]/[\text{COO}^-]$ =0.184	Sol	Viscous Sol	Gel 	N/A
$[\text{CaCl}_2]/[\text{COO}^-]$ =0.369	Gel ^b 	Gel 	Precipitation 	N/A
$[\text{CaCl}_2]/[\text{COO}^-]$ =0.738	Precipitation ^b 	Precipitation 	Precipitation 	N/A
$[\text{NaCl}]/[\text{COO}^-]$ =0.738	Sol	Sol	Sol	N/A
$[\text{NaCl}]/[\text{COO}^-]$ =1.48	Sol	Sol	Gel 	N/A
$[\text{NaCl}]/[\text{COO}^-]$ =2.95	Sol	Sol	Gel 	N/A

^a The concentration is the final concentration of the polymer after being mixed with a salt solution at a given concentration.

^b “Sol”: solution; “Gel”: gelation, the gelation is determined by the inverted vial method. The gels were left to stand overnight before the optical images were taken. No flow was observed after the vial was inverted for 1 minute, suggesting the formation of the hydrogelation; “Precipitation”: the solution turned to the mix of the macro-aggregation or failed to afford a homogenous hydrogel; “N/A”: not applicable.

5.4 Conclusions

To summarize, the novel amphiphile engineered by incorporating poly(L-glutamate) into a tyrosine-based polypeptide block copolymer can spontaneously self-assemble into macroscopic transparent membrane-like aggregates in the presence of salt solutions. The balance between hydrophobic interaction and electrostatic repulsion can be manipulated by the addition of Ca^{2+} to screen the carboxylates of poly(L-glutamate), resulting in the changes of conformation and self-assembly. More importantly, amphiphilic poly(L-glutamate-*b*-L-tyrosine) at certain concentrations (typically 1.0-4.0 wt%) can be triggered by the sufficient electrostatic screening to form the three-dimensional network as the matrix of the hydrogel.

5.5 References

- ¹ (a) Zhao, X. B.; Pan, F.; Xu, H.; Yaseen, M.; Shan, H.; Hauser, C. A. E.; Zhang, S.; Lu, J. R. *Chem. Soc. Rev.* **2010**, *39*, 3480. (b) Hamley I. W. *Soft Matter* **2011**, *7*, 4122. (c) Cui, H.; Webber, M. J.; Stupp, S. I.; *Biopolymers* **2010**, *94*, 1. (d) Hauser, C. A. E.; Zhang, S. G. *Chem. Soc. Rev.* **2010**, *39*, 2780. (e) Stupp, S. I. *Nano Lett.* **2010**, *10*, 4783.
- ² (a) Childers, W. S.; Ni, R.; Mehta, A. K.; Lynn, D. G. *Curr. Opin. Chem. Biol.* **2009**, *13*, 652. (b) Carlsten, A.; Lecommandoux, S. *Curr. Opin. Colloid Interface Sci.* **2009**, *14*, 329. (c) Rabotyagova, O. S.; Cebe, P.; Kaplan, D. L. *Biomacromolecules* **2011**, *12*, 269.
- ³ (a) Fletcher, N. L.; Lockett, C. V.; Dexter, A. F. *Soft Matter* **2011**, *7*, 10210. (b) Tang, C.; Ulijn, R. V.; Saiani, A. *Langmuir* **2011**, *27*, 14438. (c) Rodriguez-Hernandez, J.; Lecommandoux, S. *J. Am. Chem. Soc.* **2005**, *127*, 2026.
- ⁴ (a) Ozbas, B.; Kretsinger, J.; Rajagopal, K.; Schneider, J. P.; Pochan, D. J. *Macromolecules* **2004**, *37*, 7331. (b) Caplan, M. R.; Moore, P. N.; Zhang, S. G.; Kamm, R. D.; Lauffenburger, D. A. *Biomacromolecules* **2000**, *1*, 627. (c) Beniash, E.; Hartgerink, J. D.; Storrie, H.; Stupp, S. I. *Acta Biomater.* **2005**, *1*, 387.
- ⁵ (a) Jana, P.; Maity, S.; Maity, S. K.; Ghorai, P. K.; Haldar, D. *Soft Matter* **2012**, *8*, 5621. (b) Raeburn, J.; McDonald, T. O.; Adams, D. J. *Chem. Commun.* **2012**, *48*, 9355.
- ⁶ (a) Huang, Z.; Lee, H.; Lee, E.; Kang, S. K.; Nam, J. M.; Lee, M. *Nat. Commun.* **2011**, *2*, 459. (b) Maslovskis, A.; Tirelli, N.; Saiani, A.; Miller, A. F. *Soft Matter* **2011**, *7*, 6025.
- ⁷ (a) Zelzer, M.; Todd, S. J.; Hirst, A. R.; McDonald, T. O.; Ulijn, R. V. *Biomater. Sci.* **2013**, *1*, 11. (b) Williams, R. J.; Mart, R. J.; Ulijn, R. V. *Biopolymers* **2010**, *94*, 107. (c) Zelzer, M.; Ulijn, R. V. *Chem. Soc. Rev.* **2010**, *39*, 3351.
- ⁸ Missirlis, D.; Chworos, A.; Fu, C. J.; Khant, H. A.; Krogstad, D. V.; Tirrell, M. *Langmuir* **2011**, *27*, 6163.
- ⁹ (a) Stendahl, J. C.; Rao, M. S.; Guler, M. O.; Stupp, S. I. *Adv. Funct. Mater.* **2006**, *16*, 499. (b) Greenfield, M. A.; Hoffman, J. R.; de la Cruz, M. O.; Stupp, S. I.

Langmuir **2010**, *26*, 3641. (c) Zhang, S.; Greenfield, M. A.; Mata, A.; Palmer, L. C.; Bitton, R.; Mantei, J. R.; Aparicio, C.; de la Cruz, M. O.; Stupp, S. I. *Nat. Mater.* **2010**, *9*, 594.

¹⁰ (a) Luo, Z. L.; Zhang, S. G. *Chem. Soc. Rev.* **2012**, *41*, 4736. (b) Hauser, C. A. E.; Zhang, S. G. *Chem. Soc. Rev.* **2010**, *39*, 2780. (c) Zhao, X. B.; Pan, F.; Xu, H.; Yaseen, M.; Shan, H.; Hauser, C. A. E.; Zhang, S.; Lu, J. R. *Chem. Soc. Rev.* **2010**, *39*, 3480.

¹¹ (a) Zhang, S. G.; Holmes, T.; Lockshin, C.; Rich, A. *Proc. Natl. Acad. Sci. USA* **1993**, *90*, 3334. (b) Zhang, S. G.; Lockshin, C.; Cook, R.; Rich, A. *Biopolymers* **1994**, *34*, 663. (c) Caplan, M. R.; Moore, P. N.; Zhang, S. G.; Kamm, R. D.; Lauffenburger, D. A. *Biomacromolecules* **2000**, *1*, 627. (d) Vauthey, S.; Santoso, S.; Gong, H. Y.; Watson, N.; Zhang, S. G. *Proc. Natl. Acad. Sci. U.S.A.* **2002**, *99*, 5355.

¹² Chen, L.; Pont, G.; Morris, K.; Lotze, G.; Squires, A.; Serpell, L. C.; Adams, D. J. *Langmuir* **2011**, *27*, 14425.

¹³ (a) Roy, S.; Javid, N.; Frederix, P. W. J. M.; Lamprou, D. A.; Urquhart, A. J.; Hunt, N. T.; Halling, P. J.; Ulijn, R. V. *Chemistry A European Journal* **2012**, *18*, 11723. (b) Roy, S.; Javid, N.; Sefcik, J.; Halling, P. J.; Ulijn, R. V. *Langmuir* **2012**, *28*, 16664.

¹⁴ Zhang, Y.; Kuang, Y.; Gao, Y.; Xu, B. *Langmuir* **2011**, *27*, 529.

¹⁵ (a) Bertin, A.; Hermes, F.; Schlaad, H. *Adv. Polym. Sci.* **2010**, *224*, 167. (b) Cheng, J.; Deming, T. J. *Top. Curr. Chem.* **2012**, *310*, 1. (c) Habraken, G. J. M.; Heise, A.; Thornton, P. D. *Macromol. Rapid Commun.* **2012**, *33*, 272. (d) Colin, B.; Huang, J.; Ibarboure, E.; Heise, A.; Lecommandoux, S. *Chem. Commun.* **2012**, *48*, 8353. (e) Huang, J.; Bonduelle, C.; Thévenot, J.; Lecommandoux, S.; Heise, A. *J. Am. Chem. Soc.* **2012**, *134*, 119. (f) Schatz, C.; Louguet, S.; Le Meins, J.-F.; Lecommandoux, S. *Angew. Chem., Int. Ed.* **2009**, *48*, 2572.

¹⁶ (a) Nowak, A. P.; Breedveld, V.; Pakstis, L.; Ozbas, B.; Pine, D. J.; Pochan, D.; Deming, T. J. *Nature* **2002**, *417*, 424. (b) Breedveld, V.; Nowak, A. P.; Sato, J.; Deming, T. J.; Pine, D. J. *Macromolecules* **2004**, *37*, 3943. (c) Nowak, A. P.; Breedveld, V.; Pine, D. J.; Deming, T. J. *J. Am. Chem. Soc.* **2003**, *125*, 15666. (d) Nowak, A. P.; Sato, J.; Breedveld, V.; Deming, T. J. *Supramol. Chem.* **2006**, *18*, 423.

(e) Deming, T. J. *Soft Matter* **2005**, *1*, 28. (f) Li, Z. B.; Deming, T. J. *Soft Matter* **2010**, *6*, 2546.

¹⁷ (a) Choi, Y. Y.; Jang, J. H.; Park, M. H.; Choi, B. G.; Chi, B.; Jeong, B. *J. Mater. Chem.* **2010**, *20*, 3416. (b) Oh H. J.; Joo, M. K.; Sohn, Y. S.; Jeong B. *Macromolecules* **2008**, *41*, 8204. (c) Jeong, Y.; Joo, M. K.; Bahk, K. H.; Choi, Y. Y.; Kim, H.-T.; Kim, W.-K.; Lee, H. J.; Sohn, Y. S.; Jeong, B. *J. Control. Release* **2009**, *137*, 25. (d) Kang E. Y.; Yeon, B.; Moon, H. J.; Jeong, B. *Macromolecules* **2012**, *45*, 2007. (e) Shinde, U. P.; Joo, M. K.; Moon, H. J.; Jeong, B. *J. Mater. Chem.* **2012**, *22*, 6072. (f) Park M. H.; Joo, M. K.; Choi, B. G.; Jeong, B. *Acc. Chem. Res.* **2012**, *45*, 42.

¹⁸ Huang, J.; Hastings, C.; Duffy, G.; Kelly, H.; Raeburn, J.; Adams, D. J.; Heise, A. *Biomacromolecules* **2013**, *14*, 200.

¹⁹ (a) Habraken, G. J. M.; Peeters, M.; Dietz, C. H. J. T.; Koning, C. E.; Heise, A. *Polym. Chem.* **2010**, *1*, 514. (b) Habraken, G. J. M.; Wilsens, K. H. R. M.; Koning, C. E.; Heise, A. *Polym. Chem.* **2011**, *2*, 1322.

²⁰ Antosiewicz, J. M.; Shugar, D. *Mol. BioSyst.* **2011**, *7*, 2923.

²¹ Barth, A. *Prog. Biophys. Mol. Biol.* **2000**, *74*, 141.

²² (a) Lesser, G. J.; Rose, G. D. *Proteins: Struct. Funct. Genet.* **1990**, *8*, 6. (b) Glazer, A. N.; Smith, E. L. *J. Biol. Chem.* **1961**, *236*, 2948. (c) Tanford, C.; Hauenstein, J. D.; Rands, D.G. *J. Am. Chem. Soc.* **1955**, *77*, 6409. (d) Tachibana, A.; Murachi, T. *Biochemistry* **1966**, *5*, 2756.

²³ (a) Kühnle, R. I.; Gebauer, D.; Börner, H. G. *Soft Matter* **2011**, *7*, 9616. (b) Kühnle, R. I.; Börner, H. G. *Angew. Chem. Int. Ed.* **2011**, *50*, 4499.

²⁴ Martinez-Avila, O.; Wu, S.; Kim, S. J.; Cheng, Y.; Khan, F.; Samudrala, R.; Sali, A.; Horst, J. A.; Habelitz, S. *Biomacromolecules* **2012**, *13*, 3494.

²⁵ Ozbas, B.; Kretsinger, J.; Rajagopal, K.; Schneider, J. P.; Pochan, D. J. *Macromolecules* **2004**, *37*, 7331.

²⁶ (a) Whitmore, L.; Wallace, B. A. *Biopolymers* **2008**, *89*, 392. (b) Whitmore, L.; Wallace, B. A. *Nucleic Acids Research* **2004**, *32*, 668.

²⁷ (a) Sreerema, N.; Woody, R. W. *Anal. Biochem.* **1993**, *209*, 32. (b) Sreerema, N.; Venyaminov, S. Y.; Woody, R. W. *Protein Sci.* **1999**, *8*, 370.

- ²⁸ Lu, H.; Wang, J.; Bai, Y.; Lang, J. Liu, S. Lin, Y.; Cheng, J. *Nature Communications* **2011**, 2, 206.
- ²⁹ Bowerman, C. J.; Liyanage, W.; Federation, A. J.; Nilsson, B. L. *Biomacromolecules* **2011**, 12, 2735.
- ³⁰ Kyte, J.; Doolittle, R. F. *J. Mol. Biol.* **1982**, 157, 105.
- ³¹ Caplan, M. R.; Moore, P. N.; Zhang, S. G.; Kamm, R. D.; Lauffenburger, D. A. *Biomacromolecules* **2000**, 1, 627.
- ³² Stendahl, J. C.; Rao, M. S.; Guler, M. O.; Stupp, S. I. *Adv. Funct. Mater.* **2006**, 16, 499.

Chapter 6

Summary and Outlook

Synthetic peptides are of great interest as biomimetic materials because of their vast potential in biomedicine and biotechnology such as tissue engineering, drug delivery, and as therapeutics due to their biocompatibility and ability to self-organise. The polymerisation of α -amino acid N-carboxyanhydrides (NCA) is the most versatile and controllable technique for the large-scale preparation of high molecular weight synthetic polypeptides or polypeptide-based polymers. In order to design new polypeptides as biomaterials in medical applications, novel synthetic strategies and materials with well-defined structures as well as selective responsiveness are needed. Particularly, stimuli-responsive polypeptides (“smart” polypeptides) have been extensively explored. “Smart” polypeptides are capable of undergoing conformational changes and/or phase transition accompanied by variations in the chemical and physical changes of the polypeptides in response to an external stimulus such as biologically relevant species (i.e. enzyme, biomarker), chemicals, the environment (i.e. temperature, pH), the irradiation with light or exposure to a magnetic field. By design these materials can be placed at the interface between natural and synthetic polymeric materials. They combine natural building blocks (amino acids) with the flexibility of modern synthetic methodologies to achieve enhanced properties, which opens significant prospects for a new biomaterials platform.

The aim of this PhD project was the development of novel synthetic polypeptides, which can selectively bind to biomolecules and/or respond to environmental changes for applications in drug delivery and tissue engineering. The synthetic tools were amino-acid NCA polymerisation and precise orthogonal conjugation chemistries. Whilst being a “chemistry project”, translational biomedical data were sought thereafter to bridge the gap between synthesis and application.

Platform 1: Biologically active glycopolypeptides: Much attention has been drawn to the synthesis and application of glycopeptides during the last few years since natural glycoproteins are involved in many complex biologically responsive processes as diverse as signal transmission, fertilization, inflammation, protein folding and many more. To omit the tedious synthesis of glycosylated NCA

monomers and to allow the facile side-chain functionalization, for the first time unnatural amino acid propargylglycine without any potentially hydrolytically unstable ester bond was used to prepare glycopeptides by the combination of NCA polymerisation and quantitative Huisgen [3+2] cycloaddition click reaction with azide-functionalized galactose. First evidence for the highly selective bioactivity of the glycosylated poly(DL-propargylglycine) was demonstrated by galactose specific lectin recognition experiment. In particular, no adverse effect of the triazole ring on the lectin binding was observed. Proven by the selective hydrolysis of the benzyl ester groups in the glycosylated block copolymer poly(γ -benzyl-L-glutamate-*co*-DL-propargylglycine), the peptide-sugar linkage is hydrolytically stable, which presents a major advantage for the application of these materials in the design and synthesis of more complex biomimic structures. Noteworthy, using Huisgen [3+2] cycloaddition click reaction as the post-modification approach for the synthesis of glycopolypeptides also allows incorporating a wide variety of azide-functionalized groups (such as azide-functionalized thermoresponsive or pH-responsive moieties) for the preparation of multistimuli-responsive glycopolypeptides in a simple “one-pot” synthesis manner.

Based on the developed chemistry, in collaboration with Prof. Sebastien Lecommandoux from University of Bordeaux, a versatile route to bioactive polymersomes fully based on glycopeptides was developed. Poly(γ -benzyl-L-glutamate-*b*-galactosylated propargylglycine) copolymers were proposed as candidates to prepare glycopeptidic vesicles with lectin-binding galactose presented at the polymersome surface. In this amphiphilic block copolymer design, carbohydrates were introduced on the side chains of the hydrophilic segment that fulfill a dual function by promoting self-assembly and specific binding. Composed entirely of amino acids and natural carbohydrates, our approach omits the use of synthetic polymers and offers a fully biocompatible system. Depending on the block copolymer composition and the self-assembly protocol, the morphology of the self-assembly could be controlled, ranging from (wormlike) micelles to polymersomes. Poly(γ -benzyl-L-glutamate₂₀-*b*-galactosylated propargylglycine₂₅) at a hydrophilic weight ratio of 63% can self-assemble into stable polymersomes with an average diameter below 100 nm and an estimated thickness of 5-10 nm. More importantly,

the selective bioactivity of these polymersomes was revealed by carbohydrate-lectin binding experiment. These biologically responsive materials hold promise as nanosized drug carriers for targeted delivery. In a further variation of the glycopeptide architecture, “tree-like” glycopeptide architectures were synthesized by using Huisgen 1, 3-dipolar cycloaddition between poly(γ -benzyl-L-glutamate-*b*-propargylglycine) and two different oligosaccharides, dextran or hyaluronan. These glycopeptides show unprecedented spontaneous formation of very small micellar assemblies in water with sizes below 50 nm and low polydispersity. These materials will be further investigated for drug loading and targeted release.

Another research interest was to understand how the self-assemblies and the attached sugars would affect the lectin binding recognition by preparing a library of glycopolypeptides including galactosylated poly(γ -benzyl-L-glutamate-*b*-propargylglycine), lactosylated poly(γ -benzyl-L-glutamate-*b*-propargylglycine) and galactan-*b*-poly(γ -benzyl-L-glutamate). The galectin tests of these materials are ongoing in the laboratories of Prof. Sebastien Lecommandoux. The collaboration with Prof. David Haddleton and Dr. Remzi Becer from University of Warwick was to investigate the binding kinetics of the glycopeptides to dendritic cell lectin (DC-SIGN) and their inhibition potential for DC-SIGN and HIV-1 glycoprotein (gp120) binding. Through quantitative characterization techniques such as surface plasmon resonance (SPR), it has been studied whether the glycopolypeptides would have a more efficient binding affinity to the specific protein over polyacrylate-based glycopolymers, and how the secondary structure and sugar density of synthetic glycopolypeptides can influence the binding interactions. The results suggest that these novel glycopeptides could potentially be used more effectively as inhibitory agents to prevent HIV-1 gp120 binding to DC-SIGN. The feasibility of these polymers as components in novel therapeutics will be investigated further.

Platform 2: Responsive tyrosine-based polypeptide hydrogels: The gelation of protein- or polypeptide-based polymers synthesized either chemically or biologically has been extensively studied because of its potential application in drug delivery and tissue engineering. In particular, thermoresponsive hydrogels are highly amenable to the localised delivery of small-molecule drugs and other

therapeutic molecules, due to their tendency to maintain a liquid state at room temperature, thereby enabling a minimally invasive administration via syringing, and subsequent ability to rapidly form a robust gel bolus upon heating to physiological temperature, and enforcing drug cohesion and facilitating sustained release at the intended site of action. Within this project, a new PEGylated tyrosine-based polypeptide obtained by facile NCA polymerisation was developed. In this concept, tyrosine building blocks in the amphiphiles are able to display multiple interactions triggering self-assembly into the hydrogel matrix. The gel formation can be attributed to the precise hydrophobicity interaction between PEG and tyrosine building blocks as well as the unique feature of the tyrosine, that is, a polar but hydrophobic phenol group in the side chain. The hydrogelation profile is highly sensitive to the polymer composition as it was observed that only PEG2000-Tyr₆ formed transparent hydrogels in deionized (DI) water at a range of concentrations. Most interestingly, PEGylated tyrosine-based polypeptide can undergo sol-gel transition at a low polymer concentration range of 0.25-3.0 wt% when the temperature increases, which is rarely observed as most gels melt with increasing temperature. As demonstrated by the stronger β -sheet conformation at elevated temperature from CD spectra as a function of temperature, better packing of the β -sheet tyrosine block and the dehydration of PEG at increasing temperature induces a reverse thermogelation. Therefore, amphiphilic PEG2000-Tyr₆ block copolymers in aqueous solution can entangle with each other through hydrogen bonding or other non-covalent interactions to form a fibrous three-dimensional network as the matrix of the hydrogel. This opens up unique possibilities for injectable gels (liquid at room temperature, gelling at body temperature). In collaboration with Royal College of Surgeons in Ireland (RCSI), preliminary results confirmed the excellent biocompatibility and biodegradation of the novel hydrogel. Moreover, the sustained release of the small-molecule drug revealed that the PEG2000-Tyr₆ hydrogel could potentially function as an injectable drug depot.

Learning that tyrosine is a promising amino acid candidate for the formation of hydrogel owing to its unique features, tyrosine was further explored for the design of novel stimuli-responsive hydrogel materials. The amphiphilic copolypeptides poly(L-glutamate-*b*-L-tyrosine) were prepared via NCA polymerisation, followed

by deprotection and deprotonation of poly(L-glutamic acid). Poly(L-glutamate) was incorporated into the amphiphiles as polyelectrolyte segments, as in this molecular design salt was utilized to trigger the self-assemblies into three-dimensional networks and further macroscopic hydrogels. The hydrogelation of amphiphilic poly(L-glutamate-*b*-L-tyrosine) at certain concentrations (typically 1.0-4.0 wt%) can be triggered by the addition of the salt (i.e. CaCl_2). The driving force of salt-triggered hydrogelation is believed to be the cooperativity between hydrophobic and electrostatic interactions upon the addition of the salt. Furthermore, divalent ions such as Ca^{2+} can also cross-link the deprotonated carboxylates of self-assemblies as salt bridges to promote the hydrogelation. Meanwhile, the amphiphilic poly(L-glutamate-*b*-L-tyrosine) can spontaneously self-assemble into macroscopic transparent membrane-like aggregates when the amphiphile solution was drawn into the salty medium, which proved these materials might be useful for biological applications such as slow-diffusion drug-delivery systems and artificial skin. At present, rheological properties of the hydrogels triggered by different amounts of CaCl_2 are evaluated to understand the interactions of the salt and the amphiphiles. Moreover, TEM will be employed to confirm the microstructure of the salt-induced hydrogels and macroscopic transparent membrane-like aggregates. Further studies to explore the feasibility of these hydrogels are ongoing at present.

To summarize, through developing different novel stimuli-responsive polypeptides in this PhD project, it was demonstrated that amino-acid NCA ring-opening polymerisation alone or in combination with different orthogonal conjugation chemistries is able to provide enormous possibilities to prepare the next generation of “smart” polypeptide-based biomaterials, significantly advancing the development of biomaterials. However, the work presented here is just a starting point of this exciting area. We are still very interested in exploring more biomimic and “smarter” polypeptides by incorporating different functionalities into polypeptides via the combination of NCA polymerisation and other synthetic chemistries. Meanwhile, in terms of the application (i.e. *in vivo*) and commercialization of those developed novel polypeptides, there is still a long way to go. From aspects of chemistry, although NCA ring-opening polymerisation can be well controlled in the lab

synthesis, it is quite challenging to scale up the polypeptide synthesis in a manufacturing manner as the NCA monomer is highly unstable and sensitive, and also the purification of monomer would be tedious. The design and preparation of novel “smart” polypeptides (i.e. multistimuli-responsive polypeptide), which is more practical and useful, in particular for end-users in biological applications, is also another big challenge for the development of new biomaterials. This will have to rely on the continuous progress of synthetic chemistries as well as the closer collaboration between chemistry and biology.